Calhoun
Institutional Archive of the Naval Postgraduate School

Calhoun: The NPS Institutional Archive

DSpace Repository

Theses and Dissertations 1. Thesis and Dissertation Collection, all items

1967

Effect of stator blade orientation on the performance of an axial flow compressor

Marshall, Bruce Cameron

Monterey, California. U.S. Naval Postgraduate School

http://hdl.handle.net/10945/12064

This publication is a work of the U.S. Government as defined in Title 17, United States Code, Section 101. Copyright protection is not available for this work in the United States.

Downloaded from NPS Archive: Calhoun

DUDLEY
KNOX
LIBRARY

http://www.nps.edu/library

Calhoun is the Naval Postgraduate School's public access digital repository for research materials and institutional publications created by the NPS community. Calhoun is named for Professor of Mathematics Guy K. Calhoun, NPS's first appointed -- and published -- scholarly author.

Dudley Knox Library / Naval Postgraduate School
411 Dyer Road / 1 University Circle
Monterey, California USA 93943

NPS ARCHIVE
1967
MARSHALL, B.

EFFECT OF SLATOR BLADE ORIENTATION ON THE PERFORMANCE OF AN AXIAL FLOW COMPRESSOR

BRUCE CAMERON MARSHALL

LIBRARY
NAVAL POSTGRADUATE SCHOOL
MONTEREY, CALIF 93940

S 7

EFFECT OF STATOR BLADE ORIENTATION ON THE PERFORMANCE OF AN AXIAL FLOW COMPRESSOR

by

Bruce Cameron Marshall
Lieutenant, United States Navy
B. Ch. E., Cornell University, 1959

Submitted in partial fulfillment of the
requirements for the degree of

AERONAUTICAL ENGINEER

from the

NAVAL POSTGRADUATE SCHOOL
September 1967

SARCHIVE ~~Thesis M3555~~ c.1
67
ARSHALL, B.

ABSTRACT

A mean streamline analysis of the effect of stator blade orientation on the performance of an axial flow compressor was performed by means of a computer program. Measurements were made on a 3-stage axial flow compressor at the Naval Postgraduate School at six stator stagger angles between 23.8° and 44.3° for a fixed orientation of the rotor blades. Maximum efficiency and pressure ratio were measured at a stator stagger angle of 31.8°. Results at other blade settings showed that by varying stator stagger angle with flow rate optimum efficiencies and pressure ratios can be achieved over a wide range of operating conditions.

The results of the analysis were compared with the measured results. Suggestions are made for improving the manner of adapting cascade test data to performance predictions.

By applying a non-dimensional deflection coefficient it could be shown that minimum work input corresponded to maximum efficiency.

The test compressor has a tip diameter of 36 in. and a hub/tip ratio of 0.6. The blading tested is of the free-vortex type with a design degree of reaction of 0.5. Tip speed was about 185 ft/sec.

LIBRARY
NAVAL POSTGRADUATE SCHOOL
MONTEREY, CALIF. 93940

Thesis by Bruce C. Marshall entitled: "Effect of Stator Blade Orientation on the Performance of an Axial Flow Compressor"

ERRATA SHEET

Page	Line	Change	To
17	3	g/cm^3	dimensionless
17	5	temperatve	temperature
28	6	assessories	accessories
28	17/18	dia-meter	diam-eter
45	20/21	analy-tically	analyt-ically
59	9	delete "(g/cm^3)"	
78	Fig.15	Note 2: "DEMENSIONS"	DIMENSIONS
100	Fig.37	Maximum 3-Stage Effiency	Maximum 3-Stage Efficiency

TABLE OF CONTENTS

Section		Page
1	Introduction	21
2	O. N. R. 3-Stage Axial Flow Compressor	25
3	Flow Rate Calibration	33
4	Measurement of Compressor Performance	38
5	Performance Prediction Program	43
6	Discussion of Results	50
7	Conclusions and Recommendations	63
8	Illustrations	64
9	References	111
Appendix A	Calibration of Instruments	113
Appendix B	Flow Rate Calibration Details	122
Appendix C	Performance Measurements	135
Appendix D	Details of Prediction Program	157
Appendix E	Proposed Design of an Improved Inlet Duct	196

LIST OF TABLES

Table		Page
A-1	Calibration of BLH Torque Meter	116
A-2	Calibration of 0-12 in. Hg Bourdon Tube	118
A-3	Calibration of Inlet Pitot-Static Tube	120
B-1	Precision and Time to Damp for Various Lengths of Capillary Tube in Total and Static Pressure Lines	128
B-2	Listing of Program ONRFLO	129
B-3	Sample Output of Program ONRFLO-Input for Run 14	132
B-4	Sample Output of Program ONRFLO-Velocities for Run 14	133
B-5	Sample Output of Program ONRFLO-Calibration Constant for Run 14	134
C-1	Investigation of Axisymmetry of Flow	143
C-2	Listing of Program ONRETA	144
C-3	Output of Program ONRETA, Run 1, Stator Stagger Angle = 27.8^o	146
C-4	Output of Program ONRETA, Run 2, Stator Stagger Angle = 27.8^o	147
C-5	Output of Program ONRETA, Run 3, Stator Stagger Angle = 27.8^o	148
C-6	Output of Program ONRETA, Run 4, Stator Stagger Angle = 23.8^o	149
C-7	Output of Program ONRETA, Run 5, Stator Stagger Angle = 23.8^o	150
C-8	Output of Program ONRETA, Run 6, Stator Stagger Angle = 31.8^o	151

LIST OF TABLES (Cont.)

Table Page

C-9 Output of Program ONRETA, Run 7, Stator Stagger Angle = 31.8° 152

C-10 Output of Program ONRETA, Run 8, Stator Stagger Angle = 35.8° 153

C-11 Output of Program ONRETA, Run 9, Stator Stagger Angle = 35.8° 154

C-12 Output of Program ONRETA, Run 10, Stator Stagger Angle = 39.8° 155

C-13 Output of Program ONRETA, Run 11, Stator Stagger Angle = 44.3° 156

D-1 Listing of Program AXCO3 160

D-2 Sample Output of Program AXCO3 173

D-3 Output of Program AXCO3, Case 11, $C_{Dmin} = 0.000$ 177

D-4 Output of Program AXCO3, Case 12, $C_{Dmin} = 0.006$ 178

D-5 Output of Program AXCO3, Case 13, $C_{Dmin} = 0.008$ 179

D-6 Output of Program AXCO3, Case 21, $C_{Dmin} = 0.000$ 180

D-7 Output of Program AXCO3, Case 22, $C_{Dmin} = 0.006$ 181

D-8 Output of Program AXCO3, Case 23, $C_{Dmin} = 0.008$ 182

D-9 Output of Program AXCO3, Case 31, $C_{Dmin} = 0.000$ 183

D-10 Output of Program AXCO3, Case 32, $C_{Dmin} = 0.006$ 184

D-11 Output of Program AXCO3, Case 33, $C_{Dmin} = 0.008$ 185

D-12 Output of Program AXCO3, Case 41, $C_{Dmin} = 0.000$ 186

D-13 Output of Program AXCO3, Case 42, $C_{Dmin} = 0.006$ 187

D-14 Output of Program AXCO3, Case 43, $C_{Dmin} = 0.008$ 188

LIST OF TABLES (Cont.)

Table Page

D-15 Output of Program AXCO3, Cases 51, 52, and 53, All C_{Dmin} 189

D-16 Output of Program AXCO3, Cases 61, 62, and 63, All C_{Dmin} 190

D-17 Program CHECK, Listing and Output 191

LIST OF ILLUSTRATIONS

Figure Page

1 Compressor Installation 64

2 Accessories to Compressor 65

3 Compressor Casing 66

4 Rotor Blades, Drum and Shaft Mounted in Supporting Strut Assemblies 67

5 Assembly of Rotor in Lower Casing 68

6 Compressor Sectional View 69

7 Location of Radial Survey Holes 70

8 Detail of Free-Vortex Rotor 71

9 Detail of Free-Vortex Stator 72

10 Free-Vortex Stator Blade 73

11 Rotor Stagger Angle Adjustment 74

12 External Stagger Angle Adjustment 75

13 Inlet Bellmouth 76

14 Inlet Pitot-Static Traverse 77

15 Detail of Inlet Pitot-Static Traverse 78

16 Three-Hole Probe Detail 79

17 Permanent Pitot-Static Tube 80

18 Permanent Pitot-Tube and Three-Hole Probe Ahead of First Rotor 81

19 Pressure Readout Instrumentation 82

20 Pressure Selection by Scanner Valve 83

21 Simplified Pressure Selection System 84

22 Traverse Carriage and Three-Hole Probe Behind Third Stator 85

LIST OF ILLUSTRATIONS (Cont.)

Figure Page

23 Relation of Traverse Carriage to Survey Holes 86

24 Torque Meter During Calibration 87

25 Traverse of Inlet Duct Run D-1 88

26 Traverse of Inlet Duct Run D-7 89

27 Extent of Boundary Layer in Cylindrical Inlet Duct 90

28 Temperature-Entropy Diagram of Compression Process in 3-Stage Machine 91

29 Assumed Performance of Blading 92

30 3-Stage Efficiency Versus Referred Flow Rate Predicted by AXC03, Rotor Stagger Angle = 43.8°, Various Stator Stagger Angles 93

31 3-Stage Pressure Ratio and 3-Stage Efficiency Versus Referred Flow Rate, Stator Stagger Angle = 23.8° 94

32 3-Stage Pressure Ratio and 3-Stage Efficiency Versus Referred Flow Rate, Stator Stagger Angle = 27.8° 95

33 3-Stage Pressure Ratio and 3-Stage Efficiency Versus Referred Flow Rate, Stator Stagger Angle = 31.8° 96

34 3-Stage Pressure Ratio and 3-Stage Efficiency Versus Referred Flow Rate, Stator Stagger Angle = 35.8° 97

35 3-Stage Pressure Ratio and 3-Stage Efficiency Versus Referred Flow Rate, Stator Stagger Angle = 39.8° 98

36 3-Stage Pressure Ratio and 3-Stage Efficiency Versus Referred Flow Rate, Stator Stagger Angle = 44.3° 99

37 Maximum 3-Stage Efficiency Versus Referred Flow Rate for Various Stator Stagger Angles 100

LIST OF ILLUSTRATIONS (Cont.)

Figure | Page
38 Maximum 3-Stage Pressure Ratio Versus Referred Flow Rate for Various Stator Stagger Angles 101

39 3-Stage Efficiency, Deflection Coefficient and Pressure Coefficient Versus Flow Coefficient, Stator Stagger Angle = 23.8° 102

40 3-Stage Efficiency, Deflection Coefficient and Pressure Coefficient Versus Flow Coefficient, Stator Stagger Angle = 27.8° 103

41 3-Stage Efficiency, Deflection Coefficient and Pressure Coefficient Versus Flow Coefficient, Stator Stagger Angle = 31.8° 104

42 3-Stage Efficiency, Deflection Coefficient and Pressure Coefficient Versus Flow Coefficient, Stator Stagger Angle = 35.8° 105

43 3-Stage Efficiency, Deflection Coefficient and Pressure Coefficient Versus Flow Coefficient, Stator Stagger Angle = 39.8° 106

44 3-Stage Efficiency, Deflection Coefficient and Pressure Coefficient Versus Flow Coefficient, Stator Stagger Angle = 44.3° 107

45 Maximum 3-Stage Efficiency and Corresponding Deflection Coefficient and Stator Stagger Angles Versus Flow Coefficient 108

46 Maximum Pressure Coefficient and Corresponding Stator Stagger Angles Versus Flow Coefficient 109

LIST OF ILLUSTRATIONS (Cont.)

Figure		Page
47	Off-Design Conditions of Axial Compressor Stage	110
A-1	Torque Meter Calibration	117
A-2	Bourdon Tube Calibration	119
A-3	Inlet Traverse Pitot-Static Calibration	121
B-1	Variable Length Capillary Damping Device	126
B-2	Variable Length Capillary Damping Device Operation	127
C-1	Radial Integration for Total Pressure	141
C-2	Survey of Pressure Reading in Peripheral Direction	142
E-1	Proposed Improved Inlet Duct	198

LIST OF SYMBOLS

Symbol	Meaning	Fortran	Units
ALE	air flow angle after the inlet guide vanes	ALE	deg
b	number of blades in rotor or stator row	BLDR BLDS	-
c	blade chord length of rotor or stator	CHR CHS	in.
CCC	volume flow rate calibration constant	CCC	ft^3/sec per ft/sec
C_D	profile drag coefficient of blading	-	-
C_{Dmin}	minimum profile drag coefficient for rotor or stator blade	CDR CDS	-
c_f	conversion factor for barometric pressure	-	psfa/in. of Hg
c_p	specific heat at constant pressure	CP	Btu/lbm, ^oR
d	mean diameter of blading	DD	in.
DW	referred flow rate increment, $\dot{w}\sqrt{T_{to}}/P_A$	DW	lbm$\sqrt{^oR}$/sec psia
h	height of part of annulus area ΔA	-	in.
L	diffuser length proposed in Appendix E	-	in.
LMAX	number of stages for program AXCO3	LMAX	-

LIST OF SYMBOLS (Cont.)

Symbol	Meaning	Fortran	Units
m	slope factor which modifies $(i_o)_{10}$ for the camber of the blade section	SLOPM	-
n	slope factor which modifies δ_o for the camber of the blade section	SLOPM	-
N	compressor speed measured by electronic counter	TACH	rpm
NCASE	run number of programs ONRFLO and ONRETA	NCASE	-
NRUN	number of data points per run of program ONRETA	NRUN	-
NUM	case number of program AXCO3	NUM	-
P_A	atmospheric pressure	PA	psfa
P_{Bar}	barometric pressure	PBAR	in. of Hg
P_i	static pressure in inlet duct	PI	psfa
P_{r3-s}	ratio of total pressure behind third stator to total pressure ahead of first rotor	PRATS3	-
P_o	static pressure at permanent Pitot-static tube	PO	psfa
P_{sd}	static pressure with reference to atmospheric after the third stator	-	counts
P_{sda}	static pressure after the third stator	-	psfa
P_{si}	static pressure with reference to atmospheric in inlet duct	PSI	counts

LIST OF SYMBOLS (Cont.)

Symbol	Meaning	Fortran	Units
P_{so}	static pressure with reference to atmospheric at permanent Pitot-static tube	PSO	counts
P_{td}	total pressure with reference to atmospheric after the third stator	-	counts
P_{tda}	total pressure after the third stator	-	psfa
$\overline{P_{tda}}$	average total pressure after the third stator, integrated radially	-	psfa
P_{tig}	total pressure with reference to atmospheric between the inlet guide vanes and the first rotor	PTIG	counts
P_{tiga}	total pressure ahead of the first stage or after the inlet guide vanes	PTIGA	psf
P_{Wa}	actual horsepower of compressor	-	(ft-lbf)/sec
P_{Wth}	theoretical horsepower of compressor	-	(ft-lbf)/sec
q_d	velocity head after the third stator	-	counts
q_{d1}	velocity head after the third stator	-	psf

LIST OF SYMBOLS (Cont.)

Symbol	Meaning	Fortran	Units
q_i	dynamic head in inlet duct, below atmospheric	QI	counts
q_{i1}	dynamic head in inlet duct	QI1	psf
q_o	dynamic head of permanent Pitot-static tube, below atmospheric	QO	counts
q_{o1}	dynamic head of permanent Pitot-static tube	QO1	psf
r	radius in program ONRFLO	R	in.
RN	referred speed of program AXCO3 $N/\sqrt{T_{to}}$	RN	$rpm/\sqrt{^oR}$
r_o	outside radius	-	in.
RSTAG	rotor stagger angle measured from the blade chord at the mid-radius to a line parallel to the axis	STAGR	deg
s	spacing of blades $\pi d/b$	-	in.
SMAX	maximum limit $(i - i_{10})/\epsilon_{10}$ determined from Fig. 29	SMAX	-
SMI	minimum limit $(i - i_{10})/\epsilon_{10}$ determined from Fig. 29	SMI	-
SSTAG	stator stagger angle measured from the blade chord at the mid-radius to a line parallel to the axis	STAGS	deg

LIST OF SYMBOLS (Cont.)

Symbol	Meaning	Fortran	Units
sy	specific gravity of mercury	-	g/cm^3
T_{Bar}	temperature at barometer	TBAR	^oF
T_o	static temperatue at inlet screen	TO	^oF
T_r	reading of torque meter	TRAW	lb
T_{rq}	actual torque	TRQ	ft-lb
T_{td}	total temperature after the third stator	-	^oR
T_{td}'	total temperature at the discharge of an isentropic compression from P_{tiga} to P_{td}	-	^oR
T_{tiga}	total temperature ahead of the first stage or after the inlet guide vanes	-	^oR
T_{to}	total temperature at inlet screen	TTO	^oR
U_{av}	peripheral speed at mean radius	UAV	ft/sec
V_a	axial or through flow velocity in compressor annulus	-	ft/sec
V_d	velocity after the third stator	-	ft/sec
V_D	difference in inlet velocity at 16.0 in. radius and that measured in boundary layer	VD	ft/sec
V_i	velocity in the inlet duct	VI	ft/sec

LIST OF SYMBOLS (Cont.)

Symbol	Meaning	Fortran	Units
V_{iad}	velocity in inlet duct adjusted for slight compressor speed variations	VIAD	ft/sec
V_{iav}	average of four values of V_{iad} at each radius	VA	ft/sec
V_o	velocity at the permanent Pitot-static probe	VO	ft/sec
V_{oav}	average velocity at the permanent Pitot-static probe	VOAV	ft/sec
V_u	peripheral component of velocity	VU	ft/sec
$\mathcal{V}_c$	actual volume flow rate	VFC	ft^3/sec
$\mathcal{V}_D$	volume flow deficiency due to losses in inlet duct boundary layer	VFD	ft^3/sec
$\mathcal{V}_t$	volume flow rate neglecting losses in inlet duct boundary layer	VFT	ft^3/sec
W	air velocity realtive to the rotating blade row	W	ft/sec
W_u	peripheral component of relative velocity	WU	ft/sec
$\dot{w}$	weight flow rate	WDOT	lbm/sec
$\dot{w}_r$	referred weight flow rate $\dot{w}\sqrt{T_{to}}/P_A$	WREM	lbm $\sqrt{{}^oR}$/sec psia

LIST OF SYMBOLS (Cont.)

Symbol	Meaning	Fortran	Units
α_1	inlet angle of absolute flow	A	deg
β_1	inlet angle of relative flow	A	deg
γ	ratio of specific heat at constant pressure and specific heat at constant volume	GAM	-
δ	deviation angle of blade row	SD	deg
ΔA	part of the annulus area in the center of which V_{iav} is measured	A	ft^2
Δh_{is}	isentropic specific enthalpy difference for frictionless compression	-	Btu/lbm°R
ΔP_{3-S}	total pressure difference across the three stages	DELP	counts
ΔP_{3-SA}	actual total pressure difference	DELTAP	psf
ΔP_{3-Sth}	theoretical total pressure difference across the three stages	-	psf
ΔS	entropy difference	-	Btu/lbm°R
$\Delta T'_{t3-S}$	isentropic temperature difference from T_{tiga} to T'_{td}	-	°R
ϵ	actual deflection for blade row	DFACT	deg
ϵ_{10}	nominal deflection for blade row at incidence for minimum profile drag loss	DFSTAR	deg
η_{3-S}	three stage total-to-total efficiency	ETAST3	-

LIST OF SYMBOLS (Cont.)

Symbol	Meaning	Fortran	Unit
i	actual incidence angle of blade row	SI	deg
i_{10}	nominal incidence of blade row for minimum profile drag loss	STARI	deg
π	geometrical constant 3.14159	-	-
ρ_d	air density after the third stator	-	lb sec^2/ft^4
ρ_i	air density at the inlet	RHOI	lb sec^2/ft^4
ρ_o	air density at the permanent Pitot-static probe	-	lb sec^2/ft^4
σ	blading solidity	SO	-
τ_{av}	average dimensionless deflection coefficient	TAUAV	-
ϕ_{av}	flow coefficient, ratio of through flow velocity to peripheral speed	PHIVA	-
ψ_{av}	average dimensionless pressure coefficient	PSIAV	-
ω	angular velocity	OMEG	rad/sec

SECTION 1

INTRODUCTION

Axial flow compressors have a wide range of application. They are usually matched to a turbine in a set. Both open-cycle sets, such as aircraft turbo-jet engines, and closed-cycle sets for power generation are in service. In every application compressor efficiency is the critical factor in set performance. Accurate predictions of off-design compressor performance must be made during the design stage to be able to make corrections prior to manufacturing.

Theoretical analysis of the flow in an axial compressor involves three-dimensional partial differential equations of a complex nature (1). In these equations it is difficult to account for real gas effects such as boundary layer growth on machine walls and blade surfaces. The resulting wakes behind blade rows create non-uniform conditions; hence, it becomes necessary to base prediction methods on experimental data.

These data would be obtained best on an actual compressor. However, most compressors have relatively short blades and small flow annuli. Even if only small pressure probes were inserted between the rows of blades, the flow in these machines would be substantially altered. Test rigs must therefore be used that have large dimensions.

A first approximation of the flow in axial turbomachines can be obtained in rectilinear cascade test rigs. The intersections of a co-axial cylinder with the blades of a row produce a series of identical and identically oriented profiles which are unwrapped into a plane to establish the corresponding rectilinear cascade. A finite number of straight blades with profiles similar to, but larger than those obtained, is then arranged in a rectangular duct through which air is blown at the appropriate inflow angle. Flow surveys taken ahead of and behind the blade row give experimental data of air turning angle and total pressure loss for various blade geometries. Such a rectilinear cascade is in use at the Naval Postgraduate School. The results of extensive testing of compressor airfoil shapes at NASA have been summarized by Lieblein (2).

The usual problem in compressor design consists in selecting flow areas, blade shapes and blade layout to satisfy design specifications. Additional studies are frequently necessary if the design performance is not reached. An example is the study of Vavra which was made when the so-called Clark CSN-1 compressor of the ML-1 nuclear gas turbine of Aerojet-General Nucleonics failed to perform as required. Vavra analyzed the design changes proposed by the manufacturers and made further recommendations (3). However the ML-1 project was cancelled before the improved compressor could be built so that it was not possible to verify the suggested changes by experiments.

The so-called inverse problem consists in predicting the performance of an existing machine with a known blading by means of rectilinear cascade data and other experience factors. Such an approach was carried out by Gibbons and Bartels (4) for the 12-stage Allis-Chalmers axial flow compressor which supplies air to the turbine test facilities at the Naval Postgraduate School. Because of the unorthodox performance of the first stages, and also due to small flow annuli and short blade heights, it was not possible to predict the performance of the machine accurately. However, the analysis gave important indications for design changes to improve the performance of the compressor.

This thesis makes another attempt to solve the inverse problem for a 3-stage axial flow compressor built by the California Institute of Technology with the support of the Office of Naval Research. The compressor is sufficiently large so that the insertion of pressure probes causes relatively small flow perturbations. The machine was designed to permit variations in blade shapes, blade angles, tip clearances, and staging. The installation at the California Institute of Technology is described by Bowen, *et al*. (5) This report also describes a theory of perfect fluid flow in axial flow turbomachines. The results of this theory are compared with the measured data of the first stage of a so-called "free-vortex" type blading. Part 2 of the report by Bowen, *et al*. (6), gave a detailed investigation of multi-stage flow for both "free-vortex" blading and a more complex "solid body rotation" blading. Measurements of blade skin friction losses were greater than expected from cascade tests. The growth of boundary layer along the inner and the outer annulus walls of the flow was less than expected. Alsworth and Iura (7) conducted extensive and detailed measurements of flow patterns in a single stage of "free-vortex" blading. They carried out accurate measurements of the blade skin friction losses and the radial distribution of work input. The final report from the California Institute of Technology was a hot-wire anemometer study of compressor stall by Iura and Rannie (8). They observed that stalled flow regions rotate in the direction of blade rotation without changing shape but with a speed that is not proportional to rotor speed.

After the Turbo-Propulsion Laboratory of the Naval Postgraduate School was built, the compressor was relocated there. Since then it has been used for laboratory courses to supplement instruction in basic theories of turbomachines.

The present study was conducted for this compressor because of the possibility of changing its blade angles. For fixed stator and rotor blade angles a highly peaked curve of efficiency versus flow rate is usually obtained with axial flow compressors. At a slightly changed stator blade angle the peak will be displaced somewhat. A family of efficiency curves for various stator stagger angles is expected to yield a flatter efficiency curve over a wider range of flow rates for fixed rotor blade angles. The wide variation in flow rates required of the engines for the supersonic transport has led to design proposals by General Electric for compressors where the stator blade angles can be changed during operation of the jet engine. Hence, the thesis topic is of current interest.

For the tests it was necessary to obtain extremely accurate pressure measurements. An extremely sensitive bourdon tube pressure indicator was added to the instrumentation. A permanent Pitot-static tube was installed, and accurate flow rate calibrations were carried out. A parallel theoretical effort produced predictions of compressor performance by an existing computer program which was modified and adapted for use on the I. B. M. Model 360 computer system installed at the Naval Postgraduate School.

The author wishes to express a debt of gratitude to the faculty of the Department of Aeronautics of the Naval Postgraduate School for his engineering education. Particular thanks are due to Professor M. H. Vavra for his enthusiasm and guidance in showing what can be done with that education.

SECTION 2

O. N. R. 3-STAGE AXIAL FLOW COMPRESSOR

The compressor installation is shown in Fig. 1. The compressor inlet is in the background of the picture. The exit section is equipped with a throttle valve. A torque meter is installed on the shaft between the drive motor and the compressor. The overall dimensions of the equipment are given in Fig. 2.

A basic criterion of the design of the compressor was flexibility of operation. Each blade row may be removed. The angle setting of each blade is adjustable in 0.5° increments. In order to minimize flow disturbances by pressure probes the outside diameter of the blading is 36 in. For the same reason, the compressor has a hub/tip ratio of 0.6, giving an inside diameter of 21.6 in. and a blade height of 7.2 in. To permit simulation of conditions in a multistage unit, the machine has three stages. One row of inlet guide vanes simulates the effects of previous stages. Two rows of exit guide vanes remove the whirl component after the third stage. To insure that general alignment and tip clearances are maintained the compressor casing is very rigid.

The outer casing consists of two cast iron half-cylindrical shells bolted together along the horizontal plane through the axis. The rows of inlet guide vanes, stator blades, and exit guide vanes are held by bolts extending through the casing (Fig. 3). Inside the casing a hollow steel shaft carries three cast iron drums for each of the rows of rotor blades. The shaft is supported by two roller bearings whose outer races are pressed into the supporting strut assemblies (Fig. 4). These assemblies rest in close fitting channels in the casing (Fig. 5). The six assembly struts have symmetrical airfoil sections. Figure 6 shows the nine blade rows after assembly.

The casing was designed to give maximum accessibility for measuring instruments. Six rectangular instrument ports are located in the upper half at 30° from either side of the vertical (Fig. 3). They are placed in the second and third rotor planes, the first, second and third stator planes, and behind the third stator. The ports hold a special instrument carriage permitting detailed flow surveys in any axial plane. The casing has numerous radial survey holes whose locations are specified in Fig. 7.

The blades are made of ALCOA 356 aluminum alloy without heat treatment. There are thirty rotor blades and thirty-two stator blades per row. The details of construction of the blades are illustrated in Figs. 8 and 9. The blading is designed to have a degree of reaction of 0.5 at the mean radius. The rotor blades are twisted by 49° from hub to tip, and the stator blades by 13°. At the mean radius, the important blade parameters are:

Parameter	Rotor	Stator
Camber angle	20.32°	29.98°
Design stagger angle	43.80°	28.80°
Thickness-to-chord ratio	0.1	0.1
Chord length	2.60 in.	2.60 in.

The values of the blade parameters at other radii, and the method used for calculating the thickness distribution, are specified in Ref. 5.

The point of maximum thickness was set at 0.35 of the chord length from the leading edge. The thickness was modified over the rear 15 per cent of the section to provide a trailing edge thickness 0.02 in. The thickness distribution is applied about a parabolic mean camber line. Figure 10 is a picture of a "free-vortex" stator blade. Tip clearances of 0.020 in. for stator, and 0.037 in. for rotor, are maintained by the use of shims at the point of attachment.

The attaching device permits variation of rotor and stator blade stagger angle. Figure 11 shows how these changes are made. The blade shaft extends through the rotor drum at the hub. An adjusting plate is secured to the blade shaft by a tapered pin. The plate has a series of eleven taps on a circle about the shaft axis which are spaced at intervals of 4.5^{o}. Between the adjusting plate and the rotor drum is a fixed sector which is attached to the drum by a pin which guarantees its alignment. The fixed sector has eleven holes which are spaced at intervals of 4.0^{o} of arc about the blade shaft axis. Blade alignment is maintained by a set screw through both holes in the adjusting plate and the fixed sector. If the center holes of the plate and the sector are lined up, the blade is at the design stagger angle of 43.8^{o} for the "free-vortex" rotor. An angle change of 4.0^{o} can be accomplished by keeping the set screw in the center hole of the adjusting plate and moving the blade so the screw is inserted into the next hole of the fixed sector. Small angle changes of 0.5^{o} are accomplished by moving the blade slightly so that the two holes immediately adjacent to the center holes are lined up since blade angle is changed only by the difference in arc between the two holes. A similar arrangement is used for the stator blade settings (Fig. 10). Figure 12 illustrates stator blade settings which are one degree smaller than the design stagger angle. The two blades on the right-hand side of the figure belong to the first stator row. The set screw is two holes away from the center or reference holes. The blades on the left-hand side of Fig. 12 belong to the row of inlet guide vanes. They are set at an angle which is by 0.5^{o} smaller than the design stagger angle.

The assessories to the basic compressor will be described by following a path from the inlet to the exit and to the power source. The instrumentation of the compressor will be described in its appropriate place in the same sequence. Details of instrument calibrations are contained in Appendix A.

The inlet duct is seen in the background of Fig. 1. It consists of a screen, an entrance bellmouth, and a length of straight pipe. Figure 13 shows the large mesh screen which prevents the ingestion of foreign matter from the compressor bay apron. Mounted on the screen is a mercury thermometer used to determine ambient temperature. It has provisions for psychrometric analysis of the incoming air. Immediately behind the screen is the bellmouth. It changes the diameter rather abruptly from almost two diameters at the flare, to 36 in. in the axial distance of about 15 in. A cylindrical inlet duct two diameters long connects the bellmouth to the compressor proper. The inner surface of the duct is enameled to give smooth flow surfaces.

The flow rate through the compressor was determined by surveys in the inlet duct. Details of the calibration are given in Appendix B. The survey plane is about midway between the bellmouth and the compressor. The surveys were made with a Prandtl-type Pitot tube. In Fig. 14 the probe is installed for taking a vertical traverse. It is possible to disassemble the probe while the compressor is running (Fig. 15).

It may then be remounted for a horizontal traverse. Traverses at 30° and 60° from the vertical direction are possible. These traverses can be made by unbolting the entire inlet duct from the compressor and rotating it on its cradle. The design of the probe prevents measurements closer than 0.25 in. to the inlet duct wall.

A honeycomb straightener is installed behind the inlet Pitot tube to equalize the flow entering the compressor (Fig. 14). Attached to the forward strut assembly is an ogival wooden fairing (Fig. 5) to provide a smooth transition of the flow from the inlet duct to the compressor annulus.

Pressure measurements may be taken at any one of the radial survey ports described. Figure 16 shows the probe used for these measurements. It is a United Sensor three-hole probe, model YC-120. A central hole measures stagnation or total pressure. A static port is located on each of two faces of a wedge at an angle of 45° from the total pressure hole. The static pressures are balanced on a water manometer to insure alignment of the probe in flow direction. The probe is mounted on a probe holder which has vernier scales permitting radius adjustments to 0.01 in. and angle adjustments to 0.1°.

The accurate determination of flow rate is essential to compressor analysis. For this purpose a modified Prandtl type Pitot-static probe was installed. Figure 17 shows the installation details. The probe is inserted in a radial survey hole located ahead of the inlet guide vane row. It protrudes forward into a channel between two adjacent struts of the supporting assembly which is shown in Fig. 5. The probe is approximately at the center of the channel between struts. The probe is positioned in the radial survey hole by a brass plug, and secured to the casing by a simple locking device. Figure 18 shows the probe and its locking device in the background. In the middle of the figure are seen the three-hole probe and its holder located between the inlet guide vanes and the first rotor. In the foreground, a plug, originally located at the same axial position as the probe, has been removed to show a hole through which the probe can be inserted.

Pressures obtained by the probes were measured by a Texas Instruments Fused Quartz Precision Pressure Gauge which is shown in Fig. 19. The velocity head in the inlet is about 0.6 in. of water. A low-pressure bourdon tube was obtained for the gauge which measures from 0 to 166 in. of water with the instrument reading from 0 to 200,000 counts. The calibration constant of the low pressure bourdon tube was determined to be 240.423 counts/psf of the pressure gauge (See Appendix A.). The pressure gauge operates both in manual and servo modes, the latter providing automatic nulling of the unit.

Since flexibility of pressure selection was desirable, two Giannini Sp-101A pressure scanners were connected to the pressure and reference ports of the bourdon tube. One of the scanners is seen in the foreground of Fig. 19. The arrangement of pressures to the 12-channel switches is shown in Fig. 20. Later in the study a simpler system of five valves and two manifolds was constructed (Fig. 21) to eliminate leakage flows that seem to have occurred in the scanners. At this time the original 3-hole probe was placed permanently behind the third stator (Fig. 22). Another 3-hole probe was placed ahead of the first stage rotor. This arrangement permitted direct measurement of the pressure increase across the three stages, ΔP_{3-S}.

Figure 22 also shows the instrument traverse carriage mentioned before. It was used for a survey of total pressure in peripheral direction behind the third stator at two different radii (See Appendix C.). It is possible to vary the radial locations of the probe with an accuracy of 0.01 in. The probe may be rotated through 360° about its axis. The carriage can move the probe 15° in peripheral direction, which covers a whole blade spacing since a stator blade channel covers 11.25°, and a rotor blade channel 12.0° in peripheral direction. The locations of the radial survey holes with reference to the indicated meridional angle of the carriage are shown in Fig. 23. The represented stator profiles are at the design stagger angle at the mean radius. The actual stagger angle measured with respect to a plane through the axis is the complement of the indicated angle.

A short cylindrical duct connects the compressor to the exit elbow, which is equipped with sheet metal turning vanes to minimize losses. A transition piece connects the elbow to the throttle valve which is seen in Fig. 1. The valve consists of two rectangular metal doors which move in slides. The position of the doors is controlled by a right- and left-hand threaded lead screw which is rotated by a Graham variable-speed transmission. A revolution counter indicates the approximate valve opening.

The compressor is driven by a 50 HP Fairbanks Morse induction motor. It requires a three-phase, sixty-cycle, 440 volt power supply, and can operate at two fixed speeds; namely, at about 900 rpm or 1200 rpm.

Attached to the motor shaft is a Baldwin-Lima-Hamilton SR-4 torque meter type A. It is shown in Fig. 24 during calibration with known weights attached to a lever. In the background may be seen a Brown Instruments strain gauge readout which is of the standard Wheatstone bridge type. A conversion constant of 4.1565 ft-lb/lb of torque meter readout was determined (See Appendix A.). Under the protective cover next to the torque meter in Fig. 24 is installed a six lobe flux cutter to measure the motor speed by means of an electronic counter.

SECTION 3

FLOW RATE CALIBRATION

The permanent Pitot-static tube was installed to provide rapid and accurate measurements of volume flow rate. At a given throttle valve setting this probe was calibrated against the result of two traverses of the cylindrical inlet duct. Through-flow velocities in the flow annulus ahead of the inlet guide vanes were varied from 110 ft/sec to 70 ft/sec, so that compressibility effects could be ignored. The objective of the calibration was to determine a calibration constant which gave the volume flow rate when multiplied by the velocity measured at the permanent probe.

An initial survey of the inlet duct was made at the highest possible flow rate of 512 ft^3/sec. Figure 25 shows a plot of the measured velocities of both horizontal and vertical traverses. The smooth velocity profile in the duct is evident. Figure 26 is a graph of the measured velocities in the inlet duct at the lower flow rate of 310 ft^3/sec, which shows a higher degree of scatter. For these tests the pressure indicator was operated in the servo mode. Even in the meter mode the indicated pressure oscillated considerably. Pressure fluctuations seemed to have been initiated by the vibration of the brass rod on which the traversing Pitot-static tube was mounted in the inlet duct. The pressure indicator corrects a disparity between the angular position of a mirror of the bourdon tube and the indicator dial at the rate of the full scale reading of 200,000 counts in 120 seconds. With the oscillating pressure applied to the sensitive instrument, oscillations of 50 counts were observed for a pressure corresponding to a reading of 600 counts. To reduce these oscillations, variable length capillary tube damping devices were installed both in the total and static pressure lines of the traverse Pitot-static tube. Details of the arrangement and the results of tests are shown in Appendix B-1.

A special survey was made to determine the thickness of the boundary layer on the walls of the cylindrical inlet duct. However, construction of the traverse probe prevented taking readings closer than 0.25 in. from the wall. Figure 27 is a plot of the readings at high and low flow rates. In each case it is evident that large losses occur near the walls. With the velocity distributions of Fig. 27 the flow rate is about 2.5 per cent smaller than the value obtained without considering the changes near the walls.

Data were taken in the boundary layer at intervals of 0.25 in. from 17.75 in. to 16.00 in. In the main stream, data were taken at 4.0 in. intervals from 16.00 in. to the centerline. With horizontal and vertical traverses, four points were obtained at each radius and two at the axis for a total of 46 locations. At each station the following measurements were taken:

q_i - velocity head in the inlet duct (counts)

q_o - velocity head of the permanent Pitot-static probe (counts)

P_{si} - static pressure with reference to atmosphere in inlet duct (counts)

P_{so} - static pressure with reference to atmosphere at permanent Pitot-static probe (counts)

T_o - temperature at the inlet screen (^oF)

P_{Bar} - barometric pressure (in. of Hg)

T_{Bar} - temperature of column of mercury (^oF)

The barometric pressure P_{Bar} (in. Hg) was converted into pounds per square foot to obtain the atmospheric pressure P_A by

$$P_A = P_{Bar} \ (71.467) \qquad \text{(psfa)} \qquad (1)$$

where the constant was obtained by correcting the height of the column of mercury for temperature variations in specific gravity of the liquid. The inlet temperature was converted to absolute temperature,and was considered to be the total temperature T_{to} because of the low velocities, or

$$T_{to} = T_o + 459.7 \qquad (^oR) \qquad (2)$$

The static pressure P_i at the inlet was converted from the meter reading to an absolute pressure by

$$P_i = P_A - \frac{P_{si}}{240.423} \qquad \text{(psfa)} \qquad (3)$$

where the constant was obtained by the calibration procedure described in Appendix A. The pressure P_o measured at the permanent probe was obtained in a similar manner. The local air density ρ_i at the inlet was computed from

$$\rho_i = \frac{0.002378 \ P_i}{(14.696)(144)} \frac{518.7}{T_{to}} = \frac{P_i}{T_{to}}\left(5.82 \times 10^{-4}\right) \ (\text{lb sec}^2/\text{ft}^4) \qquad (4)$$

and similarly ρ_o at the permanent probe. The velocity head in the inlet q_{i1} was converted from the meter reading,

$$q_{i1} = \frac{q_i}{240.423} \qquad \text{(psf)} \qquad (5)$$

The dynamic head at the permanent probe q_{o1} was obtained similarly. The velocity V_i in the inlet is then

$$V_i = \sqrt{\frac{2 \ q_{i1}}{\rho_i}} \qquad \text{(ft/sec)} \qquad (6)$$

A similar procedure gave the velocity V_o at the permanent probe. The arithmetic average of the 46 values of V_o obtained during the carrying out of the traverses gives the average value V_{oav} of

$$V_{oav} = \frac{1}{46} \sum_{j=1}^{46} V_{oj} \qquad \text{(ft/sec)}$$

The measured values of V_i were adjusted to account for variations in flow rate due to slight compressor speed variations

$$V_{iad} = V_i \frac{V_{oav}}{V_o} \qquad \text{(ft/sec)}$$

The four values of V_{iad} obtained at each radius were averaged by

$$V_{iav} = \frac{1}{4} \sum_{j=1}^{4} V_{iadj} \qquad \text{(ft/sec)}$$

The volume flow rate was first calculated by neglecting the losses in the boundary layer to give $\mathcal{V}_t$. In general the volume flow rate is obtained by

$$\mathcal{V} = 2\pi \int_0^{r_o} V\, r\, dr \qquad (\text{ft}^3/\text{sec})$$

If the above equation were integrated directly, the velocity at the axis would not be included in the volume flow rate calculation because the zero radius is a member of the product under the integral. Therefore the integral was replaced by a summation.

$$\mathcal{V}_t = \sum V_{iav} \; \Delta A \qquad (\text{ft}^3/\text{sec})$$

The quantity $\Delta A = 2 \pi r h/144$ represented that part of the annulus area in the center of which V_{iav} was measured, where h is the height of the area. This method assumed that the velocity measured at the radius of 16.0 in. exists also at the wall. A volume flow rate deficiency was then calculated to account for the difference in velocities at 16.0 in. radius and those measured in the boundary layer, or

$$V_D = V_{iav\,16''} - V_{iav\,B.L.} \qquad \text{(ft/sec)}$$

By a trapezoidal integration the volume flow deficiency $\mathcal{VF}_D$ becomes

$$\mathcal{VF}_D = 2\pi \int_{16.0}^{18.0} V_D \; r \, dr \qquad \text{(ft}^3\text{/sec)}$$

Then the actual volume flow rate is

$$\mathcal{VF}_c = \mathcal{VF}_t - \mathcal{VF}_D \qquad \text{(ft}^3\text{/sec)}$$

A calibration constant CCC for each run was obtained from

$$\text{CCC} = \frac{\mathcal{VF}_c}{V_{oav}} \qquad \text{(ft}^3\text{/sec per ft/sec)}$$

A first series of calibration runs was invalidated when a leakage hole was discovered in the traversing Pitot-static tube. After repairs, the calibration constants CCC were obtained with a maximum relative error of 0.1 per cent. The final calibration constant was 4.4050 ft^3/sec per ft/sec velocity obtained from the readings of the permanently installed Pitot-static probe.

A data reduction computer program, ONRFLO, for these calibration procedures, was generated for the I. B. M. Model 360 computer. A listing of the program is included as Appendix B-2. Sample output data from the final run is given in Appendix B-3.

SECTION 4

MEASUREMENT OF COMPRESSOR PERFORMANCE

The objective of the study was to determine the effect of changes of the stator blade orientation on compressor performance. It was decided to restrict performance investigation to the three stages only; namely, from a station ahead of the first rotor to a station after the last stator, or between locations SP-2 and SP-8 of Fig. 7. The effects of the inlet, the inlet guide vanes, the exit guide vanes, and the diffuser were not considered.

For tests at a particular stator stagger angle the barometric pressure P_{Bar} was determined first. For various settings of the throttle valve the following measurements were taken:

T_o - ambient temperature (^oF)

P_{so} - static pressure with reference to atmosphere at the permanent Pitot-static probe (counts)

q_o - velocity head at the permanent Pitot-static probe (counts)

P_{tig} - total pressure with reference to atmospheric between the inlet guide vanes and the first rotor (counts)

ΔP_{3-S} - total pressure difference across the three stages (counts)

T_r - reading of torque meter (lb)

N - compressor speed measured by electronic counter (rpm)

With the relations listed on p. 35 these measuring data establish the following quantities:

$$P_A = P_{Bar}\,(71.467) \qquad \text{(psfa)} \qquad (1)$$

$$T_{to} = T_o + 459.7 \qquad (^oR) \qquad (2)$$

$$P_o = \frac{P_{so}}{240.423} \qquad \text{(psfa)} \qquad (3)$$

$$\rho_o = \frac{0.002378\ P_o\ 518.7}{(14.696)(144)\quad T_{to}} = \frac{P_o}{T_{to}}(5.82\times10^{-4})\ (\text{lb sec}^2/\text{ft}^4) \qquad (4)$$

$$q_{o1} = \frac{q_o}{240.423} \qquad (\text{psf}) \qquad (5)$$

$$V_o = \sqrt{\frac{2\ q_{o1}}{\rho_o}} \qquad (\text{ft/sec}) \qquad (6)$$

The absolute total pressure ahead of the first stage, or after the inlet guide vane, P_{tiga}, is

$$P_{tiga} = P_A - \frac{P_{tig}}{240.423} \qquad (\text{psf}) \qquad (7)$$

The pressure difference across the three stages ΔP_{3-SA} is obtained from

$$\Delta P_{3-SA} = \frac{\Delta P_{3-S}}{240.423} \qquad (\text{psfa})$$

From the torque meter reading T_r the actual torque T_{rq} is

$$T_{rq} = T_r\ (4.1565) \qquad (\text{ft-lbf})$$

where the constant was obtained by the calibration procedure described in Appendix A. The angular velocity ω is with the measured speed, N

$$\omega = \frac{2\pi N}{60} \qquad (\text{rad/sec})$$

Both volume and weight flow rates were calculated. The volume flow rate VF_c is then

$$VF_c = V_o\ (4.4050) \qquad (\text{ft}^3/\text{sec}) \qquad (8)$$

where the constant was obtained by the calibration procedure described in the preceding section and Appendix B. The weight flow rate $\dot{w}$ is

$$\dot{w} = \sqrt{F_c}\,\frac{32.174\ P_A\ 518.7}{(14.696)(144)\ T_{to}} = \sqrt{F_c}\,\frac{P_A}{T_{to}}\,(7.886) \qquad \text{(lbm/sec)} \qquad (9)$$

For comparison with the prediction program a referred flow rate $\mathring{w}_r$ is defined by

$$\dot{w}_r = \frac{\dot{w}\sqrt{T_{to}}}{P_A/144} \qquad (\text{lbm}\sqrt{^{o}R}/\text{sec psia}) \qquad (10)$$

Two basic indices of performance were computed; namely, the 3-stage pressure ratio P_{r3-s}, where

$$P_{r\,3-S} = \frac{P_{tiga} + \Delta P_{3-SA}}{P_{tiga}} \qquad (11)$$

and the 3-stage total-to-total efficiency η_{3-S} obtained from

$$\eta_{3-s} = \frac{P_{Wth}}{P_{WA}} \qquad (12)$$

where P_{Wth} and P_{Wa} are the theoretical and actual horsepower, respectively. The theoretical power is P_{Wth}, given by

$$P_{Wth} = \dot{w}\ \Delta h_{is}(778.3) \qquad \text{(ft-lbf/sec)}$$

where Δh_{is} is the isentropic specific enthalpy difference for a frictionless compression from P_{tiga} to P_{td} after the third stator. Assuming a perfect gas there is

$$\Delta h_{is} = c_p\ \Delta T'_{t\,3-S} \qquad (\text{Btu/lbm},\ ^{o}R)$$

where $\Delta T'_{t3-s}$ is the isentropic temperature difference from the total temperature T_{tiga} ahead of the first stage, to T'_{td} after the third stator (See Fig. 28.). Since T_{tiga} very nearly equals the ambient temperature T_{to}, there is

$$\Delta h_{is} = c_p T_{to} \left(\frac{T_{td}'}{T_{tiga}} - 1 \right) \qquad \text{(Btu/lbm, }^{o}\text{R)}$$

With the isentropic relation

$$\frac{T_{td}'}{T_{tiga}} = \left(\frac{P_{td}}{P_{tiga}} \right)^{\frac{\gamma-1}{\gamma}}$$

the final expression for the determination of the theoretical power is

$$P_{Wth} = \dot{w}\, c_p T_{to} \left[\left(P_{r3\text{-}S} \right)^{\frac{\gamma-1}{\gamma}} - 1 \right] 778.3 \qquad \text{(ft-lbf/sec)} \qquad (13)$$

The actual power is obtained from

$$P_{WA} = T_{rq}\, \omega \qquad \text{(ft-lbf/sec)}$$

The total-to-total efficiency at the three stages is then

$$\eta_{3\text{-}S} = \frac{\dot{w}\, c_p T_{to}}{T_{rq}\, \omega} \left[\left(P_{r3\text{-}S} \right)^{\frac{\gamma-1}{\gamma}} - 1 \right] 778.3 \qquad (14)$$

For comparison with other compressor data certain non-dimensional parameters are introduced. The average flow function ϕ_{av} is the ratio of through flow velocity V_a and peripheral speed at the mean diameter U_{av}, or with

$$V_a = \frac{VF_c}{651.4/144} = VF_c\,(0.221) \qquad \text{(ft/sec)}$$

and, for the mean diameter of 14.4 in.

$$U_{av} = \omega\, \frac{14.4}{12} \qquad \text{(ft/sec)}$$

there is

$$\phi_{av} = \frac{VF_c \quad (12)(144)}{\omega \quad (14.4)(651.4)} = \frac{VF_c}{\omega}\,(0.1842) \qquad (15)$$

An average dimensionless stage pressure coefficient Ψ_{av} is defined by

$$\frac{\Delta P_{3-SA}}{3} = \Psi_{av} \, \rho_o \, U_{av}^{2} \qquad \text{(psf)}$$

or

$$\Psi_{av} = \frac{\Delta P_{3-SA}}{3 \, \rho_o \, U_{av}^{2}} \tag{16}$$

The so-called dimensionless deflection coefficient τ_{av} is defined by

$$\frac{\Delta P_{3-S\,th}}{3} = \frac{\Delta P_{3-SA}}{3 \, \eta_{3-S}} = \frac{\Psi_{av}}{\eta_{3-S}} \rho_o \, U_{av}^{2} \qquad \text{(psf)}$$

$$= \tau_{av} \, \rho_o \, U_{av}^{2} \qquad \text{(psf)}$$

Hence,

$$\tau_{av} = \frac{\Psi_{av}}{\eta_{3-S}} \tag{17}$$

The performance calculations were made for the conditions along the mean radius of the stage, 14.4 in., by assuming that these conditions are representative of the performance of the 3-stage compressor. Detailed investigations which support this simplification are given in Appendix C. The data reduction was accomplished by the computer program ONRETA, which is listed also in Appendix C.

Data were taken on 11 occasions for the following settings of stator stagger angle:

Run	Stator Stagger Angle
1, 2, 3	27.8^{o}
4, 5	23.8^{o}
6, 7	31.8^{o}
8, 9	35.8^{o}
10	39.8^{o}
11	44.3^{o}

SECTION 5

PERFORMANCE PREDICTION PROGRAM

The program used to predict the performance of multi-stage compressors is called AXCO3. It is listed in Appendix D and represents an adaptation of a program by Vavra (3), modified by Gibbons and Bartels (4).

The method assumes that the flow is axisymmetric. Computations are made for the streamlines at the mean radius of a stage. A stage by stage analysis of the machine is performed. The output of one stage is used as input for the next stage. The computation is started at a flow rate less than that anticipated for surge, and the flow rate is then increased by small increments to cover the whole operating range of the machine.

Program AXCO3 uses two principal subroutines; namely, one called ROTOR and the other called STATOR. They establish the velocity triangles of a rotor or a stator row of blades, respectively, from the known geometry of the bladings, flow rate, and discharge conditions of the preceding row of blades. Both subroutines make use of three additional subroutines.

Subroutine THEORY calcualates the flow conditions for minimum profile losses. Cascade data by Lieblein are used for this purpose (2). These data are presented as curves for zero-camber incidence angle $(i_0)_{10}$, slope factor n, zero camber deviation angle $(\epsilon_0)_{10}$, and slope factor m, all given as functions of the inlet air angles β_1 or α_1, with the blading solidity σ as a parameter. The solidity σ is defined as the ratio of blade chord c and blade spacing s.

The curves described above have been expressed by polynomials in powers of solidity and inlet air angle which are used in subroutine THEORY. The accuracy of the polynomials has been verified, and the errors are listed in Appendix D. The incidence angle for minimum loss is determined by an iteration procedure which changes the inlet air angle until agreement is reached within a tolerance of 0.02°. The deflection which occurs at the minimum profile loss can then be calculated with the established polynomials also.

The subordinate subroutine CASCAD calculates the performance of the blading at the actual incidence or inlet flow angle of the blade row by using a graph of Lieblein that establishes the change of the deviation angle with incidence angle ($d\delta/di$) as a function of inlet flow angle and solidity.

In the earlier computer programs the curves of this graph were expressed by a polynomial that covered the range of solidities from 0.0 to 1.8. Since the curves have nearly exponential character, which cannot be expressed with ease by polynomial functions, it was found that an error of the order of 10 per cent was possible. Therefore, a new polynomial was established for solidities between 0.6 and 1.4 which limits the error to less than 1.9 per cent.

Subroutine CASCAD further utilizes experimental limits on blading performance by Howell (9) which are illustrated in Fig. 29. Howell found that for most cascades the ratio of the profile drag coefficient C_D at an arbitrary incidence angle i and C_{Cmin} at the minimum loss incidence i_{10} is a unique function of the quantity $(i-i_{10})/\epsilon_{10}$, where ϵ_{10} is the optimum flow deflection for the incidence angle i_{10}. Since the applicability of the data presented in Ref. 2 is limited to design point calculations, where the incidence angles are close to the nominal incidence i_{10}, the curves cannot be used for off-design analyses without restrictions. Without such limits the flow deflections ϵ could be increased simply by increasing the incidence angle i, since the data of Ref. 2 do not establish criteria for flow separations which are associated with a radical increase in profile losses. Experimental results of Howell show that the flow deflection ϵ at incidence i should not exceed the optimum deflection ϵ_{10} by more than 25 per cent to avoid excessive losses. He states that this limit occurs if the profile loss coefficient C_D is about twice the minimum loss coefficient C_{Dmin}. The solid curve in Fig. 29, labeled ϵ/ϵ_{10}, is supposed to be the relation between ϵ/ϵ_{10} and $(i-i_{10})/\epsilon_{10}$ as obtained from subroutine CASCAD with the data from Ref. 2. It will be assumed that this curve holds for negative values of $(i-i_{10})/\epsilon_{10}$ only. For positive values of this parameter the dashed curve will be applied to satisfy the limitations of Howell. This curve is somewhat arbitrary but represents the best estimate for the actual operating condition of compressor cascades. Figure 29 further shows a curve relating the ratio C_D/C_{Dmin} to $(i-i_{10})/\epsilon_{10}$, which is adapted from Ref. 9. Both this curve and the dashed curve for the deflection ratio have been expressed analytically in subroutine CASCAD. If the ratio C_D/C_{Dmin} exceeds a value of 2.0 for positive quantities $(i-i_{10})/\epsilon_{10}$, the program prints out "surge in blade row xx" and proceeds with calculations at an increased flow rate. The positive value of $(i-i_{10})/\epsilon_{10}$ at which this occurs is the input quantity SMAX. If C_D/C_{Dmin} exceeds a value of 2.0 at incidence angles i smaller than i_{10}, the program prints out "minimum pressure in blade row xx" and halts computation. The negative value of

$(i - i_{10})/\epsilon_{10}$ at which this occurs is the input quantity SMI. In both instances the symbol xx refers to the number of the blade row, and indications are given also whether the row is a stator or a rotor. For any incidence angle within the useful operating range, the values of the deflection ratio and of the ratio C_D/C_{Dmin} are computed by subroutine CASCAD and control returned to the blade row subroutines ROTOR or STATOR.

The efficiency of a blade row is determined by subroutine ETACAL. Losses due to tip clearances, secondary flows, and wall friction are taken into account with the relations proposed by Vavra (1).

If conditions of surge exist, the flow rate is increased by about 1.0 per cent and the entire computation is repeated. If the incidence angles are in the so-called useful operating region of Fig. 29, the output of subroutine ROTOR or STATOR becomes the input for the subroutine that calculates the next row of blades. Interstage data are printed out as the program progresses from one stage to the next. If all blade rows of a machine have been processed, the overall compressor efficiency and pressure ratio are computed for the particular flow rate. This flow rate is then increased by a specified amount, and the calculating process is repeated. If the so-called minimum pressure is reached, the computation stops and a summary of the overall performance parameters is printed out.

The details of the calculation of the flow through the inlet duct, the inlet guide vanes, the exit guide vanes, the diffuser and the discharge passages are not described in this thesis since it is concerned only with the performance prediction of the three stages of the compressor from a station ahead of the first rotor to the discharge at the third stator. The methods applied for the flow analysis in these passages may be found in Vavra (3) and Gibbons and Bartels (4).

According to Howell there occur additional effects that influence the off-design calculations. The growth of boundary layers on the walls of the annular flow channel will change the velocity profiles and can reduce significantly the effective flow area. The program takes account of this effect by a blockage factor that can vary from stage to stage. This boundary layer growth is responsible also for increasing peaks in the radial distribution of the axial velocity components in succesive stages. These higher velocities outside of the wall boundary layers produce smaller incidence angles for the main portion of the flow, thereby decreasing the actual flow deflection and reducing the work absorbed by the fluid in the stage. Hence in a compressor that consists of stages with identical bladings, the last stages will produce smaller pressure ratios than the stages at the compressor inlet. Experience shows the efficiency in successive stages is not reduced by the peaking of the velocity profiles, and their effects are usually taken into account by a so-called work-done factor that is about unity for the first stage and gradually decreases for the successive stages. Such work-done factors can be introduced in program AXCO3, but for the present compressor they will be taken as unity because of the small number of stages and the large blade heights. For the same reasons the blockage factor is assumed to be equal to unity also.

The geometry of the blades could be obtained from the information of Ref. 5. Values at the mean radius were used for the analysis. Bowen (5) determined that the average flow angle at the mean radius after the inlet guide vanes ALE was 20.0° for the design inlet guide vane stagger angle of 11.4°, independent of flow rate. From Fig. 12 it can be recognized that the inlet guide vanes were set at a stagger angle of 10.9° for the tests. Therefore a value of 19.5° was used in the analysis program for the average flow angle leaving the inlet guide vanes. Reference 5 does not give values of C_{Dmin} for the blading. It is possible to introduce in the program various values of C_{Dmin} both for rotor and stator blading. Hence it was possible to estimate an average apparent value of C_{Dmin} for blading by comparing measured results to predictions of the analysis program for several assumed values of C_{Dmin}.

A prediction of the 3-stage efficiency for different stator stagger angles is shown in Fig. 30 for an assumed value of C_{Dmin} of 0.020. The light line connecting the individual peak efficiencies represents the calculated operating envelope which could be obtained if continuous control of stator stagger angle for maximum efficiency were possible.

For comparison with measured performance a series of calculations were made for stator stagger angles of 23.8°, 27.8°, 31.8°, 35.8°, 39.8°, and 44.3°. For each stagger angle, values of C_{Dmin} of 0.000, 0.006, and 0.008 were assumed. To avoid confusion with the computations of actual performance based on measured quantities, which have been called runs, each calculation of the analytical prediction program has been assigned a two-digit case number. The first digit identifies the stator stagger angle of the case as follows:

First Digit	Stator Stagger Angle
1	23.8°
2	27.8°
3	31.8°
4	35.8°
5	39.8°
6	44.3°

The second digit identifies the assumed value of C_{Dmin} of the case as follows:

Second Digit	Assumed Value of C_{Dmin}
1	0.000
2	0.006
3	0.008

For example, case 42 is the predicted performance at a stator stagger angle of 35.8° with a value of C_{Dmin} of 0.006. The summary output of each case is presented in Appendix D.

SECTION 6

DISCUSSION OF RESULTS

Experimental data for performance measurements were taken during 55 hours of running time. Another 81 hours of operation were used for miscellaneous calibration and testing, including 44 hours for flow rate calibrations.

The rotor stagger angle was set at 43.8^o for all runs. The design stator stagger angle is 28.8^o. For the performance tests, the stator stagger angle was set at 23.8^o, 27.8^o, 31.8^o, 35.8^o, 39.8^o, and 44.3^o. Measured performance is presented in comparison with the predicted results of AXCO3,and also by establishing dimensionless performance parameters. Figures 31 through 36 are graphs of measured performance in comparison with the prediction by AXCO3 for each stator blade angle setting. Figures 37 and 38 are summary plots of maximum efficiency and pressure ratio for all stator blade angle settings. Figures 39 through 44 are graphs of the non-dimensional parameters at each stator stagger angle. Figure 45 is a summary plot of maximum efficiencies and associated deflection coefficients for all stator blade angle settings. Figure 46 is a summary plot of maximum pressure coefficients for all stator blade angle settings.

On each of Fig. 31 through Fig. 36 the 3-stage efficiency reaches a peak value for each stator stagger angle. The referred flow rate at which this peak occurs decreases as the stator stagger angle increases.

Also plotted on each of Fig. 31 through Fig. 34 are the results predicted by AXCO3 for the three estimated values of C_{Dmin} of 0.000, 0.006 and 0.008. The predicted 3-stage efficiency reaches a peak for each C_{Dmin}. The referred flow rate associated with predicted peak efficiency decreases with increase in stator stagger angle. The referred flow rate at which the predicted peak efficiency occurs decreases with increase in C_{Dmin} at a given stator stagger angle.

AXC03 predicts the condition of surge for each case according to the criteria of Howell shown in Fig. 29. The surge condition is assumed to exist whenever the parameter $(i-i_{10})/\epsilon_{10}$ exceeds the maximum positive value SMAX which has been inserted in the program. The incidence angle for the rotor blade rows becomes larger as the through-flow velocity decreases until a surge condition is indicated. AXC03 predicts surge at the same referred flow rate for each setting of stator stagger angle. This is due to the fixed angle of the inlet guide vanes. The assumption has been made that the air flow angle leaving a blade row does not change with variations in flow rate in the incompressible flow regime. This result was verified by Bowen (5). The inlet guide vanes were not rotated as the stator stagger angle was varied. At all stator stagger angle settings the first stage rotor had the same incidence angle at particular flow rates. In the stage-by-stage analysis, "surge in rotor 1" was indicated at the same flow rate in each run, regardless of the stator stagger angle setting of subsequent stators. The region of referred flow rates smaller than that at which surge is indicated by the program is marked with a dashed line on Figs. 31 through 34, and is less than 41.5 lbm$\sqrt{^{\circ}R}$/sec psia for every case.

When the value of the parameter $(i-i_{10})/\epsilon_{10}$ is determined to be less than SMI, the negative value of the parameter which has been inserted in AXC03, the program stops the computation and prints "minimum pressure in blade row xx." The referred flow rate at which computation is stopped decreases as stator stagger angle is increased. At stator stagger angles of 31.8^{o} and lower (Figs. 31 through 33) the referred flow rate at which computation is stopped is larger than the maximum flow rate of the graph. At a stator stagger angle of 35.8^{o} (Fig. 34), the computation stops at a referred flow rate of 45.5 lbm$\sqrt{^{o}R}$/sec psia. At stator stagger angles of 39.8^{o} and 44.3^{o} (Figs. 35 and 36), the program did not establish useful data. At the high stator angles the referred flow rate at which computation was stopped was lower than the referred flow rate for surge in the first stage rotor. The latter flow rate remained unchanged at a fixed inlet guide vane angle.

This difficulty illustrates some of the limitations of program AXC03 when applied to an actual machine. The program assumes that the compressor is designed properly. Changes from stage to stage must be gradual. For example the annulus area may change gradually from stage to stage with no adverse effects. The checks for minimum pressure and surge limits are applied in each blade row. Surge in any blade row is interpreted as surge in the machine, and similar limitations are imposed for minimum pressure. The program cannot cope with discontinuities similar to those that occur by leaving the angle of the inlet guide vanes unchanged. It is possible to imagine a situation where the angle setting of the inlet guide vanes might have to remain unchanged; for instance, if the inlet guide vanes must support the front bearing of the rotor shaft. In such a design the first rotor would have higher blade efficiencies than succeeding blade rows at large flow rates, while at lower flow rates the blade efficiencies of the first rotor would be smaller than for succeeding blade rows. The 3-stage efficiency of an actual machine is an overall parameter which includes the effect of the different blading efficiencies for different blade rows. In an actual machine the flow will adjust itself to these conditions,whereas program AXC03 cannot cope with these peculiar circumstances. For these reasons the program did not produce performance data for the higher stator stagger angles of 39.8° and 44.3°.

The detection of the actual surge point during the tests is difficult with the available instrumentation and must be based on acoustic phenomena. Incipient surge,probably due to rotating stall, was associated with an unmistakable oscillating change in sound level produced by the compressor. This effect appeared suddenly even when flow rate was decreased slowly. To eliminate the sound due to this surge condition it was necessary to increase the flow rate by about 5 to 10 per cent. A flow rate slightly above the surge point could then be reached by gradual throttling. For each run one test point was taken in the surge region and one test point as close as possible to the surge point. Efficiency at test points in the surge region was below 0.90 for all stator stagger angles. The efficiency at the data point close to stall rose from 0.89 to 0.94 as the stator stagger angle was increased from 23.8° to 31.8°, and efficiency decreased to 0.89 with further increase in stator stagger angle to 44.3°. As the surge condition is approached the rate of decrease of efficiency is set by the relative location on the efficiency versus referred flow rate graph of the two data points in the surge region and close to surge. At a stator stagger angle of 31.8° which produced the maximum

3-stage efficiency and at 35.8°, efficiency decreased most rapidly as the surge condition was approached. For other stator stagger angles the efficiency decreased less rapidly. It is not possible to make a meaningful comparison between measured surge point data and the surge condition calculated by AXCO3 because surge was predicted to occur at the same referred flow rate for each case.

It is possible to compare measured values of maximum 3-stage efficiency with the maxima calculated by program AXCO3. For all four stagger angles at which computations were made, the maximum 3-stage efficiencies were predicted to occur at flow rates about 5 per cent greater than the flow rates at which the measured maxima occurred. According to Howell the point of maximum efficiency occurs for a value of the parameter $(i-i_{10})/\epsilon_{10}$ about equal to +0.19 (Fig. 29). At greater positive values of the parameter the losses are believed to increase rapidly. Since the measured maximum efficiency occurred at a flow rate which was about 5 per cent less than was predicted, an analysis of off-design performance of a compressor stage was made. The method of Vavra (Ref. 1) assumes that the air flow angles leaving a blade row do not change with flow rate in incompressible flow. The velocity triangle changes caused by a reduction from design flow rate are shown in Fig. 47. The subscript d refers to the design condition, and the primed quantities refer to off-design. The analysis was conducted at the maximum efficiency point for a stator stagger angle of 27.8°. The following quantities were measured:

Design flow coefficient ϕ_d = 0.517

Inlet flow angle α_1 (fixed) = 20.0°

The off-design flow rate was fixed at 5 per cent less than the design flow rate, to correspond to the flow rate at which the measured maximum efficiencies occurred. The off-design flow coefficient is

$$\phi' = (0.95)\ (0.517)$$

The peripheral components of velocity are:

$$\frac{V_{u1d}}{U} = \phi_d \tan \alpha_1$$

$$\frac{V_{u1}'}{U} = 0.95\ \phi_d \tan \alpha_1$$

$$\frac{W_{u1d}}{U} = \frac{U - V_{u1d}}{U} = 1 - \phi_d \tan \alpha_1$$

$$\frac{W_{u1}'}{U} = \frac{U - V_{u1}'}{U} = 1 - 0.95\ \phi_d \tan \alpha_1$$

The relative inlet flow angles for both conditions are:

$$\beta_{1d} = \arctan \frac{W_{u1d}/U}{\phi_d} = \arctan\left[\frac{1}{\phi_d} - \tan \alpha_1\right]$$

$$\beta_1' = \arctan \frac{W_{u1}'/U}{0.95\ \phi_d} = \arctan\left[\frac{1}{0.95\phi_d} - \tan \alpha_1\right]$$

With the same rotor stagger angle, the difference in incidence angle i between design flow rate and off-design flow rate is the difference in β_1

$$i' - i_d = \beta_1' - \beta_{1d} = 59.2^\circ - 57.5^\circ = +1.7^\circ$$

The difference between the parameter $(i - i_{10})/\epsilon_{10}$ at the design flow rate and the parameter at a flow rate 5 per cent less than design is

$$\Delta \frac{(i - i_{10})}{\epsilon_{10}} = \frac{+1.7}{+11.2} = +0.15$$

where ϵ_{10} was calculated by AXC03. The measured maximum efficiencies occurred at a value of the parameter $(i - i_{10})/\epsilon_{10}$ which was greater by 0.15 than the value of the parameter for which the program AXC03 predicted maximum efficiencies.

Lieblein's data were obtained from compilations and reductions of cascade test data primarily for blade profiles which were NACA

65 (A_{10}) - series airfoils built up on equivalent circular arc camber lines. The free-vortex blades installed in the compressor have a thickness distribution which was derived from the theory of Ref. 1 applied to a parabolic mean camber line. If the actual incidence for minimum profile loss for the installed blades were smaller by 1.7° than calculated by subroutine THEORY, all values of the parameter $(i-i_{10})/\epsilon_{10}$ calculated in subroutine CASCAD would be larger by 0.15 than they actually are. The flow rate at which the maximum efficiency is calculated would be 5 per cent greater than the flow rate at which maximum efficiency was actually measured.

Howell presented results of cascade tests of British C-1 and C-2 airfoil shapes for several values of solidity. The C_D/C_{Dmin} curve of Fig. 29 was obtained by interpolation for a solidity of 0.8. If the upper limit of the parameter $(i-i_{10})/\epsilon_{10}$ for minimum loss were extended by 0.15 from 0.19 to 0.34, the flow rate at which maximum efficiency was calculated analytically would coincide with the flow rate for measured maximum efficiency.

The measured efficiency curves are more peaked than the curve computed by AXCO3. If the C_D/C_{Dmin} curve of Fig. 29 had a greater slope in regions where C_D/C_{Dmin} approaches a value of 2.0, the predicted efficiency curves would be less flat and would more nearly approximate the curves of measured performance.

It was one object of this thesis to attempt to determine the value of C_{Dmin} for the installed blade profile. Vavra (1), p. 377, indicates that these values usually do not exceed 0.008. For each stator stagger angle, analytical calculations were made for estimated C_{Dmin} of 0.000, 0.006 and 0.008. The results for the smaller stator stagger angles are plotted on Fig. 31 through Fig. 34. The value of C_{Dmin} was estimated for each stator stagger angle:

Stator Stagger Angle	Estimated C_{Dmin}
23.8	0.008
27.8	0.004
31.8	0.003
35.8	0.007

The arithmetic average of the estimated values is 0.0055, but there is is obviously considerable scatter in the experimental data.

A summary plot of maximum peak efficiencies is presented in Fig. 37. If continuous control of stator stagger angle were possible, as in the proposed SST engine, Fig. 37 would be an operating curve for maximizing efficiency at any flow rate. The peak maximum 3-stage efficiency was 0.956, measured at a stator stagger angle of 31.8. Also shown is a flatter curve of predicted peak 3-stage efficiencies using C_{Dmin} of 0.006 for the four lower stator stagger angles. The maximum predicted value is 0.942 at a stator stagger angle of 30°. The predicted values occur at flow rates 5 per cent higher than corresponding measured values. The measured values decline more steeply at stagger angles other than the angles for maximum efficiency than do the analytically calculated values. The curve relating stator stagger angle to performance shows that, in the region near the maximum efficiency, relatively small changes in angle are required for large variations in flow rate. Between stator stagger angle settings of 27.8° and 35.8°, a 10 per cent variation in flow rate requires only an 8° angle change. In the regions more distant from the maximum efficiency point, large angle changes are required to handle small flow rate changes.

Figures 31 through 36 also contain plots of 3-stage pressure ratio versus referred flow rate for each stator stagger angle.

As expected, the measured maximum pressure ratio occurred at a referred flow rate between that for maximum efficiency and for surge. It was not possible to determine maxima for the calculated data of AXCO3 because for each case the largest pressure ratio occurred at the flow rate tagged "surge." The program does not compute performance at lower flow rates. The check for surge occurs in subroutine CASCAD. Based on cascade data, Howell stated that unacceptable losses occur at values of ϵ / ϵ_{10} greater than 1.25. This conservative criterion is particularly applicable in a design where a wide range of flow rates is not required. However for the purpose of evaluating pressure ratio for an existing machine, the criterion appears to be too restrictive. It would be more advantageous if AXCO3 used the criterion to predict surge but then proceeded to complete the calculations at that flow rate rather than stopping computation.

The measured pressure ratio was in general by 0.25 per cent greater than predicted by AXCO3, and the measured ΔP_{3-SA} was about 11 per cent greater. Total pressure is relatively simple to measure. The yaw and pitch errors of the 3-hole probe are very small. Any error in total pressure measurement is expected to produce a total pressure lower than expected. Since the predictions are lower at every flow rate, it is possible that the difference in blading between the installed blade profiles and the NACA airfoils, which are represented by Liebleins's data, may be the cause of the difference as was suggested in the discussion of 3-stage efficiency. A summary plot of maximum 3-stage pressure ratio on an expanded scale is presented in Fig. 38. The peak value of maximum pressure ratio occurred at a stator stagger angle of 31.8^{o}

While writing the thesis, an error was discovered in Eq. 1, which converts the reading of the mercury barometer P_{Bar} in in. of mercury to P_A in psfa and corrects for the temperature variation of the specific gravity of the liquid. The incorrect equation

$$P_A = P_{Bar} \left(0.4928 + T_{Bar} \ 0.5/10{,}000\right) 144 \quad \text{(psfa)}$$

was used. At 70.0°F the constant by which P_{Bar} was multiplied was 71.457 psfa/in. of Hg. Reference 10 lists the specific gravity of mercury "sy" for the temperature range 0°F to 150°F as

$$sy = 13.638 - 1.354 \times 10^{-3} (T_{Bar}) \quad \text{(g/cm}^3\text{)}$$

The conversion factor is

$$c_f = 69.892 \ \frac{sy}{13.59} \quad \text{(psfa/in. of Hg)}$$

At 70°F the correct conversion factor is 69.55, or the atmospheric pressure on which all calculations were based was 3 per cent higher than the actual atmospheric pressure. By Eqs. 3, 4 and 7 the calculated static pressure P_o and air density ρ_o at the permanent Pitot-static tube, and the total pressure after the inlet guide vanes P_{tiga}, were 3 per cent higher than actual also. By Eqs. 6, 8 and 10 the calculated velocity V_o, volume flow rate VF_c, and referred flow rate $\dot{w}_r$ were 0.983 of the actual values. The calculated pressure ratio P_{r3-s} was 0.998 of the actual value by Eq. 11. By Eqs. 9 and 14 the values of weight flow rate $\dot{w}$ and 3-stage efficiency were calculated to be 1.2 per cent higher than the actual values.

The test results are presented in non-dimensional form in Figs. 39 through 44. Plotted against the flow coefficient ϕ_{av}, the efficiencies follow the same pattern as when plotted against referred flow rate, since Eqs. 10 and 13 differ only by a constant. Figure 45 is a summary plot of the maximum 3-stage efficiciency for each stator stagger angle versus flow coefficient and is similar to Fig. 37 for the same reason. Figure 46 is a summary plot of maximum pressure rise coefficient for each stator stagger angle. The pressure rise reaches a maximum at a blade angle of 33° and a flow coefficient of 0.475. The curve of corresponding stator stagger angles has an almost constant slope.

Theoretically, the deflection coefficient τ_{av} represents the change in peripheral flow components in a blade row divided by the peripheral speed. Figure 47 is a stage velocity triangle showing design and off-design conditions in a compressor stage. At the design condition

$$\tau_d = \frac{\Delta W_{ud}}{U} = \frac{\Delta V_{ud}}{U}$$

An assumption in this analysis is that the air leaving angle from a blade row does not vary with incidence. Hence the angles α_1 and β_1 remain constant. The relation between the off-design deflection coefficient τ' and the off-design flow coefficient ϕ' is fixed by similar triangles

$$\frac{1 - \tau'}{1 - \tau_d} = \frac{\phi'}{\phi_d}$$

and

$$\tau' = 1 - (1 - \tau_d)\frac{\phi'}{\phi_d}$$

or τ' is expected to vary linearly with ϕ'.

At flow coefficients greater than that for maximum 3-stage efficiency, calculated deflection coefficients τ_{av} varied linearly with flow coefficient in Figs. 39 through 44. For most runs the graph of τ_{av} broke sharply from the linear segment at the maximum efficiency point. For each case the curve continued at a reduced slope in the region between the break and prior to surge. Experience seems to indicate this identifies a region of incipient stall. As the blades become fully stalled, the nature of the flow changes drastically. It has been suggested that this change is reflected in a sharp increase in the slope of the deflection curve. The author was reluctant to operate the compressor in the region of stall for extended periods of time because of related vibration and noise problems. However a slight upturn of the deflection coefficient curve was apparent at stator stagger angles of 23.8° and 27.8° (Figs. 39 and 40).

The deflection coefficient τ is a measure of work input. It will be necessary to make an approximation for the theoretical power P_{Wth}. Equation 11 can be rewritten

$$P_{r\,3\text{-}S} = 1 + \frac{\Delta P_{3\text{-}S}}{P_{tiga}} \qquad \text{(psfa)}$$

Making a first order expansion, Eq. 13 can be rewritten

$$P_{Wth} = \dot{w} R_G \frac{\gamma}{\gamma-1} T_{to} \left[1 + \frac{\gamma-1}{\gamma} \frac{\Delta P_{3\text{-}S}}{P_{tiga}} - 1 \right] \qquad \text{(ft-lbf)/sec}$$

$$= \frac{\dot{w} R_G T_{to}}{P_{tiga}} \Delta P_{3\text{-}S} = V\!F_c \, \Delta P_{3\text{-}S} \qquad \text{(ft-lbf)/sec}$$

Substituting P_{Wth} in Eq. 12, the efficiency becomes

$$\eta_{3\text{-}S} = \frac{V\!F_c \, \Delta P_{3\text{-}S}}{T_{rq} \, \omega}$$

Rewriting Eq. 15

$$V\!F_c = A \, \phi_{av} \, U_{av} \qquad (\text{ft}^3/\text{sec})$$

and introducing Eq. 16 into Eq. 17, there is

$$\tau_{av} = \frac{T_{rq}}{3 \rho_o U_{av}^2 A R \phi_{av}}$$

or the deflection coefficient is a direct function of the torque T_{rq} or work input.

Figure 45 is a graph of the τ_{av} which was calculated at maximum 3-stage efficiency for each stator stagger angle. The minimum of these deflection coefficients occurs at the maximum efficiency. At maximum efficiency the minimum work input was required.

SECTION 7

CONCLUSIONS AND RECOMMENDATIONS

It has been shown that maximum efficiency can be achieved for each flow rate. The computer program AXCO3 can be used to predict efficiency within 2 per cent, with an error of 5 per cent in flow rate. Pressure ratio may be predicted within 0.25 per cent.

It is recommended that further measurements be made at increased rotor stagger angles. Inlet guide vane angles should be varied to simulate the effects of preceding blade rows. Blade shapes with higher blade loadings should be tested.

Scatter in the data may be caused by variations in inlet flow and accentuated by oscillations of the pressure gauge. A proposed improved inlet duct is described in Appendix E.

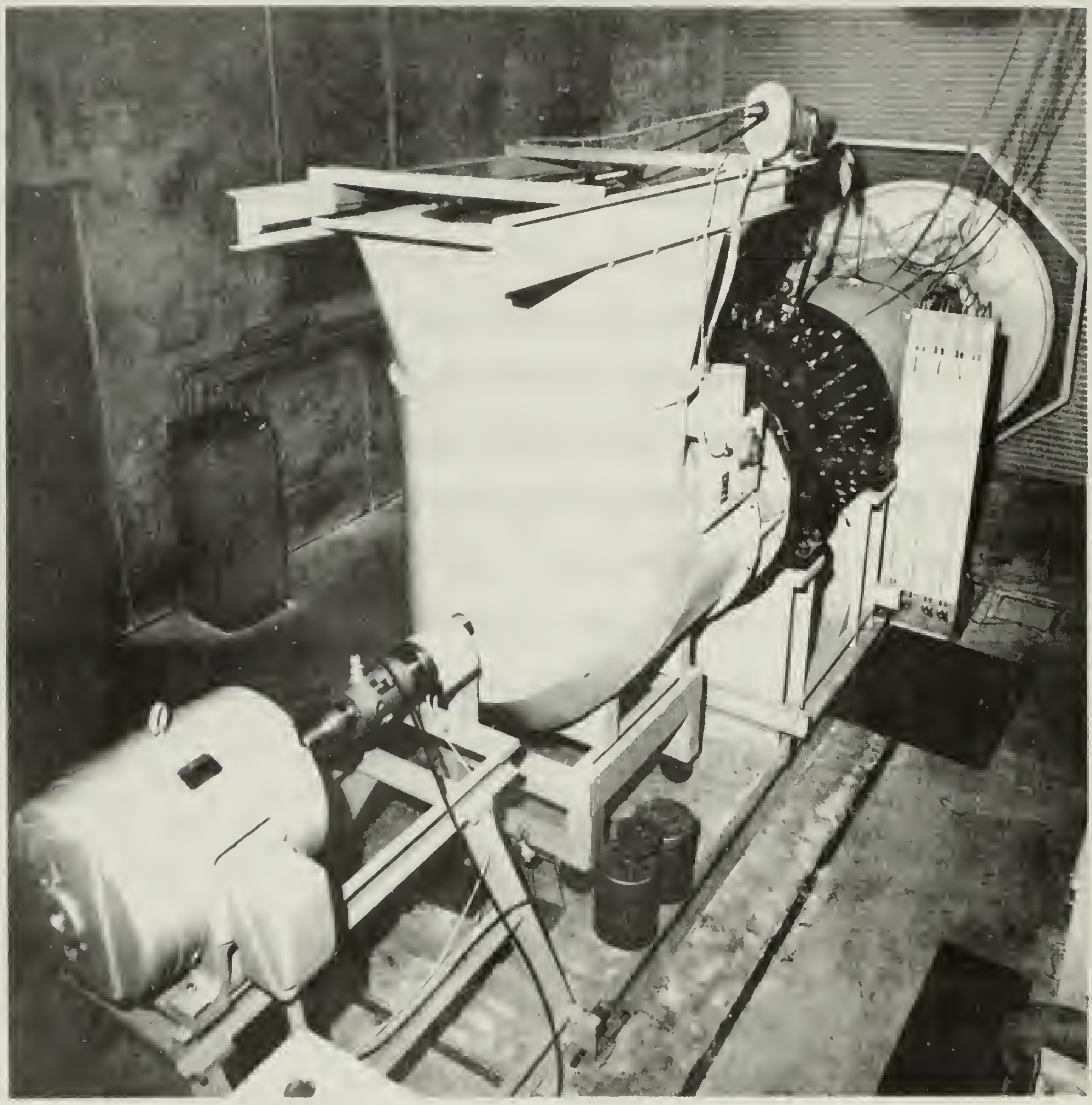

FIGURE I COMPRESSOR INSTALLATION

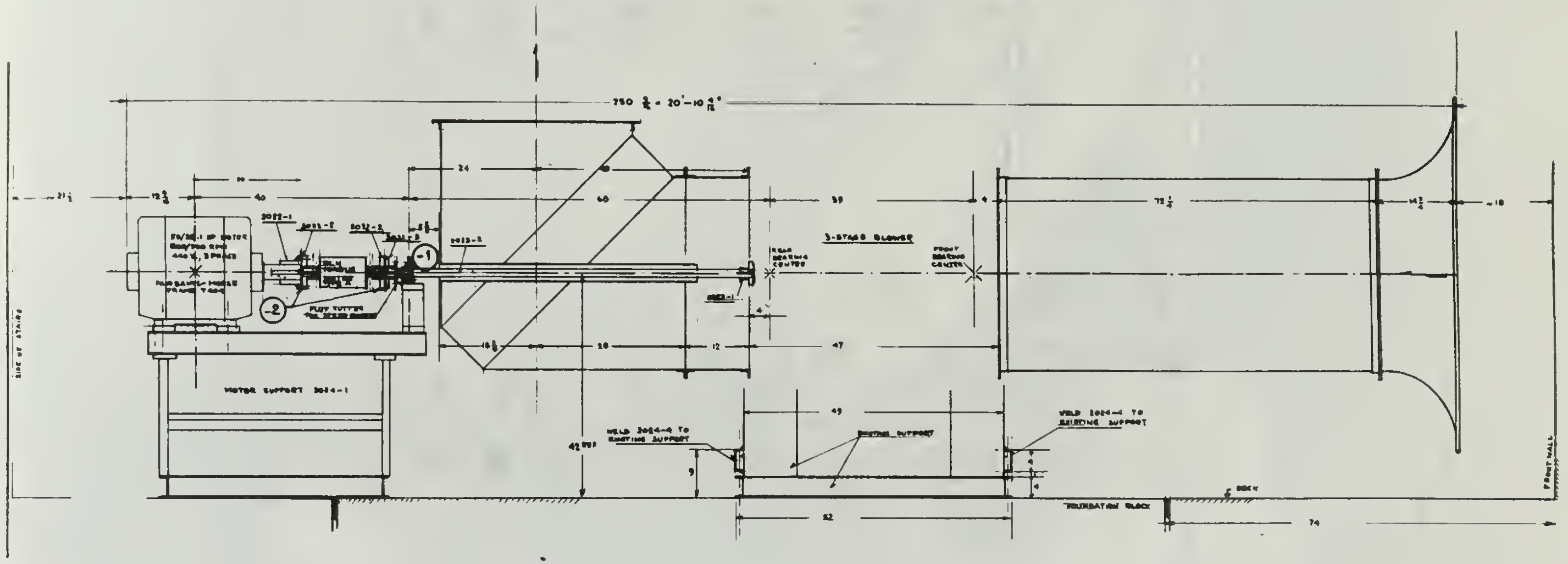

FIGURE 2 ACCESSORIES TO COMPRESSOR

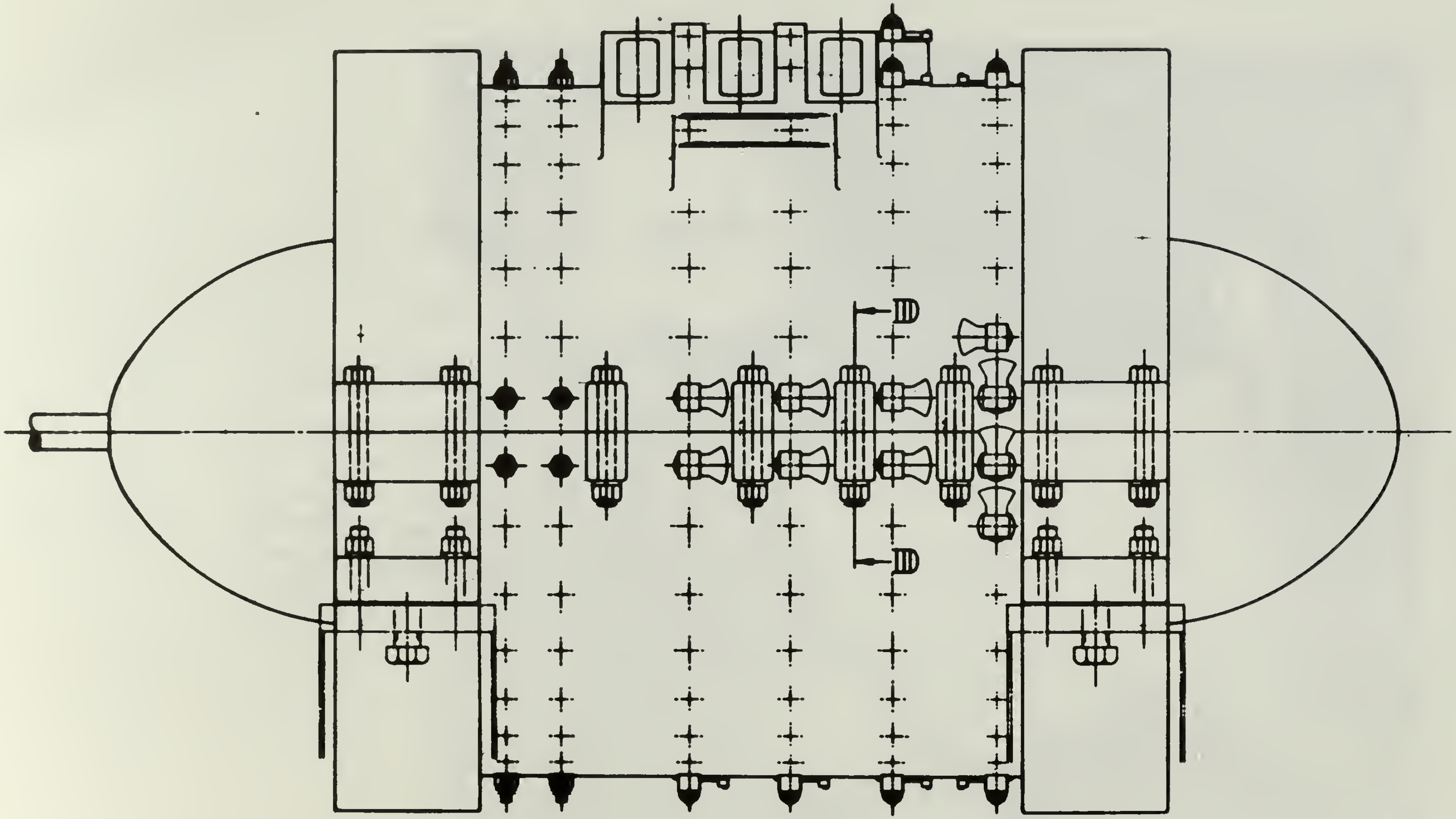

FIGURE 3 COMPRESSOR CASING

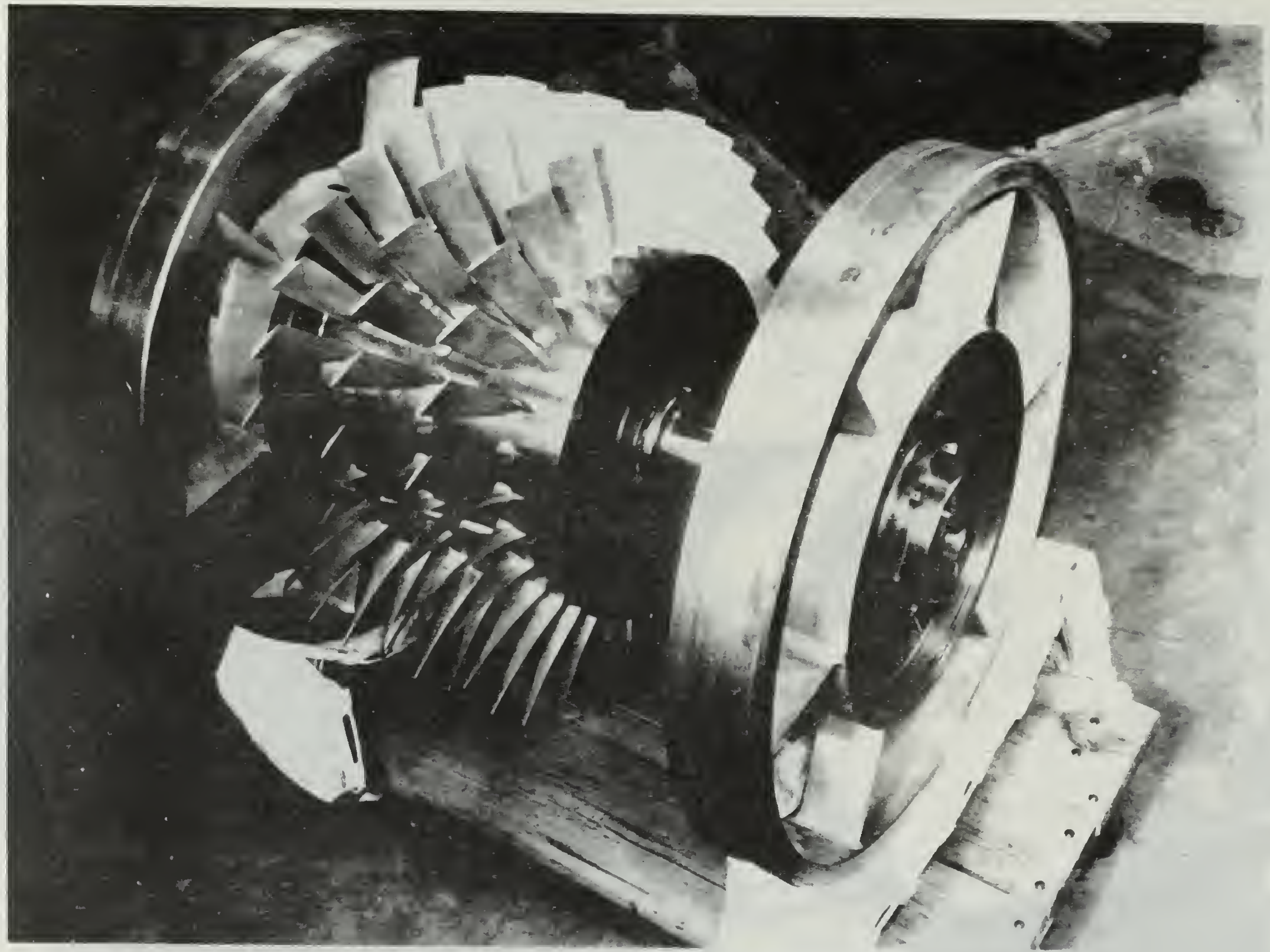

FIGURE 4 ROTOR BLADES, DRUM AND SHAFT MOUNTED IN SUPPORTING STRUT ASSMBLIES

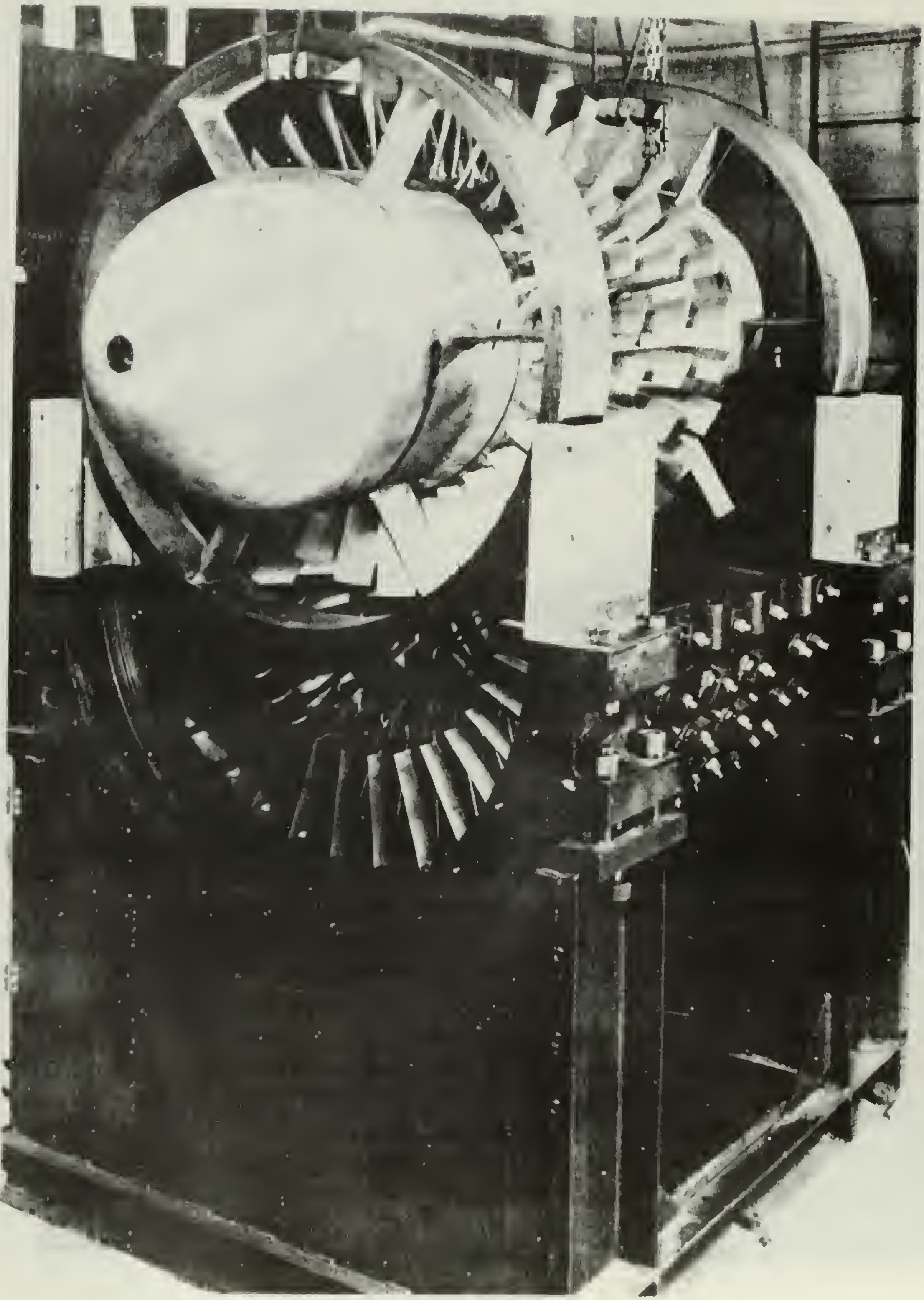

FIGURE 5 ASSEMBLY OF ROTOR IN LOWER CASING

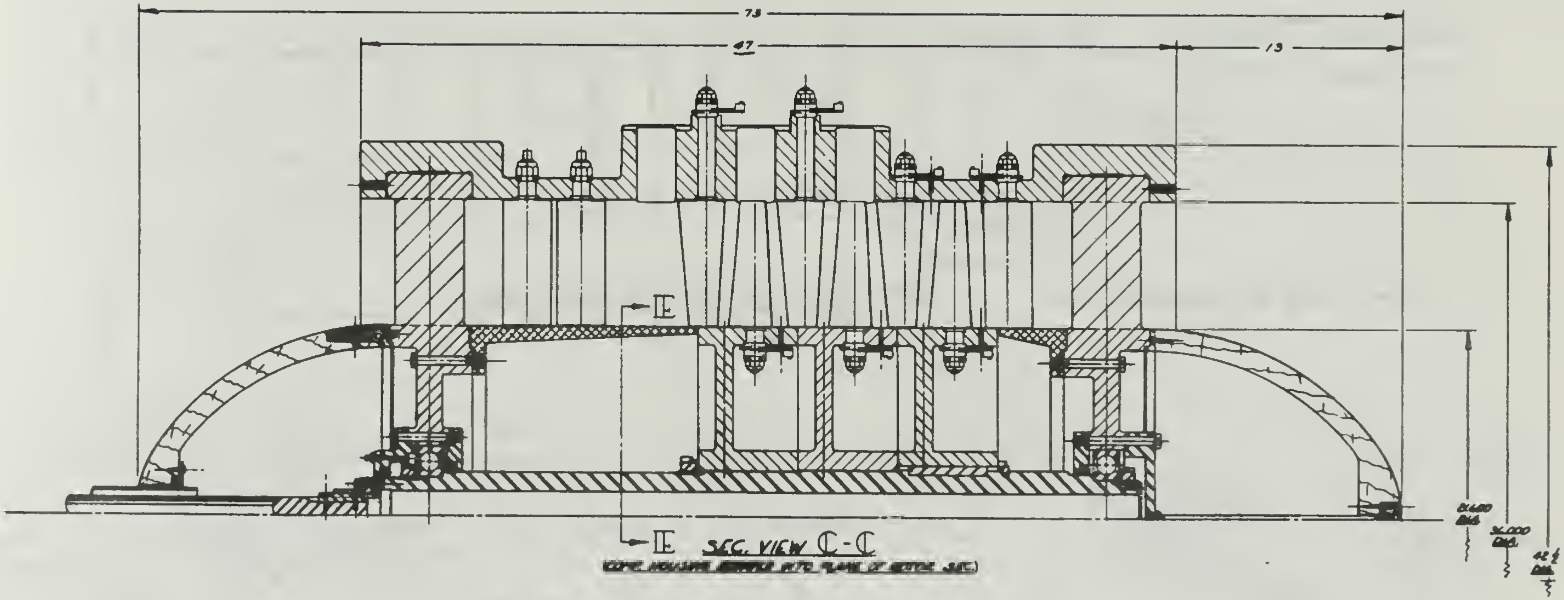

FIGURE 6 COMPRESSOR SECTIONAL VIEW

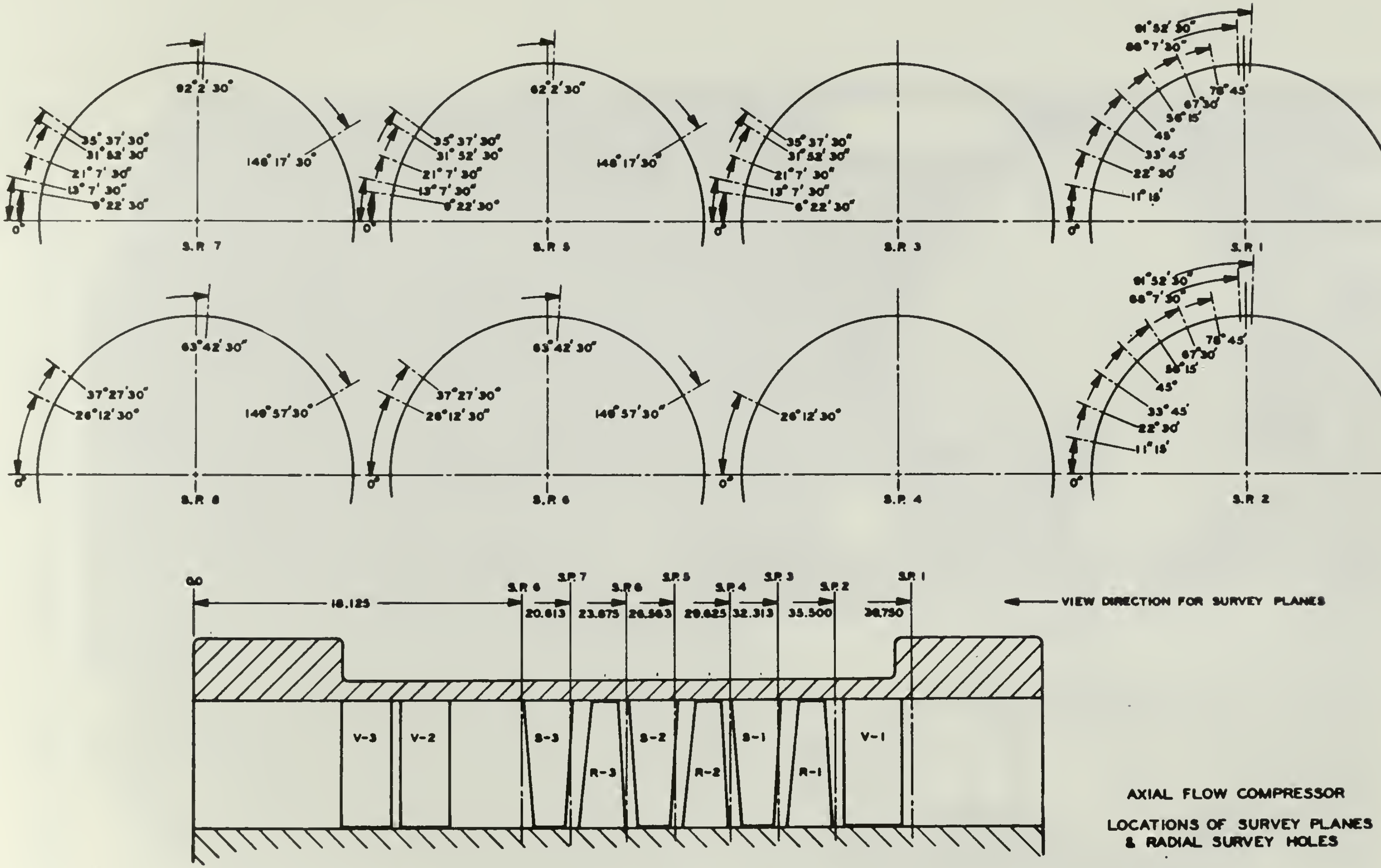

FIGURE 7 LOCATION OF RADIAL SURVEY HOLES

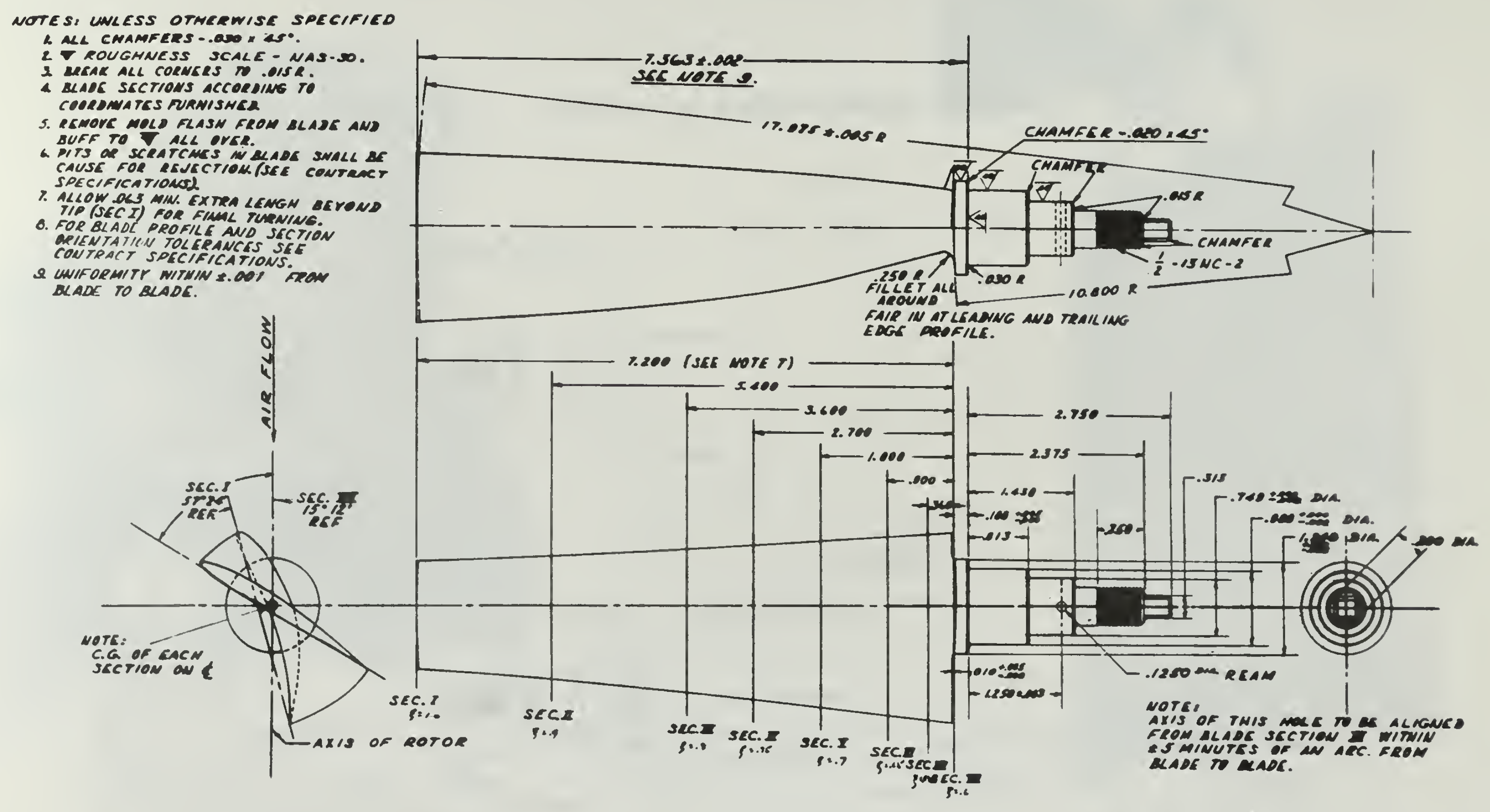

NOTES: UNLESS OTHERWISE SPECIFIED

1. ALL CHAMFERS -.030 x 45°.
2. ▼ ROUGHNESS SCALE - NAS-30.
3. BREAK ALL CORNERS TO .015 R.
4. BLADE SECTIONS ACCORDING TO COORDINATES FURNISHED.
5. REMOVE MOLD FLASH FROM BLADE AND BUFF TO ▼ ALL OVER.
6. PITS OR SCRATCHES IN BLADE SHALL BE CAUSE FOR REJECTION. (SEE CONTRACT SPECIFICATIONS).
7. ALLOW .063 MIN. EXTRA LENGH BEYOND TIP (SEC I) FOR FINAL TURNING.
8. FOR BLADE PROFILE AND SECTION ORIENTATION TOLERANCES SEE CONTRACT SPECIFICATIONS.
9. UNIFORMITY WITHIN ±.001 FROM BLADE TO BLADE.

NOTE:
C.G. OF EACH SECTION ON ℄

NOTE:
AXIS OF THIS HOLE TO BE ALIGNED FROM BLADE SECTION VII WITHIN ±5 MINUTES OF AN ARC. FROM BLADE TO BLADE.

FIGURE 8 DETAIL OF FREE - VORTEX ROTOR

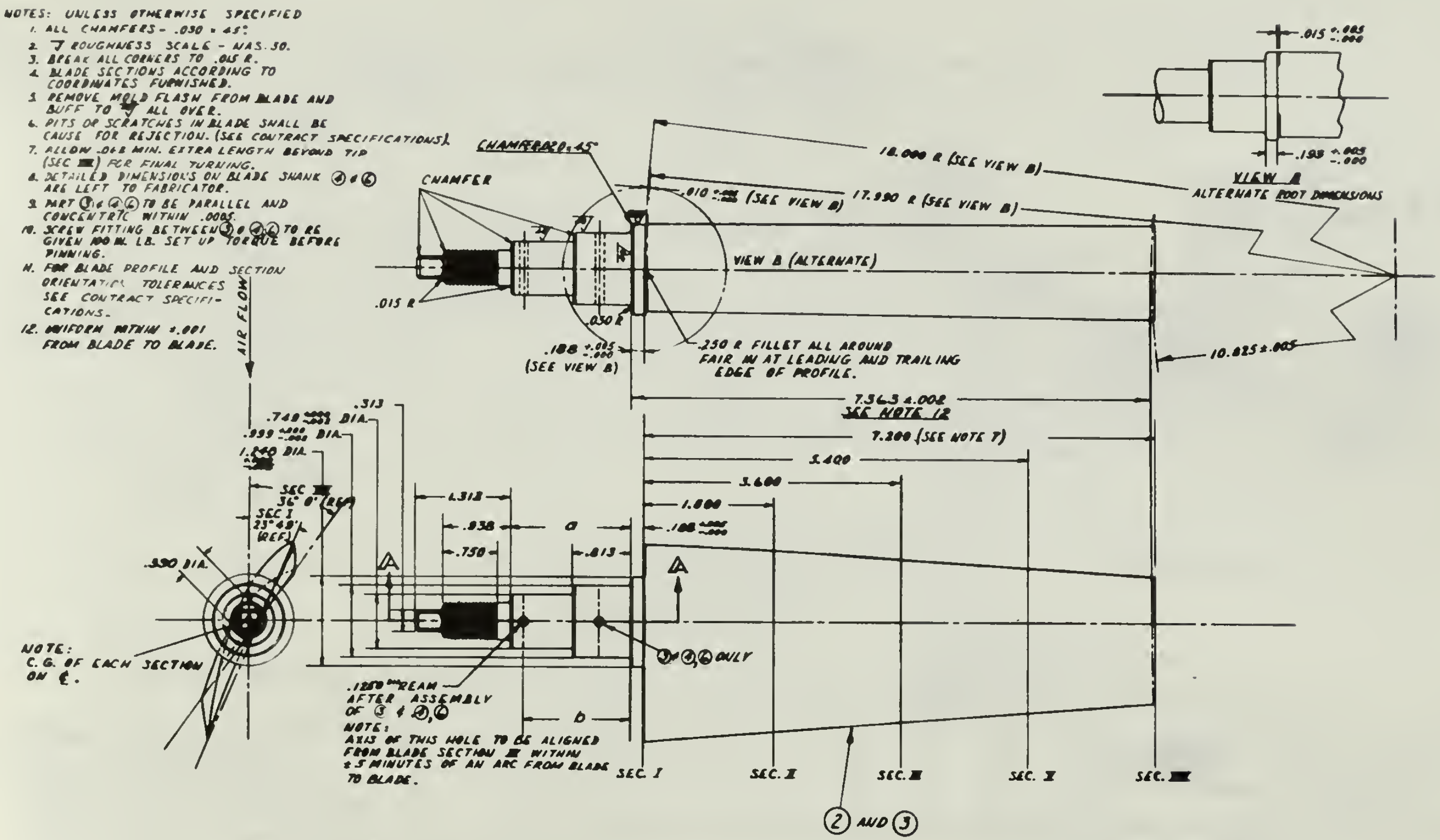
NOTES: UNLESS OTHERWISE SPECIFIED
1. ALL CHAMFERS - .030 × 45°.
2. ∇ ROUGHNESS SCALE - NAS. 30.
3. BREAK ALL CORNERS TO .015 R.
4. BLADE SECTIONS ACCORDING TO COORDINATES FURNISHED.
5. REMOVE MOLD FLASH FROM BLADE AND BUFF TO ∇ ALL OVER.
6. PITS OR SCRATCHES IN BLADE SHALL BE CAUSE FOR REJECTION. (SEE CONTRACT SPECIFICATIONS).
7. ALLOW .062 MIN. EXTRA LENGTH BEYOND TIP (SEC VI) FOR FINAL TURNING.
8. DETAILED DIMENSIONS ON BLADE SHANK ④ & ⑥ ARE LEFT TO FABRICATOR.
9. PART ③ & ④ ⑥ TO BE PARALLEL AND CONCENTRIC WITHIN .0005.
10. SCREW FITTING BETWEEN ③ & ④ ⑥ TO BE GIVEN 100 IN. LB. SET UP TORQUE BEFORE PINNING.
11. FOR BLADE PROFILE AND SECTION ORIENTATION TOLERANCES SEE CONTRACT SPECIFICATIONS.
12. UNIFORM WITHIN ±.001 FROM BLADE TO BLADE.
AIR FLOW
CHAMFER
.015 R
CHAMFER .020 × 45°
.010 (SEE VIEW B)
18.000 R (SEE VIEW B)
17.990 R (SEE VIEW B)
VIEW B (ALTERNATE)
.030 R
.188 +.005 -.000 (SEE VIEW B)
.250 R FILLET ALL AROUND FAIR IN AT LEADING AND TRAILING EDGE OF PROFILE.
.015 +.005 -.000
.193 +.005 -.000
VIEW B
ALTERNATE ROOT DIMENSIONS
10.025 ± .005
7.363 ± .002 SEE NOTE 12
7.200 (SEE NOTE 7)
5.400
3.600
1.800
.188 +.000 -.000
.313
.748 DIA.
.999 +.000 -.000 DIA.
1.240 DIA.
SEC VI 36° 0' (REF)
SEC I 23° 48' (REF)
.330 DIA.
1.312
.938
.750
a
.813
A
A
③ ④ ⑥ ONLY
.1250 REAM AFTER ASSEMBLY OF ③ & ④ ⑥
NOTE: AXIS OF THIS HOLE TO BE ALIGNED FROM BLADE SECTION III WITHIN ±5 MINUTES OF AN ARC FROM BLADE TO BLADE.
b
NOTE: C.G. OF EACH SECTION ON ℄.
SEC. I
SEC. II
SEC. III
SEC. V
SEC. VI
② AND ③

FIGURE 9 DETAIL OF FREE-VORTEX STATOR

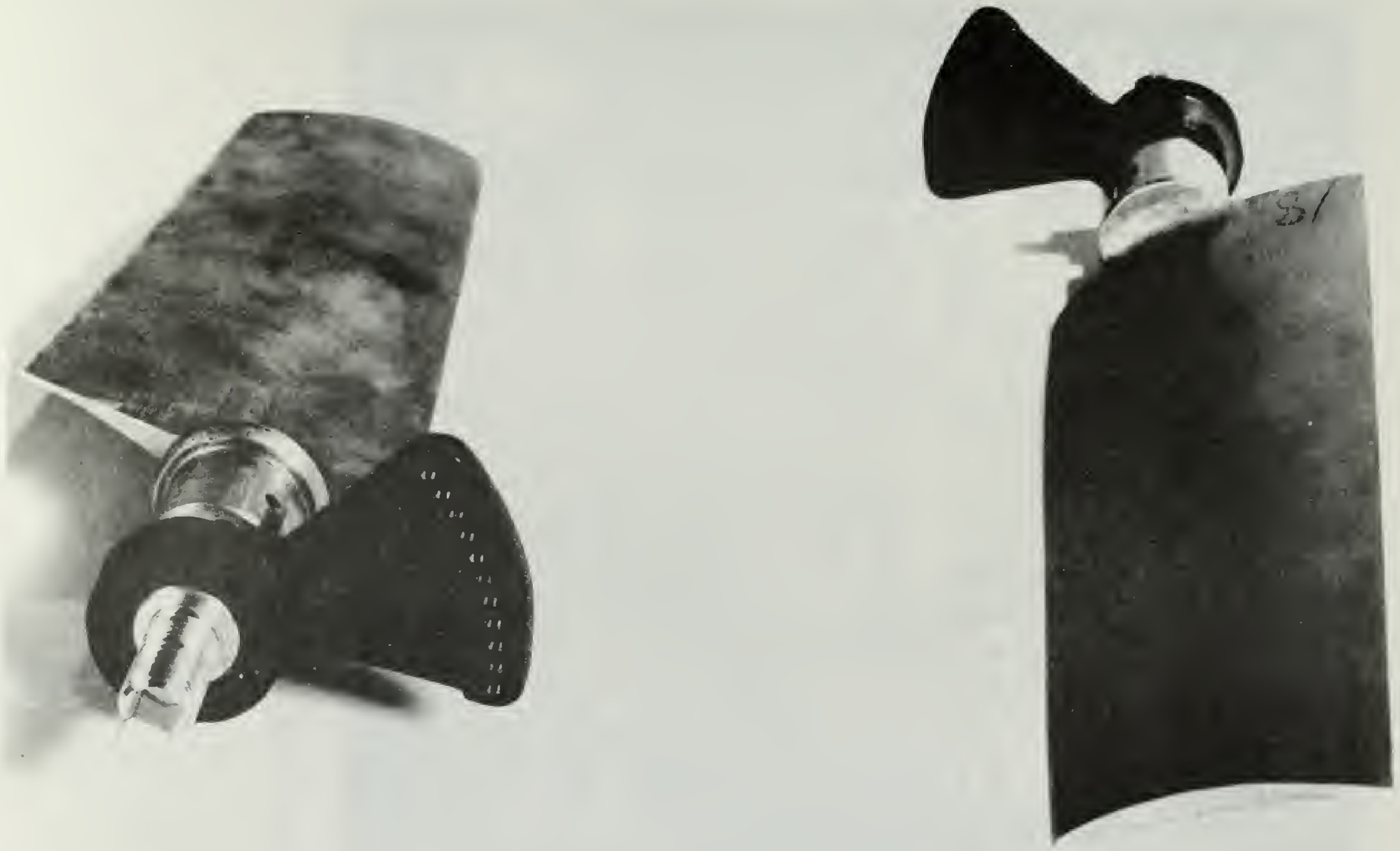

FIGURE 10 FREE-VORTEX STATOR BLADE

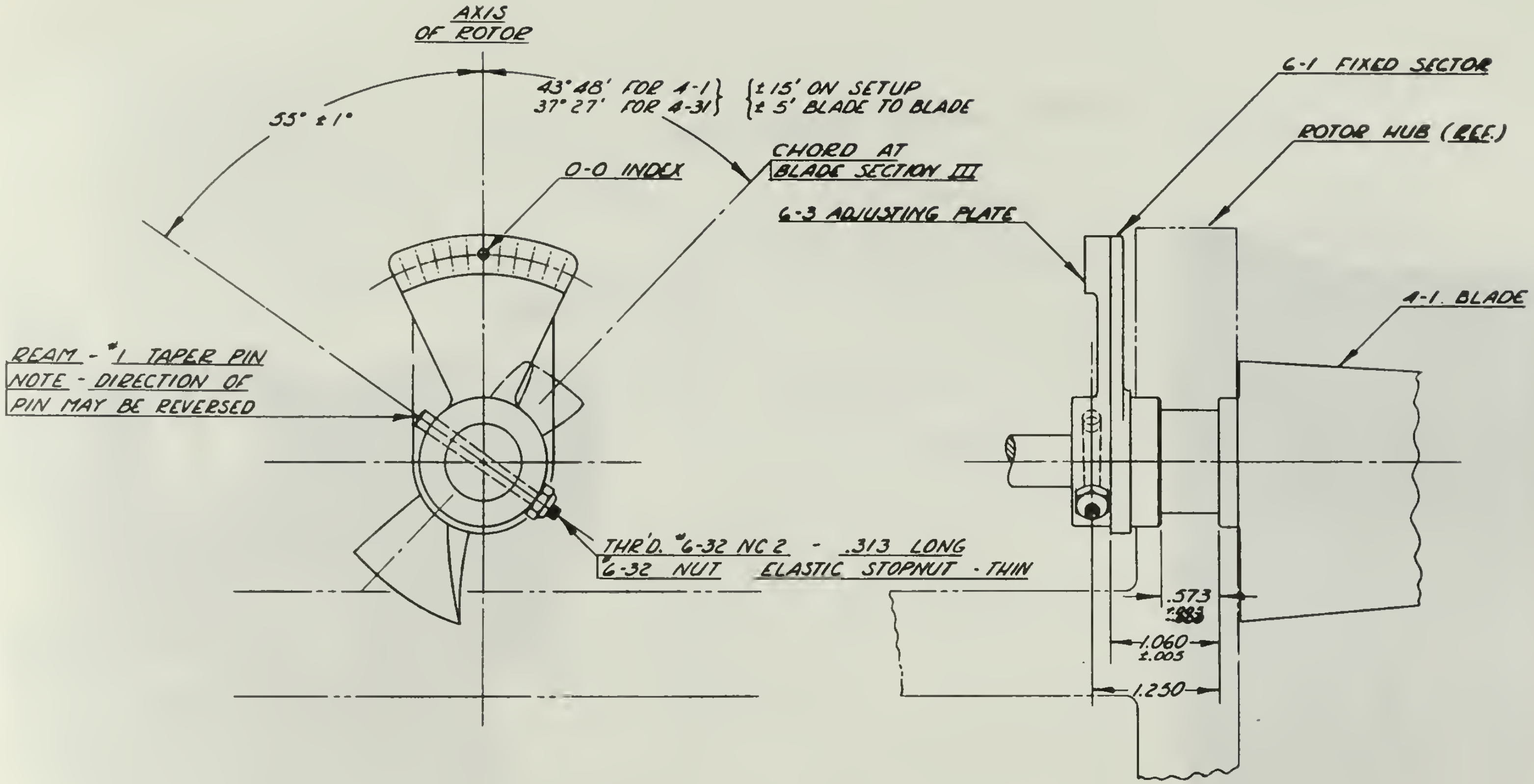

FIGURE 11 ROTOR STAGGER ANGLE ADJUSTMENT

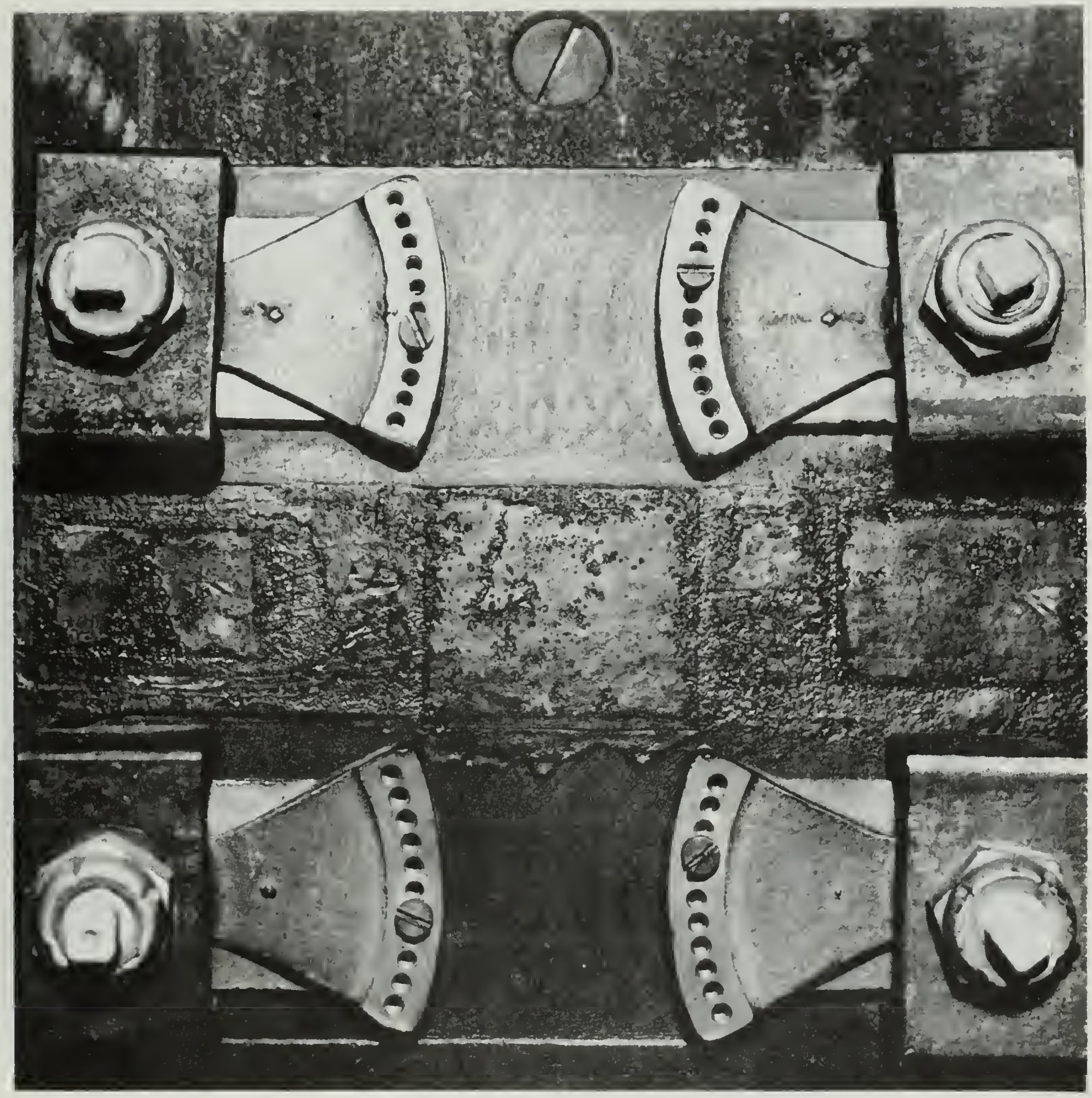

FIGURE 12 EXTERNAL STAGGER ANGLE ADJUSTMENT

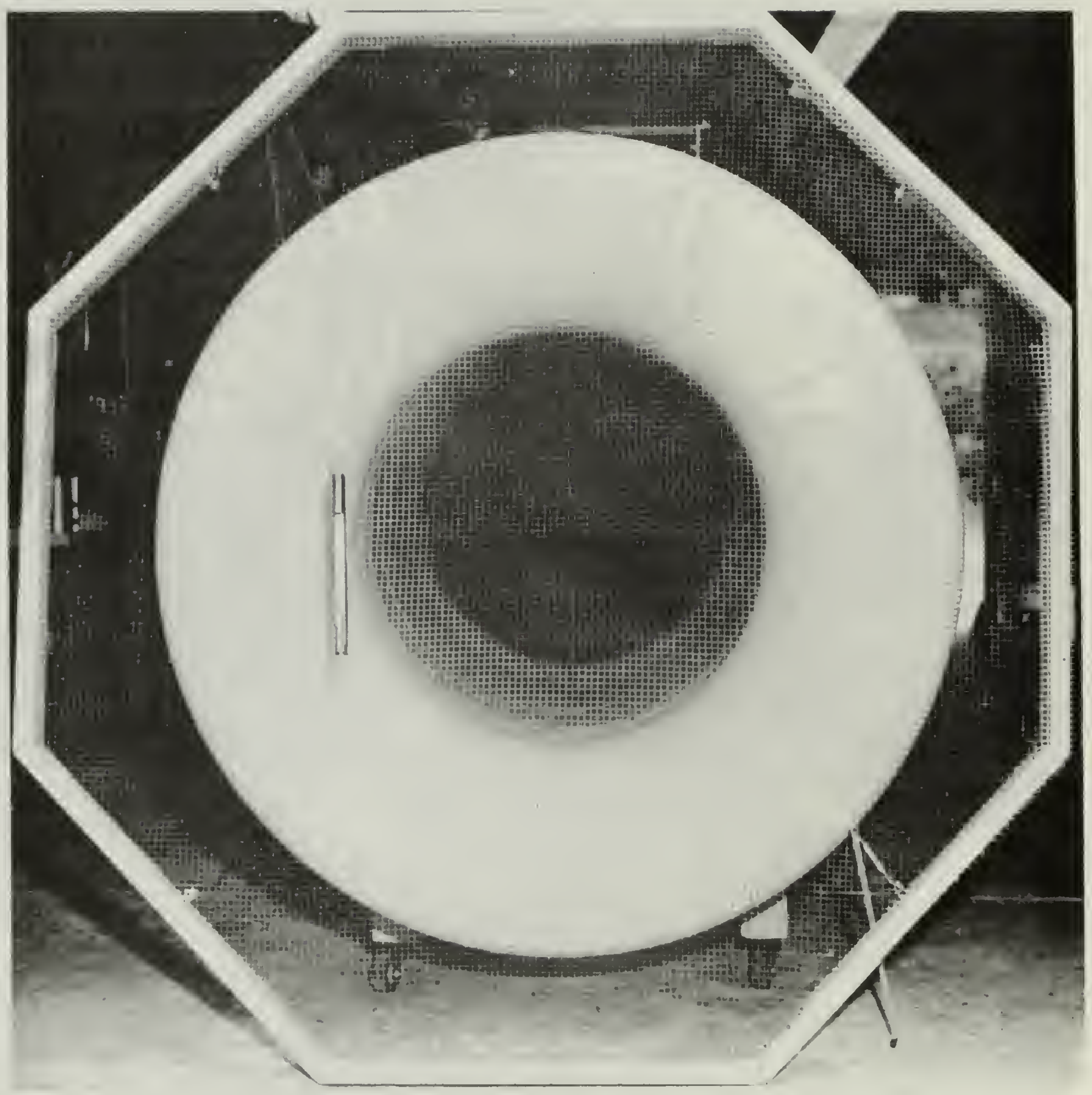

FIGURE 13 INLET BELLMOUTH

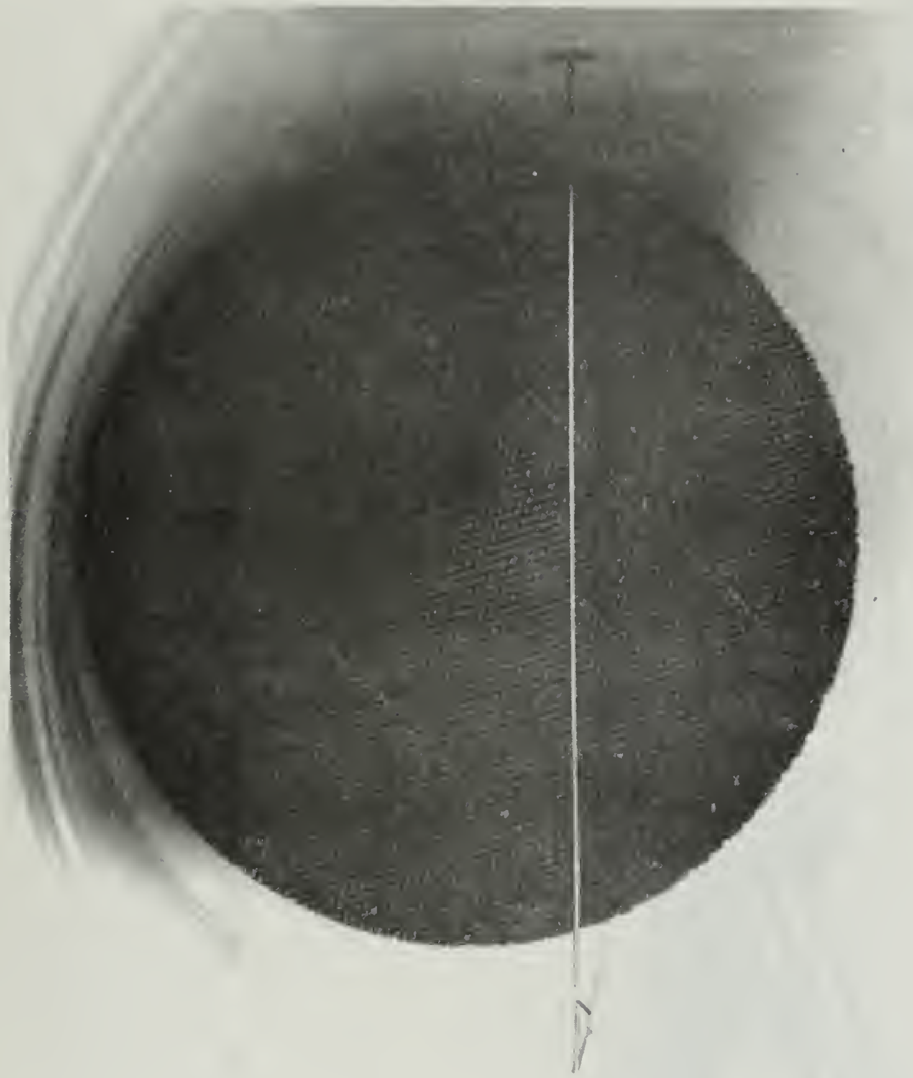

FIGURE 14 INLET PITOT-STATIC TRAVERSE

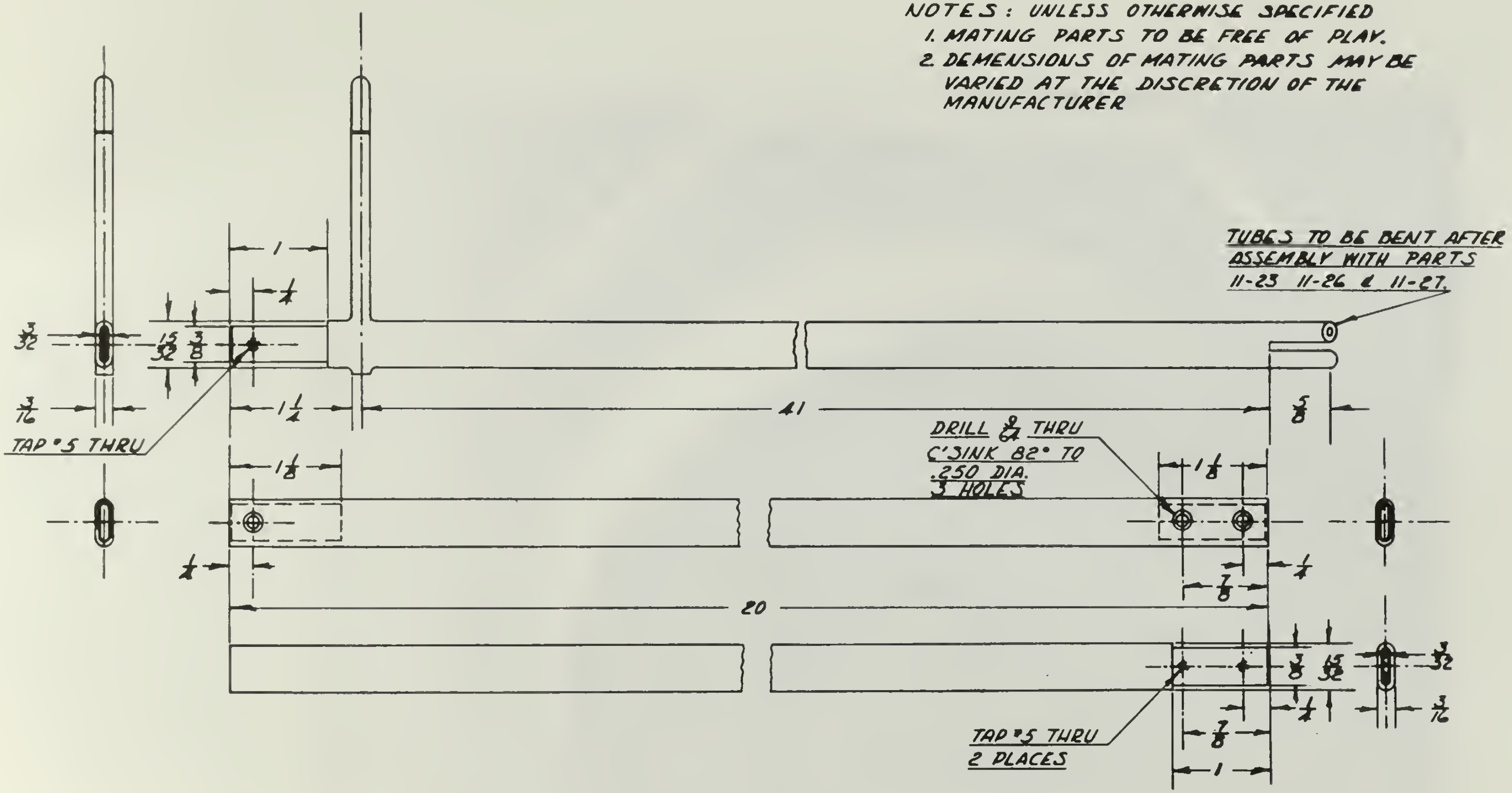
NOTES: UNLESS OTHERWISE SPECIFIED
1. MATING PARTS TO BE FREE OF PLAY.
2. DEMENSIONS OF MATING PARTS MAY BE VARIED AT THE DISCRETION OF THE MANUFACTURER
TUBES TO BE BENT AFTER ASSEMBLY WITH PARTS 11-23 11-26 & 11-27.
DRILL 9/64 THRU C'SINK 82° TO .250 DIA. 3 HOLES
TAP #5 THRU
TAP #5 THRU 2 PLACES
3/32
3/16
15/32
3/8
1
1/4
1 1/4
41
5/8
1 1/8
20
7/8

FIGURE 15 DETAIL OF INLET PITOT–STATIC TRAVERSE

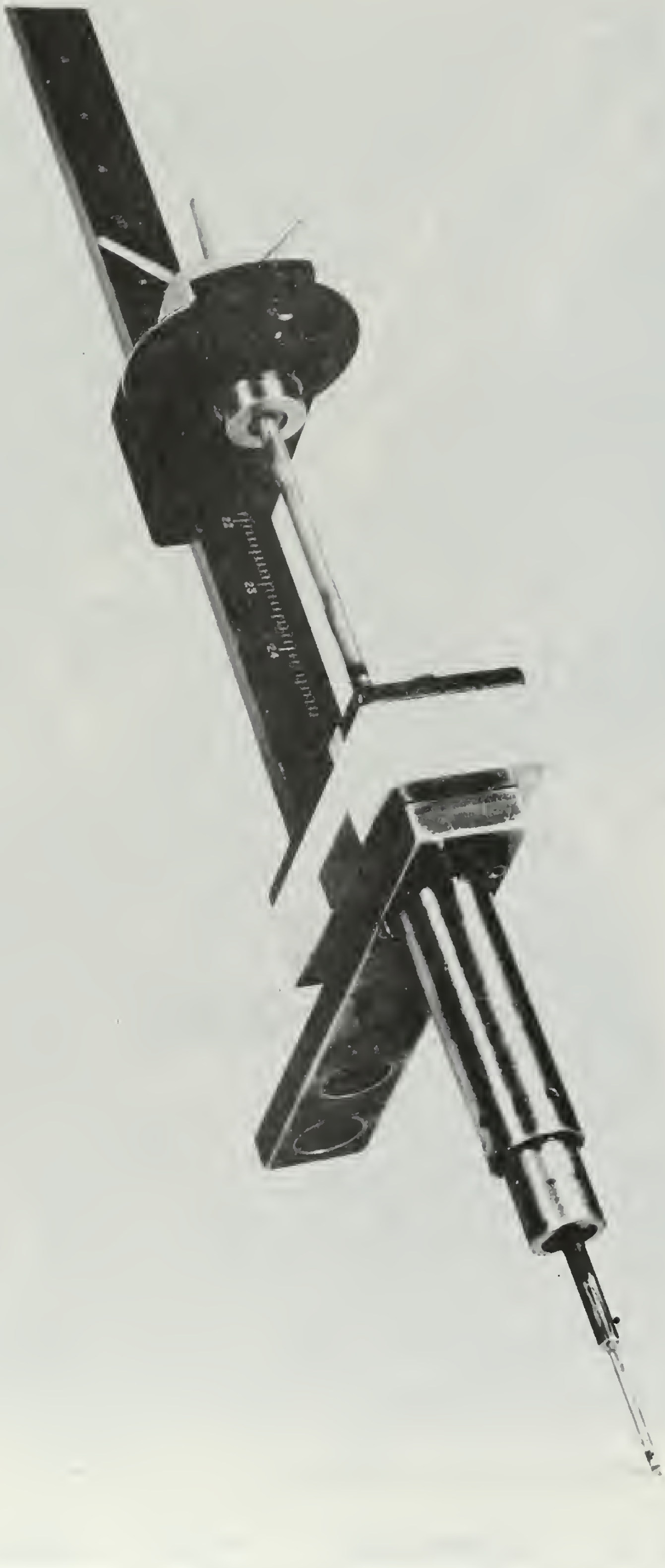

FIGURE 16   THREE-HOLE PROBE DETAIL

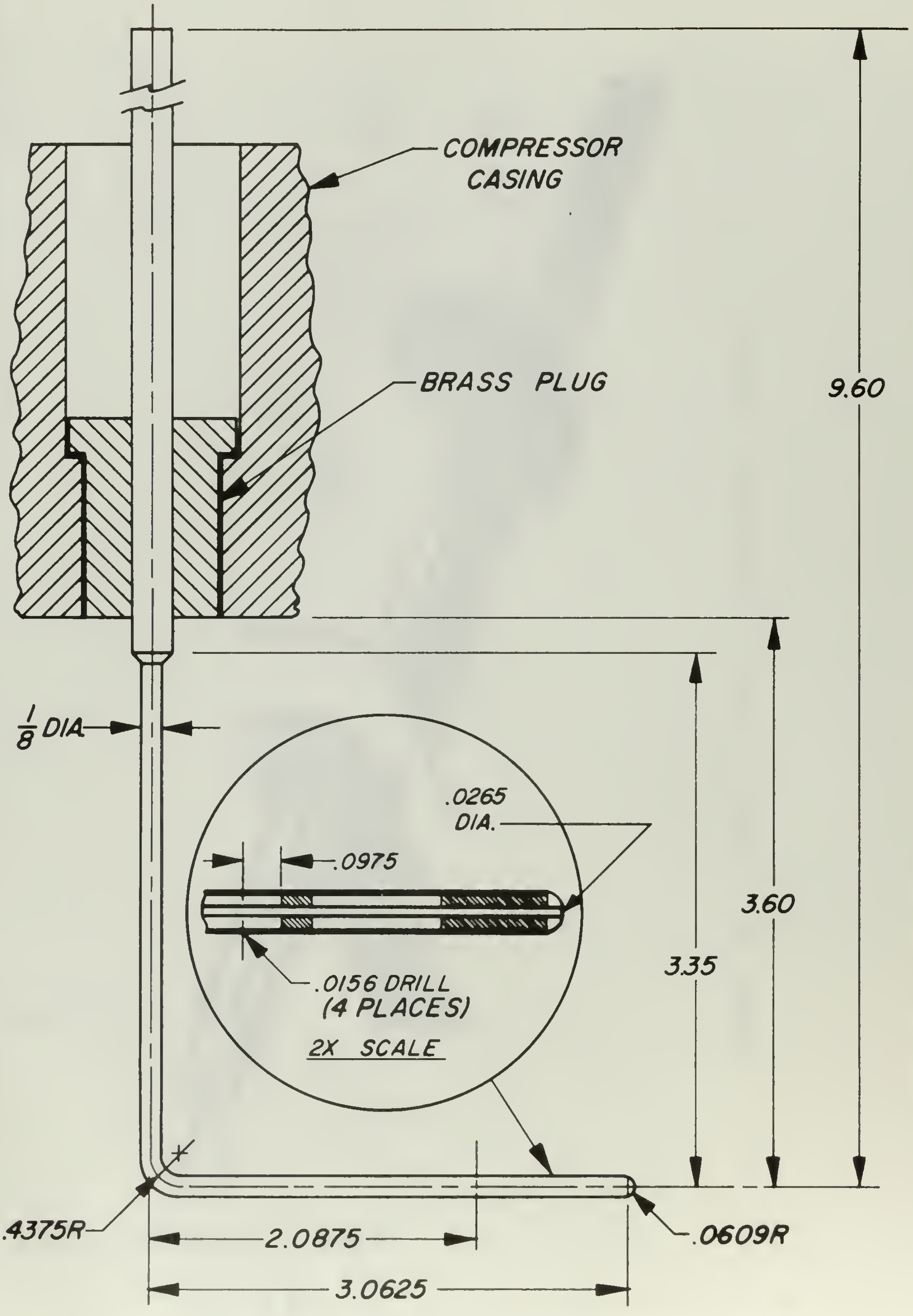

FIG. 17 PERMANENT PITOT—STATIC TUBE

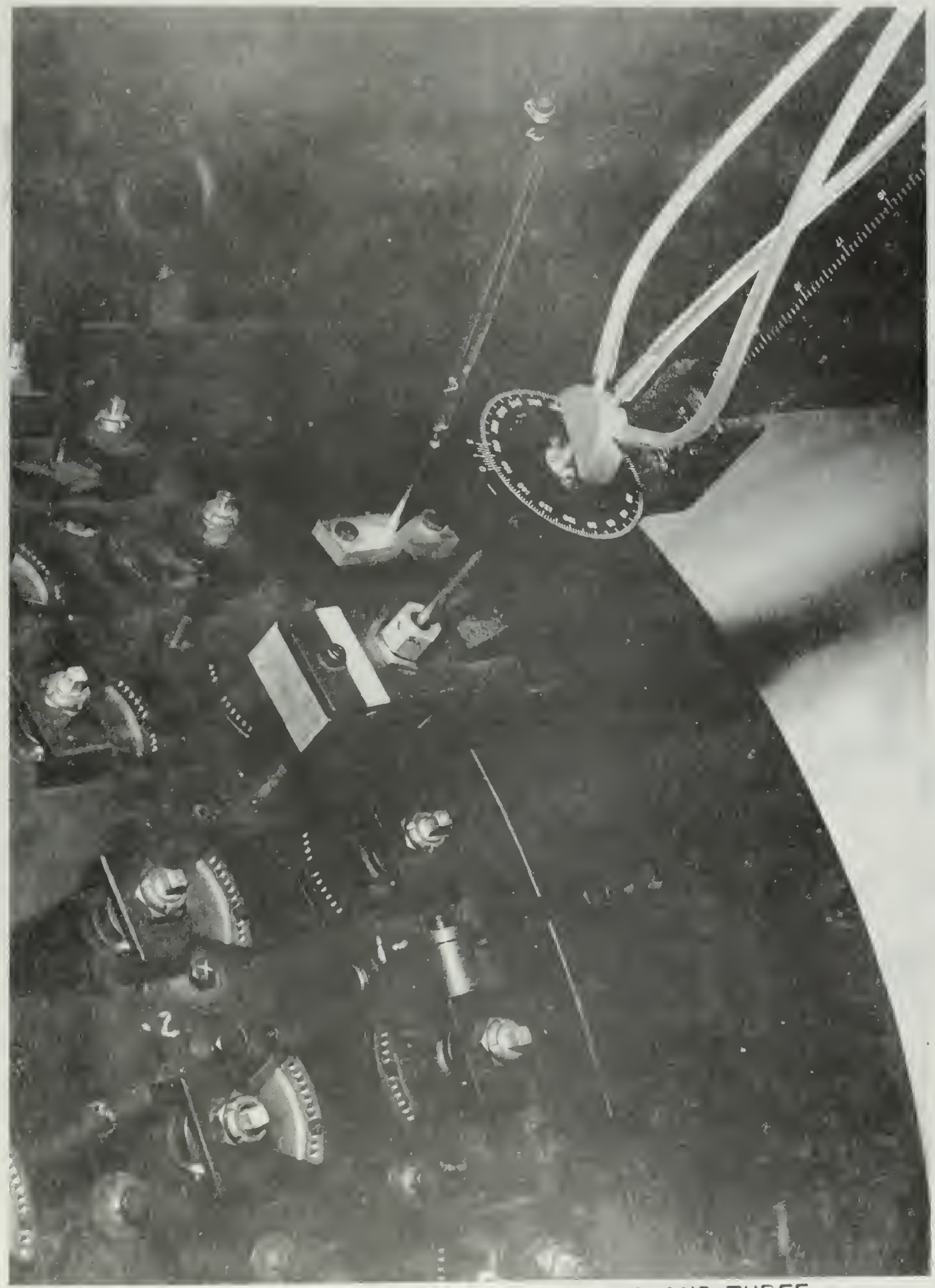

FIGURE 18 PERMANENT PITOT – TUBE AND THREE – HOLE PROBE AHEAD OF FIRST ROTOR

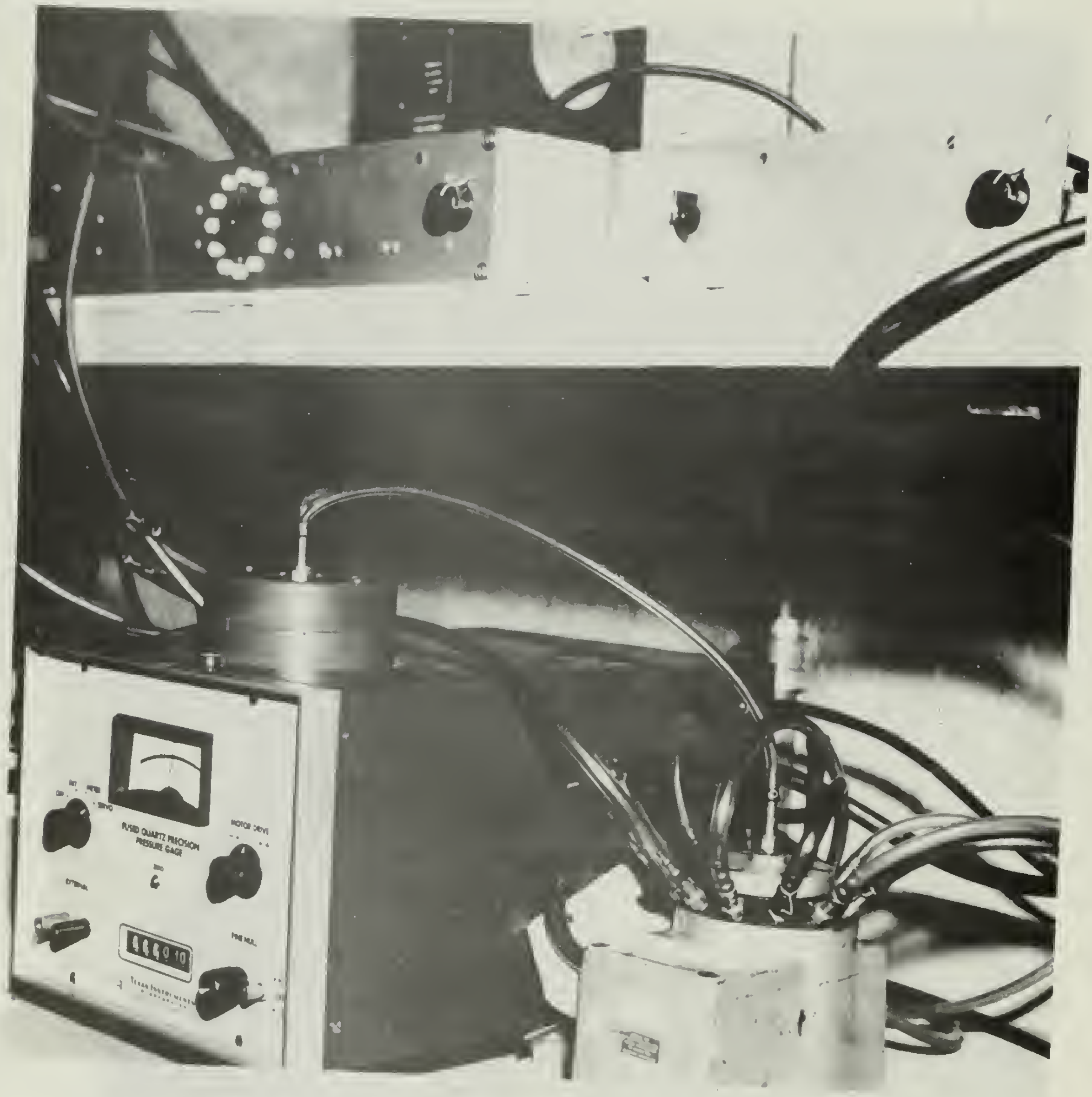

FIGURE 19 PRESSURE READOUT INSTRUMENTATION

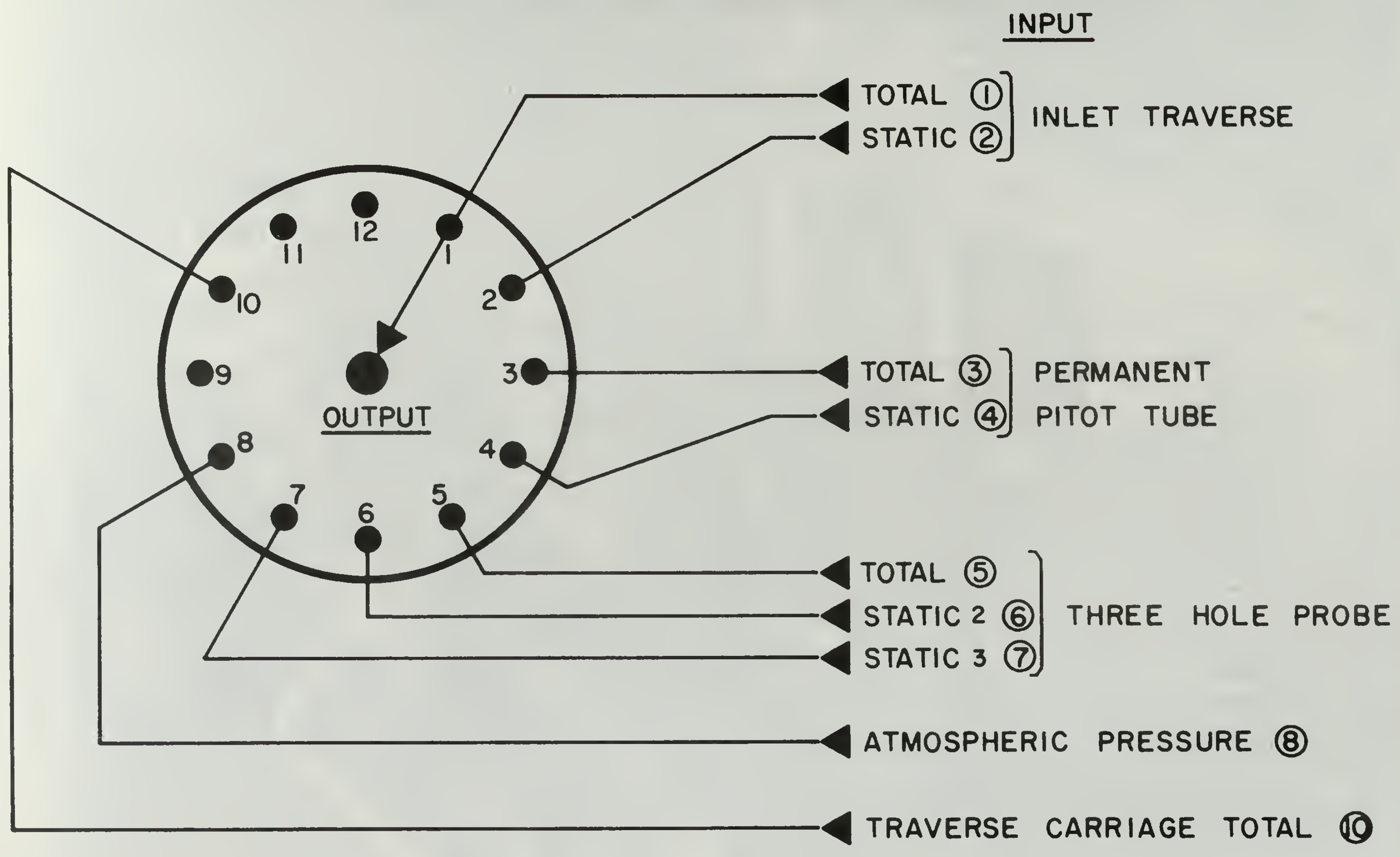

FIG. 20 PRESSURE SELECTION BY SCANNER VALVE

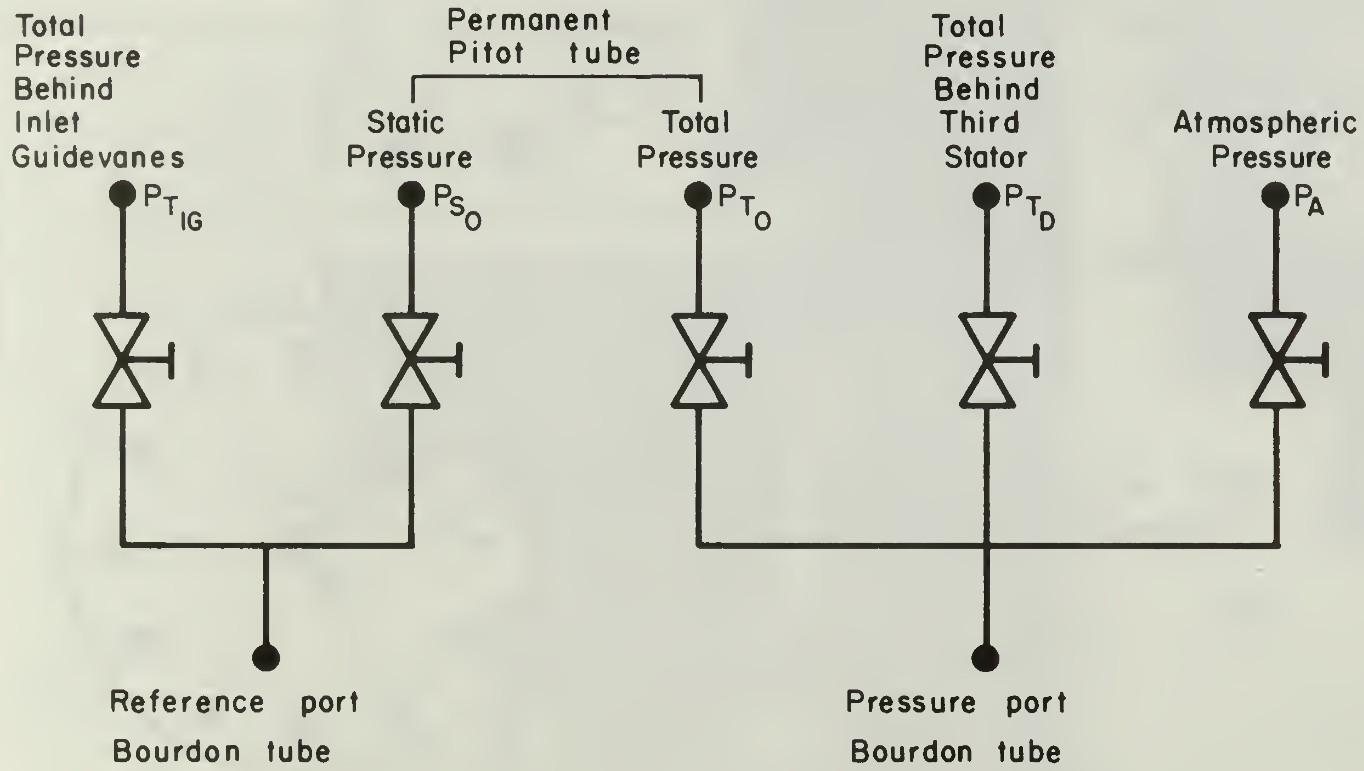
Total Pressure Behind Inlet Guidevanes
$P_{T_{IG}}$
Permanent Pitot tube
Static Pressure
P_{S_O}
Total Pressure
P_{T_O}
Total Pressure Behind Third Stator
P_{T_D}
Atmospheric Pressure
P_A
Reference port Bourdon tube
Pressure port Bourdon tube

FIG. 21 SIMPLIFIED PRESSURE SELECTION SYSTEM.

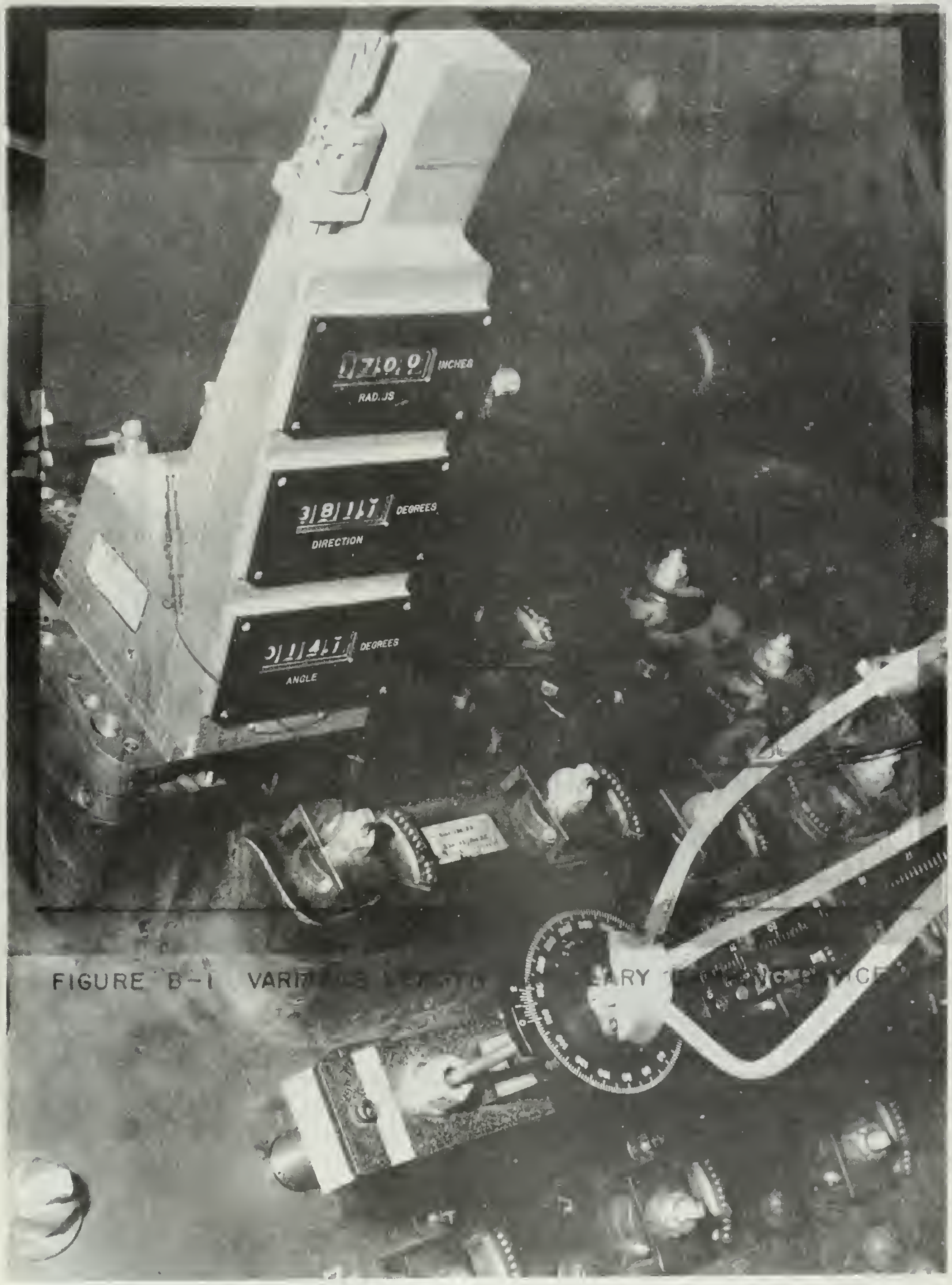

FIGURE 22 TRAVERSE CARRIAGE AND THREE-HOLE PROBE BEHIND THIRD STATOR

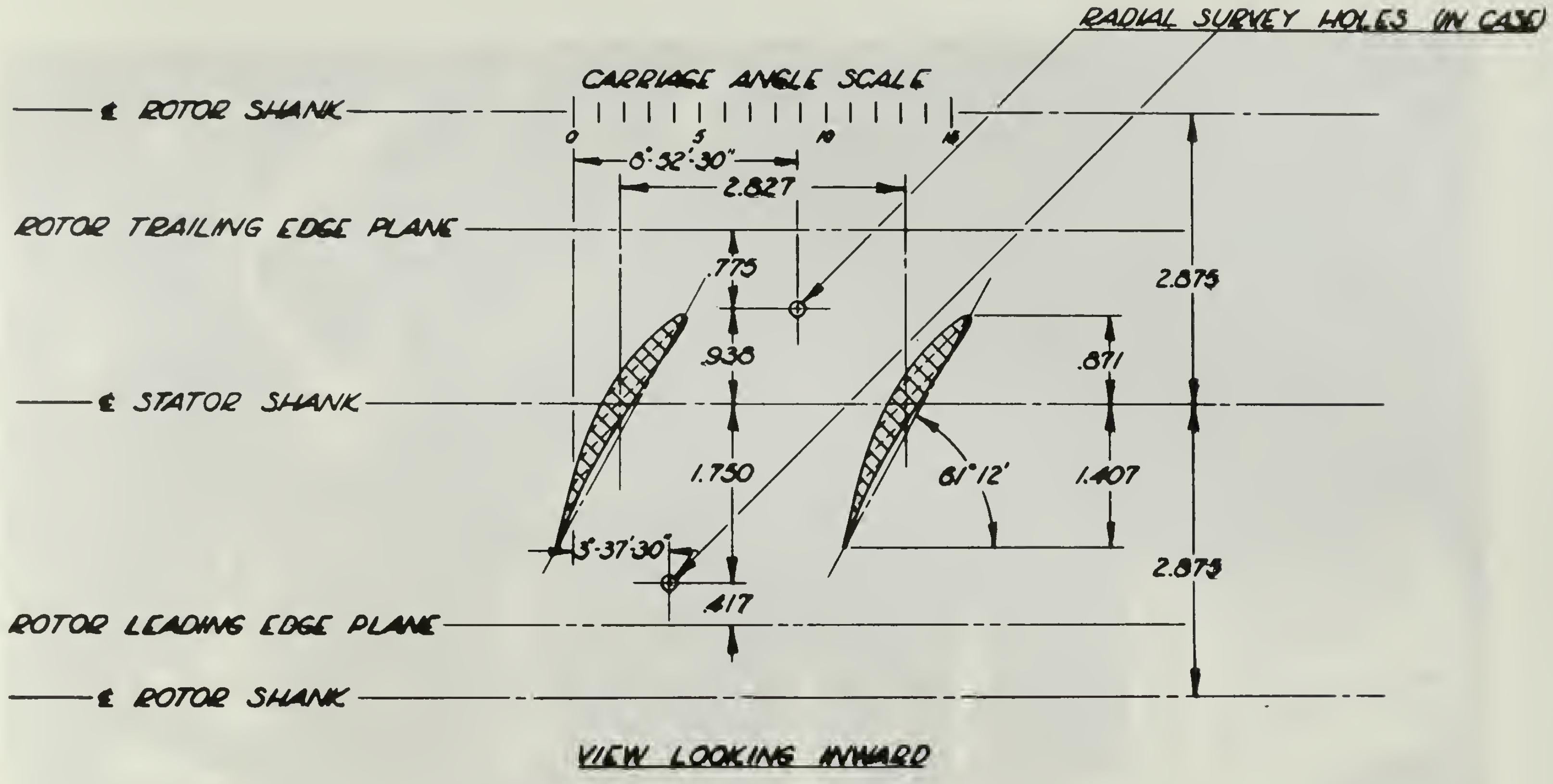

FIGURE 23 RELATION OF TRAVERSE CARRIAGE TO SURVEY HOLES

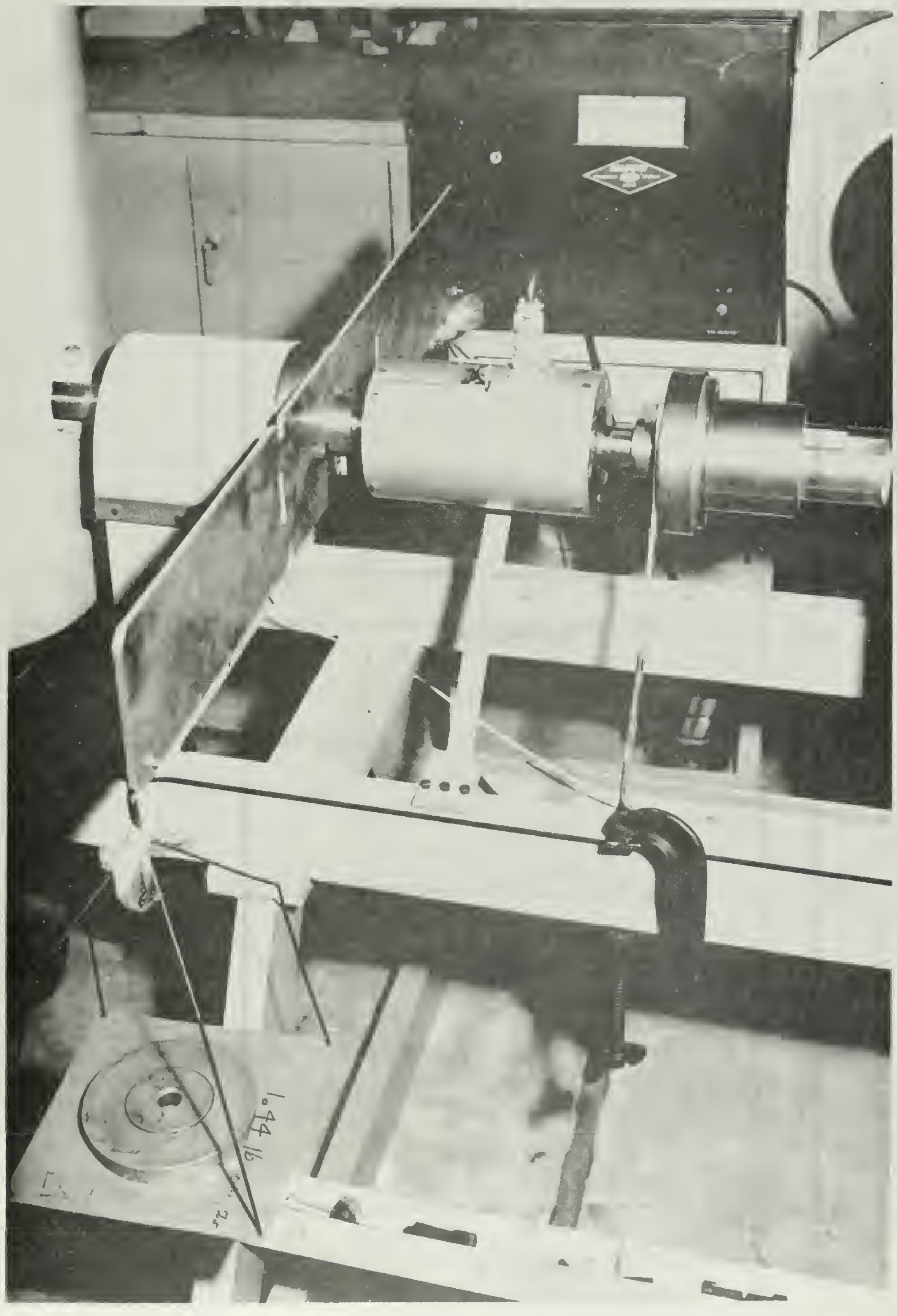

FIGURE 24 TORQUE METER DURING CALIBRATION

FIGURE 25 TRAVERSE OF INLET DUCT RUN D-1
VOLUME FLOW RATE 512 FT^3/SEC

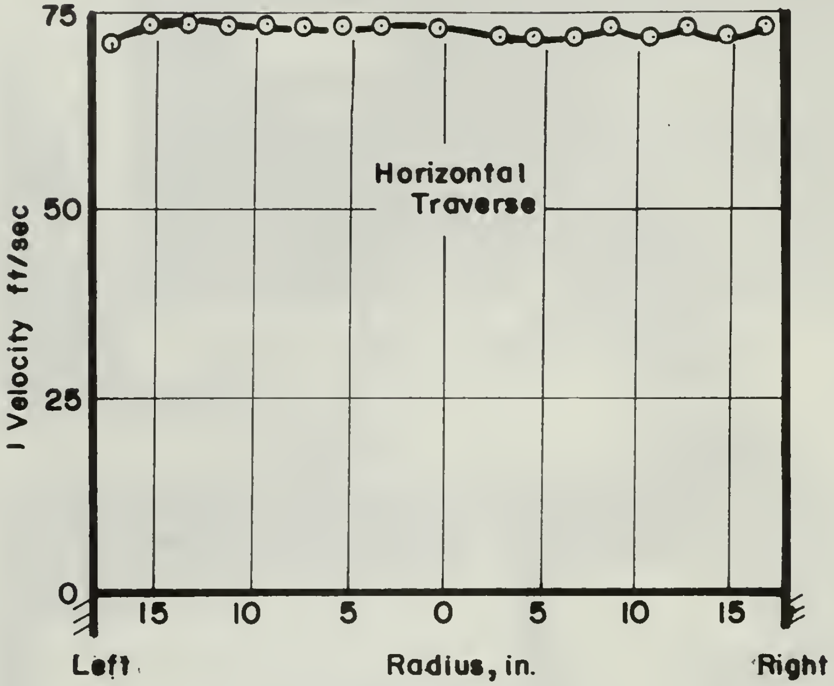

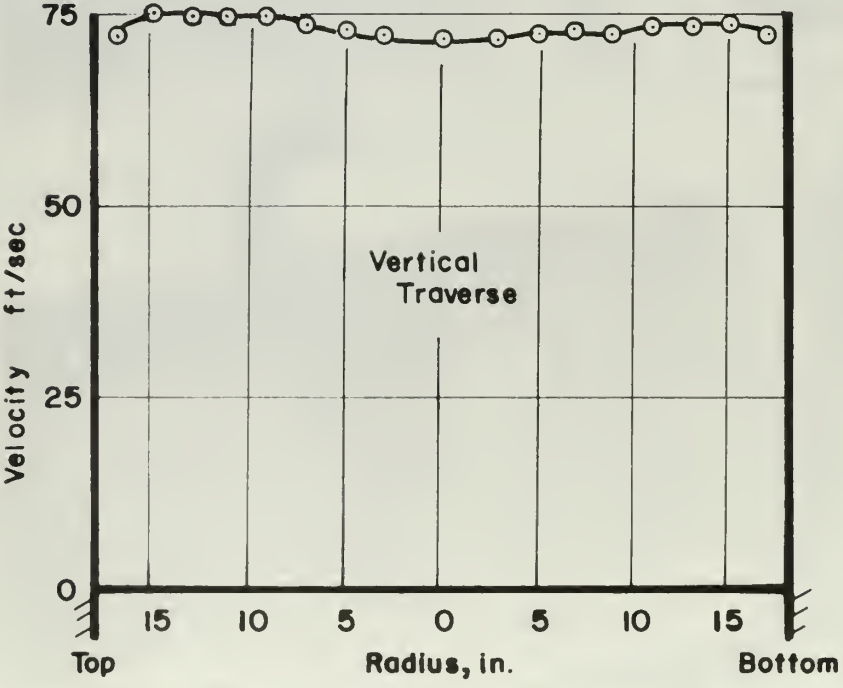

FIGURE 26 TRAVERSE OF INLET DUCT RUN D-7
VOLUME FLOW RATE 310 FT^3/SEC.

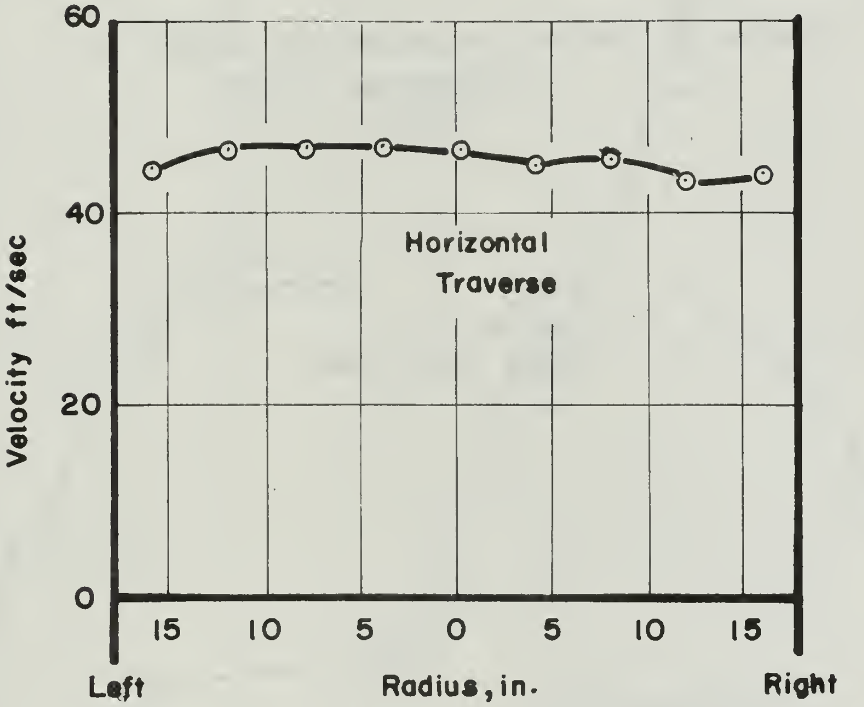

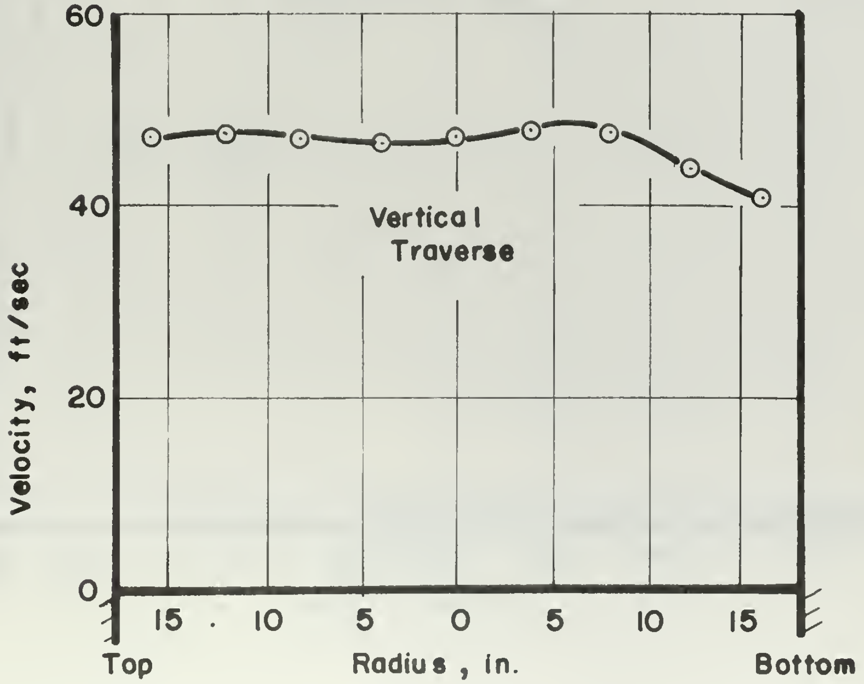

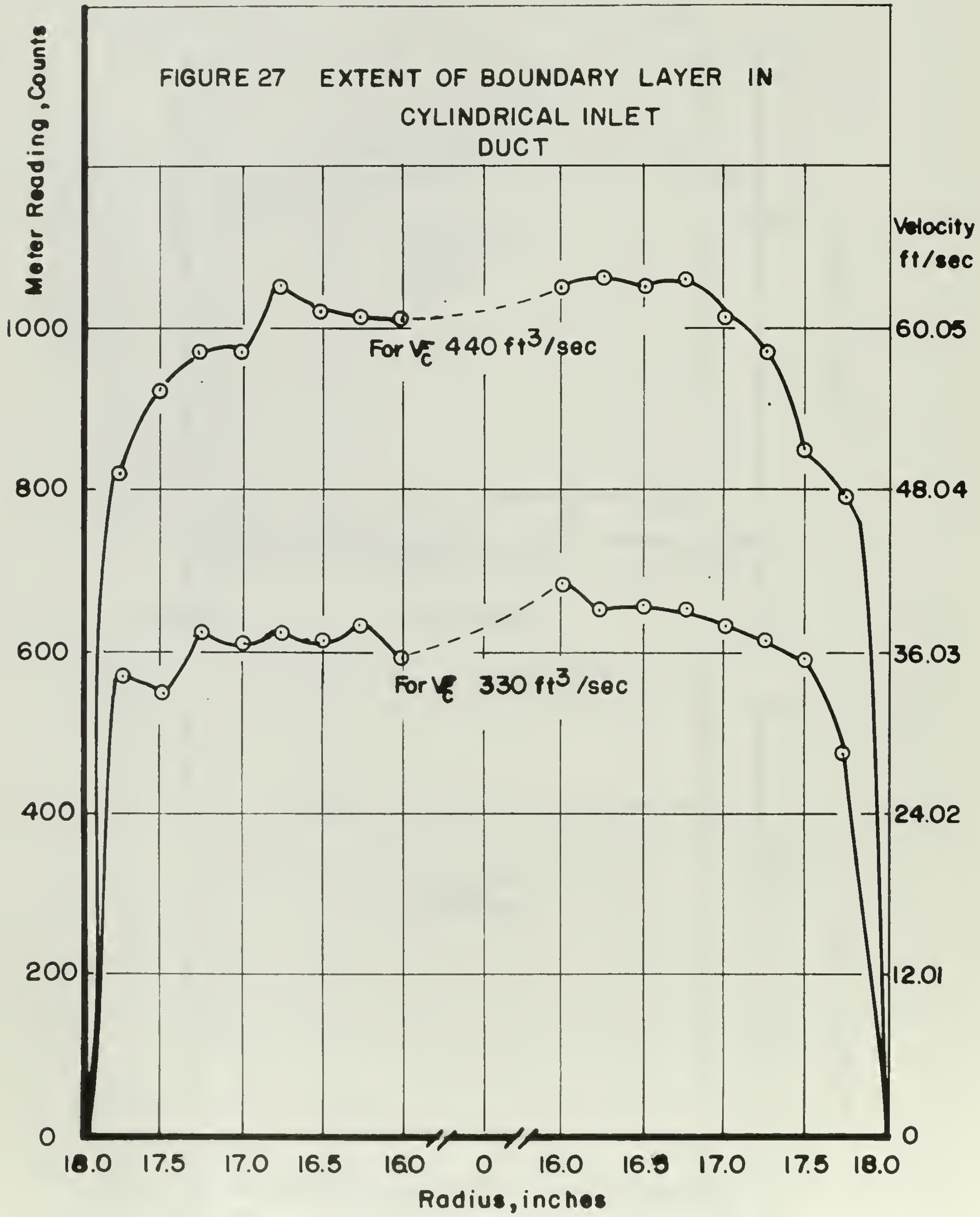

FIGURE 27 EXTENT OF BOUNDARY LAYER IN CYLINDRICAL INLET DUCT

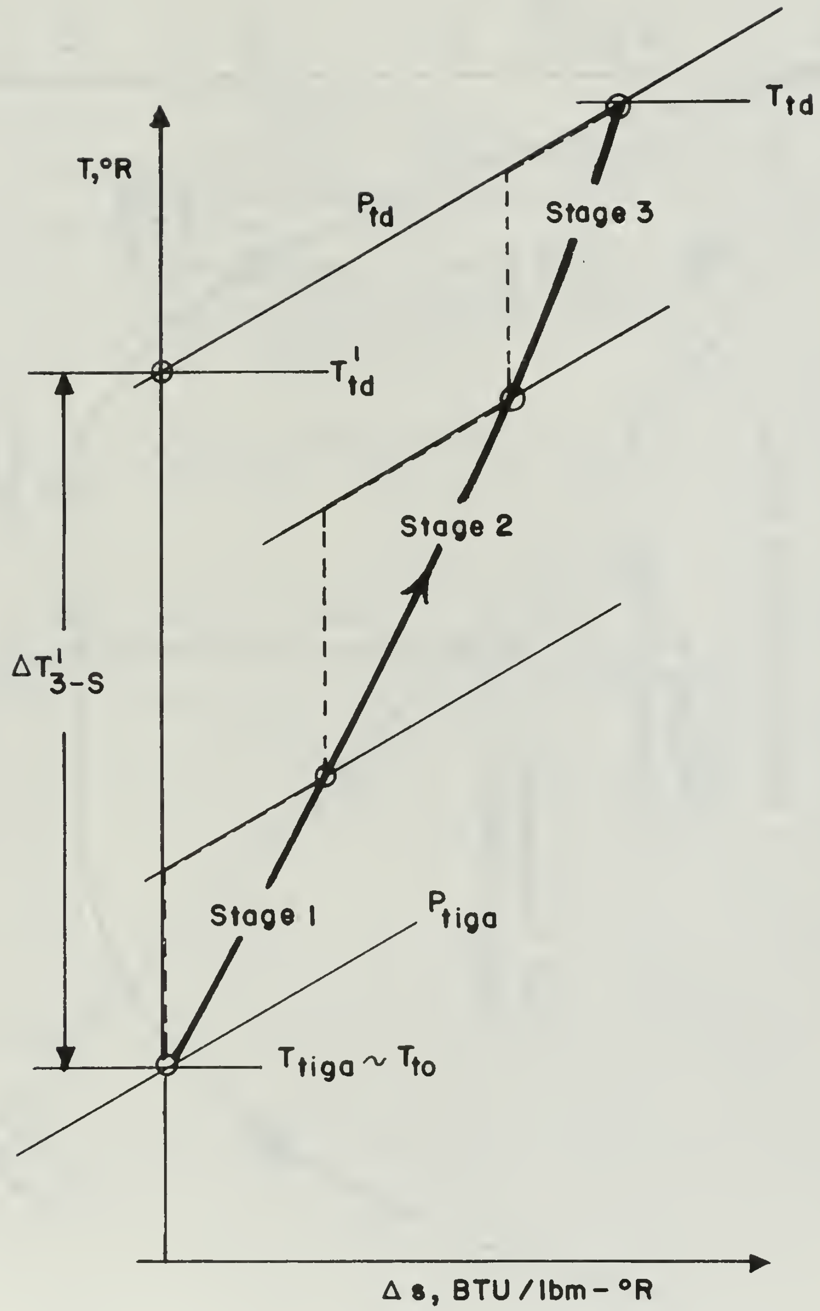

FIGURE 28 TEMPERATURE—ENTROPY DIAGRAM OF COMPRESSION PROCESS IN 3-STAGE MACHINE

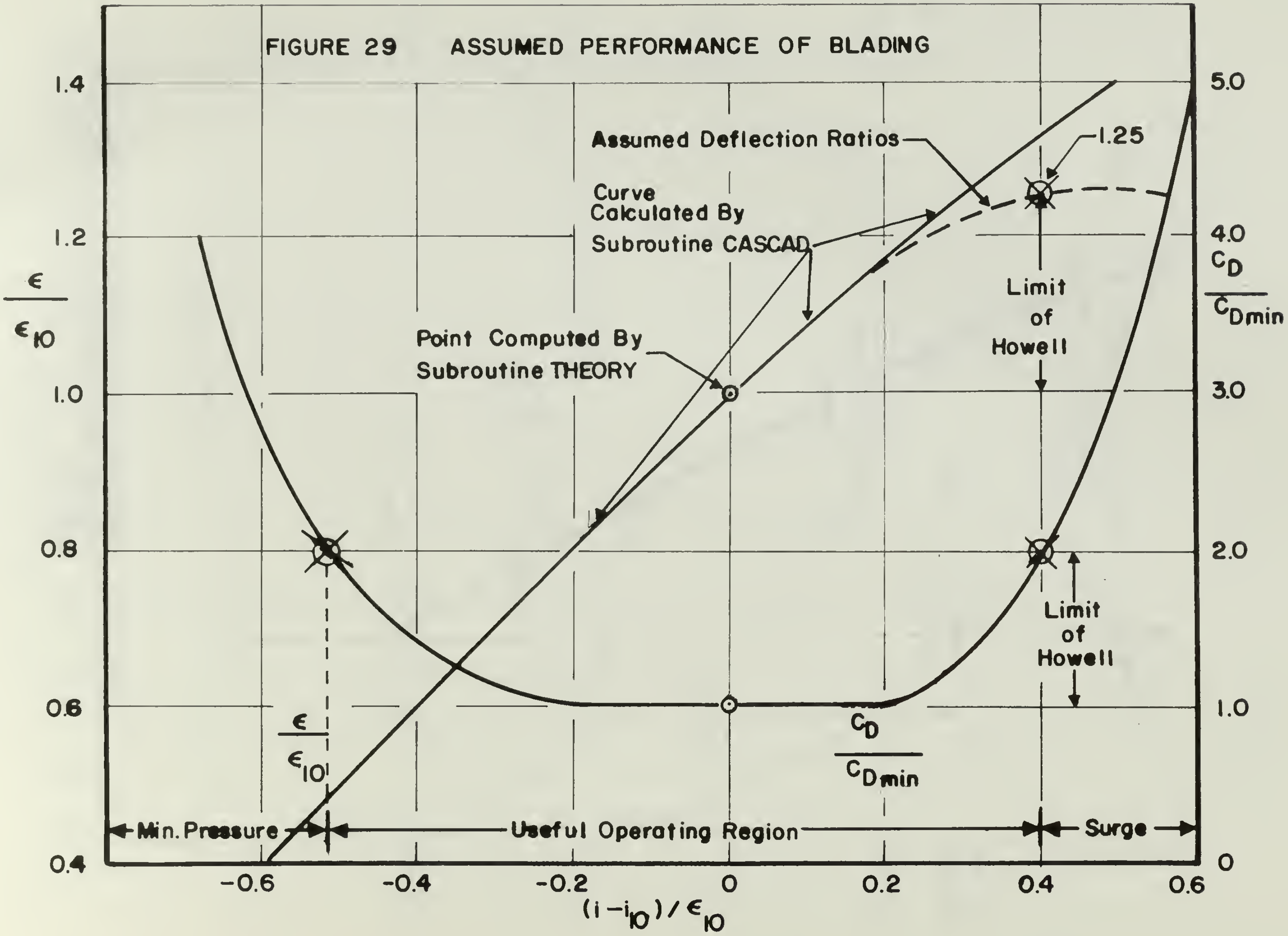
FIGURE 29 ASSUMED PERFORMANCE OF BLADING

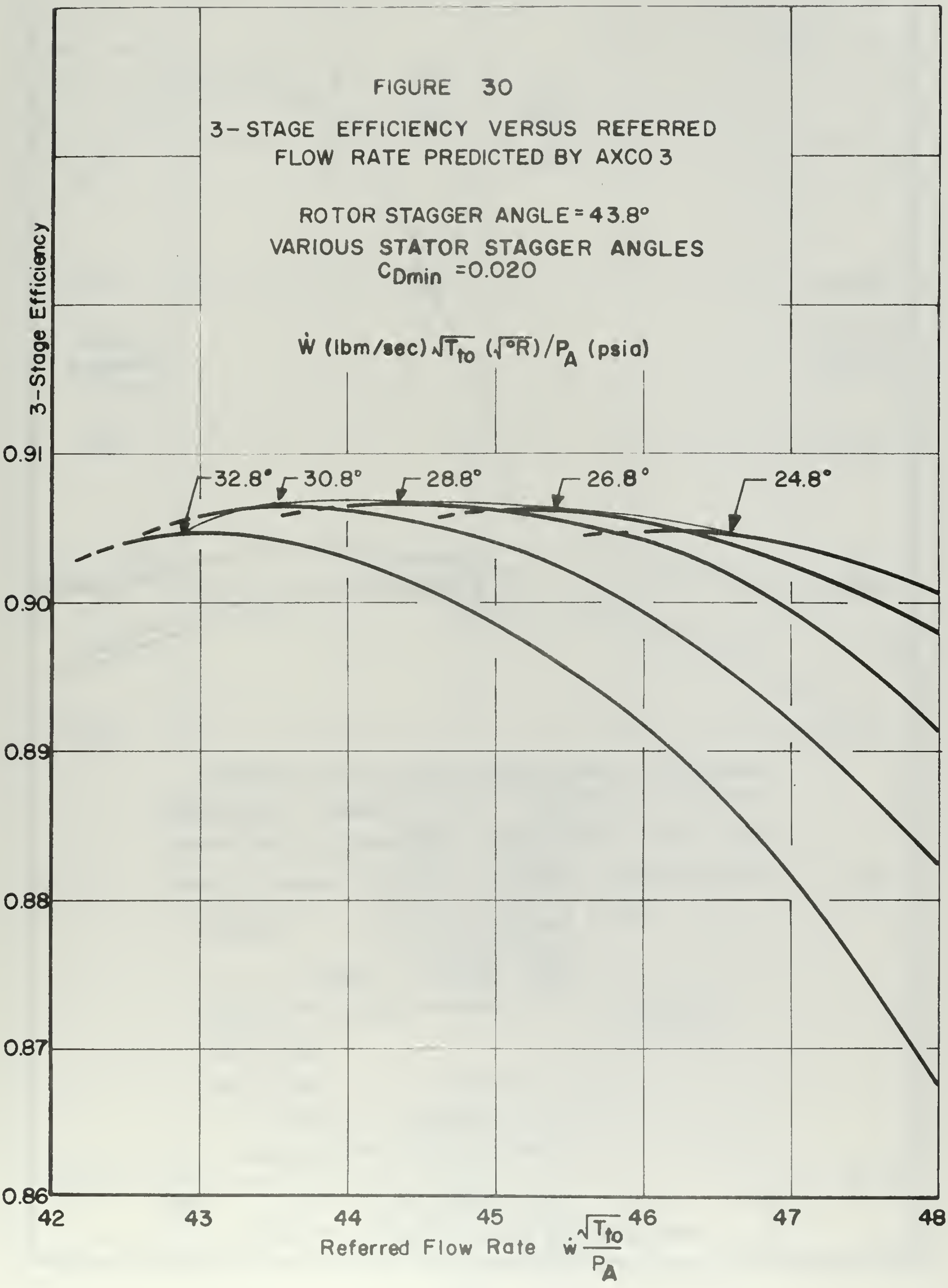

FIGURE 30

3-STAGE EFFICIENCY VERSUS REFERRED FLOW RATE PREDICTED BY AXCO 3

ROTOR STAGGER ANGLE = 43.8°
VARIOUS STATOR STAGGER ANGLES
$C_{D_{min}} = 0.020$

$\dot{W}$ (lbm/sec) $\sqrt{T_{to}}$ ($\sqrt{°R}$)/P_A (psia)

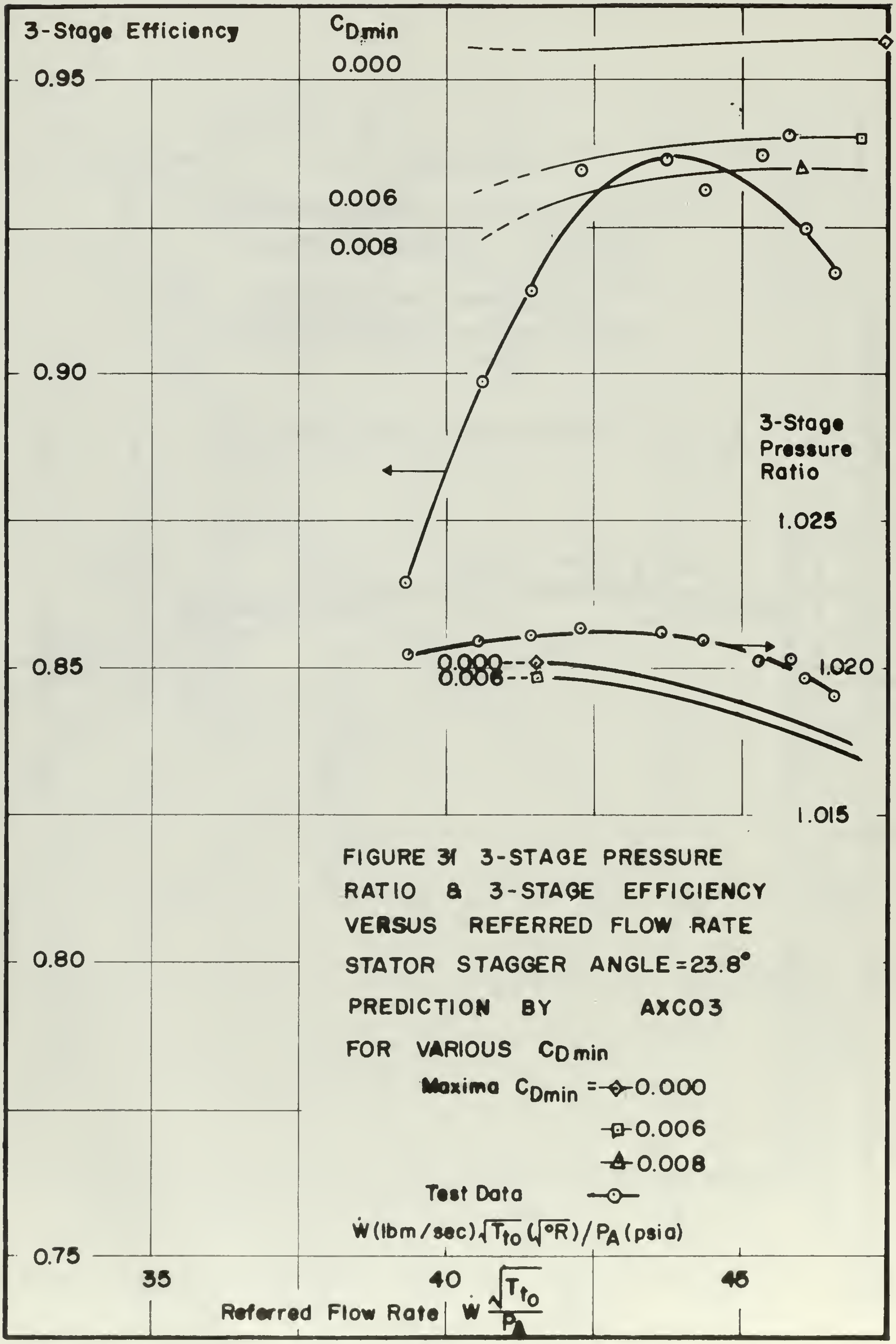

FIGURE 31 3-STAGE PRESSURE RATIO & 3-STAGE EFFICIENCY VERSUS REFERRED FLOW RATE STATOR STAGGER ANGLE = 23.8° PREDICTION BY AXCO3 FOR VARIOUS $C_{D\,min}$

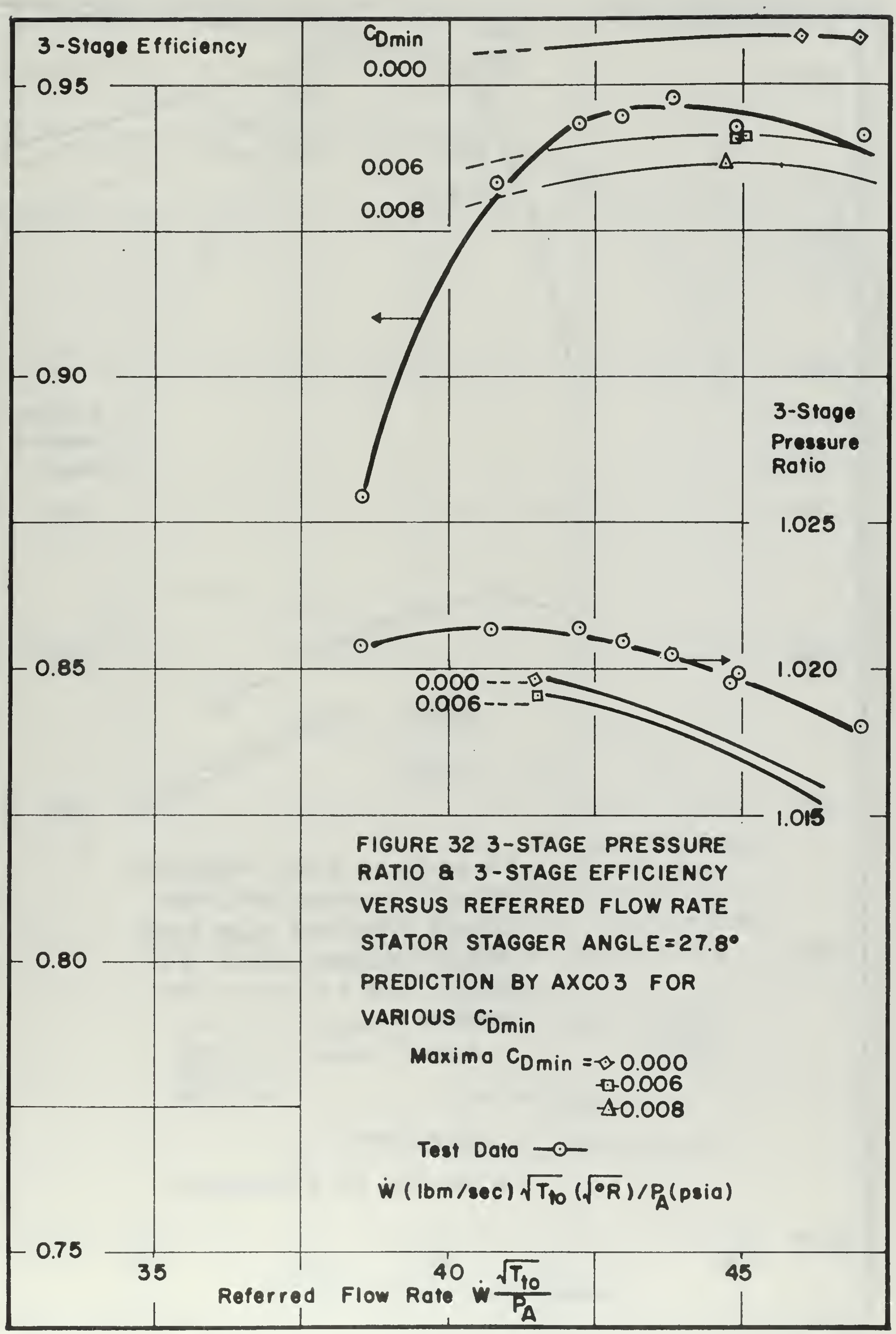

FIGURE 32 3-STAGE PRESSURE RATIO & 3-STAGE EFFICIENCY VERSUS REFERRED FLOW RATE STATOR STAGGER ANGLE = 27.8° PREDICTION BY AXCO3 FOR VARIOUS C_{Dmin}

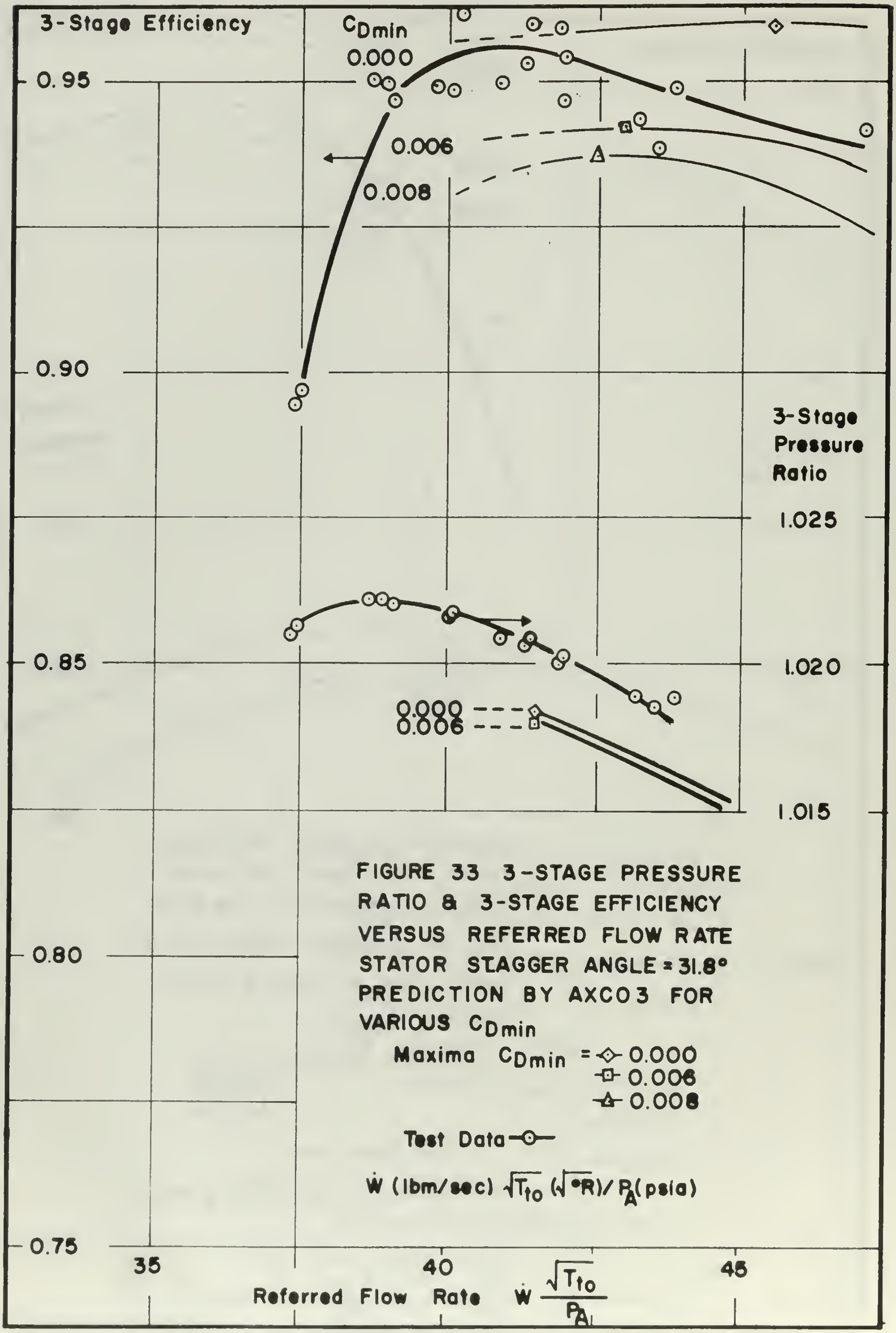

FIGURE 33 3-STAGE PRESSURE RATIO & 3-STAGE EFFICIENCY VERSUS REFERRED FLOW RATE STATOR STAGGER ANGLE = 31.8° PREDICTION BY AXCO3 FOR VARIOUS C_{Dmin}

Maxima C_{Dmin} = ◇ 0.000
□ 0.006
△ 0.008

Test Data —⊙—

$\dot{W}$ (lbm/sec) $\sqrt{T_{t0}}$ ($\sqrt{°R}$)/ P_A(psia)

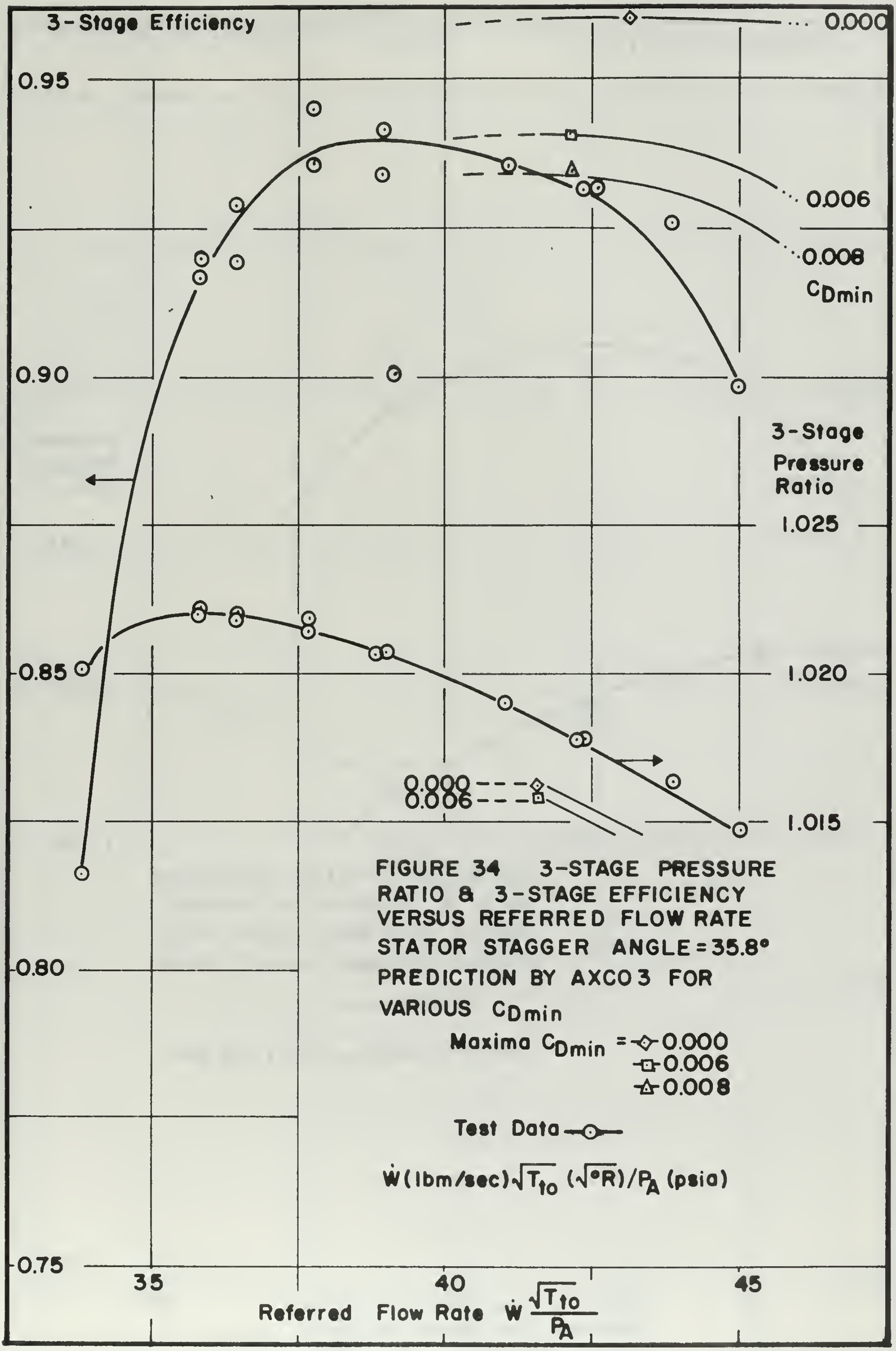

FIGURE 34 3-STAGE PRESSURE RATIO & 3-STAGE EFFICIENCY VERSUS REFERRED FLOW RATE STATOR STAGGER ANGLE = 35.8° PREDICTION BY AXCO3 FOR VARIOUS C_{Dmin}

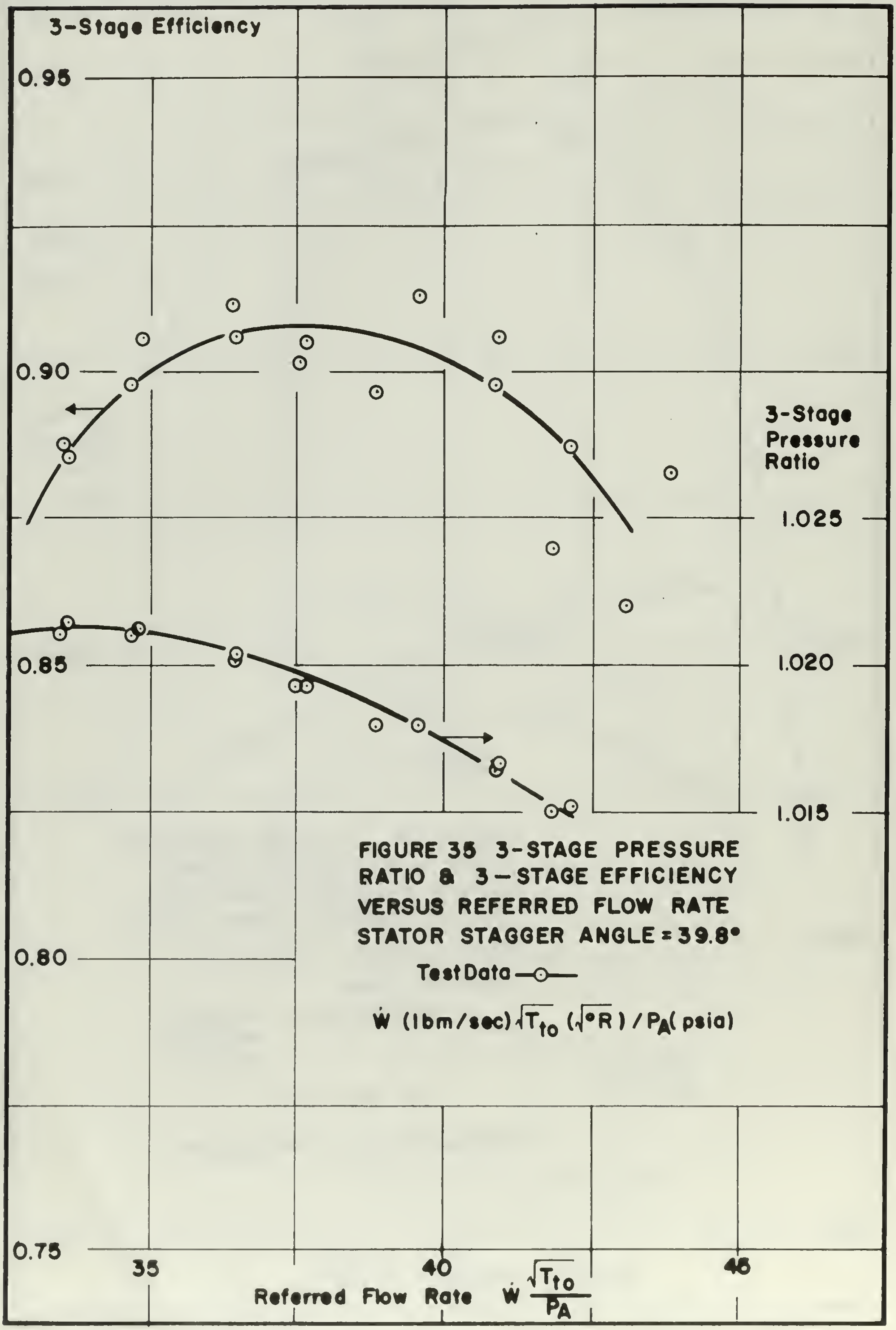

FIGURE 35 3-STAGE PRESSURE RATIO & 3-STAGE EFFICIENCY VERSUS REFERRED FLOW RATE STATOR STAGGER ANGLE = 39.8°

Test Data —⊙—

$\dot{W}$ (lbm/sec) $\sqrt{T_{to}}$ ($\sqrt{°R}$) / P_A (psia)

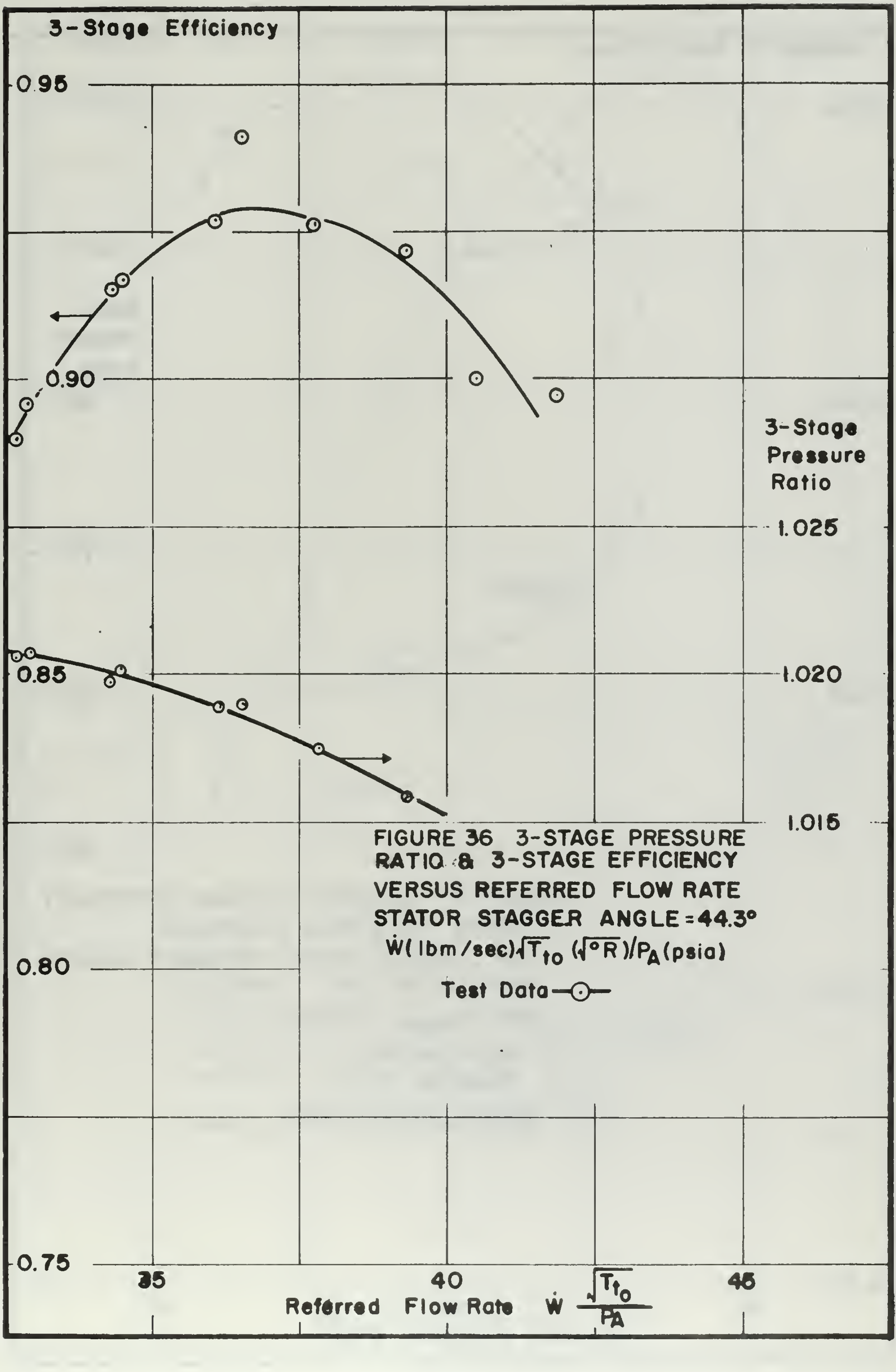

FIGURE 36 3-STAGE PRESSURE RATIO & 3-STAGE EFFICIENCY VERSUS REFERRED FLOW RATE STATOR STAGGER ANGLE = 44.3°

$\dot{W}$ (lbm/sec) $\sqrt{T_{t0}}$ ($\sqrt{°R}$)/P_A (psia)

Test Data —⊙—

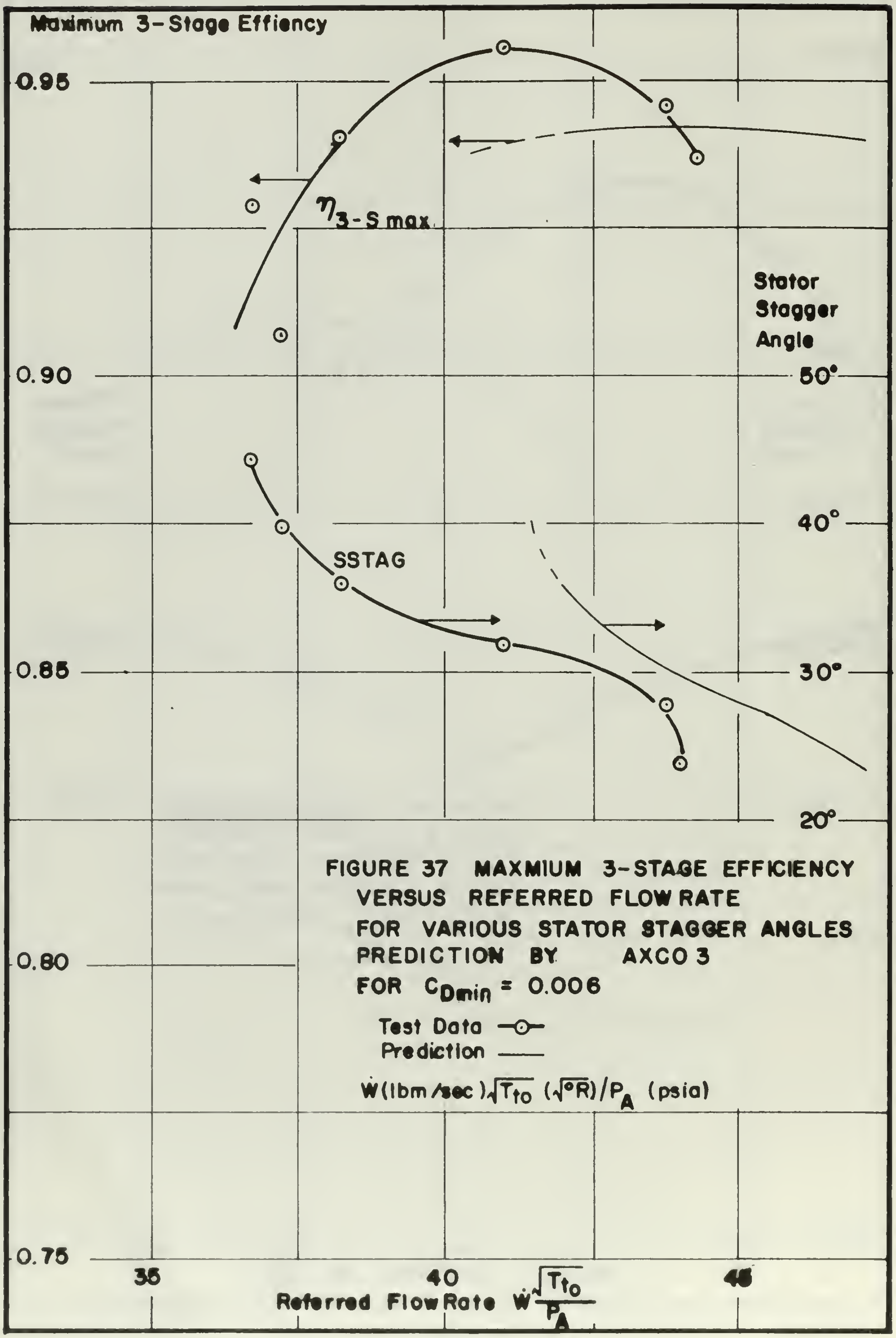

FIGURE 37 MAXMIUM 3-STAGE EFFICIENCY VERSUS REFERRED FLOW RATE FOR VARIOUS STATOR STAGGER ANGLES PREDICTION BY AXCO 3 FOR C_{Dmin} = 0.006

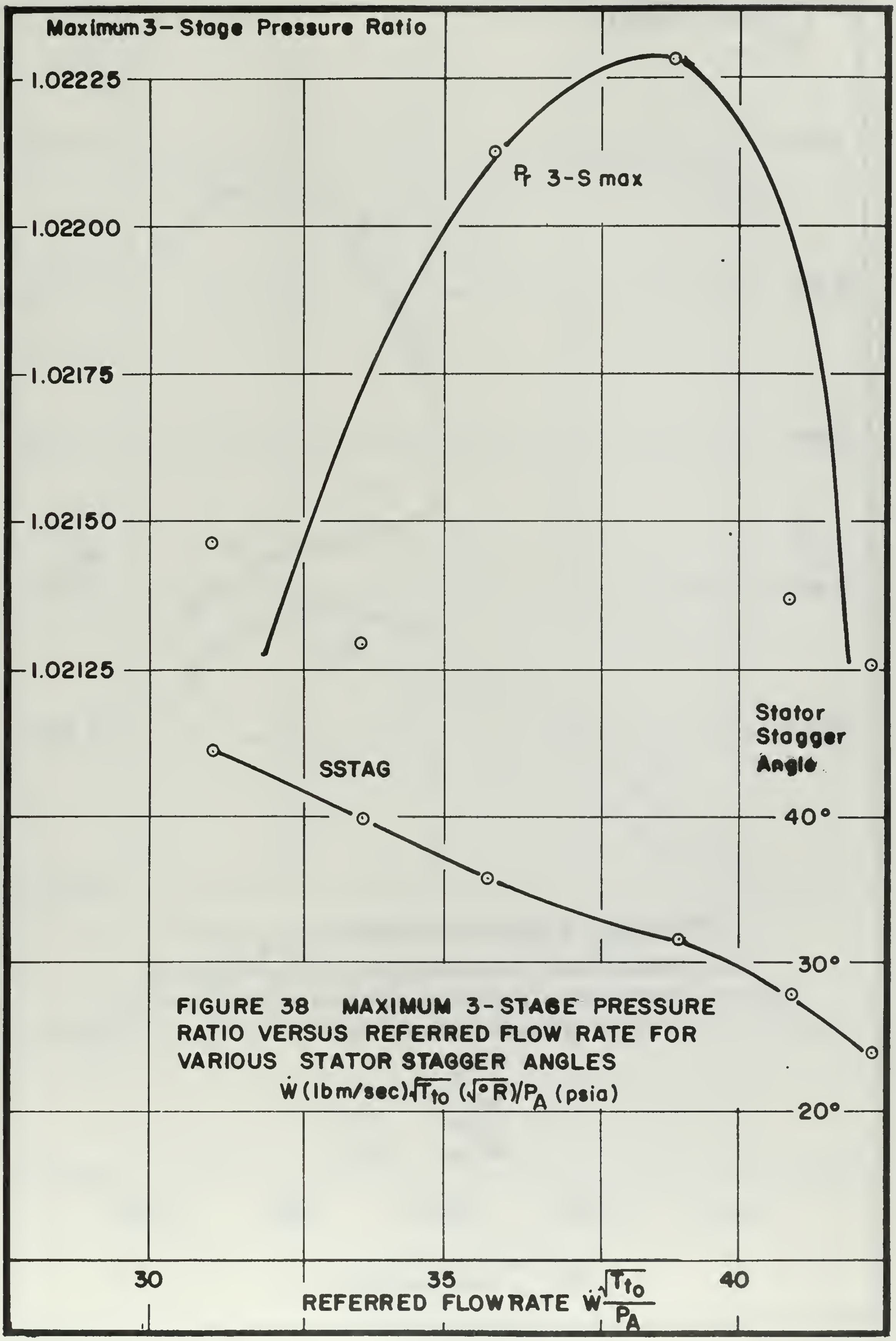

FIGURE 38 MAXIMUM 3-STAGE PRESSURE RATIO VERSUS REFERRED FLOW RATE FOR VARIOUS STATOR STAGGER ANGLES

$\dot{W}$ (lbm/sec)$\sqrt{T_{t0}}$ ($\sqrt{°R}$)/P_A (psia)

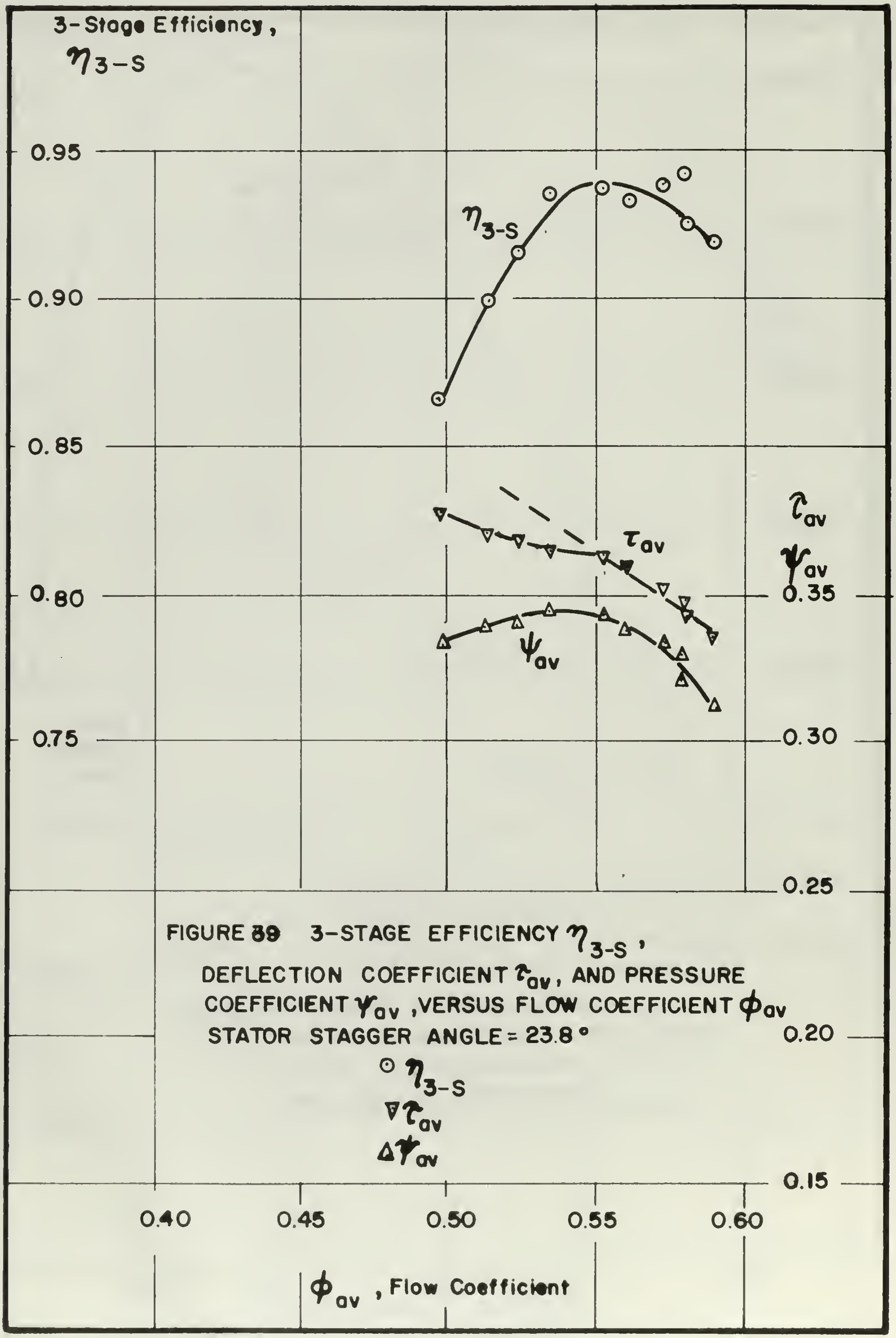

FIGURE 39 3-STAGE EFFICIENCY η_{3-S}, DEFLECTION COEFFICIENT τ_{av}, AND PRESSURE COEFFICIENT ψ_{av}, VERSUS FLOW COEFFICIENT ϕ_{av} STATOR STAGGER ANGLE = 23.8°

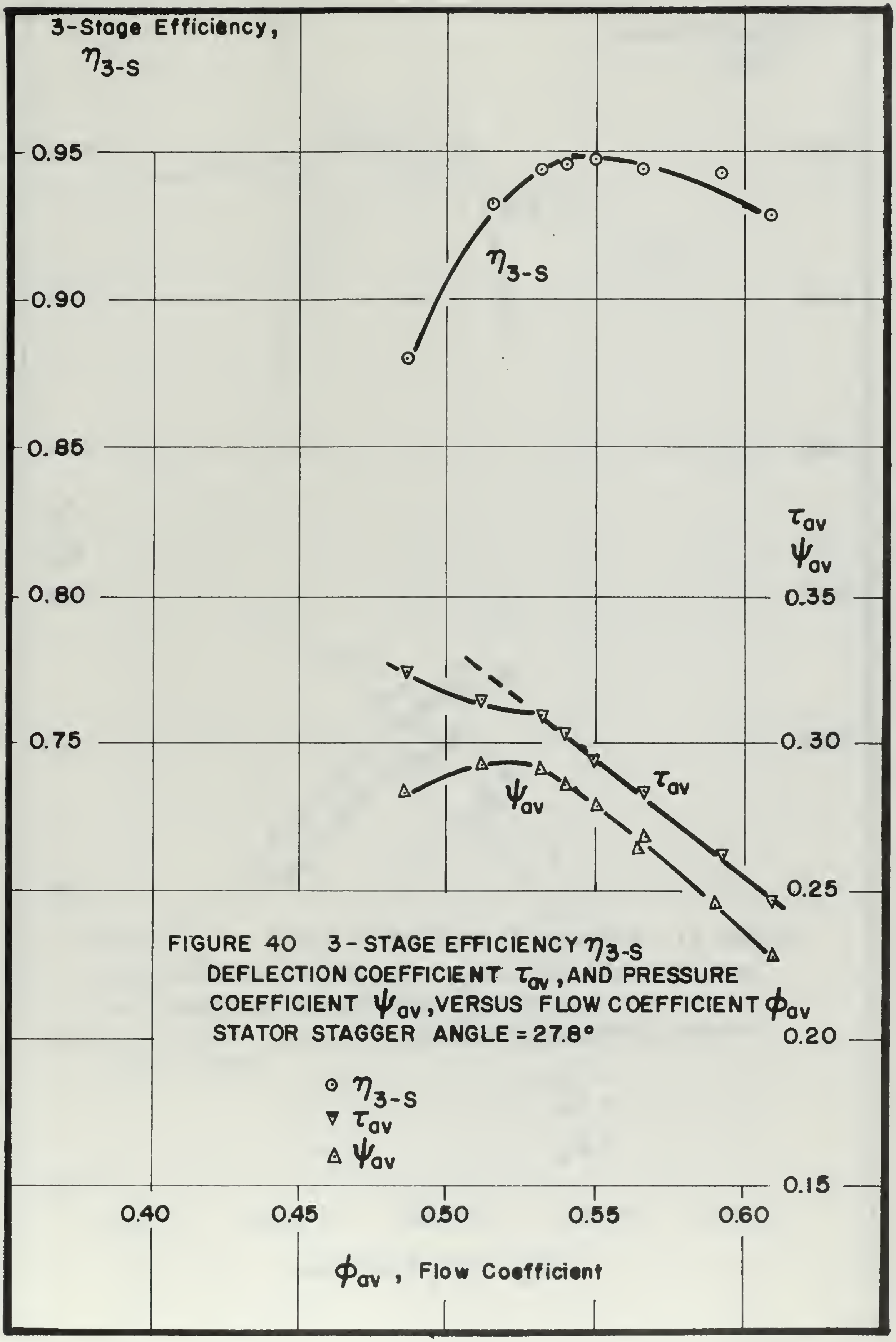

FIGURE 40 3-STAGE EFFICIENCY η_{3-S} DEFLECTION COEFFICIENT τ_{av}, AND PRESSURE COEFFICIENT ψ_{av}, VERSUS FLOW COEFFICIENT ϕ_{av} STATOR STAGGER ANGLE = 27.8°

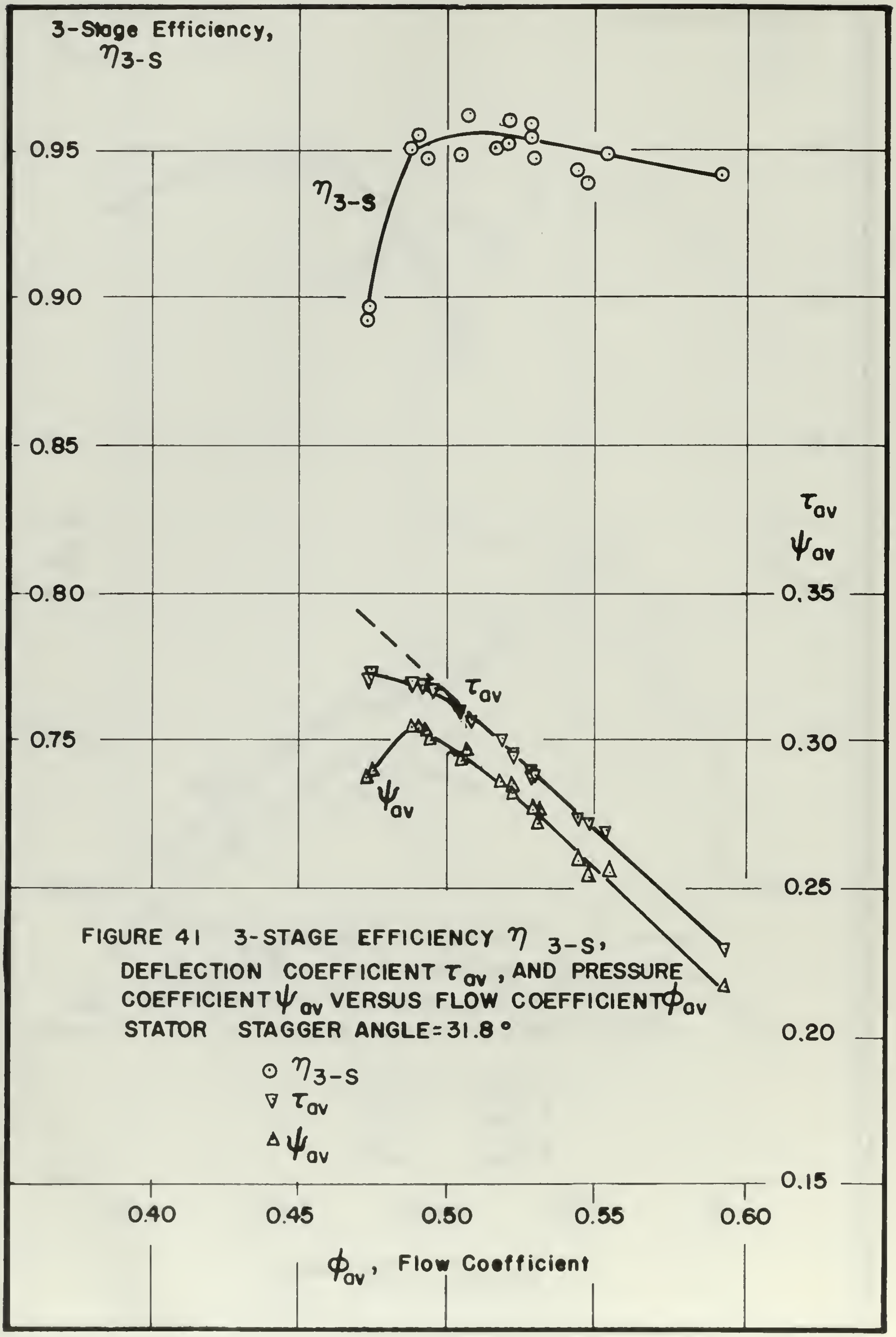

FIGURE 41 3-STAGE EFFICIENCY η_{3-S}, DEFLECTION COEFFICIENT τ_{av}, AND PRESSURE COEFFICIENT ψ_{av} VERSUS FLOW COEFFICIENT ϕ_{av} STATOR STAGGER ANGLE = 31.8°

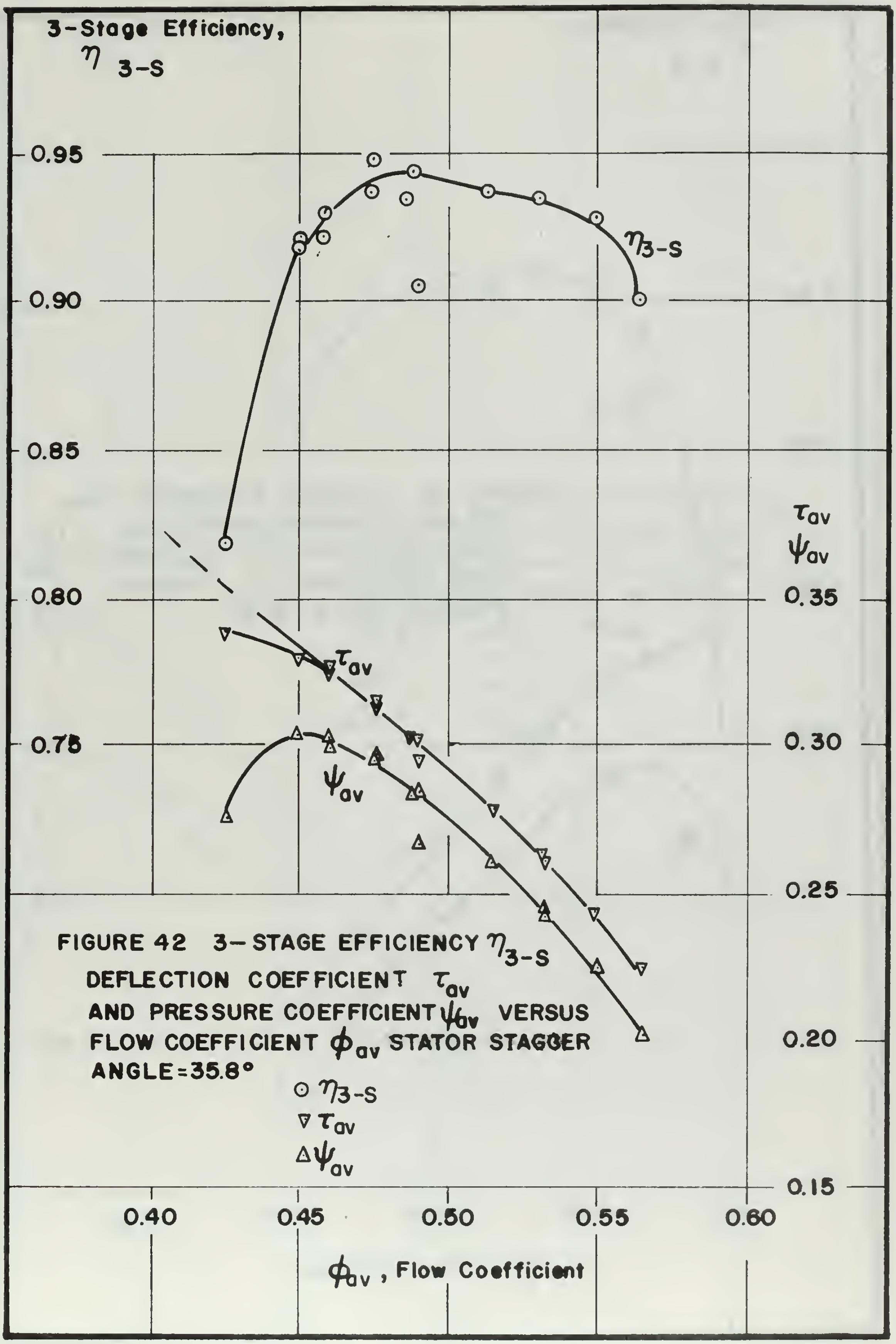

FIGURE 42 3-STAGE EFFICIENCY $\eta_{3\text{-}S}$ DEFLECTION COEFFICIENT τ_{av} AND PRESSURE COEFFICIENT ψ_{av} VERSUS FLOW COEFFICIENT ϕ_{av} STATOR STAGGER ANGLE=35.8°

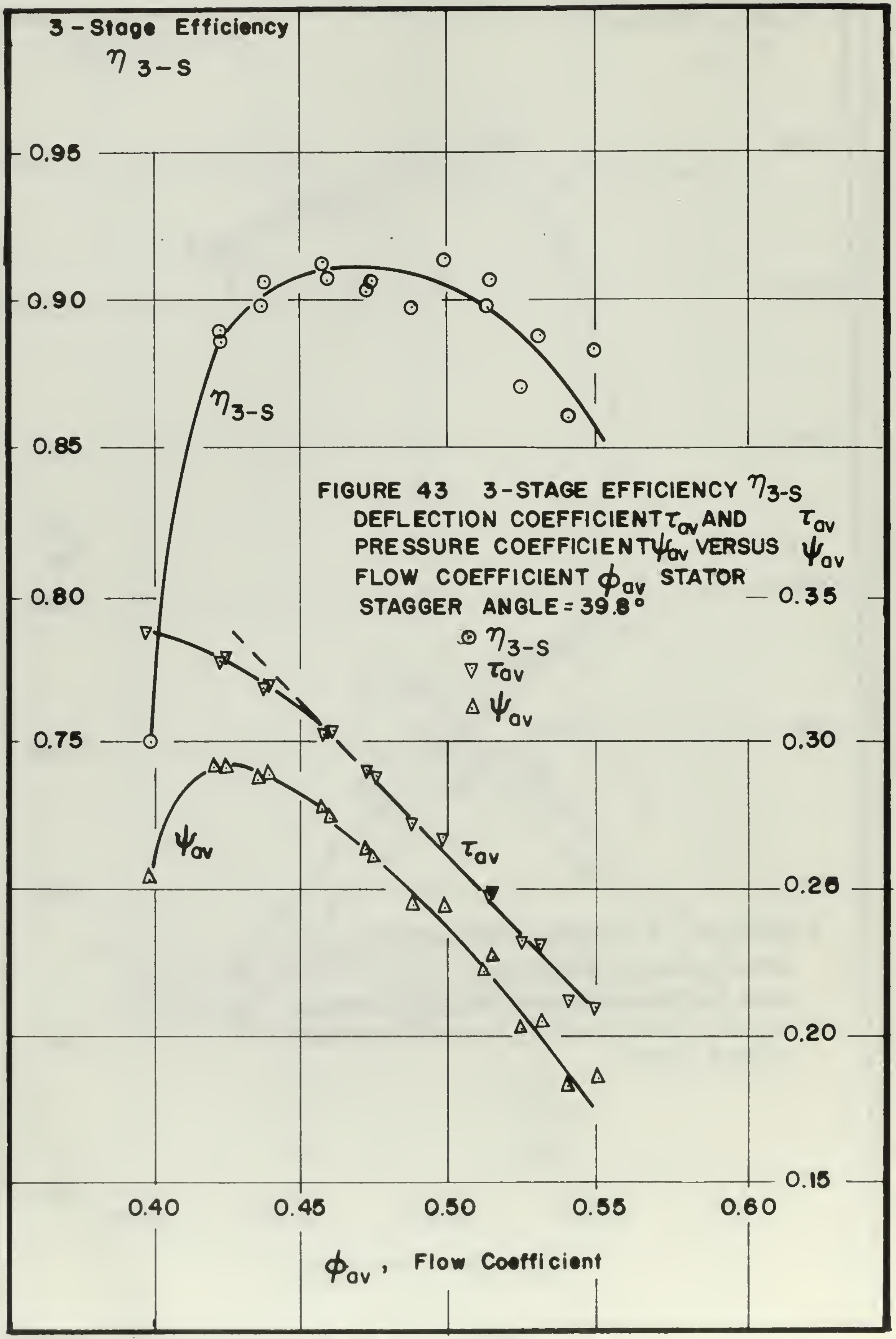

FIGURE 43 3-STAGE EFFICIENCY η_{3-S} DEFLECTION COEFFICIENT τ_{av} AND PRESSURE COEFFICIENT ψ_{av} VERSUS FLOW COEFFICIENT ϕ_{av} STATOR STAGGER ANGLE = 39.8°

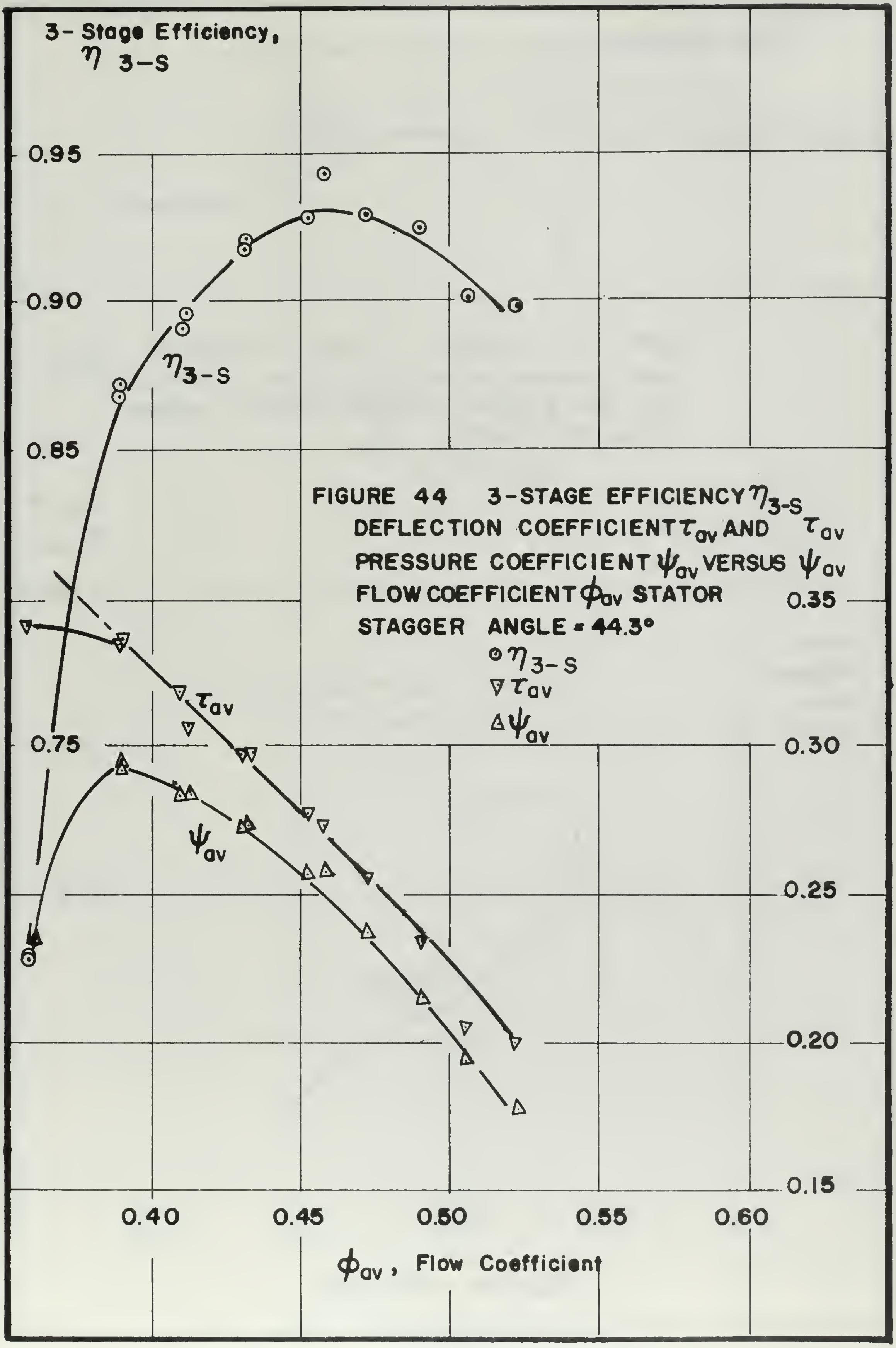

FIGURE 44 3-STAGE EFFICIENCY η_{3-S} DEFLECTION COEFFICIENT τ_{av} AND PRESSURE COEFFICIENT ψ_{av} VERSUS FLOW COEFFICIENT ϕ_{av} STATOR STAGGER ANGLE = 44.3°

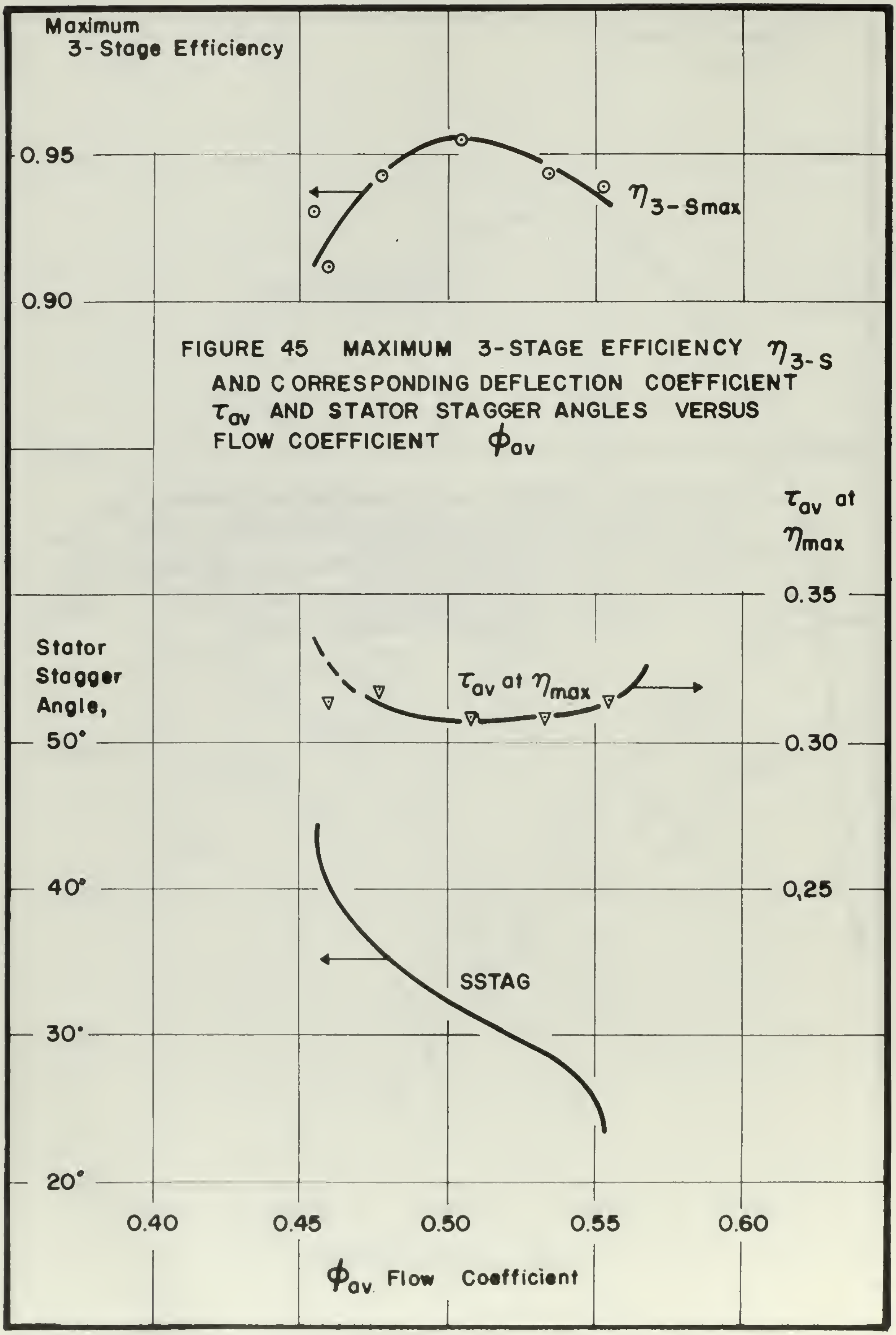

FIGURE 45 MAXIMUM 3-STAGE EFFICIENCY η_{3-S} AND CORRESPONDING DEFLECTION COEFFICIENT τ_{av} AND STATOR STAGGER ANGLES VERSUS FLOW COEFFICIENT ϕ_{av}

FIGURE 46 MAXIMUM PRESSURE COEFFICIENT $\psi_{av,\,max}$ AND CORRESPONDING STATOR STAGGER ANGLES VERSUS FLOW COEFFICIENT ϕ_{av}

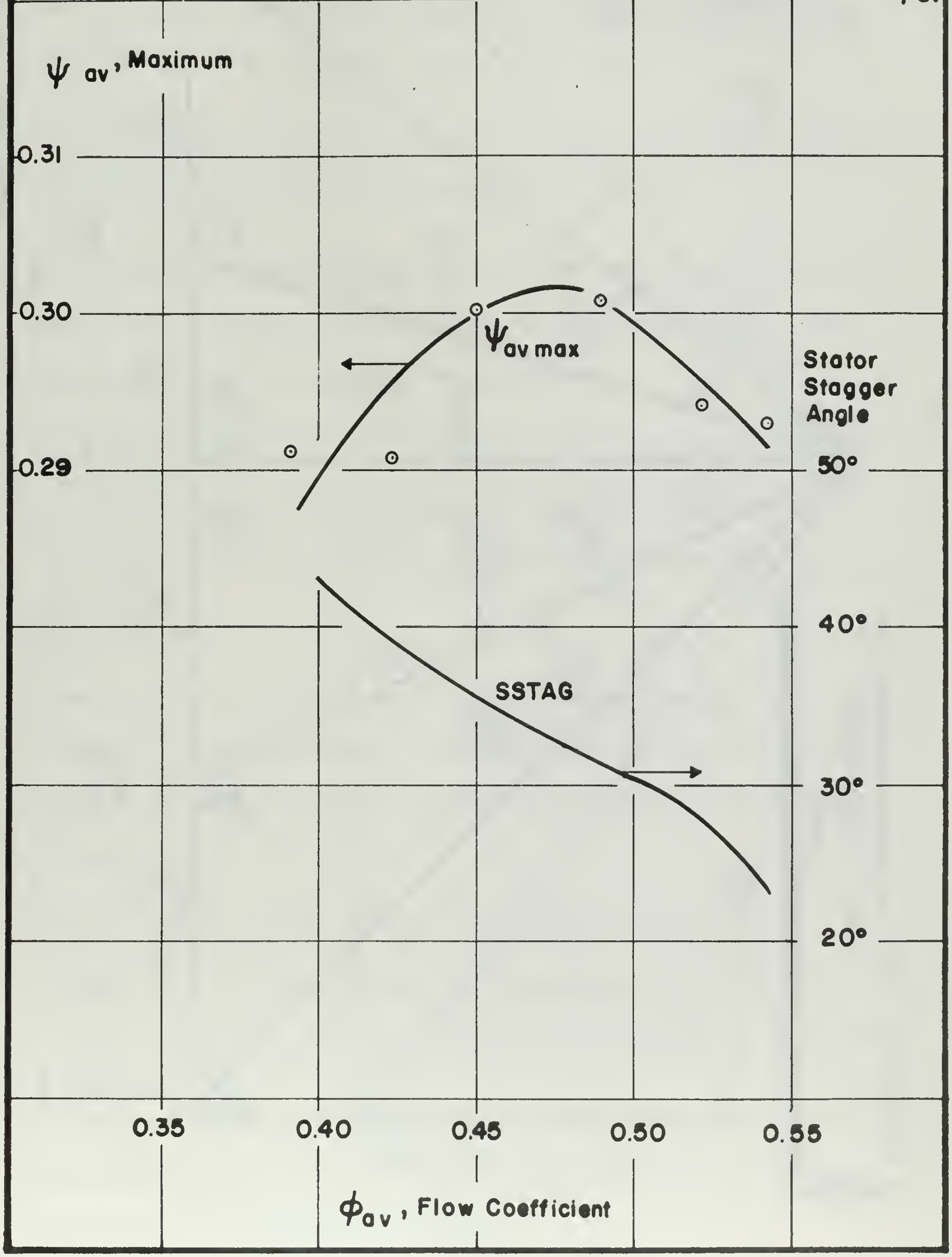

FIGURE 47 OFF-DESIGN CONDITIONS OF AXIAL COMPRESSOR STAGE

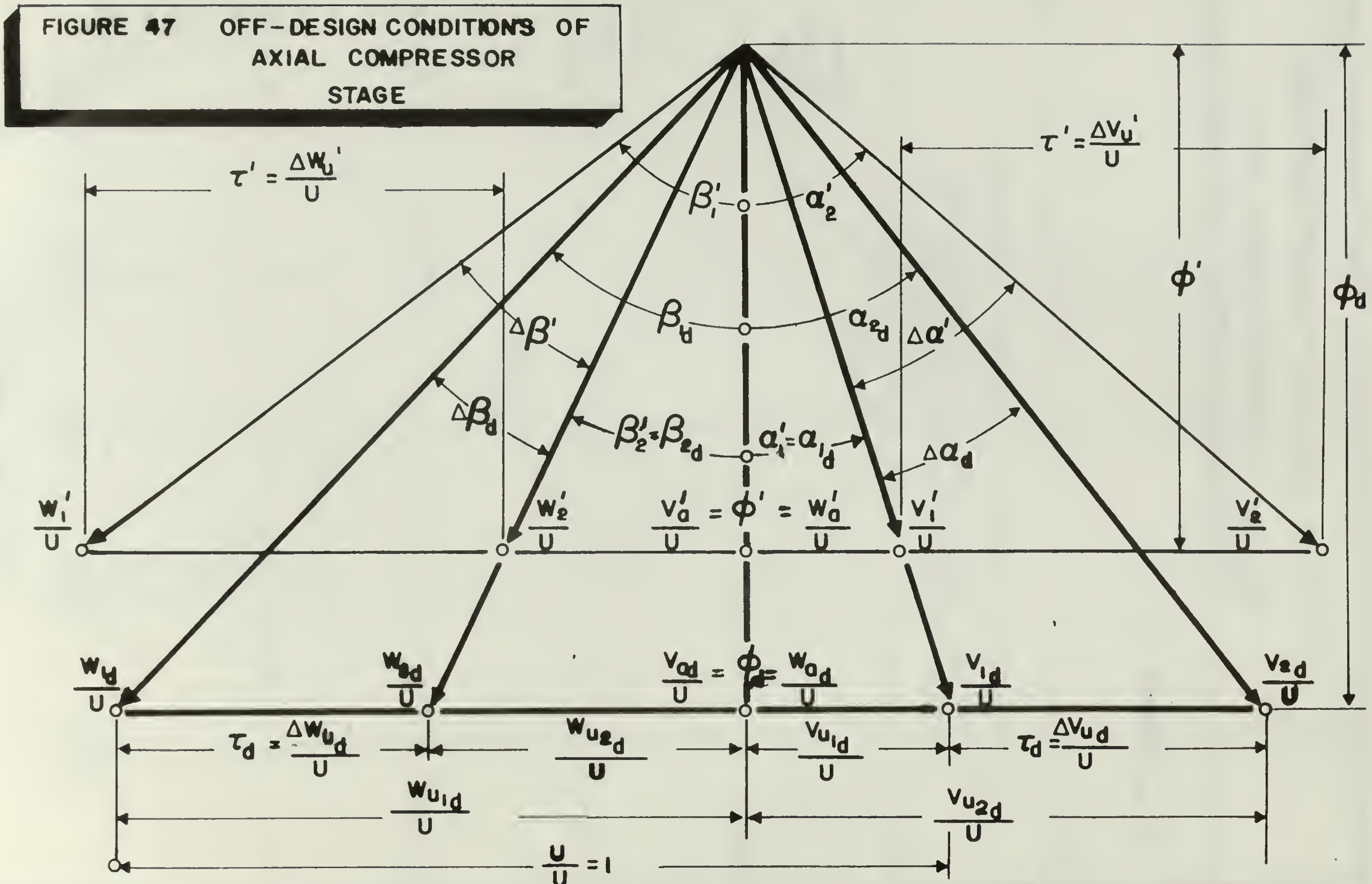

After Vavra (1) p.348

SECTION 9

REFERENCES

1. Vavra, M. H., "Aero-Thermodynamics and Flow in Turbomachines," John Wiley & Sons, Inc., New York, N. Y., 1960.

2. Lieblein, Seymour, "Experimental Flow in Two-Dimensional Cascades," Chapter VI of NASA SP-36, Washington, D. C., 1965.

3. Vavra, M. H., "Analysis of Performance of Clark CSN-2 Axial-Flow Compressor for ML-1", Report AGN-VA #26, Aerojet-General Nucleonics, San Ramon, California, November 1963.

4. Gibbons, Thomas and Bartels, Harlan B., "An Analytical Investigation of Off-Design Performance in Multi-Stage Axial Flow Compressors" Unpublished Masters Thesis, Naval Postgraduate School, May 1966.

5. Bowen, John T., Sabersky, Rolf H. and Rannie, Duncan W., "Theoretical and Experimental Investigations of Axial Flow Compressors (Summary Report)," California Institute of Technology, January 1949.

6. Bowen, John T., Sabersky, Rolf H. and Rannie, Duncan W., "Theoretical and Experimental Investigations of Axial Flow Compressors, Part 2," California Institute of Technology, July 1949.

7. Alsworth, Charles C. and Iura, Toru, "Theoretical and Experimental Investigations of Axial Flow Compressors, Part 3," California Institute of Technology, July 1951.

REFERENCES (Cont.)

8. Iura, Toru, and Rannie, Duncan W., "Observations of Propagating Stall in Axial Flow Compressors," California Institute of Technology, April 1953.

9. Howell, A. R., "Axial Compressor Design," Rpt. E3946, Royal Aircraft Establishment, Farnborough, England, June 1942.

10. National Research Council, "International Critical Tables, Vol. III," McGraw-Hill, 1928.

11. Waitman, B. A., Reneau, L. R. and Kline, S. J., "Effects of Inlet Conditions on Performance of Two Dimensional Subsonic Diffusers," Journal of Basic Engineering, Transactions of the A. S. M. E., Sept. 1961, pp. 349-360.

APPENDIX A

CALIBRATION OF INSTRUMENTS

The measuring devices were calibrated to determine their accuracy and precision.

The Berkeley digital counter is located near a Hewlett-Packard digital counter in the control room. At a given flow rate, there was no difference between the two instruments. The Hewlett-Packard device was recently calibrated with a cesium wave length frequency standard in the Standards Laboratory of the Electrical Engineering Department of the Naval Postgraduate School. The speed measured is considered accurate to 0.5 rpm.

The Baldwin-Lima-Hamilton torque meter was calibrated statically as illustrated in Fig. 24. A bar was attached to the drive end of the shaft and was clamped to the stand. A symmetrical lever bar was attached to the rotor end of the shaft. The lever arm is 20.0 in. Two weight pans were adjusted to 1.44 lb. each with lead shot in a plastic bag. The weights themselves were checked on the Toledo Precision Scales of the Cascade Laboratory. On the first run, different readings were obtained while loading and unloading the pans. This problem was overcome in subsequent runs by tapping the stand with a mallet prior to recording the reading. This simulated the vibration of dynamic operation which eliminated any frictional effects. Good agreement was obtained during tests where the loading was increased and decreased. The possibility of temperature effects on the strain gauges was explored in a third test. The torque meter cannot be calibrated while the motor is running, but it was calibrated immediately after shutdown. The shaft was only slightly warmer to the touch than ambient temperature.

The data of the three calibration runs are shown in Table A-1. The results are plotted in Fig. A-1. Run A-3 revealed no temperature effect. A fourth run was made later for checking purposes and did not reveal any discrepancies. The calibration tests established a constant for the torque meter of 4.1565 foot-pounds of torque per pound reading of the meter. The maximum relative error among the runs is 0.6 per cent. The meter may be read to within 0.03 pounds, or 1 per cent of the meter reading.

The newly acquired low range bourdon tube was calibrated also. Run B-1 was made by using the mercury manometer board in the control room of the Compressor Laboratory. The transsonic turbine test rig was used to provide the pressure difference for the higher pressure range. The present compressor tests required pressure measurements down to 0.6 in. of water. Runs B-3 and B-5 were made at low pressure difference with a Merriam water micro-manometer. Pressure was supplied from a static source.

The data of the three calibration runs are shown in Table A-2. The results are plotted in Fig. A-2. The calculation of velocities was set up using pressure difference in lb/ft^2. Measured pressures are therefore very small numbers. An inverse calibration constant was used. The bourdon tube has a constant of 240.423 counts per lb/ft^2. The maximum relative error among the calibration runs was 0.12 per cent. The meter may be read to within 5 counts. The meter's servo system tends to overcorrect. In the manual null mode the meter needle tends to wander a similar amount. The five count reading error amounts to 1 per cent of the velocity head reading in the inlet duct during flow rate calibration. The error is 0.5 per cent of the velocity head reading at the permanent Pitot tube. The error is only 0.05 per cent of the measured pressure difference across the three stages.

The Pitot-static tube used to traverse the inlet duct during flow rate calibration is a modified Prandtl-type tube. Another Pitot-static tube was attached to the traverse shaft and the tubes compared. Sufficient difference existed between the two to justify further tests. The low speed calibration tunnel in the Cascade Laboratory was modified to receive the Pitot-static tube from the inlet duct.

The data of the calibration runs are shown in Table A-3. The results are plotted in Fig. A-3. Each point represents the average of four readings. Run C-3 indicated that the velocity head of the Pitot-static tube from the inlet duct was at most 1.1 per cent less than that of the calibration tunnel. Run C-4 indicated that the static pressure below atmospheric was at most 1.8 per cent less than that of the calibration tunnel. These maximum errors occurred at the lower pressure differences. It is probable that the effect recorded is in part the reading error due to bourdon tube oscillation.

TABLE A-1

CALIBRATION OF BLH TORQUE METER

RUN A-2

APPLIED TORQUE FT-LB	METER READING LB
4.167	0.995
8.333	2.005
12.500	3.000
16.667	3.985
20.833	4.995
25.000	5.985
29.167	6.980
33.333	7.960
37.500	8.940
41.667	9.970
45.833	10.925
50.000	11.950
54.167	12.915
58.333	13.930
62.500	14.905
66.667	15.925
70.833	16.935
75.000	17.945
79.167	18.910
83.333	19.970

RUN A-3

APPLIED TORQUE FT-LB	METER READING LB
19.792	4.745
39.583	9.620
59.375	14.540
77.708	18.445
92.708	22.400
109.375	26.345
126.042	30.285

RUN A-4

APPLIED TORQUE FT-LB	METER READING LB
19.792	4.77
38.958	9.610
59.792	14.545
76.458	18.510
93.125	22.435
109.792	26.405
126.458	30.370
130.675	31.340

FIGURE A-I TORQUE METER CALIBRATION

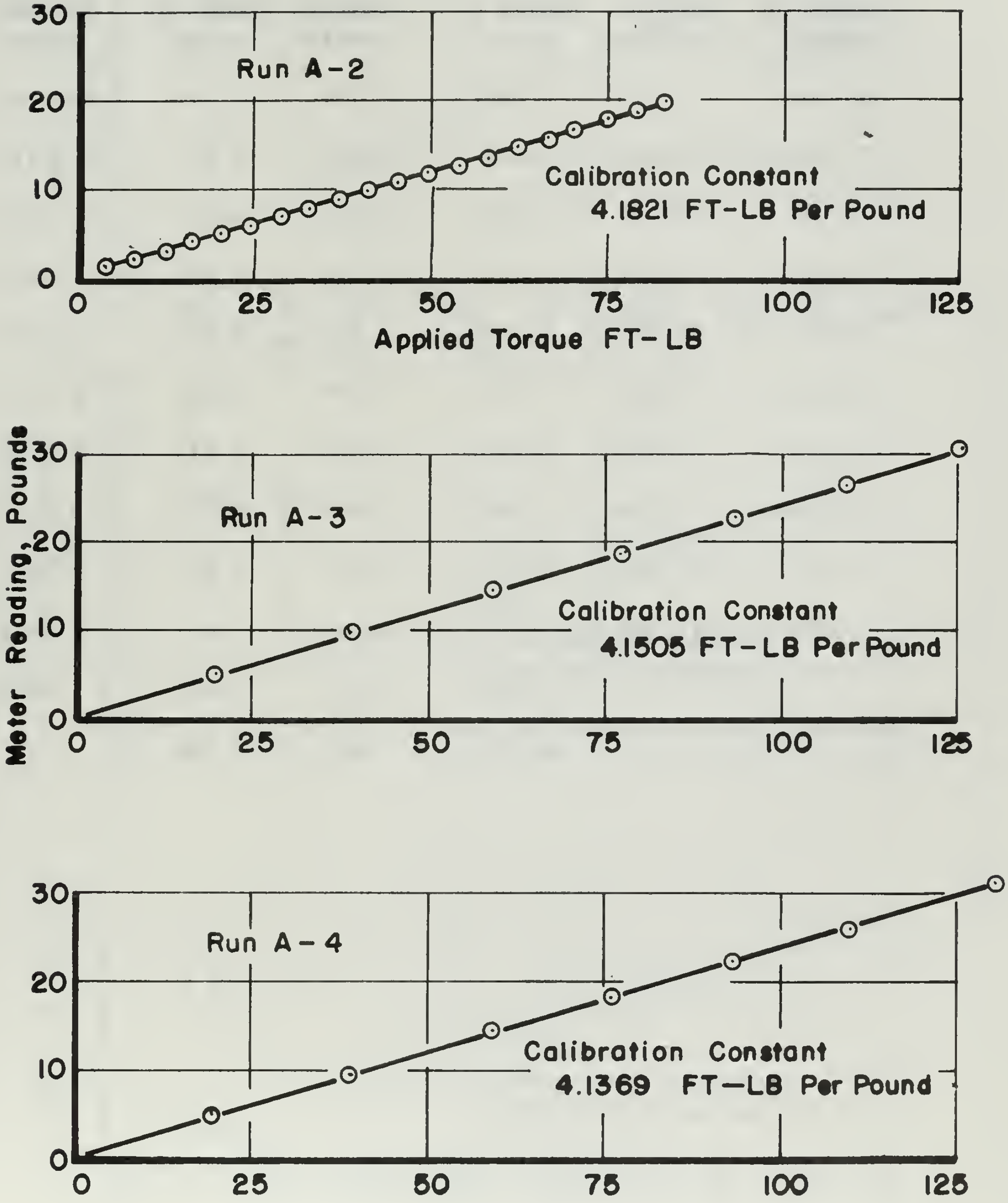

Average Calibration Constant 4.1565 FT-LB Per Pound

TABLE A-2

CALIBRATION OF 0-12 in. Hg BOURDON TUBE

RUN B-1		RUN B-3		RUN B-5	
PRESSURE INCHES OF MERCURY	METER READING COUNTS	PRESSURE INCHES OF WATER	METER READING COUNTS	PRESSURE INCHES OF WATER	METER READING COUNTS
10.260	174,300	13.978	17.409	14.519	18,218
8.290	139,450	12.459	15,518	12.914	16,119
7.445	125,750	11.062	13,784	11.397	14,222
6.065	102,900	9.853	12,276	9.913	12,368
5.235	88,200	6.993	8,737	8.471	10,560
4.440	74,800	6.198	7,738	6.989	8,715
4.035	67,950	4.992	6,230	5.471	6.826
3.320	57,100	3.996	4,993	4.493	5,613
2.415	40,900	3.036	3,794	3.470	4,398
1.000	16,300	2.195	2,741	2.401	2,994
		1.602	1,997	1.512	1,885
		0.785	982	0.620	762

FIGURE A-2 BOURDON TUBE CALIBRATION

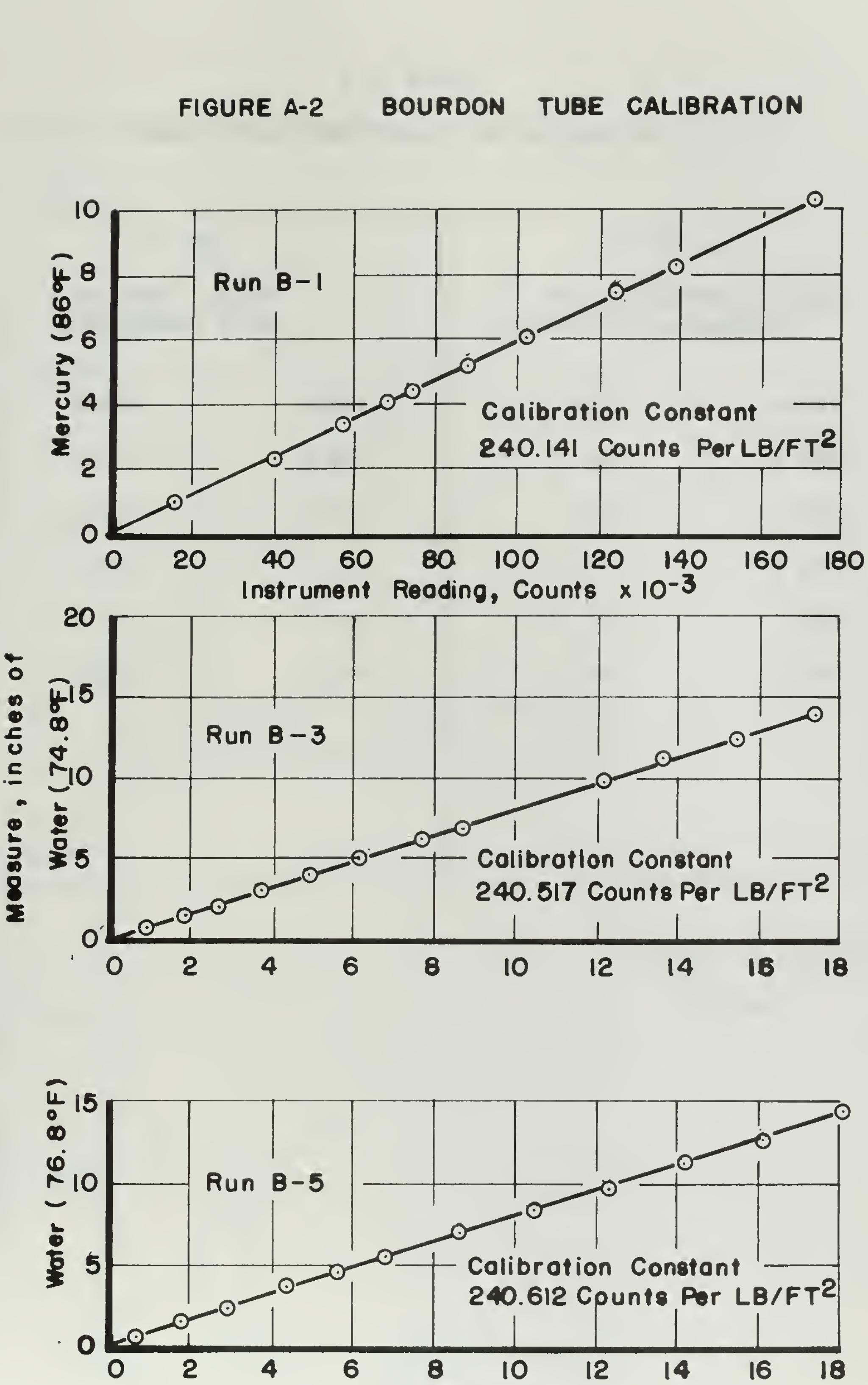

Average Calibration Constant 240.423

TABLE A-3

CALIBRATION OF INLET PITOT-STATIC TUBE

RUN C-3 TOTAL PRESSURE MINUS STATIC PRESSURE		RUN C-4 STATIC PRESSURE BELOW ATMOSPHERIC	
PROBE	TUNNEL	PROBE	TUNNEL
2486.25	2508.75	2450.0	2455.0
2157.5	2182.5	2190.0	2190.0
1413.75	1421.25	1422.5	1425.0
1002.5	1011.25	1087.5	1012.5
793.75	797.5	795.0	810.0

FIGURE A-3 INLET TRAVERSE PITOT-STATIC CALIBRATION

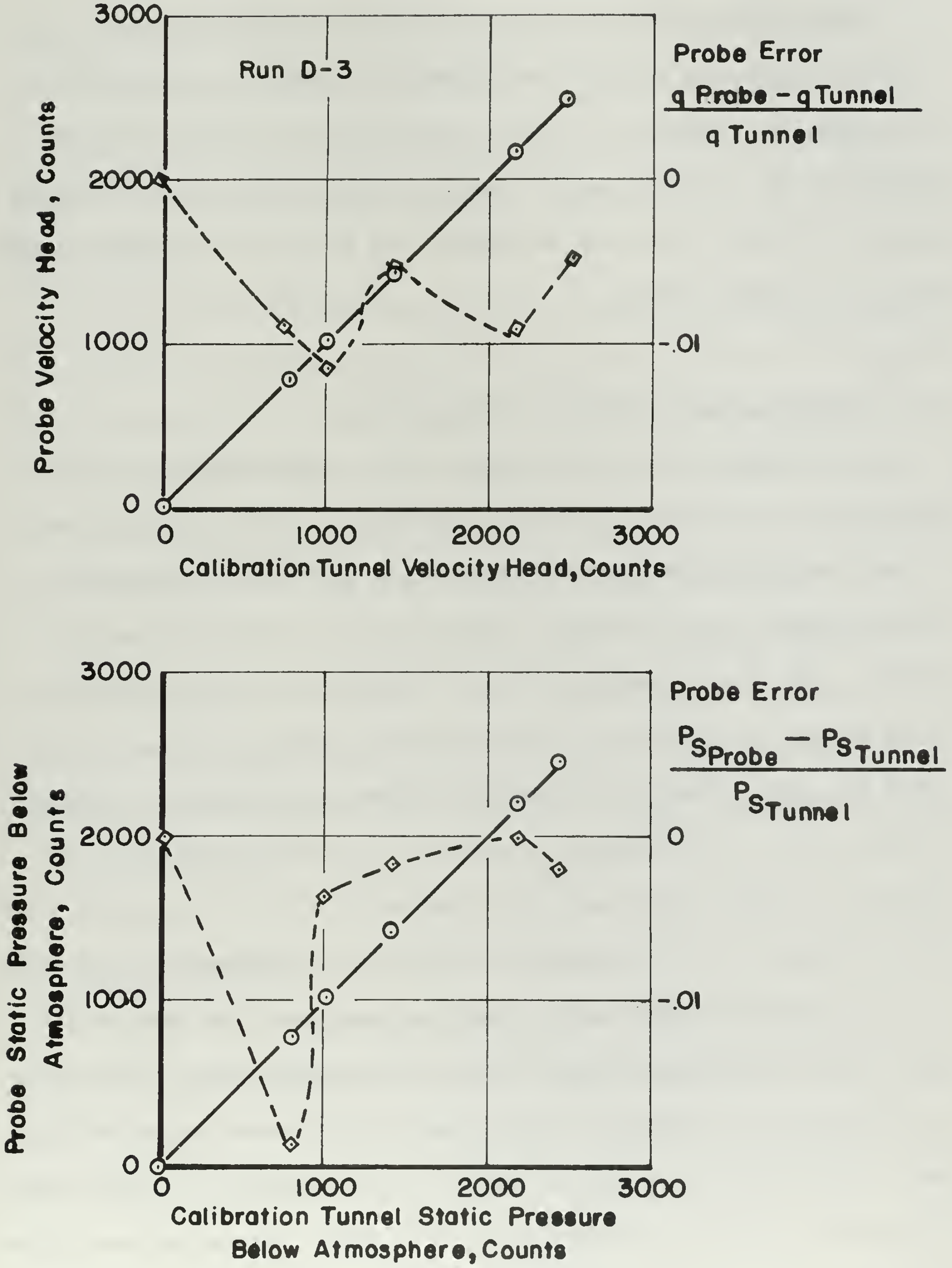

APPENDIX B

FLOW RATE CALIBRATION DETAILS

Particulars of the flow rate calibration scheme which may be of special interest to a restricted number of readers are included in this Appendix. Section B-1 gives details of the construction and testing of the variable length capillary damping devices. Section B-2 gives a listing of the program ONRFLO, and Section B-3 presents sample output of program ONRFLO.

B-1 Variable Length Capillary Damping Devices

The problem of oscillating pressures at the traversing Pitot-static tube in the inlet has been described. Pressure oscillations in the tubing were damped with alternating sections of smaller and larger diameter flow passages. Figure B-1 is a picture of such a device. The device consists of three lengths of needle stainless steel tubing, of 0.020 in. inside diameter, which are 4 in., 6 in., and 8 in. long. They are connected as shown to polyethylene tubing by brass "T's." By clamping the tubing at various positions it is possible to obtain total capillary lengths of 4 in., 6 in., 8 in., or 18 in. Figure B-2 is a schematic showing the operation of the device.

Two variable length damping devices were used, one each in the total and static pressure lines from the traversing Pitot-static tube in the inlet. Two effects of these devices were observed on velocity head, the difference between total and static pressure. As the length of capillary tube was increased, the fluctuation of the pressure gauge was decreased. But as the length of capillary tubing was increased, the time to come to a steady reading was also increased. Table B-1 presents the results of tests of various lengths of capillary tubing.

Immediately before taking the velocity head reading the traverse probe was placed at a new radial position. This task took about 20 sec. to perform. The best precision for a time to damp of 20 sec or less was used. The combination of a total pressure capillary length of 18 in. and a static pressure length of 8 in. satisfied this requirement.

Later in the investigation, when the simplified pressure selection system was used, it became possible to use both 18 in. lengths of tubing and have a time to damp to a steady reading of less than 20 sec. It appears that the 12-channel pressure scanners increased the time required for the system to stabilize. This was probably due to admittance of air from other channels during sequencing of the scanner. However as the survey progressed, flow rate measurements were made at lower flow rates. As the machine was operated nearer to the stalled condition, greater pressure oscillations were observed. The meter precision was no better than ± 15 counts, and sometimes as much as ± 50 counts.

B-2 Program ONRFLO

The flow rate calculations described in Section 3 were accomplished by program ONRFLO which is included as Table B-2. Since the calculations are straightforward and have been described earlier, they will not be repeated here.

The input format is as follows:

Card 1:	NCASE	run number (arbitrary)
(I7,3F7.2)	PBAR	reading of barometer (in.)
	TBAR	temperature at barometer (°F)
	TO	temperature at inlet screen (°F)
Cards 2, 3, and 4: (8F10.2)	R	the 23 radii at which data were taken (17.75, 17.50, ...4.00, 0.00, 4.00...17.50,17.75) (in.)
Cards 5 through 50:	QI	velocity head in inlet duct (counts)
(4F7.0)	PSI	static pressure with reference to atmospheric in inlet duct (counts)
	QO	velocity head at permanent Pitot-static tube (counts)
	PSO	static pressure with reference to atmospheric at permanent Pitot-static tube (counts)

The radii of cards 2, 3 and 4 are repeated internally to account for the cross traverse. Cards 5 through 27 introduce measurements made at the data points for one traverse, and data for the cross traverse are introduced on cards 28 through 50.

B-3 Output of ONRFLO

Table B-3 is a sample of the output of ONRFLO. It is for the final calibration, run 14. The first data block is a list of input data. For each point on the two traverses, QI, PSI, QO, and PSO are listed. The second data block is a list of computed velocities VI, VO, and VIAD. The third block shows how the "no boundary layer" flow rate, VFT, is computed by summing the product of VA and A. The fourth block shows how the flow rate deficiency, VFD, is computed. It lists the inputs to and outputs from SUBROUTINE QTFE, which performs the integration by the trapezoidal rule. The final statements list the final computed flow rate VFC and the final calibration constant CCC.

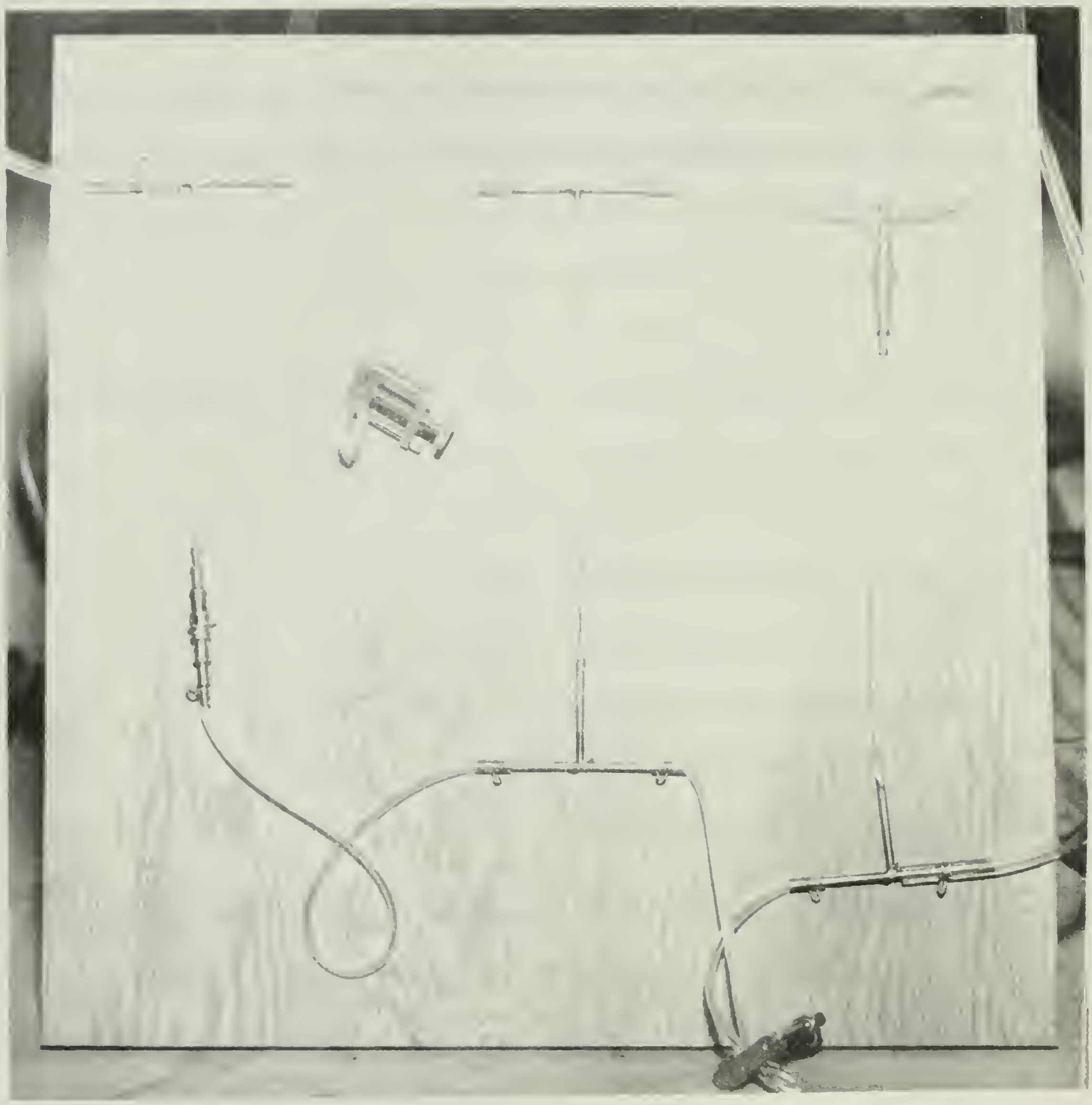

FIGURE B-1 VARIABLE LENGTH CAPILLARY DAMPING DEVICE

VARIABLE LENGTH CAPILLARY
DAMPING DEVICE
OPERATION

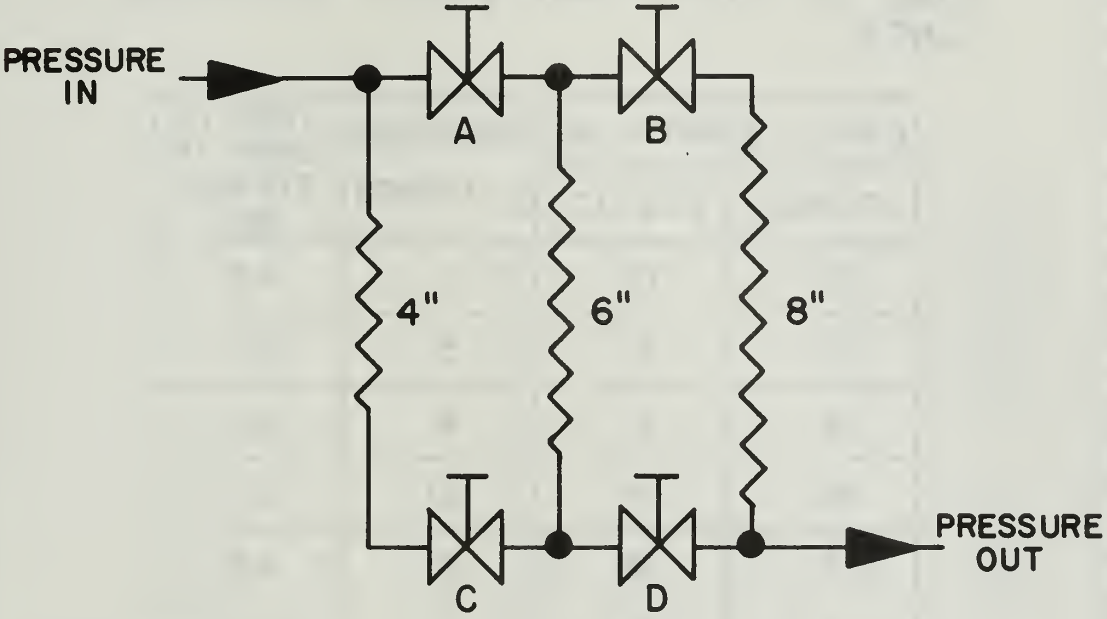

MATERIALS

CAPILLARY: NEEDLE STAINLESS TUBE 0.020" I.D.
VALVE: POLYETHYLENE TUBE & LAB CLAMPS.

CAP. LENGTH DESIRED	VALVES			
	A	B	C	D
4"	CLOSED	CLOSED	OPEN	OPEN
6"	OPEN	CLOSED	CLOSED	OPEN
8"	OPEN	OPEN	CLOSED	CLOSED
18"	CLOSED	OPEN	OPEN	CLOSED

FIG. B-2

PRECISION & TIME TO DAMP FOR VARIOUS LENGTHS OF CAPILLARY TUBE IN TOTAL AND STATIC PRESSURE LINES.

CAP. LENGTH IN.		PRECISION, ± COUNTS	TIME TO DAMP TO STEADY, SEC.
TOTAL	STATIC		
18	18	1	45
18	8	5	20
18	6	8	10
18	4	10	5
8	18	5	45
8	8	5	35
8	6	10	20
8	4	10	5
6	18	5	30
6	8	10	15
6	6	10	10
6	4	20	10
4	18	15	30
4	8	25	15
4	6	30	10
4	4	40	8

TABLE BI

```
FORTRAN IV G LEVEL 0, MOD 0                MAIN                DATE = 67228            22/56/36

          DIMENSION QI(50),PSI(50),QO(50),PSO(50),VI(50),VO(50),VIAD(50),A(5
         1),VA(5),VF(5),R(50),V3(10),VD(10),VR(10),VFD(10)
    11    READ(5,700,END=999)(NCASE,PBAR,TBAR,TO)
          WRITE(6,749)
          WRITE(6,750)
          WRITE(6,751) NCASE
          READ(5,701)(R(N),N=1,23)
          DO 1 N=24,46
          K=N-23
     1    R(N)=R(K)
          DO 2 N=1,46
          READ(5,702)(QI(N),PSI(N),QO(N),PSO(N))
     2    WRITE(6,752)(R(N),QI(N),PSI(N),QO(N),PSO(N))
          C1=.49280 + TBAR*.5/10000
          PA=PBAR*C1*144.
          TTO=TO + 459.7
          C2=SQRT((2.*2115.36)/(.002378*518.7))
          C3=240.329
          DO 3 N=1,46
          PI=PA-PSI(N)/C3
          QI1 = QI(N)/C3
          VI(N)=C2*SQRT(TTO)* SQRT(QI1/PI)
          PO=PA-PSO(N)/C3
          QO1 = QO(N)/C3
     3    VO(N)=C2 * SQRT(TTO)* SQRT(QO1/PO)
          VOT=0.
          DO 4 N=1,46
     4    VOT=VOT+VO(N)
          VOAV = VOT/46.
          DO 5 N=1,46
     5    VIAD(N)=VI(N) * VOAV  /VO(N)
          WRITE(6,753)
          DO 6 N=1,23
     6    WRITE(6,754)(R(N),VI(N),VO(N),VIAD(N))
          WRITE(6,755)
          DO 7 N=24,46
     7    WRITE(6,754)(R(N),VI(N),VO(N),VIAD(N))
          A(1)=3.14159 *2.*2./144.
          A(2)=2.*3.14159*4.0*4./144.
          A(3)=2.*3.14159*8.0*4./144.
          A(4)=2.*3.14159*12.*4./144.
          A(5)=2.*3.14159*16.*4./144.
          VA(1) = (VIAD(12) + VIAD(35))/2.
          VA(2) = (VIAD(11) + VIAD(13) + VIAD(34) + VIAD(36))/4.
          VA(3) = (VIAD(10) + VIAD(14) + VIAD(33) + VIAD(37))/4.
          VA(4) = (VIAD( 9) + VIAD(15) + VIAD(32) + VIAD(38))/4.
          VA(5) = (VIAD( 8) + VIAD(16) + VIAD(31) + VIAD(39))/4.
          WRITE(6,749)
```

Table B-2. Listing of Program ONRFLO

```
      WRITE(6,756)
      VFT=0.
      DO 8 N=1,5
      VF(N)=A(N)*VA(N)
      VFT=VFT+VF(N)
    8 WRITE(6,757)(N,VA(N),A(N),VF(N),VFT)
      CC=VFT/VOAV
      WRITE(6,758)(VFT,VOAV,CC)
      VB(1)=VA(5)
      VB(2) = (VIAD( 7) + VIAD(17) + VIAD(30) + VIAD(40))/4.
      VB(3) = (VIAD( 6) + VIAD(18) + VIAD(29) + VIAD(41))/4.
      VB(4) = (VIAD( 5) + VIAD(19) + VIAD(28) + VIAD(42))/4.
      VB(5) = (VIAD( 4) + VIAD(20) + VIAD(27) + VIAD(43))/4.
      VB(6) = (VIAD( 3) + VIAD(21) + VIAD(26) + VIAD(44))/4.
      VB(7) = (VIAD( 2) + VIAD(22) + VIAD(25) + VIAD(45))/4.
      VB(8) = (VIAD( 1) + VIAD(23) + VIAD(24) + VIAD(46))/4.
      VB(9)=0.
      DO 9 N=1,9
    9 VD(N)=VA(5)-VB(N)
      DO 10 N=1,8
      K=15+N
   10 VR(N)=VD(N)*R(K)*2.*3.14159/12.
      VR(9)=VD(9)*18.*2.*3.14159/12.
      H=.25/12.
      NDIM=9
      CALL QTFE(H,VR,VFD,NDIM)
      WRITE(6,755)
      WRITE(6,760)
      DO 12 N=1,8
      K=15+N
   12 WRITE(6,761)(R(K),VD(N),VR(N),VFD(N))
      VFF = VFD(9)
      VFC=VFT-VFF
      CCC=VFC/VOAV
      WRITE(6,759)(VFF,VFC,CCC)
  700 FORMAT(I7,3F7.2)
  701 FORMAT(8F10.2)
  702 FORMAT(4F7.0)
  749 FORMAT(1H1)
  750 FORMAT(23X,52HNAVAL POSTGRADUATE SCHOOL TURBOPROPULSION LABORATORY
     1///23X53HO.N.R. 3-STAGE AXIAL COMPRESSOR FLOW RATE CALIBRATION//)
  751 FORMAT(13X,18HINPUT DATA FOR RUN13,27X,15HN = 1200 R.P.M.//5X,11HR
     1ADIUS FROM,7X,14HINLET VELOCITY,7X,12HINLET STATIC,7X,14HPROBE VEL
     2OCITY,7X,12HPROBE STATIC/1X,18HCENTERLINE, INCHES,5X,12HHEAD, COUN
     3TS,6X,16HPRESSURE, COUNTS,6X,12HHEAD, COUNTS,6X,16HPRESSURE, COUNT
     4S)
  752 FORMAT(F13.2,4F20.0)
  753 FORMAT(1H1,21X,38HCALCULATED VELOCITIES, FEET PER SECOND//5X,11HRA
```

Table B-2. Listing of Program ONRFLO (cont.)

```
FORTRAN IV G LEVEL 0, MOD 0                 MAIN                 DATE = 67228          22/56/36

                    1DIUS FROM,12X,5HINLET,14X,5HPROBE,11X,14HADJUSTED INLET/1X,18HCENT
                    2ERLINE, INCHES,7X,8HVELOCITY,12X,8HVELOCITY,12X,8HVELOCITY/)
  0091         754 FORMAT(F13.2,3F20.3)
  0092         755 FORMAT(//)
  0093         756 FORMAT(//4X,74HCALCULATION OF VOLUME FLOW RATE ASSUMING NO BOUNDAR
                    1Y LAYER EXISTS IN INLET//3X,6HSECTOR,4X16HAVERAGE VELOCITY,8X,5H A
                    2REA,4X,16HSECTOR FLOW RATE,5X,15HTOTAL FLOW RATE/)
  0094         757 FORMAT(I6,4F18.3)
  0095         758 FORMAT(//1X,19HVOLUME FLOW RATE = ,F10.3,5X,25HAVERAGE PROBE VELOC
                    1ITY = ,F8.3//1X,48HTHE "NO BOUNDARY LAYER" CALIBRATION CONSTANT IS
                    2 ,F8.4,2X,39HCUBIC FEET PER SECOND / FOOT PER SECOND)
  0096         759 FORMAT(//1X,25HVOLUME FLOW DEFICIENCY = ,F8.3,5X,25HFINAL VOLUME F
                    1LOW RATE = ,F10.3//1X,34HTHE FINAL CALIBARTION CONSTANT IS ,F8.4,2
                    2X,39HCUBIC FEET PER SECOND / FOOT PER SECOND)
  0097         760 FORMAT(9X,55HCALCULATION OF VOLUME FLOW DEFICIENCY IN BOUNDARY LAY
                    1ER//5X,11HRADIUS FROM,10X,8HVELOCITY,12X,8HVALUE OF,12X,9HFLOW RAT
                    2E/1X,18HCENTERLINE,INCHES,6X,11HDEFICIENCY ,10X,9HINTEGRAND,11X,10
                    3HDEFICIENCY//)
  0098         761 FORMAT(F13.2,3F20.3)
  0099             GO TO 11
  0100         999 RETURN
  0101             END
```

```
FORTRAN IV G LEVEL 0, MOD 0                 QTFE                 DATE = 67228          22/56/36

  0001               SUBROUTINE QTFE(H,Y,Z,NDIM)
  0002               DIMENSION Y(9),Z(9)
  0003               SUM2=0.
  0004               IF(NDIM-1)4,3,1
  0005             1 HH=.5*H
  0006               DO 2 N=2,NDIM
  0007               I=N
  0008               SUM1=SUM2
  0009               SUM2=SUM2+HH*(Y(I)+Y(I-1))
  0010             2 Z(I-1)=SUM1
  0011             3 Z(NDIM)=SUM2
  0012             4 RETURN
  0013               END
```

Table B-2. Listing of Program ONRFLO (cont.)

```
                         NAVAL POSTGRADUATE SCHOOL TURBOPROPULSION LABORATORY

                         C.N.R. 3-STAGE AXIAL COMPRESSOR FLOW RATE CALIBRATION

          INPUT DATA FOR RUN 14                                N = 1200 R.P.M.

     RADIUS FROM          INLET VELOCITY         INLET STATIC          PROBE VELOCITY          PROBE STATIC
  CENTERLINE, INCHES       HEAD, COUNTS       PRESSURE, COUNTS          HEAD, COUNTS        PRESSURE, COUNTS
        17.75                  545.                 825.                   1785.                  2465.
        17.50                  605.                 865.                   1795.                  2490.
        17.25                  665.                 860.                   1775.                  2480.
        17.00                  685.                 870.                   1755.                  2495.
        16.75                  705.                 845.                   1780.                  2485.
        16.50                  700.                 845.                   1800.                  2475.
        16.25                  700.                 835.                   1790.                  2515.
        16.00                  695.                 830.                   1775.                  2475.
        12.00                  720.                 875.                   1785.                  2490.
         8.00                  725.                 895.                   1780.                  2495.
         4.00                  715.                 915.                   1775.                  2505.
         0.0                   750.                 905.                   1780.                  2480.
         4.00                  740.                 935.                   1800.                  2450.
         8.00                  710.                 970.                   1770.                  2495.
        12.00                  750.                 880.                   1760.                  2470.
        16.00                  725.                 860.                   1795.                  2455.
        16.25                  700.                 855.                   1775.                  2470.
        16.50                  695.                 835.                   1780.                  2480.
        16.75                  700.                 830.                   1795.                  2460.
        17.00                  670.                 840.                   1845.                  2485.
        17.25                  635.                 830.                   1780.                  2455.
        17.50                  585.                 845.                   1775.                  2505.
        17.75                  525.                 815.                   1760.                  2480.
        17.75                  515.                 785.                   1785.                  2480.
        17.50                  655.                 835.                   1790.                  2465.
        17.25                  685.                 800.                   1795.                  2470.
        17.00                  705.                 815.                   1785.                  2480.
        16.75                  705.                 840.                   1780.                  2450.
        16.50                  705.                 850.                   1775.                  2470.
        16.25                  710.                 860.                   1780.                  2465.
        16.00                  720.                 825.                   1810.                  2450.
        12.00                  735.                 870.                   1830.                  2465.
         8.00                  735.                 880.                   1790.                  2475.
         4.00                  760.                 935.                   1765.                  2485.
         0.0                   730.                 875.                   1800.                  2465.
         4.00                  730.                 820.                   1645.                  2450.
         8.00                  730.                 930.                   1665.                  2465.
        12.00                  710.                 835.                   1735.                  2440.
        16.00                  685.                 860.                   1780.                  3475.
        16.25                  680.                 835.                   1775.                  2440.
        16.50                  700.                 835.                   1790.                  2455.
        16.75                  695.                 845.                   1780.                  2465.
        17.00                  670.                 815.                   1805.                  2465.
        17.25                  645.                 845.                   1810.                  2465.
        17.50                  625.                 855.                   1800.                  2445.
        17.75                  545.                 885.                   1795.                  2475.
```

Table B-3. Sample Output of Program ONRFLO-Input for Run 14

```
                      CALCULATED VELOCITIES, FEET PER SECOND
   RADIUS FROM            INLET              PROBE          ADJUSTED INLET
CENTERLINE, INCHES       VELOCITY           VELOCITY           VELOCITY

      17.75               44.116             79.968             44.052
      17.50               46.483             80.193             46.285
      17.25               48.733             79.745             48.799
      17.00               49.461             79.295             49.809
      16.75               50.177             79.857             50.174
      16.50               49.999             80.304             49.717
      16.25               49.998             80.084             49.854
      16.00               49.819             79.744             49.886
      12.00               50.709             79.970             50.635
       8.00               50.886             79.858             50.882
       4.00               50.535             79.746             50.602
       0.0                51.757             79.857             51.753
       4.00               51.412             80.302             51.124
       8.00               50.361             79.633             50.499
      12.00               51.755             79.406             52.046
      16.00               50.884             80.191             50.669
      16.25               49.999             79.744             50.067
      16.50               49.819             79.857             49.816
      16.75               49.998             80.191             49.786
      17.00               48.915             81.302             48.043
      17.25               47.620             79.855             47.618
      17.50               45.707             79.746             45.768
      17.75               43.299             79.407             43.541

      17.75               42.883             79.969             42.820
      17.50               48.364             80.080             48.227
      17.25               49.458             80.192             49.248
      17.00               50.175             79.969             50.102
      16.75               50.177             79.854             50.175
      16.50               50.177             79.744             50.245
      16.25               50.355             79.856             50.353
      16.00               50.707             80.525             50.283
      12.00               51.235             80.969             50.527
       8.00               51.235             80.080             51.089
       4.00               52.102             79.520             52.319
       0.0                51.060             80.303             50.773
       4.00               51.058             76.767             53.110
       8.00               51.063             77.233             52.795
      12.00               50.354             78.838             51.002
      16.00               49.461             79.935             49.410
      16.25               49.279             79.741             49.347
      16.50               49.998             80.079             49.856
      16.75               49.820             79.856             49.817
      17.00               48.914             80.414             48.572
      17.25               47.994             80.526             47.593
      17.50               47.245             80.301             46.980
      17.75               44.119             80.192             43.932
```

Table B-4. Sample Output of Program ONRFLO-Velocities for Run 14

```
  CALCULATION OF VOLUME FLOW RATE ASSUMING NO BOUNDARY LAYER EXISTS IN INLET
 SECTOR    AVERAGE VELOCITY          AREA    SECTOR FLOW RATE     TOTAL FLOW RATE

   1            51.263              0.087          4.474               4.474
   2            51.789              0.698         36.155              40.629
   3            51.316              1.396         71.651             112.280
   4            51.052              2.094        106.924             219.203
   5            50.062              2.793        139.800             359.003

VOLUME FLOW RATE =    359.003     AVERAGE PROBE VELOCITY =   79.852
THE "NO BOUNDARY LAYER" CALIBRATION CONSTANT IS   4.4959  CUBIC FEET PER SECOND / FOOT PER SECOND


      CALCULATION OF VOLUME FLOW DEFICIENCY IN BOUNDARY LAYER
   RADIUS FROM          VELOCITY              VALUE OF            FLOW RATE
CENTERLINE,INCHES,     DEFICIENCY            INTEGRAND           DEFICIENCY

       16.00              0.0                  0.0                 0.0
       16.25              0.157                1.337               0.014
       16.50              0.153                1.325               0.042
       16.75              0.074                0.649               0.062
       17.00              0.931                8.286               0.155
       17.25              1.743               15.785               0.406
       17.50              3.247               29.753               0.880
       17.75              6.476               60.184               1.817

VOLUME FLOW DEFICIENCY =    7.359    FINAL VOLUME FLOW RATE =    351.644
THE FINAL CALIBARTION CONSTANT IS   4.4037  CUBIC FEET PER SECOND / FOOT PER SECOND
```

Table B-5. Sample Output of Program ONRFLO-Calibration Constant for Run 14

APPENDIX C

PERFORMANCE MEASUREMENTS

It was decided to take flow measurements at the mean streamline, using the radial survey holes. The assumption was made that measurements made at this point accurately represented the flow in the entire flow annulus. The truth of the assumption is verified in Section C-1. Section C-2 presents details concerning the data reduction program ONRETA.

C-1 Verification of Assumptions

The assumption that measurements made at the mean streamline using the radial survey holes accurately represent the flow in the entire flow annulus was verified in three ways. The total pressure measured at the mean radius was shown to be nearly equal to the integrated average of total pressure at each radius. It was demonstrated that the total pressure measured at the peripheral location of a radial survey hole was nearly equal to the integrated average of total pressure at each peripheral location in a blade channel. The flow was shown to be nearly axisymmetric.

Concerning the radial variation of total pressure, the existence of a boundary layer at the outer radius in the inlet has already been shown. It was further shown that a boundary layer existed ahead of the first stage and behind the last stage. With the stator stagger angle at 27.8° and the flow rate at about 400 ft^3/sec., a radial traverse was made at the radial survey hole labeled $37^{\circ}27'30''$ in survey plane 8 of Fig. 7. Data points were established each 0.3 in.

from a radius of 11.1 in. to 18.0 in. After recording the barometric pressure P_{Bar} and ambient temperature T_o the following measurements were taken:

P_{td} - total pressure with reference to atmospheric after third stator (counts)

P_{sd} - static pressure with reference to atmospheric after third stator (counts)

q_d - velocity head after the third stator (counts)

The total pressure at the inner radius could not be measured but was assumed to be the static pressure at 11.1 in. With the relations listed on p. 35 these measuring data establish the following quantities:

$$P_A = P_{Bar} \ (71.467) \qquad \text{(psfa)} \qquad (1)$$

$$T_{to} = T_o + 459.7 \qquad ({}^{o}\text{R}) \qquad (2)$$

$$P_{tda} = P_A + \frac{P_{td}}{240.423} \qquad \text{(psfa)} \qquad (3)$$

$$P_{sda} = P_A + \frac{P_{sd}}{240.423} \qquad \text{(psfa)} \qquad (3)$$

With the assumption that the total temperature after the third stator T_{td} is nearly equal to the inlet total temperature T_{to}

$$\rho_d = \frac{0.002378 \ P_{sda} \ 518.7}{(14.696)(144) \quad T_{to}} = \frac{P_{sda}}{T_{to}} \left(5.82 \times 10^{-4}\right) (\text{lb sec}^2/\text{ft}^4) \qquad (4)$$

$$q_{d1} = \frac{q_d}{240.423} \qquad \text{(psf)} \qquad (5)$$

$$V_d = \sqrt{\frac{2\, q_{d1}}{\rho_d}} \qquad \text{(ft/sec)} \qquad (6)$$

The average total pressure was calculated from the integral expression

$$\overline{P_{tda}} = \frac{\int_{10.8}^{18.0} 2\pi\, V_d \frac{r}{12}\, P_{tda} \frac{dr}{12}}{\int_{10.8}^{18.0} 2\pi\, V_d \frac{r}{12} \frac{dr}{12}}$$

Both integrations were performed by the trapezoidal rule. Figure C-1 is a graphical representation of the integration. The integrated average total pressure $\overline{P_{tda}}$ was 2184.20 lb/ft^2 while the total pressure measured at the mean streamline was 2184.34 lb/ft^2. The relative error between the two pressures is 0.006 per cent. A second radial survey was made at the radial survey hole labeled 149°57'30" in the plane called S. P. 8 on Fig. 7. The integrated average pressure for this survey was 2183.92 lb/ft^2. The total pressure measured at the mean radial position was 2184.32 lb/ft^2. The relative error between the two pressures was 0.018 per cent. Since the pressure measured at the mean radius was nearly equal to the integrated average of pressure at each radial location, mean streamline values were used to measure compressor performance.

The traverse carriage was used for peripheral surveys. Since it would be necessary to remove the first stage rotor to survey in the axial plane ahead of the first stage, the investigation was confined to the plane behind the third stage stator where measurements could be made simply. The locations of the radial survey holes with reference to the indicated meridional angle of the carriage are shown in Fig. 23.

There are 32 stator blades. Each blade channel is 11.25° in peripheral direction. With the stator stagger angle at 27.8° a peripheral survey was made at the mean radius, 14.4 in. The average reading over the entire 15° of carriage travel was 9256 counts. The reading taken at the radial survey hole marked 37°27'30" on Fig. 7 was 9246 counts, a relative error of 0.11 per cent. The average over the first 11.25° of carriage travel, representing one blade channel, was 9218 counts, a relative error of 0.30 per cent. Figure C-2 illustrates the results of this mean radius survey. A second survey was conducted near the hub at a radius of 11.2 in. The average pressure reading of the traverse was 9532.47 counts. The pressure measurement at the radial survey hole was 9569.23 counts. A relative error of 0.36 per cent existed between the two pressures. On the basis of the surveys made behind the third stage stator the measurements taken at the radial survey taps were accepted as accurately representing the flow in the entire blade channel.

An investigation of the axisymmetry of the flow was conducted. The results are tabulated in Table C-1. The total pressure behind the inlet guide vanes, P_{tig}, was measured at eight different radial survey holes in plane S. P. 2 of Fig. 7. The average reading of P_{tig} was 578.1 counts. The nearest reading to the average was 573.9 counts, taken at the hole labeled 33°45'. This hole was used for all readings of P_{tig}. The relative error was 0.73 per cent. The average of readings taken behind the third stage stator P_{td} was 10, 821.5 counts. The nearest reading to the average was 10, 810 counts, taken at the hole marked 37°27'30" on Fig. 7. This hole was used for all readings of P_{td}. The relative error was 0.10 per cent. Within the measurement capability of the instrument, the flow was considered axisymmetric and the most representative readings have been used.

C-2 Program ONRETA

The data reduction described in Section 4 was accomplished by Program ONRETA (Table C-2). Since the calculations are straightforward and have been described in the body of the thesis, they will not be repeated here.

The input format is as follows:

Card 1:	NCASE	run number (arbitrary)
(2I8,4F8.2)	NRUN	number of data points per run
	PBAR	reading of barometer (in. of Hg)
	TBAR	temperature of barometer ($^{\circ}$F)
	RSTAG	rotor stagger angle (43.8°)
	SSTAG	stator stagger angle (various $^{\circ}$)
Card 2:	TO	temperature at inlet screen ($^{\circ}$F)
(F8.1,4F8.0 F8.1,F8.2)	QO	velocity head at permanent Pitot-static tube (counts)
	PSO	static pressure with reference to atmospheric at permanent Pitot-static tube (counts)
	PTIG	total pressure with reference to atmospheric ahead of first rotor (counts)
	DELP	pressure rise across the 3 stages (counts)
	TACH	reading of the speed counter (rpm)
	TRAW	reading of the torque meter (lb)

Cards 3 through (NRUN - 1): repeat of Card 2 for remaining data points

The first five entries on cards 2 through (NRUN - 1) are the arithmetic average of four readings taken two minutes apart. The last two entries are the average of two readings taken five minutes apart.

The first section of program output is a printout of the input data. The second section is the calculated data for the run. The third section is the calculated nondimensional coefficients.

Tables C-3 through C-13 present the results of runs 1 through 11.

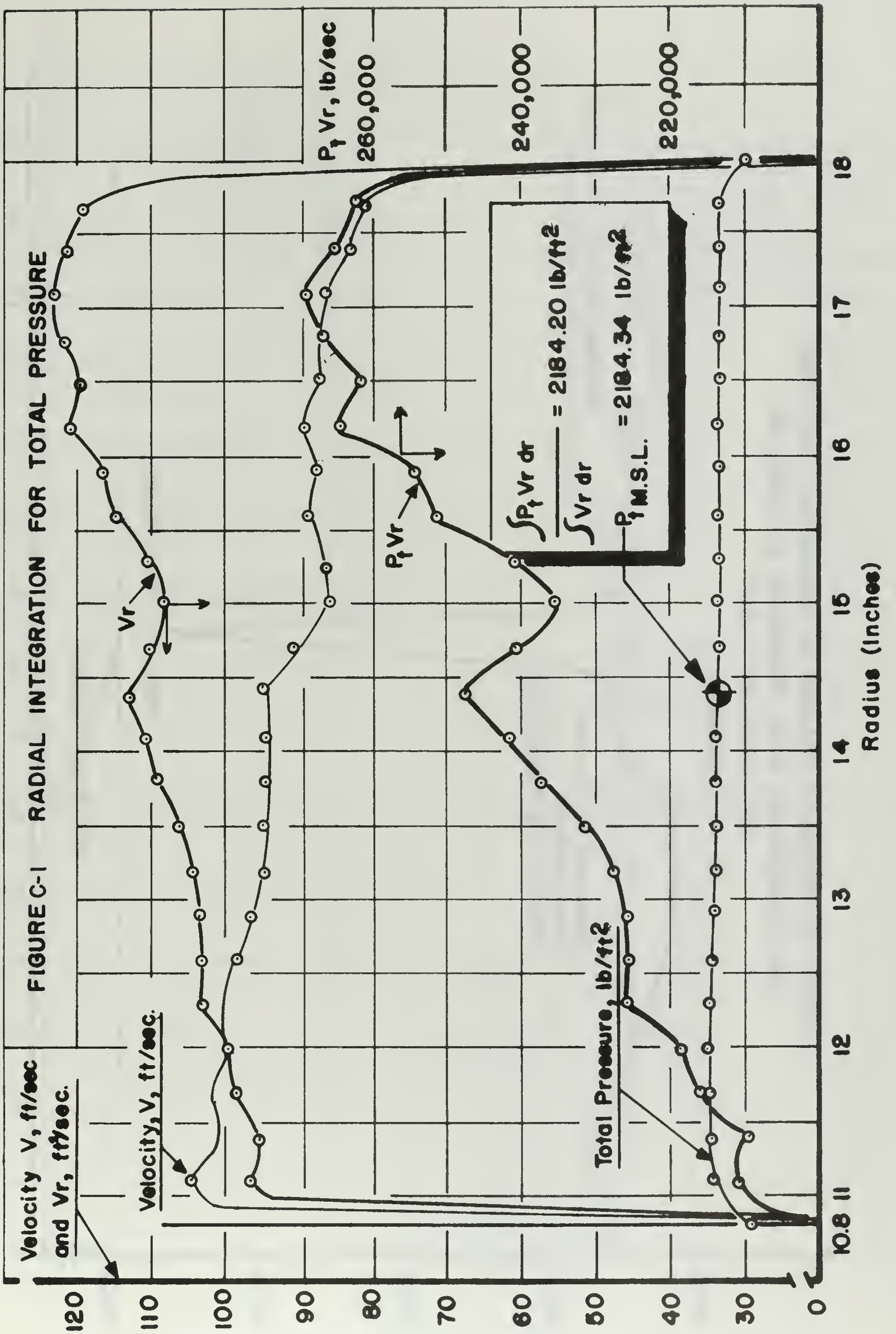

FIGURE C-1 RADIAL INTEGRATION FOR TOTAL PRESSURE

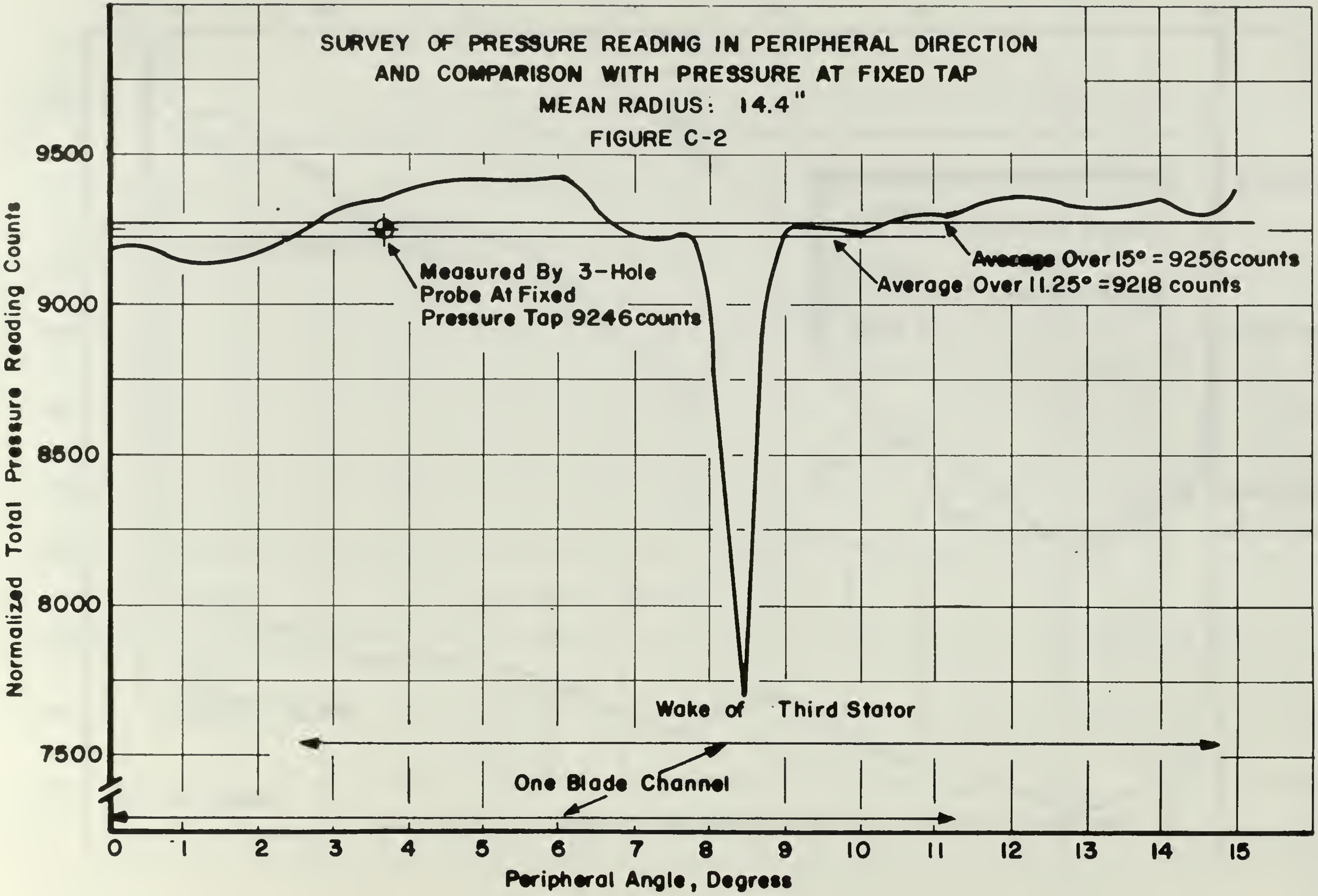

SURVEY OF PRESSURE READING IN PERIPHERAL DIRECTION AND COMPARISON WITH PRESSURE AT FIXED TAP

MEAN RADIUS: 14.4"

FIGURE C-2

TABLE C-1

INVESTIGATION OF AXISYMMETRY OF FLOW

TOTAL PRESSURE BEHIND INLET GUIDE VANES	
RADIAL SURVEY HOLE	READING
26°12'30"	10,860
* 37°27'30"	10,810
93°42'30"	10,810
149°57'30"	10,805
AVERAGE	10,821

* READING CLOSEST TO AVERAGE

TOTAL PRESSURE BEHIND THIRD STAGE STATOR	
RADIAL SURVEY HOLE	READING
11°15'	564.2
22°30'	587.2
* 33°45'	573.9
45°	601.5
56°15'	557.3
67°30'	565.9
76°45'	611.6
88°7'30"	563.2
AVERAGE	578.1

```
      DIMENSION TO(20),QO(20),PSO(20),PTIG(20),DELP(20),TACH(20),TRAW(20
     1),VFC(20),WREM(20),DELTAP(20),PRATS3(20),TRQ(20),OMEG(20),ETAST3(2
     20),PSIAV(30),PHIAV(30),TAUAV(30),PO(30),TTO(30)
   11 READ(5,700,END=9999)(NCASE,NRUN,PBAR,TBAR,RSTAG,SSTAG)
      WRITE(6,750)(NCASE,PBAR,TBAR,RSTAG,SSTAG)
      WRITE(6,1750)
      DO 12 N=1,NRUN
      READ(5,701)(TO(N),QO(N),PSO(N),PTIG(N),DELP(N),TACH(N),TRAW(N))
   12 WRITE(6,751)(TO(N),QO(N),PSO(N),PTIG(N),DELP(N),TACH(N),TRAW(N))
      WRITE(6,752)(NCASE)
      C1=.49280 + TBAR*.5/10000
      C2=SQRT((2.*14.696*144.)/(.002378*518.7))
      C3=240.423
      C4=4.1565
      CCC = 4.4050
      CP = .24
      GAM = 1.4
      EXP2 = (GAM-1.) / GAM
      AANUL=651.4/144.
      RAV=28.8/(2.*12.)
      PA=PBAR*C1*144.
      DO 13 N=1,NRUN
      TTO(N)=TO(N)+459.7
      PO(N)=PA-PSO(N)/C3
      QO1=QO(N)/C3
      VO=C2*SQRT(TTO(N)*QO1/PO(N))
      VFC(N)= CCC * VO
      WDOT = VFC(N)*32.174*.002378*518.7*PA/(TTO(N)*14.696*144.)
      WREM(N) = WDOT * SQRT(TTO(N)) * 144. / PA
      DELTAP(N) = DELP(N)/C3
      PTIGA = PA - PTIG(N)/C3
      PRATS3(N) =( PTIGA    + DELTAP(N))/ PTIGA
      TRQ(N) = TRAW(N)*C4
      OMEG(N) = TACH(N)*2.*3.14159/60.
      A = EXP2 *ALOG(PRATS3(N))
      B = EXP(A) - 1.
      ETAST3(N) =WDOT*CP*TTO(N)*B*778.3/ (TRQ(N) * OMEG(N))
   13 WRITE(6,753)(WREM(N),VFC(N),DELTAP(N),PRATS3(N),TRQ(N),OMEG(N),ETA
     1ST3(N))
      WRITE(6,754)(NCASE)
      DO 14 N=1,NRUN
      UAV=RAV*OMEG(N)
      PHIAV(N)=VFC(N)/(AANUL*UAV)
      RHOI=.002378*PO(N)*518.7/(TTO(N)*14.696*144.)
      PSIAV(N)=DELTAP(N)/(3*RHOI*(UAV**2.))
      TAUAV(N)=PSIAV(N)/ETAST3(N)
   14 WRITE(6,755)(PHIAV(N),ETAST3(N),TAUAV(N),PSIAV(N))
  700 FORMAT(2I8,4F8.2)
```

Table C-2. Listing of Program ONRETA

```
  701 FORMAT(F8.1,4F8.C,F8.1,F8.2)
  750 FORMAT(1H1,23X,52HNAVAL PCSTGRADUATE SCHOOL TURBOPROPULSION LABORA
     1TCRY///23X,51HO.N.R. 3-STAGE AXIAL COMPRESSOR, 3-STAGE EFFICIENCY/
     2/6X,18HINPUT DATA FOR RUNI3,9X,19HBAROMETRIC PRESSUREF7.2,4X,2HATF
     36.1,2X,10HDEGREES,F.//6X,19HROTOR STAGGER ANGLEF5.1,15X,20HSTATOR
     4STAGGER ANGLEF5.1)
 1750 FORMAT(//5X,5HTEMP,,7X,8HVELOCITY,6X,8HPSTATIC,,8X,5HPTIG,,9X,5HDE
     1LP,,6X,10HTACHOMETER,4X,11HTORQUEMETER/4X,7HDEG. F.,4X,12HHEAD, CO
     2UNTS,5X,6HCCUNTS,8X,6HCOUNTS,8X,6HCOUNTS,8X,6HR.P.M.,8X,6HPOUNDS/)
  751 FCRMAT(F9.1,4F14.0,F14.1,F14.2)
  752 FORMAT(///,6X,19HOUTPUT DATA FOR RUNI3,//3X,8HREFERRED,5X,10HVOLFL
     1ORATE,5X,8HPTD-PTIG,6X,8HPRESSURE,7X,6HTORQUE,9X,5HOMEGA,7X,7H3-ST
     2AGE/3X,9HFLOW RATE,4X,11HCU.FT./SEC.3X,10HLB./SQ.FT.,6X,5HRATIO,9
     3X,7HFT.-LB.,6X,9HRAD./SEC.4X,10HEFFICIENCY/)
  753 FORMAT(F10.3,F15.3,F13.3,F14.5,2F14.3,F14.5)
  754 FORMAT(///,6X,37HNON-DIMENSIONAL COEFFICIENTS FOR RUN I3,//5X,16HF
     1LOW COEFFICIENT,7X,18H3-STAGE EFFICIENCY,5X,22HDEFLECTION COEFFICI
     2ENT,4X,20HPRESSURE COEFFICIENT/)
  755 FCRMAT(F16.4,3F25.4)
      GC TO 11
 9999 RETURN
      END
```

Table C-2. Listing of Program ONRETA (cont.)

```
                    NAVAL POSTGRADUATE SCHOOL TURBOPROPULSION LABORATORY

                        O.N.R. 3-STAGE AXIAL COMPRESSOR, 3-STAGE EFFICIENCY
    INPUT DATA FOR RUN  1         BAROMETRIC PRESSURE  30.02    AT   76.7  DEGREES,F.
    ROTOR STAGGER ANGLE 42.8                    STATOR STAGGER ANGLE 27.8

   TEMP,       VELOCITY       PSTATIC,       PTIG,        DELP,       TACHOMETER    TORQUEMETER
  DEG. F.    HEAD, COUNTS     COUNTS        COUNTS       COUNTS        R.P.M.        POUNDS

   72.3         2470.          3240.         835.         8595.        1190.5         30.62
   71.0         2340.          3045.         815.         9265.        1190.0         31.60
   71.4         2135.          2825.         750.        10110.        1189.5         32.87

    OUTPUT DATA FOR RUN  1

 REFERRED     VOLFLORATE      PTO-PTIG      PRESSURE       TORQUE        OMEGA         3-STAGE
 FLOW RATE   CU.FT./SEC.     LB./SQ.FT.      RATIO         FT.-LB.     RAD./SEC.     EFFICIENCY

  48.354       413.005         35.749       1.01668       127.272       124.669       0.92725
  47.055       401.422         38.536       1.01798       131.345       124.616       0.94138
  44.937       383.498         42.051       1.01962       136.624       124.564       0.94319

    NON-DIMENSIONAL COEFFICIENTS FOR RUN   1

   FLOW COEFFICIENT        3-STAGE EFFICIENCY      DEFLECTION COEFFICIENT    PRESSURE COEFFICIENT

       0.6103                  0.9273                    0.2457                     0.2278
       0.5934                  0.9414                    0.2603                     0.2451
       0.5672                  0.9432                    0.2839                     0.2677
```

Table C-3. Output of Program ONRETA, Run 1, Stator Stagger Angle = 27.8°

```
                    NAVAL POSTGRADUATE SCHOOL TURBOPROPULSION LABORATORY

                   O.N.R. 3-STAGE AXIAL COMPRESSOR, 3-STAGE EFFICIENCY
   INPUT DATA FOR RUN  2         BAROMETRIC PRESSURE  30.04    AT  74.2  DEGREES,F.
   ROTOR STAGGER ANGLE 42.8                 STATOR STAGGER ANGLE 27.8

  TEMP,       VELOCITY     PSTATIC,      PTIG,      DELP,     TACHOMETER   TORQUEMETER
 DEG. F.   HEAD, COUNTS     COUNTS      COUNTS     COUNTS       R.P.M.       POUNDS

  70.5        2130.         2870.        727.      10087.      1189.8        32.78
  69.5        2030.         2757.        705.      10545.      1189.4        33.20
  71.0        1948.         2657.        655.      10785.      1188.9        33.40
  70.3        1890.         2553.        565.      11015.      1189.0        33.62

   OUTPUT DATA FOR RUN  2

 REFERRED    VOLFLORATE    PTD-PTIG     PRESSURE     TORQUE      OMEGA       3-STAGE
 FLOW RATE  CU.FT./SEC.  LB./SQ.FT.     RATIO       FT.-LB.    RAD./SEC.   EFFICIENCY

  44.877      382.660      41.955      1.01956     136.250     124.595     0.94128
  43.806      373.177      43.860      1.02045     137.996     124.554     0.94745
  42.908      366.044      44.858      1.02091     138.827     124.501     0.94499
  42.260      360.279      45.815      1.02135     139.742     124.512     0.94325

   NON-DIMENSIONAL COEFFICIENTS FOR RUN  2

  FLOW COEFFICIENT      3-STAGE EFFICIENCY    DEFLECTION COEFFICIENT    PRESSURE COEFFICIENT

       0.5658                0.9413                  0.2831                    0.2664
       0.5519                0.9475                  0.2936                    0.2781
       0.5416                0.9450                  0.3021                    0.2855
       0.5330                0.9433                  0.3086                    0.2911
```

Table C-4. Output of Program ONRETA, Run 2, Stator Stagger Angle = 27.8°

```
                 NAVAL POSTGRADUATE SCHOOL TURBOPROPULSION LABORATORY

                   C.N.R. 3-STAGE AXIAL COMPRESSOR, 3-STAGE EFFICIENCY
   INPUT DATA FOR RUN  3        BAROMETRIC PRESSURE  30.05    AT   74.9  DEGREES,F.
   ROTOR STAGGER ANGLE 42.8                 STATOR STAGGER ANGLE 27.8

  TEMP,       VELOCITY      PSTATIC,       PTIG,        DELP,      TACHOMETER   TORQUEMETER
 DEG. F.   HEAD, COUNTS     COUNTS        COUNTS       COUNTS       R.P.M.        POUNDS

  72.0        1765.         2347.          607.        11027.       1189.0        32.93
  72.3        1570.         2075.          550.        10750.       1189.0        32.13


   OUTPUT DATA FOR RUN  3
 REFERRED    VOLFLORATE    PTD-PTIG     PRESSURE       TORQUE        OMEGA       3-STAGE
 FLOW RATE  CU.FT./SEC.  LB./SQ.FT.      RATIO        FT.-LB.     RAD./SEC.    EFFICIENCY

  40.823      348.579      45.865       1.02137      136.874      124.512      0.93285
  38.491      328.765      44.713       1.02083      133.548      124.512      0.87917


   NON-DIMENSIONAL COEFFICIENTS FOR RUN   3
  FLOW COEFFICIENT      3-STAGE EFFICIENCY     DEFLECTION COEFFICIENT    PRESSURE COEFFICIENT

       0.5157                0.9329                  0.3131                    0.2921
       0.4864                0.8792                  0.3239                    0.2847
```

Table C-5. Output of Program ONRETA, Run 3, Stator Stagger Angle = 27.8°

```
                    NAVAL POSTGRADUATE SCHOOL TURBOPROPULSION LABORATORY

                   C.N.R. 3-STAGE AXIAL COMPRESSOR, 3-STAGE EFFICIENCY

    INPUT DATA FOR RUN  4          BAROMETRIC PRESSURE  29.92    AT   75.6  DEGREES,F.

    ROTOR STAGGER ANGLE 42.8                   STATOR STAGGER ANGLE 23.8

   TEMP,       VELOCITY      PSTATIC,      PTIG,       DELP,      TACHOMETER    TORQUEMETER
  DEG. F.    HEAD, COUNTS     COUNTS       COUNTS      COUNTS       R.P.M.        POUNDS

   74.0         2292.         3140.         780.        9730.       1189.4        33.88
   76.4         2207.         2920.         757.       10350.       1189.1        34.55
   75.2         2073.         2783.         707.       10683.       1188.9        34.85
   75.4         1880.         2520.         657.       10919.       1189.0        33.80
   74.3         1740.         2360.         593.       10743.       1189.5        33.23


    OUTPUT DATA FOR RUN  4

  REFERRED    VOLFLORATE     PTD-PTIG     PRESSURE      TORQUE       OMEGA       3-STAGE
  FLOW RATE   CU.FT./SEC.  LB./SQ.FT.     RATIO        FT.-LB.     RAD./SEC.   EFFICIENCY

   46.655      399.133       40.470      1.01894      140.822      124.554      0.91681
   45.772      392.458       43.049      1.02015      143.607      124.522      0.94022
   44.355      379.880       44.434      1.02080      144.854      124.501      0.93116
   42.229      361.739       45.416      1.02125      140.490      124.512      0.93412
   40.620      347.597       44.684      1.02091      138.120      124.564      0.89788


    NON-DIMENSIONAL COEFFICIENTS FOR RUN   4

   FLOW COEFFICIENT       3-STAGE EFFICIENCY     DEFLECTION COEFFICIENT    PRESSURE COEFFICIENT

        0.5903                  0.9168                  0.2836                    0.2600
        0.5806                  0.9402                  0.2955                    0.2779
        0.5621                  0.9312                  0.3073                    0.2862
        0.5352                  0.9341                  0.3130                    0.2924
        0.5141                  0.8979                  0.3194                    0.2868
```

Table C-6. Output of Program ONRETA, Run 4, Stator Stagger Angle = 23.8°

```
                 NAVAL POSTGRADUATE SCHOOL TURBOPROPULSION LABORATORY

                      O.N.R. 3-STAGE AXIAL COMPRESSOR, 3-STAGE EFFICIENCY
    INPUT DATA FOR RUN  5        BAROMETRIC PRESSURE  30.06    AT  75.6  DEGREES,F.

    ROTOR STAGGER ANGLE 42.8                  STATOR STAGGER ANGLE 23.8

  TEMP,       VELOCITY      PSTATIC,      PTIG,      DELP,     TACHOMETER   TORQUEMETER
 DEG. F.    HEAD, COUNTS     COUNTS       COUNTS     COUNTS      R.P.M.       POUNDS

  73.0         2240.         3075.         750.      10137.      1189.3        34.50
  74.1         2169.         2903.         737.      10587.      1189.0        35.00
  74.5         2021.         2703.         680.      10910.      1188.8        34.85
  75.3         1815.         2460.         655.      10865.      1189.1        33.70
  76.2         1635.         2102.         563.      10550.      1189.5        32.83

    OUTPUT DATA FOR RUN  5

 REFERRED    VOLFLORATE     PTD-PTIG     PRESSURE     TORQUE      OMEGA       3-STAGE
 FLOW RATE   CU.FT./SEC.    LB./SQ.FT.    RATIO       FT.-LB.    RAD./SEC.   EFFICIENCY

  46.012      393.260        42.163      1.01964     143.399     124.543     0.92405
  45.269      387.312        44.035      1.02051     145.477     124.512     0.93676
  43.689      373.932        45.378      1.02114     144.854     124.491     0.93599
  41.393      354.544        45.191      1.02105     140.074     124.522     0.91371
  39.273      336.670        43.881      1.02044     136.458     124.564     0.86446

    NON-DIMENSIONAL COEFFICIENTS FOR RUN   5

   FLOW COEFFICIENT      3-STAGE EFFICIENCY    DEFLECTION COEFFICIENT   PRESSURE COEFFICIENT

        0.5817                0.9240                 0.2913                    0.2691
        0.5730                0.9368                 0.3007                    0.2817
        0.5533                0.9360                 0.3104                    0.2905
        0.5245                0.9137                 0.3168                    0.2895
        0.4979                0.8645                 0.3252                    0.2812
```

Table C-7. Output of Program ONRETA, Run 5, Stator Stagger Angle = 23.8°

```
                    NAVAL POSTGRADUATE SCHOOL TURBOPROPULSION LABORATORY

                    O.N.R. 3-STAGE AXIAL COMPRESSOR, 3-STAGE EFFICIENCY

 INPUT DATA FOR RUN  6         BAROMETRIC PRESSURE  30.04    AT  76.2  DEGREES,F.

 ROTOR STAGGER ANGLE 42.8                      STATOR STAGGER ANGLE 31.8

  TEMP,        VELOCITY        PSTATIC,        PTIG,          DELP,       TACHOMETER     TORQUEMETER
 DEG. F.     HEAD, COUNTS       COUNTS         COUNTS         COUNTS        R.P.M.          POUNDS

  71.8          1978.           2703.           758.           9772.        1191.0          30.55
  73.5          1866.           2515.           633.          10313.        1190.3          31.23
  74.6          1810.           2400.           617.          10627.        1190.6          31.50
  74.9          1675.           2270.           598.          11138.        1190.0          31.90
  74.0          1618.           2190.           570.          11340.        1190.0          31.93
  73.6          1485.           2028.           563.          10913.        1190.3          31.18


 OUTPUT DATA FOR RUN  6

 REFERRED      VOLFLORATE       PTD-PTIG       PRESSURE        TORQUE         OMEGA         3-STAGE
 FLOW RATE    CU.FT./SEC.     LB./SQ.FT.        RATIO          FT.-LB.      RAD./SEC.      EFFICIENCY

 43.235         369.109          40.645        1.01895        126.981        124.721        0.94316
 41.985         359.014          42.895        1.01999        129.807        124.648        0.94696
 41.346         353.910          44.201        1.02060        130.930        124.679        0.95327
 39.769         340.509          46.327        1.02159        132.592        124.616        0.94931
 39.084         334.357          47.167        1.02198        132.717        124.616        0.94797
 37.437         320.150          45.391        1.02115        129.600        124.648        0.89459


 NON-DIMENSIONAL COEFFICIENTS FOR RUN   6

 FLOW COEFFICIENT       3-STAGE EFFICIENCY      DEFLECTION COEFFICIENT     PRESSURE COEFFICIENT

      0.5452                  0.9432                     0.2737                      0.2581
      0.5306                  0.9470                     0.2888                      0.2735
      0.5229                  0.9533                     0.2960                      0.2822
      0.5034                  0.9493                     0.3120                      0.2961
      0.4943                  0.9480                     0.3175                      0.3010
      0.4732                  0.8946                     0.3232                      0.2892
```

Table C-8. Output of Program ONRETA, Run 6, Stator Stagger Angle = 31.8°

```
                    NAVAL POSTGRADUATE SCHOOL TURBOPROPULSION LABORATORY

                  O.N.R. 3-STAGE AXIAL COMPRESSOR, 3-STAGE EFFICIENCY
   INPUT DATA FOR RUN  7          BAROMETRIC PRESSURE  29.88    AT  74.0  DEGREES,F.
   ROTOR STAGGER ANGLE 42.8                   STATOR STAGGER ANGLE 31.8

   TEMP,      VELOCITY       PSTATIC,       PTIG,        DELP,       TACHOMETER     TORQUEMETER
  DEG. F.   HEAD, COUNTS      COUNTS        COUNTS       COUNTS        R.P.M.         POUNDS

   70.0        2331.          3145.          760.         8139.        1191.0          27.73
   71.4        2023.          2755.          734.         9614.        1190.0          30.31
   72.6        1850.          2568.          639.        10431.        1189.9          31.10
   72.0        1764.          2464.          630.        10735.        1189.8          31.55
   71.3        1705.          2393.          626.        11135.        1189.6          31.73
   72.0        1581.          2260.          630.        11419.        1190.2          31.73
   71.9        1484.          2108.          626.        10903.        1190.5          31.11
   71.4        1594.          2276.          630.        11432.        1190.0          31.83
   71.6        1689.          2400.          626.        11071.        1190.0          31.85
   72.0        1806.          2524.          630.        10708.        1191.0          31.48
   71.6        1851.          2610.          639.        10391.        1190.5          31.12
   71.5        1994.          2801.          734.         9588.        1191.0          30.32


   OUTPUT DATA FOR RUN  7

  REFERRED    VOLFLORATE      PTD-PTIG      PRESSURE       TORQUE        OMEGA        3-STAGE
  FLOW RATE   CU.FT./SEC.   LB./SQ.FT.       RATIO        FT.-LB.      RAD./SEC.     EFFICIENCY

   47.087      401.308        33.853        1.01587       115.260       124.721       0.94195
   43.849      374.207        39.988        1.01874       125.983       124.616       0.94901
   41.924      358.187        43.386        1.02033       129.267       124.606       0.95981
   40.934      349.531        44.650        1.02093       131.138       124.595       0.95005
   40.241      343.385        46.314        1.02171       131.886       124.574       0.96252
   38.745      330.838        47.495        1.02226       131.886       124.637       0.95043
   37.532      320.450        45.349        1.02125       129.309       124.669       0.89657
   38.904      332.013        47.550        1.02228       132.301       124.616       0.95198
   40.052      341.869        46.048        1.02158       132.384       124.616       0.94886
   41.421      353.688        44.538        1.02087       130.847       124.721       0.96004
   41.937      357.962        43.220        1.02026       129.350       124.669       0.95447
   43.535      371.567        39.880        1.01869       126.025       124.721       0.93868


   NON-DIMENSIONAL COEFFICIENTS FOR RUN   7

  FLOW COEFFICIENT      3-STAGE EFFICIENCY     DEFLECTION COEFFICIENT     PRESSURE COEFFICIENT

        0.5928                0.9420                  0.2289                     0.2156
        0.5532                0.9490                  0.2693                     0.2556
        0.5295                0.9598                  0.2895                     0.2779
        0.5168                0.9501                  0.3007                     0.2857
        0.5078                0.9625                  0.3075                     0.2960
        0.4890                0.9504                  0.3194                     0.3035
        0.4735                0.8966                  0.3229                     0.2895
        0.4908                0.9520                  0.3190                     0.3037
        0.5054                0.9489                  0.3101                     0.2943
        0.5224                0.9600                  0.2962                     0.2844
        0.5289                0.9545                  0.2892                     0.2761
        0.5488                0.9387                  0.2712                     0.2546
```

Table C-9. Output of Program ONRETA, Run 7, Stator Stagger Angle = 31.8°

```
                  NAVAL POSTGRADUATE SCHOOL TURBOPROPULSION LABORATORY

                  O.N.R. 3-STAGE AXIAL COMPRESSOR, 3-STAGE EFFICIENCY

   INPUT DATA FOR RUN  8        BAROMETRIC PRESSURE  30.01    AT   77.2  DEGREES,F.

   ROTOR STAGGER ANGLE 42.8                 STATOR STAGGER ANGLE 35.8

  TEMP,      VELOCITY      PSTATIC,      PTIG,       DELP,      TACHOMETER   TORQUEMETER
 DEG. F.   HEAD, COUNTS     COUNTS      COUNTS      COUNTS        R.P.M.       POUNDS

  74.9        2124.         2915.        795.        7550.        1192.0        25.80
  75.1        2016.         2723.        710.        8384.        1192.0        27.06
  76.0        1882.         2550.        665.        9122.        1191.5        28.27

   OUTPUT DATA FOR RUN  8

 REFERRED    VOLFLORATE     PTO-PTIG     PRESSURE     TORQUE       OMEGA        3-STAGE
 FLOW RATE   CU.FT./SEC.   LB./SQ.FT.     RATIO       FT.-LB.    RAD./SEC.    EFFICIENCY

  44.832      383.855       31.403       1.01465     107.238      124.826       0.89788
  43.669      373.969       34.872       1.01627     112.475      124.826       0.92550
  42.186      361.569       37.941       1.01770     117.504      124.773       0.93184

   NON-DIMENSIONAL COEFFICIENTS FOR RUN   8

  FLOW COEFFICIENT       3-STAGE EFFICIENCY     DEFLECTION COEFFICIENT    PRESSURE COEFFICIENT

      0.5665                  0.8979                   0.2233                   0.2005
      0.5519                  0.9255                   0.2406                   0.2226
      0.5338                  0.9318                   0.2605                   0.2428
```

Table C-10. Output of Program ONRETA, Run 8, Stator Stagger Angle = 35.8°

```
               NAVAL POSTGRADUATE SCHOOL TURBOPROPULSION LABORATORY

                 O.N.R. 3-STAGE AXIAL COMPRESSOR, 3-STAGE EFFICIENCY
   INPUT DATA FOR RUN  9        BAROMETRIC PRESSURE  29.99    AT  76.2  DEGREES,F.
   ROTOR STAGGER ANGLE 42.8                 STATOR STAGGER ANGLE 35.8

  TEMP,       VELOCITY       PSTATIC,       PTIG,        DELP,      TACHOMETER   TORQUEMETER
 DEG. F.    HEAD, COUNTS      COUNTS        COUNTS       COUNTS       R.P.M.       POUNDS

  71.3         1611.          2359.         645.        10028.       1191.0        29.54
  73.4         1599.          2156.         654.        10665.       1191.0        30.06
  74.8         1503.          2044.         689.        11141.       1191.0        30.33
  75.0         1405.          1928.         629.        11290.       1191.0        30.24
  72.8         1357.          1861.         581.        11405.       1191.0        30.28
  71.9         1211.          1665.         520.        10406.       1191.0        29.37
  74.2         1356.          1866.         516.        11340.       1191.0        30.22
  75.0         1405.          1933.         524.        11200.       1191.0        30.32
  73.9         1505.          2056.         543.        11019.       1191.0        30.30
  72.5         1589.          2191.         576.        10619.       1191.0        30.06
  72.7         1775.          2416.         628.         9774.       1191.5        29.21
  72.8         1891.          2564.         671.         9128.       1191.0        28.29


   OUTPUT DATA FOR RUN  9

 REFERRED    VOLFLORATE     PTD-PTIG       PRESSURE       TORQUE       OMEGA        3-STAGE
 FLOW RATE   CU.FT./SEC.   LB./SQ.FT.       RATIO         FT.-LB.     RAD./SEC.    EFFICIENCY

  39.038      333.122        41.710        1.01947       122.783      124.721      0.90300
  38.885      332.469        44.359        1.02071       124.944      124.721      0.94143
  37.695      322.721        46.339        1.02164       126.067      124.721      0.94584
  36.442      312.046        46.959        1.02192       125.693      124.721      0.92940
  35.811      306.018        47.437        1.02214       125.859      124.721      0.91932
  33.824      288.788        43.282        1.02020       122.076      124.721      0.81657
  35.758      306.308        47.167        1.02201       125.609      124.721      0.91669
  36.442      312.047        46.585        1.02174       126.025      124.721      0.91941
  37.721      322.668        45.832        1.02139       125.942      124.721      0.93602
  38.764      331.158        44.168        1.02062       124.944      124.721      0.93361
  40.979      350.147        40.653        1.01898       121.411      124.773      0.93529
  42.303      361.493        37.966        1.01773       117.587      124.721      0.93190


   NON-DIMENSIONAL COEFFICIENTS FOR RUN  9

  FLOW COEFFICIENT      3-STAGE EFFICIENCY     DEFLECTION COEFFICIENT    PRESSURE COEFFICIENT

      0.4920                 0.9030                  0.2933                   0.2649
      0.4911                 0.9414                  0.3003                   0.2827
      0.4767                 0.9458                  0.3130                   0.2960
      0.4609                 0.9294                  0.3228                   0.3000
      0.4520                 0.9193                  0.3283                   0.3018
      0.4266                 0.8166                  0.3365                   0.2748
      0.4524                 0.9167                  0.3282                   0.3009
      0.4609                 0.9194                  0.3237                   0.2976
      0.4766                 0.9360                  0.3123                   0.2923
      0.4891                 0.9336                  0.3010                   0.2810
      0.5170                 0.9353                  0.2766                   0.2587
      0.5339                 0.9319                  0.2596                   0.2419
```

Table C-11. Output of Program ONRETA, Run 9, Stator Stagger Angle = 35.8°

```
                    NAVAL POSTGRADUATE SCHOOL TURBOPROPULSION LABORATORY

                 O.N.R. 3-STAGE AXIAL COMPRESSOR, 3-STAGE EFFICIENCY
      INPUT DATA FOR RUN 10          BAROMETRIC PRESSURE  29.88    AT   74.0  DEGREES,F.
      ROTOR STAGGER ANGLE 42.8                   STATOR STAGGER ANGLE 39.8

   TEMP,       VELOCITY        PSTATIC,        PTIG,         DELP,       TACHOMETER     TORQUEMETER
 DEG. F.    HEAD, COUNTS       COUNTS         COUNTS        COUNTS        R.P.M.          POUNDS

   72.0         2015.           2675.          430.          6986.        1193.0          23.62
   73.0         1836.           2514.          361.          7579.        1193.0          24.82
   71.9         1766.           2343.          370.          8488.        1191.0          26.17
   72.9         1653.           2198.          324.          9138.        1191.0          27.06
   72.5         1500.           2040.          296.          9794.        1191.0          27.84
   72.5         1403.           1899.          298.         10304.        1191.0          28.28
   73.2         1280.           1733.          258.         10858.        1190.5          28.50
   73.5         1191.           1618.          250.         10931.        1190.0          28.32
   73.7         1059.           1436.          228.          9504.        1191.0          27.48
   73.4         1184.           1589.          243.         10914.        1190.5          28.12
   73.2         1271.           1701.          256.         10756.        1191.5          28.35
   72.6         1398.           1889.          279.         10408.        1191.5          28.32
   73.9         1486.           2025.          314.          9814.        1191.5          27.89
   71.9         1584.           2221.          341.          9203.        1192.0          27.13
   72.3         1759.           2384.          376.          8380.        1192.0          26.00
   72.6         1876.           2500.          383.          7708.        1192.5          25.02
   72.0         1951.           2683.          401.          6860.        1193.0          23.42

      OUTPUT DATA FOR RUN 10

  REFERRED     VOLFLORATE      PTO-PTIG       PRESSURE       TORQUE        OMEGA         3-STAGE
  FLOW RATE   CU.FT./SEC.    LB./SQ.FT.       RATIO        FT.-LB.      RAD./SEC.     EFFICIENCY

   43.759       373.648        29.057        1.01361        98.176       124.930       0.88247
   41.763       356.945        31.524        1.01477       103.164       124.930       0.86985
   40.952       349.654        35.304        1.01654       108.776       124.721       0.90605
   39.615       338.553        38.008        1.01780       112.475       124.721       0.91285
   37.731       322.333        40.737        1.01908       115.717       124.721       0.90485
   36.486       311.694        42.858        1.02007       117.546       124.721       0.90598
   34.844       297.865        45.162        1.02115       118.460       124.669       0.90524
   33.607       287.372        45.466        1.02129       117.712       124.616       0.88514
   31.685       270.982        39.530        1.01851       114.221       124.721       0.74800
   33.507       286.491        45.395        1.02126       116.881       124.669       0.88693
   34.720       296.807        44.738        1.02095       117.837       124.773       0.89753
   36.420       311.165        43.290        1.02028       117.712       124.773       0.91186
   37.554       321.242        40.820        1.01912       115.925       124.773       0.90170
   38.780       331.108        38.278        1.01793       112.766       124.826       0.89593
   40.873       349.106        34.855        1.01633       108.069       124.826       0.89815
   42.215       360.672        32.060        1.01502       103.996       124.878       0.88694
   43.058       367.669        28.533        1.01337        97.345       124.930       0.85979

      NON-DIMENSIONAL COEFFICIENTS FOR RUN  10

     FLOW COEFFICIENT       3-STAGE EFFICIENCY     DEFLECTION COEFFICIENT    PRESSURE COEFFICIENT

         0.5510                  0.8825                  0.2096                   0.1850
         0.5263                  0.8699                  0.2311                   0.2010
         0.5165                  0.9061                  0.2487                   0.2253
         0.5001                  0.9128                  0.2662                   0.2430
         0.4761                  0.9049                  0.2875                   0.2601
         0.4604                  0.9060                  0.3020                   0.2736
         0.4401                  0.9052                  0.3191                   0.2888
         0.4248                  0.8851                  0.3289                   0.2911
         0.4003                  0.7480                  0.3378                   0.2527
         0.4233                  0.8869                  0.3274                   0.2904
         0.4382                  0.8975                  0.3182                   0.2856
         0.4594                  0.9119                  0.3029                   0.2762
         0.4743                  0.9017                  0.2896                   0.2611
         0.4887                  0.8959                  0.2722                   0.2438
         0.5152                  0.8981                  0.2475                   0.2223
         0.5321                  0.8869                  0.2305                   0.2044
         0.5422                  0.8598                  0.2113                   0.1817
```

Table C-12. Output of Program ONRETA, Run 10, Stator Stagger Angle = 39.8°

```
              NAVAL POSTGRADUATE SCHOOL TURBOPROPULSION LABORATORY

                 O.N.R. 3-STAGE AXIAL COMPRESSOR, 3-STAGE EFFICIENCY
    INPUT DATA FOR RUN 11          BAROMETRIC PRESSURE  29.91    AT   74.1  DEGREES,F.
    ROTOR STAGGER ANGLE 42.8                 STATOR STAGGER ANGLE 44.3

   TEMP,       VELOCITY        PSTATIC,       PTIG,        DELP,      TACHOMETER    TORQUEMETER
  DEG. F.    HEAD, COUNTS      COUNTS        COUNTS       COUNTS        R.P.M.        POUNDS

   68.0         1841.          2469.          455.         6736.        1194.0         21.31
   68.1         1730.          2331.          360.         7356.        1194.0         22.47
   68.4         1628.          2200.          345.         8155.        1193.5         23.59
   69.0         1504.          2023.          308.         8948.        1193.0         24.76
   69.3         1373.          1871.          290.         9691.        1192.5         25.62
   68.5         1256.          1708.          281.        10325.        1192.5         26.34
   69.0         1144.          1548.          245.        10700.        1192.0         26.67
   69.7         1020.          1380.          219.        11010.        1192.5         26.80
   70.4          864.          1163.          210.         8725.        1192.0         25.08
   72.2         1021.          1351.          201.        11015.        1192.0         26.59
   71.4         1128.          1545.          250.        10665.        1192.5         26.64
   71.6         1245.          1696.          253.        10246.        1192.5         26.15
   68.4         1409.          1849.          298.         9728.        1192.0         25.62

    OUTPUT DATA FOR RUN 11

  REFERRED     VOLFLORATE      PTD-PTIG      PRESSURE       TORQUE        OMEGA        3-STAGE
  FLOW RATE   CU.FT./SEC.    LB./SQ.FT.       RATIO        FT.-LB.     RAD./SEC.     EFFICIENCY

   41.797       355.552        28.017        1.01311        88.575      125.035       0.89674
   40.512       344.653        30.596        1.01432        93.396      125.035       0.89965
   39.294       334.391        33.919        1.01587        98.052      124.983       0.92163
   37.762       321.531        37.218        1.01741       102.915      124.930       0.92631
   36.074       307.250        40.308        1.01886       106.490      124.878       0.92629
   34.498       293.599        42.945        1.02009       109.482      124.878       0.91694
   32.918       280.292        44.505        1.02082       110.854      124.826       0.89602
   31.078       264.797        45.794        1.02142       111.394      124.878       0.86624
   28.597       243.818        36.290        1.01698       104.245      124.826       0.67664
   31.092       265.544        45.815        1.02143       110.937      124.826       0.87290
   32.687       278.955        44.359        1.02075       110.729      124.878       0.88949
   34.346       293.163        42.617        1.01994       108.692      124.878       0.91513
   36.543       310.981        40.462        1.01893       106.490      124.826       0.94161

    NON-DIMENSIONAL COEFFICIENTS FOR RUN  11

   FLOW COEFFICIENT        3-STAGE EFFICIENCY      DEFLECTION COEFFICIENT     PRESSURE COEFFICIENT

        0.5238                   0.8967                     0.1968                     0.1765
        0.5078                   0.8996                     0.2142                     0.1927
        0.4929                   0.9216                     0.2321                     0.2139
        0.4741                   0.9263                     0.2538                     0.2351
        0.4533                   0.9263                     0.2751                     0.2549
        0.4331                   0.9169                     0.2956                     0.2710
        0.4137                   0.8960                     0.3139                     0.2813
        0.3906                   0.8662                     0.3342                     0.2895
        0.3598                   0.6766                     0.3396                     0.2298
        0.3919                   0.8729                     0.3336                     0.2912
        0.4115                   0.3895                     0.3164                     0.2814
        0.4325                   0.9151                     0.2956                     0.2705
        0.4589                   0.9416                     0.2715                     0.2556
```

Table C-13. Output of Program ONRETA, Run 11, Stator Stagger Angle = 44.3°

APPENDIX D

DETAILS OF PREDICTION PROGRAM

This Appendix contains details concerning AXCO3 which may be of interest to a limited number of readers. Table D-1 is a listing of the main program and the seven subroutines. Section D-1 is a description of the method of inserting data. Table D-2 is a sample of program output. The rewrite of input data, a sample of interstage data, and a sample summary of one case are included. Tables D-3 through D-16 are the summary printouts of the cases which were compared to measured performance of the machine. Table D-17 is a printout of program CHECK which verified the errors in the polynomials of subroutines THEORY and CASCAD.

D-1 Input Data

There is no limit to the number of cases which may be considered, since data are read in prior to execution for each case, and output printed prior to considering the next case. The executive routine reads input data and prints it before computation begins. The input data consists of thirteen cards per case.

Card 1: (I7, 4F7.3)	NUM	case number (arbitrary)
	GAM	ratio of specific heats
	RN	referred speed (rpm/$\sqrt{^{o}R}$)
	WREM	initial referred flow rate (lbm$\sqrt{^{o}R}$/sec psia)
	DW	referred flow rate increment (lbm$\sqrt{^{o}R}$/sec psia)

Card 2:	LMAX	number of stages (3)
(I7,	ZETAI	loss coefficient of inlet duct
5F7.3)		(assumed 0.0)
	ZIGV	loss coefficient of inlet guide vanes
		(assumed 0.05)
	EGV	efficiency of exit guide vanes (assumed 0.85)
	ETD	efficiency of diffuser (assumed 1.0)
	EEX	efficiency of exit (assumed 1.0)
Card 3:	DIN	inlet pipe diameter, in.
(3F7.3,	DAV	average blade diameter, in.
4F7.1,	DOU	outlet pipe diameter, in.
3F7.3)	AEA	annulus area ahead of IGV, in.^{2}
	AIGV	annulus area after IGV, in.^{2}
	AGV	annulus area after EGV, in.^{2}
	ADI	diffuser exit area, in.^{2}
	ALE	inlet guide vane exit angle, degrees
	SMAX	maximum limit, $(i-i_{10})/\epsilon_{10}$, set by Fig. 29
	SMI	minimum limit, $(i-i_{10})/\epsilon_{10}$, set by Fig. 29
Card 4:	AAA	an array of annulus areas after rotor one,
(10F7.3)		stator one,....stator LMAX, in.^{2}
Card 5:	BH	an array of blade heights of rotor one....
(10F7.3)		stator LMAX, in.
Card 6:	BLOCK	an array of blockage factors for rotor one....
(10F7.3)		stator LMAX (assumed 1.0)
Card 7:	WDO	an array of work done factors for stage one....
(10F7.3)		stage LMAX (assumed 1.0)

Card 8: (Rotor data) (9F7.3)	BLDR	number of blades in the row
	CAMR	camber angle, degrees
	STAGR	stagger angle, degrees
	SHR	shape correction factor, (1.0)
	THR	thickness to chord ratio
	CHR	blade chord length, in.
	DIAR	mean blade diameter, in.
	DER	tip clearance, in
	CDR	minimum profile drag coefficient (assumed various)
Card 9: (Stator data) (9F7.3)	BLDS	number of blades in the row
	CAMS	camber angle, degrees
	STAGS	stagger angle, degrees
	SHS	shape correction factor (1.0)
	THS	thickness to chord ratio
	CHS	blade chord length, in.
	DIAS	blade mean diameter, in.
	DES	tip clearance, in.
	CDS	minimum profile drag coefficient (assumed various)

Cards 10 and 12 are duplicates of 8

Cards 11 and 13 are duplicates of 9

```
FORTRAN IV G LEVEL 0, MOD 0              MAIN                 DATE = 67224          00/08/30                PAGE 000

0001              DIMENSION AAA(2,15),BH(2,15),BLOCK(2,15),WDO(15),BLDR(15),BLDS(15)00000005
                 1,CAMR(15),CAMS(15),STAGR(15),STAGS(15),SHR(15),SHS(15),THR(15),THS00000006
                 2(15),CHR(15),CHS(15),DIAR(15),DIAS(15),DER(15),DES(15),CDR(15),CDS00000007
                 3(15),FLOW(30),RATIO(30),OETA(30),POCO(30),BLETA(30),ITITLE(12),LAB00000008
                 4EL(5),X(30),Y(30),XY(30),STAPR(30),STAETA(30)                     10000008
            C      USES ORIGINAL DATA OF HOWELL BETWEEN CD=0.02 AND 0.04           10000001
            C CALCULATES PERFORMANCE MAP OF AXIAL COMPRESSORS AT SPECIFIED REFERRED 00000002
            C SPEEDS BASED ON CASCADE DATA CALCULATED FROM BLADING GEOMETRY  - USES 00000003
            C NACA DATA (NACA SP-36 CHAP 6) AND DATA FROM HOWELL                    00000004
0002         3002 READ(5,700,END=3001)(NUM,GAM,RN,WREM,DW)                          0     11
0003              READ(5,701)(LMAX,ZETAI,ZIGV,EGV,ETD,EEX)                          00000012
0004              READ(5,713)(DIN,DAV,DOU,AEA,AIGV,AGV,ADI,ALE,SMAX,SMI)            00000013
0005              READ(5,703)((AAA(J,I),J=1,2),I=1,LMAX)                            00000014
0006              READ(5,703)((BH(J,I),J=1,2),I=1,LMAX)                             00000015
0007              READ(5,703)((BLOCK(J,I),J=1,2),I=1,LMAX)                          00000016
0008              READ(5,703)(WDO(I),I=1,LMAX)                                      00000017
0009              DO 1 K=1,LMAX                                                     00000018
0010              READ(5,702)(BLDR(K),CAMR(K),STAGR(K),SHR(K),THR(K),CHR(K),DIAR(K),00000019
                 1DER(K),CDR(K))                                                    00000020
0011              READ(5,702)(BLDS(K),CAMS(K),STAGS(K),SHS(K),THS(K),CHS(K),DIAS(K),00000021
                 1DES(K),CDS(K))                                                    00000022
0012            1 CONTINUE                                                          00000023
0013              WRITE(6,750)(NUM)                                                 00000024
0014              WRITE(6,751)(NUM,GAM,RN,WREM,DW)                                  00000025
0015              WRITE(6,752)(LMAX,ZETAI,ZIGV,EGV,ETD,EEX)                         00000026
0016              WRITE(6,753)(DIN,DAV,DOU,AEA,AIGV,AGV,ADI,ALE,SMAX,SMI)           00000027
0017              WRITE(6,754)                                                      00000028
0018              WRITE(6,714)((AAA(J,I),J=1,2),I=1,LMAX)                           00000029
0019              WRITE(6,755)                                                      00000030
0020              WRITE(6,703)((BH(J,I),J=1,2),I=1,LMAX)                            00000031
0021              WRITE(6,756)                                                      00000032
0022              WRITE(6,703)((BLCCK(J,I),J=1,2),I=1,LMAX)                         00000033
0023              WRITE(6,757)                                                      00000034
0024              WRITE(6,703)(WDO(I),I=1,LMAX)                                     00000035
0025              DO 20 K=1,LMAX                                                    00000036
0026              IF(1-K) 22,23,23                                                  00000037
0027           22 KL=KL+1                                                           00000038
0028              WRITE(6,758)(KL,K)                                                00000043
0029              GO TO 28                                                          00000044
0030           23 KL=K+7                                                            00000046
0031              WRITE(6,761)(KL,K)                                                00000047
0032           28 WRITE(6,702)(BLDR(K),CAMR(K),STAGR(K),SHR(K),THR(K),CHR(K),DIAR(K)00000048
                 1,DER(K),CDR(K))                                                   00000049
0033              KL=KL+1                                                           00000050
0034              WRITE(6,759)(KL,K)                                                00000051
0035              WRITE(6,702)(BLDS(K),CAMS(K),STAGS(K),SHS(K),THS(K),CHS(K),DIAS(K)00000052
                 1,DES(K),CDS(K))                                                   00000053
0036           20 CONTINUE                                                          00000054
```

Table D-1. Listing of Program AXC03

```
0037            AGV=AGV*BLOCK(2,LMAX)                                                          00000055
0038            EXP1=GAM/(GAM-1.)                                                              00000056
0039            EXP2=(GAM-1.)/GAM                                                              00000057
0040            C=2.*32.174*53.346*EXP1                                                        00000058
0041            B=1./C                                                                         00000059
0042            RAG=SQRT (53.346/32.174)                                                       00000060
0043            UAV=RN*DAV*3.14159/720.                                                        00000061
0044            MMM=1                                                                          10000061
0045            WRE=WREM                                                                       00000062
0046          3 WRITE(6,704)(NUM,RN,GAM,UAV)                                                   00000063
0047            AA=3.14159*DIN*DIN/4.                                                          00000064
0048            CALL PREX(WRE,1.,1.,0.,AA,GAM,RAG,C,XXX,PIN,XXY,XXZ)                           00000065
0049            CALL PREX(WRE,1.,PIN,ZETAI,AEA,GAM,RAG,C,YXX,YXY,PTE,YXZ)                      00000066
0050            A=AIGV*COS (ALE/57.29578)                                                      00000067
0051            CALL PREX(WRE,1.,PTE,ZIGV,A,GAM,RAG,C,TSIG,PSIG,PTIG,VE)                       00000068
0052            AL3=ALE/57.29578                                                               00000069
0053            VA1=VE*COS (AL3)                                                               00000070
0054            WRITE(6,763)(YXX,YXY,VA1,VE)                                                   00000071
0055            TS1=TSIG                                                                       00000072
0056            TT1=1.                                                                         00000073
0057            PS1=PSIG                                                                       00000074
0058            PT1=PTIG                                                                       00000075
0059            L=1                                                                            00000076
0060          4 I=1                                                                            00000077
0061            BLOK=BLOCK(I,L)                                                                00000078
0062            A2=AAA(I,L)                                                                    00000079
0063            HR=BH(I,L)                                                                     00000080
0064            WODO=WDO(L)                                                                    00000081
0065            DD=DIAR(L)                                                                     00000082
0066            BLD=BLDR(L)                                                                    00000083
0067            CAM=CAMR(L)                                                                    00000084
0068            STAG=STAGR(L)                                                                  00000085
0069            RSTAG=STAG                                                                     10000085
0070            SH=SHR(L)                                                                      00000086
0071            TH=THR(L)                                                                      00000087
0072            CH=CHR(L)                                                                      00000088
0073            DE=DER(L)                                                                      00000089
0074            CD=CDR(L)                                                                      00000090
0075            CALL ROTOR(WRE,DD,BLOK,A2,HR,WODO,BLD,CAM,STAG,SH,TH,CH,DE,VA1,AL300000091
               1,TS1,TT1,PS1,PT1,CD,B,EXP1,RN,L,SMAX,SMI,BE2,VA2,TS2,TT2,PS2,M,NCA00000092
               2SF)                                                                            10000092
0076            WRITE(6,764)(TT2,PT1)                                                          00000093
0077            GO TO (5,8,10),M                                                               00000094
0078          5 I=2                                                                            00000095
0079            BLOK=BLOCK(I,L)                                                                00000096
0080            A3=AAA(I,L)                                                                    00000097
0081            HS=BH(I,L)                                                                     00000098
0082            DD=DIAS(L)                                                                     00000099
```

Table D-1. Listing of Program AXC03 (cont.)

```
0083               BLD=BLDS(L)                                                      00000100
0084               CAM=CAMS(L)                                                      00000101
0085               STAG=STAGS(L)                                                    00000102
0086               SSTAG=STAG                                                       10000102
0087               SH=SHS(L)                                                        00000103
0088               TH=THS(L)                                                        00000104
0089               CH=CHS(L)                                                        00000105
0090               DE=DES(L)                                                        00000106
0091               CD=CDS(L)                                                        00000107
0092               CALL STATOR(WRE,DD,BLOK,A3,HS,WODO,BLD,CAM,STAG,SH,TH,CH,DE,VA2,BE00000108
                  12,TS2,PS2,CD,B,EXP1,RN,L,SMAX,SMI,AL3,VA3,TS3,PS3,PT3,K,NCASE)  00000109
0093               WRITE(6,764)(TT2,PT3)                                            00000110
0094               GO TO (6,9,11),K                                                 00000111
0095             6 L=L+1                                                            00000112
0096               IF(L-LMAX) 7,7,12                                                00000113
0097             7 VA1=VA3                                                          00000114
0098               TS1=TS3                                                          00000115
0099               TT1=TT2                                                          00000116
0100               PS1=PS3                                                          00000117
0101               PT1=PT3                                                          00000118
0102               GO TO 4                                                          00000119
0103             8 WRITE(6,711)                                                     00000120
0104               WRITE(6,705)(WRE,L)                                              00000121
0105               WRE=WRE+DW                                                       00000122
0106               GO TO 3                                                          00000123
0107             9 WRITE(6,711)                                                     00000124
0108               WRITE(6,706)(WRE,L)                                              00000125
0109               WRE=WRE+DW                                                       00000126
0110               GO TO 3                                                          00000127
0111            10 WRITE(6,711)                                                     00000128
0112               WRITE(6,707)(WRE,L)                                              00000129
0113               GO TO 2000                                                       00000130
0114            11 WRITE(6,711)                                                     00000131
0115               WRITE(6,707)(WRE,L)                                              00000132
0116               GO TO 2000                                                       00000133
0117            12 ACU=3.14159*DOU*DOU/4.                                           00000134
0118               ZEX=1.-EEX                                                       00000135
0119               CALL PRCO(WRE,TT2,TS3,PS3,EGV,AGV,GAM,RAG,C,PSEG,XXX,PTEG,TSEG)  00000136
0120               WRITE(6,709)(TSEG,PSEG)                                          00000137
0121               WRITE(6,764)(TT2,PTEG)                                           00000138
0122               CALL PRCO(WRE,TT2,TSEG,PSEG,ETD,ADI,GAM,RAG,C,PSEX,XXX,PTEX,TSEX) 00000139
0123               WRITE(6,712)(TSEX,PSEX)                                          10000139
0124               WRITE(6,764)(TT2,PTEX)                                           20000139
0125               PRATS3=PT3/PTIG                                                  30000139
0126               ETAST3=(PRATS3**EXP2-1.)/(TT2-1.)                                40000139
0127               ETAB=((PTEG/PTE)**EXP2 - 1.)/(TT2-1.)                            00000140
0128               ETT=(PTEX**EXP2 -1.)/(TT2-1.)                                    00000141
0129               AM=WRE*53.346*(TT2-1.)*1.055*GAM/((GAM-1.)*778.16)               00000142
```

Table D-1. Listing of Program AXC03 (cont.)

```
          WRITE(6,711)                                                      00000143
          WRITE(6,710)(WRE,PTEX,ETT,AM,ETAB,PRATS3,ETAST3)                  00000144
          FLOW(MMM)=WRE                                                     10000144
          RATIO(MMM)=PTEX                                                   20000144
          OETA(MMM)=ETT                                                     30000144
          POCO(MMM)=AM                                                      40000144
          BLETA(MMM)=ETAB                                                   50000144
          STAPR(MMM)=PRATS3                                                 51000144
          STAETA(MMM)=ETAST3                                                52000144
          MMM=MMM+1                                                         60000144
          WRE=WRE+DW                                                        00000145
          GO TO 3                                                           00000146
      700 FORMAT(I7,4F7.3)                                                  00000147
      701 FORMAT(I7,5F7.3)                                                  00000148
      702 FORMAT(9F7.3)                                                     00000149
      703 FORMAT(10F7.3)                                                    00000150
      713 FORMAT(3F7.3,4F7.1,3F7.3)                                         10000150
      704 FORMAT(1H1,38X,39HCALCULATED AXIAL COMPRESSOR PERFORMANCE//40X,   00000151
         1//8H RUN NO.I4,9X,16HREFERRED SPEED =F7.4,9X,7HGAMMA =F6.3,9X,35HA00000152
         2VERAGE PERIPHERAL VELOCITY RATIO =F7.4//51X,15HINTERSTAGE DATA//1100000153
         35H BLADE  INLET INLET AXIAL INLET  OUT  ROTOR BLADE INLET  OUT   C00000154
         4DP   CDP  REFERENCE REFERENCE    ACTUAL    STALLING/116H  ROW   TE00000155
         5MP. PRES. VELOC VELOC VELOC VELOC EFFIC ANGLE ANGLE  MIN  RATIO IN00000156
         6CIDENCE DEFLECTION DEFLECTION DEFLECTION//)                       00000157
      705 FORMAT(F8.3,5X,18HSURGE IN ROTOR NO.I3)                           00000158
      706 FORMAT(F8.3,5X,19HSURGE IN STATOR NO.I3)                          00000159
      707 FORMAT(F8.3,5X,26HMIN. PRESSURE IN ROTOR NO.I3)                   00000160
      708 FORMAT(F8.3,5X,27HMIN. PRESSURE IN STATOR NO.I3)                  00000161
      709 FORMAT(6H  EGV ,2F6.2)                                            00000162
      710 FORMAT(F8.3,F13.5,F10.4,F15.5,F12.4,F13.5,F13.4)                  00000163
      711 FORMAT(2X,///86H REFERRED    PRESSURE    OVERALL        POWER     00000164
         1  BLADING        3-STAGE        3-STAGE/88H FLOW RATE    RATIO    EF00000165
         2FICIENCY   COEFFICIENT  EFFICIENCY  PRESSURE RATIO  EFFICIENCY//) 00000166
      712 FORMAT(6H  DIFF,2F6.2)                                            00000167
      714 FORMAT(10F7.2)                                                    2     167
      750 FORMAT(1H1,14X,39HCALCULATED AXIAL COMPRESSOR PERFORMANCE/26X,21HI00000168
         1NPUT DATA OF RUN NO.I4//)                                         00000169
      751 FORMAT(2X,6HCARD 1//I7,4F7.3//)                                   00000170
      752 FORMAT(2X,6HCARD 2//I7,5F7.3//)                                   00000171
      753 FORMAT(2X,6HCARD 3//3F7.3,4F7.1,3F7.3//)                          00000172
      754 FORMAT(2X,22HCARD 4   ANNULUS AREAS//)                            00000173
      755 FORMAT(2X,//2X,22HCARD 5   BLADE HEIGHTS//)                       00000174
      756 FORMAT(2X,//2X,25HCARD 6   BLOCKAGE FACTORS//)                    00000175
      757 FORMAT(2X,//2X,26HCARD 7   WORK-DONE FACTORS//)                   00000176
      758 FORMAT(2X,//2X, 4HCARD,I3,3X,18HROTOR DATA   STAGE,I3//)          00000177
      759 FORMAT(2X,//2X,4HCARD,I3,3X,19HSTATOR DATA   STAGE,I3//)          00000178
      761 FORMAT(1H1,//2X,4HCARD,I3,3X,18HROTOR DATA   STAGE,I3//)          00000179
      762 FORMAT(I7)                                                        00000180
```

Table D-1. Listing of Program AXC03 (cont.)

```
FORTRAN IV G LEVEL 0, MOD 0               MAIN                 DATE = 67224         00/08/30                PAGE 000

 0169            763 FORMAT(6H  IGV ,2F6.2,F7.2,6X,F6.2)                                00000181
 0170            764 FORMAT(6X2F6.2,2X,25H(TOTAL OUTLET CONDITIONS))                    00000182
 0171            765 FORMAT(1H1,34X,53HCALCULATED AXIAL COMPRESSOR PERFORMANCE, OVERALL10000182
                    1 DATA//8H RUN NO.I4,9X,16HREFERRED SPEED =F7.4,9X,7HGAMMA =F6.3,9X20000182
                    2,35HAVERAGE PERIPHERAL VELOCITY RATIO =F7.4//)                     30000182
 0172            7660FORMAT(20X,22HROTOR STAGGER ANGLE = ,F5.2,15X,23HSTATOR STAGGER AN31000182
                    1GLE = ,F5.2//)                                                     32000182
 0173           2000 WRITE(6,765)(NUM,RN,GAM,UAV)                                       40000182
 0174                WRITE(6,766)(RSTAG,SSTAG)                                          41000182
 0175                WRITE(6,711)                                                       51000182
 0176                NNN=MMM-1                                                          60000182
 0177                DO 911 I=1,NNN                                                     70000182
 0178                X(I)= FLOW(I)                                                      80000182
 0179                Y(I)= RATIC(I)                                                     90000182
 0180                XY(I)=OETA(I)                                                      11000182
 0181            911 WRITE(6,710)(FLOW(I),RATIO(I),OETA(I),POCO(I),BLETA(I),STAPR(I),ST12000182
                    1AETA(I))                                                           13000182
 0182           3000 GO TO 3002                                                         00000183
 0183           3001 RETURN                                                             00000184
 0184                END                                                                00000184
```

Table D-1. Listing of Program AXCO3 (cont.)

```
FORTRAN IV G LEVEL 0, MOD 0               ROTOR               DATE = 67224          00/08/30              PAGE 0001

      SUBROUTINE ROTOR(W,DD,BLOK,A2,HR,WO,BL,CA,ST,SH,TH,CH,DE,VA1,AL3, 00000185
     1TS1,TT1,PS1,PT1,CD,B,EXP1,RN,L,SMA,SMI,BE2,VA2,TS2,TT2,PS2,M,NCASE00000186
     2)                                                                 10000186
C CALCULATES CONDITIONS AT ROTOR DISCHARGE                               00000187
      U=RN*DD*3.14159/720.                                              00000188
      WU1=U-VA1*TAN(AL3)                                                00000189
      BE1=ATAN(WU1/VA1)                                                 00000190
      ANG=BE1*57.29578                                                  00000191
      SO=CH*BL/(3.14159*DD)                                             00000192
      CALL THEORY(TH,SH,CA,ST,SO,STARI,STARD,BETA,ASTAR,DFSTAR)         00000193
      CALL CASCAD(STARI,STARD,DFSTAR,BETA,CA,ASTAR,ANG,SO,SMA,SMI,ALG,R,00000194
     1DFACT,DFMAX,N,NCASE)                                              00000195
      GO TO (400,405,405),N                                             00000196
  400 XX=VA1                                                            00000197
      BE2=ALG/57.29578                                                  00000198
      BE2=ATAN((1.-WO)*TAN(BE1)+WO*TAN(BE2))                            00000199
      ALG=BE2*57.29578                                                  00000200
      KK=1                                                              00000201
  401 CALL ETACAL(CD,R,BE1,BE2,VA1,XX,SO,HR,DE,CH,ETAR)                 00000202
      W1=VA1/COS(BE1)                                                   00000203
      W2=XX/COS(BE2)                                                    00000204
      D=B*(W1*W1-W2*W2)                                                 00000205
      TS2=TS1+D                                                         00000206
      TT2=TT1+2.*B*U*(WU1-XX*TAN(BE2))                                  00000207
      PS2=PS1*(1.+ETAR*D/TS1)**EXP1                                     00000208
      RA=53.346                                                         00000209
      VA2=W*TS2*RA/(A2*BLOK*PS2)                                        00000210
      XX=VA2                                                            00000211
      GO TO (450,450,450,450,450,403),KK                                00000212
  450 KK=KK+1                                                           00000213
      GO TO 401                                                         00000214
  403 WRITE(6,404)(L,TS2,PS2,VA2,W1,W2,U,ETAR,ANG,ALG,CD,R,STARI,DFSTAR,00000215
     1DFACT,DFMAX)                                                      00000216
  404 FORMAT(3H  R,I3,2F6.2,F7.2,3F6.2,F6.3,2F6.2,2F6.3,F8.3,2F11.3,F10.00000217
     13)                                                                00000218
  405 M=N                                                               00000219
      RETURN                                                            00000220
      END                                                               00000221
```

Table D-1. Listing of Program AXC03 (cont.)

```
FORTRAN IV G LEVEL 0, MOD 0              STATOR              DATE = 67224          00/08/30              PAGE 0001

 0001                SUBROUTINE STATOR(W,DD,BLOK,A3,HS,WO,BL,CA,ST,SH,TH,CH,DE,VA2,BE2,00000222
                    1TS2,PS2,CD,B,EXP1,RN,L,SMA,SMI,AL3,VA3,TS3,PS3,PT3,K,NCASE)      00000223
               C CALCULATES CONDITIONS AT STATOR DISCHARGE                            00000224
 0002                U=RN*DD*3.14159/720.                                             00000225
 0003                VU2=U-VA2*TAN(BE2)                                               00000226
 0004                AL2=ATAN(VU2/VA2)                                                00000227
 0005                AMG=AL2*57.29578                                                 00000228
 0006                SO=CH*BL/(3.14159*DD)                                            00000229
 0007                CALL THEORY(TH,SH,CA,ST,SO,STARI,STARD,BETA,ASTAR,DFSTAR)        00000230
 0008                CALL CASCAD(STARI,STARD,DFSTAR,BETA,CA,ASTAR,AMG,SO,SMA,SMI,AKG,R,00000231
                    1DFACT,DFMAX,N,NCASE)                                             00000232
 0009                GO TO (600,605,605),N                                            00000233
 0010            600 XX=VA2                                                           00000234
 0011                AL3=AKG/57.29578                                                 00000235
 0012                AL3=ATAN((1.-WO)*TAN(AL2)+WO*TAN(AL3))                           00000236
 0013                AKG=AL3*57.29578                                                 00000237
 0014                KK=1                                                             00000238
 0015            601 CALL ETACAL(CD,R,AL2,AL3,VA2,XX,SO,HS,DE,CH,FTAS)                00000239
 0016                V2=VA2/COS(AL2)                                                  00000240
 0017                V3=XX/CCS(AL3)                                                   00000241
 0018                D=B*(V2*V2-V3*V3)                                                00000242
 0019                PS3=PS2*(1.+ETAS*D/TS2)**EXP1                                    00000243
 0020                TS3=TS2+D                                                        00000244
 0021                PT3=PS3*(1.+B*V3*V3/TS3)**EXP1                                   00000245
 0022                RA=53.346                                                        00000246
 0023                VA3=W*TS3*RA/(A3*BLOK*PS3)                                       00000247
 0024                XX=VA3                                                           00000248
 0025                GO TO (650,650,650,650,650,603),KK                               00000249
 0026            650 KK=KK+1                                                          00000250
 0027                GO TO 601                                                        00000251
 0028            603 WRITE(6,604)(L,TS3,PS3,VA3,V2,V3,U,ETAS,AMG,AKG,CD,R,STARI,DFSTAR,00000252
                    1DFACT,DFMAX)                                                     00000253
 0029            604 FORMAT(3H  S,I3,2F6.2,F7.2,3F6.2,F6.3,2F6.2,2F6.3,F8.3,2F11.3,F10.00000254
                    13)                                                               00000255
 0030            605 K=N                                                              00000256
 0031                RETURN                                                           00000257
 0032                END                                                              00000258
```

Table D-1. Listing of Program AXC03 (cont.)

```
FORTRAN IV G LEVEL 0, MOD 0              THEORY              DATE = 67224          00/08/30                  PAGE 0001
0001                SUBROUTINE THEORY(TH,SH,CA,ST,SO,SI,SD,BET,AS,DFS)                          00000259
              C                                                                                 00000260
              C CALCULATES MINIMUM LOSS CONDITIONS OF COMPRESSOR CASCADES USING THE             00000261
              C METHOD OF LIEBLEIN  -  NACA SP-36  CHAP.  VI                                    00000262
              C                                                                                 00000263
              C                                                                                 00000264
              C ZERO-CAMBER INCIDENCE VS SOLIDITY AND ALPHA 1  FIG 137                          00000265
              C                                                                                 00000266
0002                FIGAF(A,S)=0.96195E-02- 0.21961E-01*S+0.10963E-01*S*S-0.42930E-02*00000267
                   1A+0.85403E-01*A*S-0.34503E-02*A*S*S+0.27923E-04*A*A-0.64301E-04*A*00000268
                   2A*S+0.32138E-04*A*A*S*S                                                     00000269
              C                                                                                 00000270
              C THICKNESS CORRECTION FACTOR (INCIDENCE) VS THICKNESS-CHORD RATIO F 14200000271
              C                                                                                 00000272
0003                FIGBF(TH)=0.03472777+17.891945*TH-118.09901*TH*TH+429.53472*TH**3-00000273
                   1685.43011*TH**4                                                             00000274
              C                                                                                 00000275
              C SLOPE FACTOR N (INCIDENCE) VS SOLIDITY AND ALPHA 1   FIG 138                    00000276
              C                                                                                 00000277
0004                FIGCF(A,S)=-0.11890+0.21192*S-0.17854*S*S+0.57160E-01*S*S*S-0.368700000278
                   13E-02*A-0.76207E-04*A*S+0.18208E-02*A*S*S-0.55334E-03*A*S*S*S-0.360000000279
                   2825E-04*A*A+0.66620E-04*A*A*S+0.16243E-04*A*A*S*S-0.22671E-04*A*A*00000280
                   3S*S*S-0.72311E-07*A*A*A-0.54986E-06*A*A*A*S-0.49472E-06*A*A*A*S*S+00000281
                   40.37471E-06*A*A*A*S*S*S                                                     00000282
              C                                                                                 00000283
              C ZERO-CAMBER DEVIATION VS SOLIDITY AND ALPHA 1   FIG 161                         00000284
              C                                                                                 00000285
0005                FIGDF(A,S)=-0.017896+0.10058*S-0.14687*S*S+0.58557E-01*S*S*S-0.11900000286
                   187E-01*A+0.65167E-01*A*S-0.44822E-01*A*S*S+0.11478E-01*A*S*S*S-0.200000287
                   24947E-03*A*A+0.66468E-03*A*A*S-0.94528E-03*A*A*S*S+0.28823E-03*A*A00000288
                   3*S*S*S+0.67269E-05*A*A*A-0.17987E-04*A*A*A*S+0.25862E-04*A*A*A*S*S00000289
                   4-0.77546E-05*A*A*A*S*S*S                                                    00000290
              C                                                                                 00000291
              C THICKNESS CORRECTION FACTOR (DEVIATION) VS THICKNESS-CHORD RATIO F 17200000292
              C                                                                                 00000293
0006                FIGEF(TH)=0.1169385+2.6167113*TH+70.722724*TH*TH-85.664637*TH**3  00000294
              C                                                                                 00000295
              C SLOPE FACTOR M (DEVIATION) VS SOLIDITY AND ALPHA 1   FIG 168                    00000296
              C                                                                                 00000297
0007                FIGGF(A,S)=1.06850-1.68830*S+1.15690*S*S-0.28879*S*S*S+0.36581E-0300000298
                   1*A-0.19185E-02*A*S+0.36235E-02*A*S*S-0.13993E-02*A*S*S*S-0.57353E-00000299
                   205*A*A+0.11329E-03*A*A*S-0.19416E-03*A*A*S*S+0.74911E-04*A*A*S*S*S00000300
                   3-0.16187E-06*A*A*A-0.79239E-06*A*A*A*S+0.22558E-05*A*A*A*S*S-0.99200000301
                   418E-06*A*A*A*S*S*S                                                          00000302
              C                                                                                 00000303
0008                BET=ST + 0.5*CA                                                             00000304
0009                CTHK=FIGBF(TH)                                                              10000304
0010                SIP=2.0                                                                     20000304
```

Table D-1. Listing of Program AXCO3 (cont.)

```
FORTRAN IV G LEVEL 0, MOD 0              THEORY              DATE = 67224          00/08/30             PAGE 0002

 0011        201 A=BET+SIP                                                                 00000305
 0012            DENCE=FIGAF(A,SO)                                                         00000306
 0013            SLOPN=FIGCF(A,SO)                                                         00000307
          C      CALCULATE SI AND COMPARE TO SIP UNTIL WITHIN 0.02 DEGREE                  00000308
 0014            SI=DENCE*SH*CTHK + SLOPN*CA                                               00000309
 0015            CHEC=ABS (SI-SIP)                                                         10000309
 0016            IF(CHEC-0.02)203,203,202                                                  20000309
 0017        202 SIP=SI                                                                    30000309
 0018            GO TO 201                                                                 40000309
 0019        203 DEVAT=FIGDF(A,SO)                                                         00000310
 0020            DTHK=FIGEF(TH)                                                            00000311
 0021            SLOPM=FIGGF(A,SO)                                                         00000312
 0022            SD=DEVAT*SH*DTHK + SLOPM*CA                                               00000313
 0023            AS = A                                                                    00000314
 0024            DFS=CA+SI-SD                                                              00000315
 0025            RETURN                                                                    00000316
 0026            END                                                                       00000317
```

Table D-1. Listing of Program AXC03 (cont.)

```
0001            SUBROUTINE CASCAD(SI,SD,DFS,BET,CA,AS,A,SO,SMA,SMI,AA,R,DFF,DFMAX,00000318
               1N,NCASE)                                                         00000319
          C                                                                      00000320
          C CALCULATES CASCADE PERFORMANCE DATA FOR COMPRESSOR BLADING USING     00000321
          C THE METHOD OF LIEBLEIN (NACA SP-36  CHAP 6                           00000322
          C                                                                      00000323
          C SLOPE FACTOR (DI/DD)* VS SOLIDITY AND ALPHA 1   FIG 177              00000324
          C                                                                      00000325
          C   CAUTION  THIS POLYNOMIAL GENERATED FOR SOLIDITIES FROM 0.6 TO 1.4  10000325
          C                                                                      20000325
0002           OFIGHF(A,S)=.81324E+00-.17818E+01*S+.13558E+01*S*S-.35174E+00*S*S*S00000326
               1-.40846E-02*A+.18322E-01*A*S-.21692E-01*A*S*S+.76075E-02*A*S*S*S+.00000327
               218174E-03*A*A-.83518E-03*A*A*S+.10421E-02*A*A*S*S-.38235E-03*A*A*S00000328
               3*S*S-.94842E-06*A*A*A+.86041E-05*A*A*A*S-.12163E-04*A*A*A*S*S+.46710000328
               421E-05*A*A*A*S*S*S                                               20000328
          C                                                                      00000329
0003            SLOPD=FIGHF(AS,SO)                                               00000330
0004            DI=A-BET                                                         00000331
0005            DEV=SD+(DI-SI)*SLOPD                                             00000332
0006            DF=CA+DI-DEV                                                     00000333
0007            Z=DF/DFS                                                         00000334
0008            X=(DI-SI)/DFS                                                    00000335
0009            DFMAX=DFS/0.80                                                   00000336
0010            IF(X) 300,300,301                                                00000337
0011        300 IF(X-SMI) 302,303,303                                            00000338
0012        302 N=3                                                              00000339
0013            RETURN                                                           00000340
0014        301 IF(X-SMA) 303,303,304                                            00000341
0015        304 N=2                                                              00000342
0016            RETURN                                                           00000343
0017        303 IF(X-0.10) 305,306,306                                           00000344
0018        305 DELZ=0.                                                          00000345
0019            GO TO 307                                                        00000346
0020        306 DELZ=0.0250-0.3250*X+1.750*X**2                                  00000347
0021        307 Y=Z-DELZ                                                         00000348
0022            DFF=Y*DFS                                                        00000349
0023            AA=A-DFF                                                         00000350
0024            R = 1.0034396+0.01430105*X+2.8807456*X**2-0.19234646*X**3+4.422982000000351
               10*X**4+22.349047*X**5+21.533222*X**6                             00000352
0025            N=1                                                              00000353
0026            RETURN                                                           00000354
0027            END                                                              00000355
```

Table D-1. Listing of Program AXC03 (cont.)

```
FORTRAN IV G LEVEL 0, MOD C            ETACAL            DATE = 67224          00/08/30            PAGE 0001

 0001               SUBROUTINE ETACAL(CD,R,ALI,ALE,VI,VE,SO,H,DE,CH,ETA)                   00000356
              C CALCULATES EFFICIENCY OF ROTOR OR STATOR                                     00000357
 0002               AI=VI*TAN(ALI)                                                           00000358
 0003               AE =VE*TAN(ALE)                                                          00000359
 0004               D=AI-AE                                                                  00000360
 0005               VU= SQRT(((AI+AE)/2.)**2+((VI+VE)/2.)**2)                                00000361
 0006               CL=2.*D/(SO*VU)                                                          00000362
 0007               E=CD*R/CL+.04*CL*CH/H+.25*CL*DE/(H* COS(ALE))+ .018 * CH/(CL*H)          00000363
 0008               T=(AI+AE)/(VI+VE)                                                        00000364
 0009               ETA=(1.-E/T)/(1.+E*T)                                                    00000365
 0010               RETURN                                                                   00000366
 0011               END                                                                      00000367
```

Table D-1. Listing of Program AXC03 (cont.)

```
FORTRAN IV G LEVEL 0, MOD 0            PREX              DATE = 67224          00/08/30              PAGE 0001

            SUBROUTINE PREX(W,TTI,PTI,Z,A,GAM,RAG,C,TSE,PSE,PTE,VE)
      C CALCULATES PRESSURE DROP IN CHANNEL FOR FLOW WITH FRICTION
            EN=GAM/(1.+Z*(GAM-1.) )
            EX1=2./EN
            EX2=(EN+1.)/EN
            EX3=(EN-1.)/EN
            PHI=W*SQRT (TTI)*RAG/(PTI*A)
            PRA=1.
            KM=1
        100 PH2=SQRT ((2.*GAM/(GAM-1.))* (PRA**EX1-PRA**EX2))
            GO TO (101,104),KM
        101 IF(PH2-PHI)102,106,103
        102 PRA=PRA-.001
            GO TO 100
        103 KM=2
        104 IF(PH2 -PHI)106,106,105
        105 PRA=PRA+.0001
            GO TO 100
        106 TSE=TTI*PRA**EX3
            VE=SQRT (C*(TTI-TSE))
            PSE=PRA*PTI
            PTE=PSE/(PRA**(1.-Z))
            RETURN
            END
```

Table D-1. Listing of Program AXC03 (cont.)

```
FORTRAN IV G LEVEL 0, MOD 0             PRC0              DATE = 67224          00/08/30              PAGE 0001

               SUBROUTINE PRC0(W,TTI,TSI,PSI,E,A,GAM,RAG,C,PSE,VE,PTE,TSE)
         C CALCULATES PRESSURE RISE IN DIFFUSOR FOR FLOW WITH FRICTION
               EN=GAM*E/(1.-GAM*(1.-E))
               EX1=2./EN
               EX2=(EN+1.)/EN
               PHI=W*SQRT (TSI)*RAG/(PSI*A)
               PRA=1.
               KM=1
           500 PH2=SQRT ((2.*GAM/(GAM-1.))*((TTI/TSI)*PRA**EX1-PRA**EX2))
               GO TO (501,504),KM
           501 IF(PHI-PH2)502,506,503
           502 PRA=PRA+.001
               GO TO 500
           503 KM=2
           504 IF(PHI-PH2)506,506,505
           505 PRA=PRA-.00005
               GO TO 500
           506 PSE=PRA*PSI
               TSE=TSI*PRA**((EN-1.)/EN)
               VE=SQRT (C*(TTI-TSE))
               PRE=(TTI/TSE)**(GAM/(GAM-1.))
               PTE=PRE*PSE
               RETURN
               END
```

Table D-1. Listing of Program AXC03 (cont.)

```
                 CALCULATED AXIAL CCMPRESSOR PERFORMANCE
                            INPUT DATA OF RUN NO.    1

 CARD 1
     1  1.400 52.474 4C.000  0.500

 CARD 2
     3  0.0    0.050  C.850  1.00C  1.000

 CARD 3
36.000 28.800 36.000  651.0  651.C  651.0 1017.0 19.500  0.400 -0.510

 CARD 4   ANNULUS AREAS

651.0C 651.00 651.00 651.00 651.0C 651.00

 CARD 5   BLADE HEIGHTS

 7.20C  7.200  7.20C  7.200  7.20C  7.200

 CARD 6   BLOCKAGE FACTORS

 1.00C  1.000  1.000  1.000  1.00C  1.000

 CARD 7   WORK-DONE FACTCRS

 1.00C  1.000  1.000
```

Table D-2. Sample Output of Program AXC03

```
 CARD  8   ROTOR DATA   STAGE  1

30.000 20.320 42.800  1.000  0.1CC  2.600 28.800  0.037  0.020

 CARC  9   STATOR DATA   STAGE  1

32.000 29.980 27.800  1.000  0.10C  2.600 28.800  0.020  0.020

 CARC 1C   ROTOR CATA   STAGE  2

30.000 20.320 42.800  1.00C  0.10C  2.600 28.800  0.037  0.020

 CARD 11   STATOR DATA   STAGE  2

32.000 29.980 27.800  1.000  0.10C  2.600 28.800  0.020  0.020

 CARD 12   ROTOR DATA   STAGE  3

30.000 20.320 42.800  1.000  0.10C  2.60C 28.800  0.037  0.020

 CARD 13   STATOR DATA   STAGE  3

32.000 29.980 27.800  1.000  0.100  2.60C 28.800  0.020  0.020
```

Table D-2. Sample Output of Program AXCO3 (cont.)

```
                                    CALCULATED AXIAL CCMPRESSOR PERFORMANCE

RUN NO.   1          REFERRED SPEEC =52.4740          GAMMA = 1.400          AVERAGE PERIPHERAL VELOCITY RATIO = 6.5941
                                                        INTERSTAGE DATA
BLADE   INLET INLET AXIAL INLET  CUT  ROTOR BLADE INLET  OUT   CDP   CDP  REFERENCE REFERENCE   ACTUAL    STALLING
 ROW    TEMP. PRES. VELOC VELOC VELOC VELOC EFFIC ANGLE ANGLE  MIN  RATIO INCIDENCE DEFLECTION DEFLECTION DFFLECTION

 IGV    1.CC  C.99   3.77        4.CC
 R  1   1.00  1.00   3.78  6.47  5.02  6.59 0.904 54.35 41.21 0.020 1.153  -1.017     11.412     13.141     14.265
        1.00  1.00  (TOTAL OUTLET CCNDITIONS)
 S  1   1.00  1.00   3.77  5.01  4.08  6.59 0.905 41.02 22.57 0.020 1.003  -1.673     18.542     18.450     23.177
        1.00  1.00  (TOTAL OUTLET CONDITIONS)
 R  2   1.00  1.00   3.76  6.28  4.97  6.59 0.907 53.11 40.79 0.020 1.036  -1.017     11.412     12.329     14.265
        1.00  1.00  (TOTAL OUTLET CONDITIONS)
 S  2   1.00  1.01   3.76  5.04  4.07  6.59 0.907 41.67 22.62 0.020 1.006  -1.673     18.542     19.054     23.177
        1.00  1.01  (TOTAL OUTLET CONDITIONS)
 R  3   1.00  1.01   3.75  6.28  4.95  6.59 0.907 53.25 40.81 0.020 1.044  -1.017     11.412     12.438     14.265
        1.01  1.01  (TOTAL OUTLET CONDITIONS)
 S  3   1.00  1.01   3.74  5.03  4.05  6.59 0.907 41.89 22.64 0.020 1.009  -1.673     18.542     19.253     23.177
        1.01  1.02  (TOTAL OUTLET CONDITIONS)
 EGV    1.00  1.01
        1.01  1.02  (TOTAL OUTLET CONDITICNS)
 DIFF   1.01  1.02
        1.01  1.02  (TCTAL CUTLET CCNDITICNS)


REFERREC    PRESSURE     OVERALL       POWER        BLADING       3-STAGE        3-STAGE
FLCW RATE    RATIC      EFFICIENCY   CCEFFICIENT   EFFICIENCY  PRESSURE RATIO  EFFICIENCY

 46.000     1.01737      0.8136       0.C7060       0.8894       1.01936        0.9058
```

Table D-2. Sample Output of Program AXC03 (cont.)

```
                         CALCULATED AXIAL COMPRESSOR PERFORMANCE, OVERALL DATA
RUN NO.    1        REFERRED SPEED =52.4740       GAMMA = 1.400       AVERAGE PERIPHERAL VELOCITY RATIO = 6.5941

                    ROTOR STAGGER ANGLE = 42.80               STATOR STAGGER ANGLE = 27.80


REFERRED     PRESSURE    OVERALL       POWER       BLADING      3-STAGE        3-STAGE
FLOW RATE     RATIO     EFFICIENCY  COEFFICIENT  EFFICIENCY  PRESSURE RATIO  EFFICIENCY

  43.500     1.01871     0.8191       0.07140      0.8854       1.02056       0.8992
  44.000     1.01860     0.8211       0.07162      0.8882       1.02045       0.9021
  44.500     1.01842     0.8220       0.07165      0.8897       1.02027       0.9040
  45.000     1.01809     0.8171       0.07158      0.8901       1.02005       0.9050
  45.500     1.01776     0.8155       0.07121      0.8899       1.01974       0.9058
  46.000     1.01737     0.8136       0.07060      0.8894       1.01936       0.9058
  46.500     1.01694     0.8070       0.07016      0.8891       1.01902       0.9058
  47.000     1.01648     0.8035       0.06929      0.8873       1.01856       0.9047
  47.500     1.01589     0.7944       0.06833      0.8852       1.01808       0.9033
  48.000     1.01543     0.7898       0.06746      0.8830       1.01764       0.9019
  48.500     1.01486     0.7827       0.06627      0.8784       1.01708       0.8988
  49.000     1.01425     0.7712       0.06513      0.8750       1.01657       0.8961
  49.500     1.01372     0.7639       0.06397      0.8707       1.01604       0.8926
  50.000     1.01308     0.7500       0.06277      0.8656       1.01551       0.8888
  50.500     1.01253     0.7405       0.06154      0.8595       1.01498       0.8841
  51.000     1.01198     0.7300       0.06028      0.8529       1.01443       0.8787
  51.500     1.01128     0.7109       0.05887      0.8441       1.01384       0.8714
  52.000     1.01073     0.6986       0.05756      0.8364       1.01329       0.8646
  52.500     1.01006     0.6773       0.05617      0.8265       1.01274       0.8572
  53.000     1.00950     0.6623       0.05479      0.8164       1.01218       0.8487
  53.500     1.00888     0.6432       0.05325      0.8040       1.01157       0.8375
  54.000     1.00820     0.6171       0.05178      0.7913       1.01100       0.8265
  54.500     1.00763     0.5961       0.05030      0.7771       1.01044       0.8153
```

Table D-2. Sample Output of Program AXC03 (cont.)

```
                          CALCULATED AXIAL COMPRESSOR PERFORMANCE, OVERALL DATA
RUN NO.  11        REFERRED SPEED =51.6500        GAMMA = 1.400        AVERAGE PERIPHERAL VELOCITY RATIO = 6.4905

                   ROTOR STAGGER ANGLE = 43.80                STATOR STAGGER ANGLE = 23.80


REFERRED    PRESSURE    OVERALL       POWER       BLADING        3-STAGE        3-STAGE
FLOW RATE    RATIO     EFFICIENCY  COEFFICIENT  EFFICIENCY   PRESSURE RATIO   EFFICIENCY

  41.500    1.02015     0.8857      0.06782      0.9434        1.02175         0.9552
  42.000    1.02001     0.8807      0.06852      0.9433        1.02172         0.9553
  42.500    1.01994     0.8805      0.06911      0.9430        1.02164         0.9552
  43.000    1.01982     0.8802      0.06956      0.9430        1.02153         0.9555
  43.500    1.01958     0.8750      0.06990      0.9429        1.02139         0.9555
  44.000    1.01938     0.8739      0.07007      0.9424        1.02120         0.9554
  44.500    1.01913     0.8726      0.07009      0.9419        1.02096         0.9555
  45.000    1.01874     0.8667      0.06992      0.9417        1.02068         0.9554
  45.500    1.01840     0.8651      0.06952      0.9414        1.02034         0.9559
  46.000    1.01803     0.8632      0.06906      0.9407        1.01997         0.9555
  46.500    1.01766     0.8572      0.06886      0.9405        1.01971         0.9558
  47.000    1.01717     0.8545      0.06791      0.9400        1.01923         0.9559
  47.500    1.01658     0.8463      0.06691      0.9392        1.01875         0.9561
  48.000    1.01611     0.8435      0.06591      0.9388        1.01827         0.9560
  48.500    1.01558     0.8396      0.06475      0.9376        1.01776         0.9559
  49.000    1.01499     0.8301      0.06365      0.9364        1.01727         0.9560
  49.500    1.01452     0.8266      0.06256      0.9360        1.01680         0.9557
  50.000    1.01392     0.8162      0.06139      0.9343        1.01632         0.9556
  50.500    1.01344     0.8112      0.06024      0.9330        1.01584         0.9553
  51.000    1.01296     0.8063      0.05904      0.9318        1.01537         0.9554
  51.500    1.01234     0.7933      0.05767      0.9295        1.01486         0.9545
  52.000    1.01186     0.7877      0.05640      0.9281        1.01439         0.9546
  52.500    1.01128     0.7743      0.05509      0.9266        1.01391         0.9540
  53.000    1.01080     0.7673      0.05376      0.9246        1.01344         0.9538
  53.500    1.01029     0.7585      0.05229      0.9222        1.01294         0.9528
  54.000    1.00970     0.7415      0.05089      0.9188        1.01246         0.9518
  54.500    1.00923     0.7330      0.04947      0.9168        1.01199         0.9511
  55.000    1.00864     0.7142      0.04800      0.9137        1.01151         0.9502
```

Table D-3. Output of Program AXC03, Case 11, C_{Dmin} = 0.000

```
                      CALCULATED AXIAL COMPRESSOR PERFORMANCE, OVERALL DATA
RUN NO.  12        REFERRED SPEED =51.6500        GAMMA = 1.400        AVERAGE PERIPHERAL VELOCITY RATIO = 6.4905

                   ROTOR STAGGER ANGLE = 43.80                  STATOR STAGGER ANGLE = 23.80


REFERRED     PRESSURE     OVERALL        POWER        BLADING       3-STAGE        3-STAGE
FLOW RATE     RATIO      EFFICIENCY   COEFFICIENT   EFFICIENCY   PRESSURE RATIO   EFFICIENCY

  41.500     1.01967      0.8645       0.06782       0.9226        1.02126        0.9340
  42.000     1.01956      0.8613       0.06851       0.9238        1.02126        0.9356
  42.500     1.01952      0.8623       0.06909       0.9250        1.02122        0.9372
  43.000     1.01942      0.8624       0.06956       0.9254        1.02114        0.9379
  43.500     1.01919      0.8581       0.06988       0.9259        1.02100        0.9387
  44.000     1.01900      0.8573       0.07005       0.9259        1.02082        0.9388
  44.500     1.01877      0.8565       0.07006       0.9259        1.02060        0.9396
  45.000     1.01840      0.8511       0.06990       0.9260        1.02033        0.9397
  45.500     1.01806      0.8496       0.06951       0.9257        1.01999        0.9399
  46.000     1.01770      0.8478       0.06904       0.9252        1.01964        0.9398
  46.500     1.01732      0.8412       0.06883       0.9245        1.01937        0.9400
  47.000     1.01684      0.8383       0.06787       0.9239        1.01890        0.9402
  47.500     1.01625      0.8299       0.06689       0.9229        1.01841        0.9395
  48.000     1.01576      0.8260       0.06586       0.9214        1.01793        0.9391
  48.500     1.01523      0.8211       0.06472       0.9191        1.01741        0.9376
  49.000     1.01465      0.8115       0.06363       0.9178        1.01693        0.9373
  49.500     1.01415      0.8062       0.06252       0.9153        1.01644        0.9358
  50.000     1.01357      0.7957       0.06138       0.9137        1.01596        0.9349
  50.500     1.01306      0.7889       0.06019       0.9109        1.01547        0.9336
  51.000     1.01256      0.7821       0.05899       0.9077        1.01497        0.9313
  51.500     1.01193      0.7675       0.05764       0.9038        1.01444        0.9282
  52.000     1.01143      0.7599       0.05636       0.9004        1.01396        0.9265
  52.500     1.01083      0.7440       0.05504       0.8962        1.01346        0.9240
  53.000     1.01034      0.7349       0.05372       0.8924        1.01297        0.9212
  53.500     1.00977      0.7214       0.05224       0.8853        1.01243        0.9167
  54.000     1.00917      0.7025       0.05083       0.8802        1.01193        0.9131
  54.500     1.00868      0.6905       0.04940       0.8748        1.01144        0.9092
  55.000     1.00807      0.6679       0.04793       0.8679        1.01094        0.9042
```

Table D-4. Output of Program AXC03, Case 12, $C_{Dmin} = 0.006$

```
                    CALCULATED AXIAL COMPRESSOR PERFORMANCE, OVERALL DATA
RUN NO.  13        REFERRED SPEED =51.6500        GAMMA = 1.400        AVERAGE PERIPHERAL VELOCITY RATIO = 6.4905

              ROTOR STAGGER ANGLE = 43.80                STATOR STAGGER ANGLE = 23.80


REFERRED    PRESSURE     OVERALL       POWER       BLADING       3-STAGE        3-STAGE
FLOW RATE    RATIO      EFFICIENCY  COEFFICIENT  EFFICIENCY  PRESSURE RATIO  EFFICIENCY

 41.500     1.01952      0.8579      0.06781      0.9158       1.02110       0.9273
 42.000     1.01941      0.8547      0.06851      0.9171       1.02111       0.9290
 42.500     1.01938      0.8561      0.06909      0.9188       1.02108       0.9309
 43.000     1.01928      0.8563      0.06956      0.9193       1.02100       0.9318
 43.500     1.01906      0.8523      0.06988      0.9202       1.02087       0.9328
 44.000     1.01888      0.8519      0.07005      0.9202       1.02070       0.9334
 44.500     1.01866      0.8514      0.07006      0.9207       1.02048       0.9341
 45.000     1.01827      0.8454      0.06990      0.9204       1.02021       0.9343
 45.500     1.01794      0.8440      0.06951      0.9202       1.01988       0.9346
 46.000     1.01759      0.8427      0.06903      0.9202       1.01953       0.9348
 46.500     1.01722      0.8361      0.06883      0.9194       1.01926       0.9346
 47.000     1.01672      0.8327      0.06787      0.9181       1.01878       0.9343
 47.500     1.01615      0.8246      0.06689      0.9174       1.01830       0.9338
 48.000     1.01565      0.8204      0.06586      0.9159       1.01782       0.9335
 48.500     1.01512      0.8152      0.06470      0.9135       1.01730       0.9320
 49.000     1.01452      0.8049      0.06362      0.9113       1.01681       0.9308
 49.500     1.01403      0.7998      0.06251      0.9092       1.01632       0.9293
 50.000     1.01344      0.7885      0.06135      0.9067       1.01583       0.9280
 50.500     1.01294      0.7818      0.06018      0.9038       1.01534       0.9259
 51.000     1.01244      0.7746      0.05899      0.9002       1.01485       0.9238
 51.500     1.01179      0.7590      0.05761      0.8953       1.01431       0.9204
 52.000     1.01129      0.7505      0.05635      0.8911       1.01381       0.9171
 52.500     1.01069      0.7347      0.05504      0.8869       1.01331       0.9139
 53.000     1.01018      0.7239      0.05370      0.8813       1.01281       0.9104
 53.500     1.00962      0.7102      0.05223      0.8741       1.01227       0.9053
 54.000     1.00901      0.6901      0.05081      0.8676       1.01176       0.9005
 54.500     1.00850      0.6764      0.04940      0.8607       1.01126       0.8945
 55.000     1.00789      0.6531      0.04792      0.8529       1.01075       0.8894
```

Table D-5. Output of Program AXC03, Case 13, C_{Dmin} = 0.008

```
                              CALCULATED AXIAL COMPRESSOR PERFORMANCE, OVERALL DATA
RUN NO.  21        REFERRED SPEED =51.6500        GAMMA = 1.400        AVERAGE PERIPHERAL VELOCITY RATIO = 6.4905

              ROTOR STAGGER ANGLE = 43.80                  STATOR STAGGER ANGLE = 27.80


REFERRED    PRESSURE    OVERALL       POWER       BLADING       3-STAGE        3-STAGE
FLOW RATE    RATIO     EFFICIENCY  COEFFICIENT   EFFICIENCY  PRESSURE RATIO  EFFICIENCY

 41.500     1.01961     0.8841      0.06612      0.9435       1.02122        0.9562
 42.000     1.01935     0.8789      0.06642      0.9434       1.02107        0.9565
 42.500     1.01917     0.8781      0.06664      0.9430       1.02089        0.9564
 43.000     1.01889     0.8771      0.06655      0.9428       1.02063        0.9569
 43.500     1.01849     0.8707      0.06636      0.9422       1.02033        0.9570
 44.000     1.01809     0.8688      0.06585      0.9416       1.01994        0.9568
 44.500     1.01774     0.8673      0.06542      0.9417       1.01960        0.9573
 45.000     1.01716     0.8599      0.06457      0.9409       1.01912        0.9574
 45.500     1.01668     0.8574      0.06364      0.9406       1.01865        0.9577
 46.000     1.01621     0.8541      0.06279      0.9393       1.01819        0.9579
 46.500     1.01561     0.8458      0.06173      0.9387       1.01769        0.9578
 47.000     1.01511     0.8425      0.06065      0.9381       1.01719        0.9579
 47.500     1.01450     0.8329      0.05951      0.9372       1.01669        0.9578
 48.000     1.01399     0.8284      0.05836      0.9359       1.01619        0.9577
 48.500     1.01344     0.8223      0.05707      0.9335       1.01566        0.9571
 49.000     1.01284     0.8112      0.05582      0.9324       1.01516        0.9574
 49.500     1.01233     0.8054      0.05459      0.9304       1.01466        0.9567
 50.000     1.01173     0.7925      0.05329      0.9287       1.01416        0.9563
 50.500     1.01123     0.7861      0.05197      0.9275       1.01367        0.9561
 51.000     1.01073     0.7785      0.05063      0.9251       1.01318        0.9557
 51.500     1.01009     0.7621      0.04912      0.9223       1.01265        0.9547
 52.000     1.00959     0.7537      0.04770      0.9195       1.01216        0.9542
 52.500     1.00900     0.7364      0.04625      0.9172       1.01166        0.9531
```

Table D-6. Output of Program AXC03, Case 21, $C_{Dmin} = 0.000$

```
                              CALCULATED AXIAL COMPRESSOR PERFORMANCE, OVERALL DATA
RUN NO.  22          REFERRED SPEED =51.6500          GAMMA = 1.400          AVERAGE PERIPHERAL VELOCITY RATIO = 6.4905

                 ROTOR STAGGER ANGLE = 43.80                      STATOR STAGGER ANGLE = 27.80


REFERRED      PRESSURE     OVERALL        POWER       BLADING       3-STAGE        3-STAGE
FLOW RATE      RATIO      EFFICIENCY   COEFFICIENT   EFFICIENCY  PRESSURE RATIO  EFFICIENCY

 41.500       1.01921      0.8662       0.06611      0.9254       1.02082        0.9382
 42.000       1.01897      0.8618       0.06640      0.9262       1.02069        0.9395
 42.500       1.01881      0.8619       0.06663      0.9269       1.02053        0.9403
 43.000       1.01855      0.8612       0.06654      0.9270       1.02027        0.9407
 43.500       1.01815      0.8555       0.06634      0.9270       1.01999        0.9414
 44.000       1.01776      0.8533       0.06582      0.9261       1.01961        0.9413
 44.500       1.01742      0.8517       0.06540      0.9259       1.01927        0.9417
 45.000       1.01684      0.8441       0.06454      0.9253       1.01880        0.9418
 45.500       1.01635      0.8408       0.06362      0.9240       1.01831        0.9411
 46.000       1.01589      0.8376       0.06278      0.9229       1.01787        0.9409
 46.500       1.01528      0.8283       0.06171      0.9212       1.01736        0.9403
 47.000       1.01477      0.8238       0.06061      0.9197       1.01685        0.9395
 47.500       1.01415      0.8130       0.05948      0.9173       1.01634        0.9385
 48.000       1.01364      0.8077       0.05832      0.9154       1.01584        0.9374
 48.500       1.01307      0.8002       0.05702      0.9115       1.01529        0.9353
 49.000       1.01245      0.7874       0.05580      0.9084       1.01477        0.9334
 49.500       1.01193      0.7795       0.05456      0.9047       1.01426        0.9308
 50.000       1.01131      0.7650       0.05325      0.9012       1.01375        0.9291
 50.500       1.01078      0.7556       0.05192      0.8969       1.01322        0.9258
 51.000       1.01026      0.7459       0.05058      0.8924       1.01272        0.9233
 51.500       1.00959      0.7251       0.04907      0.8855       1.01215        0.9184
 52.000       1.00908      0.7139       0.04765      0.8799       1.01164        0.9146
 52.500       1.00845      0.6926       0.04618      0.8738       1.01112        0.9103
```

Table D-7. Output of Program AXC03, Case 22, C_{Dmin} = 0.006

```
                              CALCULATED AXIAL COMPRESSOR PERFORMANCE, OVERALL DATA
RUN NO.  23         REFERRED SPEED =51.6500          GAMMA = 1.400          AVERAGE PERIPHERAL VELOCITY RATIO = 6.4905

                    ROTOR STAGGER ANGLE = 43.80                     STATOR  STAGGER ANGLE = 27.80


REFERRED     PRESSURE    OVERALL        POWER        BLADING       3-STAGE        3-STAGE
FLOW RATE     RATIO     EFFICIENCY   COEFFICIENT   EFFICIENCY   PRESSURE RATIO   EFFICIENCY

 41.500      1.01937     0.8611        0.06610      0.9195       1.02069        0.9326
 42.000      1.01885     0.8565        0.06640      0.9209       1.02057        0.9339
 42.500      1.01869     0.8565        0.06662      0.9215       1.02041        0.9352
 43.000      1.01843     0.8561        0.06653      0.9218       1.02016        0.9359
 43.500      1.01804     0.8501        0.06633      0.9215       1.01988        0.9362
 44.000      1.01765     0.8483        0.06581      0.9212       1.01950        0.9364
 44.500      1.01730     0.8464        0.06539      0.9207       1.01916        0.9366
 45.000      1.01673     0.8387        0.06454      0.9199       1.01869        0.9362
 45.500      1.01624     0.8356        0.06361      0.9187       1.01821        0.9361
 46.000      1.01578     0.8317        0.06275      0.9170       1.01776        0.9356
 46.500      1.01517     0.8224        0.06170      0.9152       1.01725        0.9345
 47.000      1.01466     0.8180        0.06061      0.9139       1.01675        0.9335
 47.500      1.01404     0.8070        0.05948      0.9113       1.01623        0.9319
 48.000      1.01351     0.8007        0.05831      0.9084       1.01571        0.9304
 48.500      1.01295     0.7928        0.05702      0.9041       1.01517        0.9279
 49.000      1.01232     0.7795        0.05579      0.9008       1.01465        0.9256
 49.500      1.01179     0.7710        0.05453      0.8961       1.01412        0.9224
 50.000      1.01117     0.7558        0.05324      0.8921       1.01361        0.9195
 50.500      1.01064     0.7459        0.05192      0.8873       1.01308        0.9162
 51.000      1.01011     0.7349        0.05058      0.8817       1.01256        0.9119
 51.500      1.00943     0.7136        0.04906      0.8738       1.01199        0.9065
 52.000      1.00891     0.7009        0.04764      0.8669       1.01147        0.9017
 52.500      1.00827     0.6780        0.04617      0.8592       1.01093        0.8957
```

Table D-8. Output of Program AXC03, Case 23, $C_{Dmin} = 0.008$

```
                         CALCULATED AXIAL COMPRESSOR PERFORMANCE, OVERALL DATA
RUN NO.   31          REFERRED SPEED =51.6          GAMMA = 1.400         AVERAGE PERIPHERAL VELOCITY RATIO = 6.4905

                  ROTOR STAGGER ANGLE = 43.80                    STATOR STAGGER ANGLE = 31.80


REFERRED     PRESSURE      OVERALL        POWER       BLADING      3-STAGE       3-STAGE
FLOW RATE     RATIO      EFFICIENCY    COEFFICIENT  EFFICIENCY  PRESSURE RATIO  EFFICIENCY

 41.500      1.01832      0.8796        0.06210      0.9429      1.01996       0.9579
 42.000      1.01787      0.8730        0.06179      0.9421      1.01963       0.9582
 42.500      1.01756      0.8715        0.06155      0.9418      1.01932       0.9583
 43.000      1.01713      0.8695        0.06091      0.9414      1.01891       0.9589
 43.500      1.01659      0.8623        0.06018      0.9410      1.01847       0.9592
 44.000      1.01612      0.8589        0.05939      0.9397      1.01801       0.9592
 44.500      1.01564      0.8558        0.05849      0.9388      1.01754       0.9589
 45.000      1.01505      0.8473        0.05750      0.9382      1.01705       0.9592
 45.500      1.01454      0.8434        0.05645      0.9371      1.01655       0.9589
 46.000      1.01405      0.8390        0.05545      0.9355      1.01608       0.9593
 46.500      1.01343      0.8287        0.05425      0.9344      1.01555       0.9588
 47.000      1.01290      0.8235        0.05302      0.9328      1.01504       0.9589
 47.500      1.01226      0.8105        0.05175      0.9306      1.01451       0.9583
 48.000      1.01174      0.8046        0.05046      0.9290      1.01400       0.9580
 48.500      1.01119      0.7977        0.04902      0.9269      1.01345       0.9575
 49.000      1.01055      0.7819        0.04762      0.9240      1.01292       0.9573
```

Table D-9. Output of Program AXC03, Case 31, C_{Dmin} = 0.000

```
                          CALCULATED AXIAL COMPRESSOR PERFORMANCE, OVERALL DATA
RUN NO.  32          REFERRED SPEED =51.6500        GAMMA = 1.400        AVERAGE PERIPHERAL VELOCITY RATIO = 6.4905

                  ROTOR STAGGER ANGLE = 43.80                 STATOR STAGGER ANGLE = 31.80


REFERRED     PRESSURE     OVERALL         POWER         BLADING         3-STAGE          3-STAGE
FLOW RATE    RATIO       EFFICIENCY    COEFFICIENT    EFFICIENCY   PRESSURE RATIO    EFFICIENCY

  41.500      1.01795     0.8627         0.06207        0.9258        1.01960          0.9411
  42.000      1.01752     0.8565         0.06177        0.9256        1.01928          0.9416
  42.500      1.01722     0.8551         0.06152        0.9253        1.01899          0.9423
  43.000      1.01680     0.8529         0.06089        0.9248        1.01857          0.9424
  43.500      1.01626     0.8453         0.06016        0.9241        1.01814          0.9422
  44.000      1.01579     0.8418         0.05937        0.9225        1.01768          0.9417
  44.500      1.01530     0.8378         0.05847        0.9208        1.01720          0.9412
  45.000      1.01470     0.8282         0.05748        0.9191        1.01671          0.9403
  45.500      1.01418     0.8232         0.05641        0.9171        1.01619          0.9393
  46.000      1.01370     0.8185         0.05542        0.9150        1.01572          0.9385
  46.500      1.01305     0.8058         0.05422        0.9116        1.01518          0.9362
  47.000      1.01252     0.7994         0.05299        0.9088        1.01465          0.9349
  47.500      1.01186     0.7849         0.05172        0.9051        1.01411          0.9326
  48.000      1.01132     0.7761         0.05042        0.9009        1.01357          0.9301
  48.500      1.01074     0.7660         0.04898        0.8953        1.01299          0.9261
  49.000      1.01008     0.7479         0.04759        0.8901        1.01245          0.9234
```

Table D-10. Output of Program AXC03, Case 32, $C_{Dmin} = 0.006$

```
                                   CALCULATED AXIAL COMPRESSOR PERFORMANCE, OVERALL DATA
RUN NO.   33          REFERRED SPEED =51.6500         GAMMA = 1.400          AVERAGE PERIPHERAL VELOCITY RATIO = 6.4905

                     ROTOR STAGGER ANGLE = 43.80                      STATOR STAGGER ANGLE = 31.80


REFERRED    PRESSURE      OVERALL        POWER       BLADING       3-STAGE        3-STAGE
FLOW RATE    RATIO       EFFICIENCY   COEFFICIENT   EFFICIENCY   PRESSURE RATIO  EFFICIENCY

  41.500    1.01783       0.8568       0.06207       0.9199       1.01948        0.9353
  42.000    1.01741       0.8511       0.06176       0.9204       1.01916        0.9361
  42.500    1.01711       0.8499       0.06152       0.9201       1.01888        0.9370
  43.000    1.01669       0.8474       0.06088       0.9194       1.01846        0.9369
  43.500    1.01614       0.8394       0.06015       0.9181       1.01802        0.9366
  44.000    1.01568       0.8359       0.05936       0.9168       1.01757        0.9361
  44.500    1.01520       0.8324       0.05846       0.9155       1.01710        0.9357
  45.000    1.01459       0.8220       0.05748       0.9131       1.01660        0.9342
  45.500    1.01407       0.8168       0.05641       0.9106       1.01608        0.9326
  46.000    1.01358       0.8111       0.05542       0.9076       1.01560        0.9311
  46.500    1.01294       0.7988       0.05422       0.9046       1.01505        0.9288
  47.000    1.01239       0.7914       0.05298       0.9008       1.01452        0.9268
  47.500    1.01172       0.7756       0.05170       0.8958       1.01397        0.9233
  48.000    1.01117       0.7666       0.05039       0.8915       1.01343        0.9204
  48.500    1.01059       0.7556       0.04896       0.8850       1.01285        0.9161
  49.000    1.00992       0.7365       0.04759       0.8784       1.01229        0.9115
```

Table D-11. Output of Program AXC03, Case 33, C_{Dmin} 0.008

```
                         CALCULATED AXIAL COMPRESSOR PERFORMANCE, OVERALL DATA
RUN NO.  41        REFERRED SPEED =51.6500       GAMMA = 1.400       AVERAGE PERIPHERAL VELOCITY RATIO = 6.4905

              ROTOR STAGGER ANGLE = 43.80                  STATOR STAGGER ANGLE = 35.80


REFERRED     PRESSURE    OVERALL      POWER       BLADING       3-STAGE        3-STAGE
FLOW RATE     RATIO     EFFICIENCY  COEFFICIENT  EFFICIENCY  PRESSURE RATIO  EFFICIENCY

  41.500     1.01634    0.8700      0.05604     0.9401       1.01804        0.9600
  42.000     1.01582    0.8621      0.05544     0.9391       1.01763        0.9599
  42.500     1.01538    0.8587      0.05476     0.9376       1.01720        0.9599
  43.000     1.01495    0.8566      0.05399     0.9375       1.01677        0.9604
  43.500     1.01437    0.8466      0.05313     0.9356       1.01630        0.9599
  44.000     1.01389    0.8430      0.05218     0.9346       1.01583        0.9599
  44.500     1.01339    0.8385      0.05115     0.9334       1.01535        0.9603
  45.000     1.01277    0.8271      0.05002     0.9316       1.01483        0.9598
  45.500     1.01223    0.8215      0.04880     0.9298       1.01430        0.9597
```

Table D-12. Output of Program AXC03, Case 41, C_{Dmin} 0.000

```
                              CALCULATED AXIAL COMPRESSOR PERFORMANCE, OVERALL DATA
RUN NO.  42           REFERRED SPEED =51.6500        GAMMA = 1.400         AVERAGE PERIPHERAL VELOCITY RATIO = 6.4905

                      ROTOR STAGGER ANGLE = 43.80                    STATOR STAGGER ANGLE = 35.80


REFERRED   PRESSURE    OVERALL       POWER       BLADING      3-STAGE       3-STAGE
FLOW RATE   RATIO     EFFICIENCY  COEFFICIENT  EFFICIENCY  PRESSURE RATIO  EFFICIENCY

 41.500    1.01597     0.8508      0.05601      0.9208      1.01767       0.9408
 42.000    1.01547     0.8432      0.05542      0.9202      1.01727       0.9409
 42.500    1.01504     0.8399      0.05474      0.9188      1.01685       0.9406
 43.000    1.01459     0.8361      0.05397      0.9169      1.01640       0.9398
 43.500    1.01400     0.8252      0.05311      0.9142      1.01593       0.9383
 44.000    1.01351     0.8204      0.05215      0.9122      1.01545       0.9377
 44.500    1.01300     0.8144      0.05111      0.9094      1.01495       0.9361
 45.000    1.01236     0.8011      0.04998      0.9057      1.01442       0.9339
 45.500    1.01182     0.7940      0.04878      0.9023      1.01388       0.9318
```

Table D-13. Output of Program AXC03, Case 42, C_{Dmin} 0.006

```
                                    CALCULATED AXIAL COMPRESSOR PERFORMANCE, OVERALL DATA
RUN NO.  43        REFERRED SPEED =51.6500        GAMMA = 1.400        AVERAGE PERIPHERAL VELOCITY RATIO = 6.4905

                 ROTOR STAGGER ANGLE = 43.80                      STATOR STAGGER ANGLE = 35.80


REFERRED    PRESSURE    OVERALL       POWER       BLADING       3-STAGE       3-STAGE
FLOW RATE    RATIO     EFFICIENCY  COEFFICIENT   EFFICIENCY  PRESSURE RATIO  EFFICIENCY

 41.500     1.01585     0.8444      0.05601       0.9143       1.01754       0.9342
 42.000     1.01534     0.8364      0.05540       0.9134       1.01714       0.9343
 42.500     1.01491     0.8331      0.05473       0.9121       1.01673       0.9342
 43.000     1.01447     0.8295      0.05396       0.9104       1.01628       0.9332
 43.500     1.01388     0.8184      0.05308       0.9076       1.01581       0.9319
 44.000     1.01338     0.8126      0.05214       0.9045       1.01532       0.9299
 44.500     1.01286     0.8062      0.05111       0.9010       1.01482       0.9279
 45.000     1.01222     0.7924      0.04998       0.8972       1.01428       0.9252
 45.500     1.01168     0.7847      0.04877       0.8930       1.01374       0.9227
```

Table D-14. Output of Program AXC03, Case 43, $C_{Dmin} = 0.008$

```
                              CALCULATED AXIAL COMPRESSOR PERFORMANCE, OVERALL DATA
RUN NO.  51          REFERRED SPEED =51.6500          GAMMA = 1.400          AVERAGE PERIPHERAL VELOCITY RATIO = 6.4905

                     ROTOR STAGGER ANGLE = 43.80                    STATOR STAGGER ANGLE = 39.80


REFERRED     PRESSURE     OVERALL        POWER       BLADING      3-STAGE        3-STAGE
FLOW RATE     RATIO      EFFICIENCY   COEFFICIENT  EFFICIENCY  PRESSURE RATIO  EFFICIENCY

 41.500       1.01515     0.8081        0.05595      0.8781       1.01683        0.8976
```

Table D-15. Output of Program AXC03, Cases 51, 52, and 53, All C_{Dmin}

```
                         CALCULATED AXIAL COMPRESSOR PERFORMANCE, OVERALL DATA
RUN NO.   61        REFERRED SPEED =51.6500        GAMMA = 1.400        AVERAGE PERIPHERAL VELOCITY RATIO = 6.4905

                 ROTOR STAGGER ANGLE = 43.80                 STATOR STAGGER ANGLE = 44.30


REFERRED    PRESSURE     OVERALL         POWER        BLADING        3-STAGE         3-STAGE
FLOW RATE    RATIO      EFFICIENCY    COEFFICIENT   EFFICIENCY   PRESSURE RATIO    EFFICIENCY

 41.500     1.01515      0.8081         0.05595       0.8781        1.01683          0.8976
```

Table D-16. Output of Program AXC03, Cases 61, 62, and 63, All C_{Dmin}

```
FORTRAN IV G LEVEL 0, MOD 0             MAIN                DATE = 67160          16/30/48                PAGE 0001
 0001                0DIMENSION BETA(15),ADENCE(15),CDENCE(15),DDENCE(15),ASLOPN(15),CSL        2
                     1OPN(15),DSLOPN(15),ADEVAT(15),CDEVAT(15),DDEVAT(15),ASLOPM(15),CSL        3
                     2OPM(15),DSLOPM(15),ASLOPD(15),CSLOPD(15),DSLOPD(15),PDENCE(15),PSL        4
                     3OPN(15),PDEVAT(15),PSLOPM(15),PSLOPD(15)                           1      4
                  C  THIS PROGRAM CHECKS THE ACCURACY WITH WHICH THE POLYNOMIALS IN AXCOM4
                  C  REPRESENT THE FIGURES IN NACA SP-36
                  C                                                                     00000264
                  C ZERO-CAMBER INCIDENCE VS SOLIDITY AND ALPHA 1  FIG 137              00000265
                  C                                                                     00000266
 0002                 FIGAF(A,S)=0.96195E-02- 0.21961E-01*S+0.10963E-01*S*S-0.42930E-02*00000267
                     1A+0.85403E-01*A*S-0.34503E-02*A*S*S+0.27923E-04*A*A-0.64301E-04*A*00000268
                     2A*S+0.32138E-04*A*A*S*S                                           00000269
                  C                                                                     00000275
                  C SLOPE FACTOR N (INCIDENCE) VS SOLIDITY AND ALPHA 1   FIG 138        00000276
                  C                                                                     00000277
 0003                 FIGCF(A,S)=-0.11890+0.21192*S-0.17854*S*S+0.57160E-01*S*S*S-0.368700000278
                     13E-02*A-0.76207E-04*A*S+0.18208E-02*A*S*S-0.55334E-03*A*S*S*S-0.3600000279
                     2825E-04*A*A+0.66620E-04*A*A*S+0.16243E-04*A*A*S*S-0.22671E-04*A*A*00000280
                     3S*S*S-0.72311E-07*A*A*A-0.54986E-06*A*A*A*S-0.49472E-06*A*A*A*S*S+00000281
                     40.37471E-06*A*A*A*S*S*S                                           00000282
                  C                                                                     00000283
                  C ZERO-CAMBER DEVIATION VS SOLIDITY AND ALPHA 1   FIG 161             00000284
                  C                                                                     00000285
 0004                 FIGDF(A,S)=-0.017896+0.10058*S-0.14687*S*S+0.58557E-01*S*S*S-0.11900000286
                     187E-01*A+0.65167E-01*A*S-0.44822E-01*A*S*S+0.11478E-01*A*S*S*S-0.200000287
                     24947E-03*A*A+0.66468E-03*A*A*S-0.94528E-03*A*A*S*S+0.28823E-03*A*A00000288
                     3*S*S*S+0.67269E-05*A*A*A-0.17987E-04*A*A*A*S+0.25862E-04*A*A*A*S*S00000289
                     4-0.77546E-05*A*A*A*S*S*S                                          00000290
                  C                                                                     00000295
                  C SLOPE FACTOR M (DEVIATION) VS SOLIDITY AND ALPHA 1   FIG 168        00000296
                  C                                                                     00000297
 0005                 FIGGF(A,S)=1.06850-1.68830*S+1.15690*S*S-0.28879*S*S*S+0.36581E-0300000298
                     1*A-0.19185E-02*A*S+0.36235E-02*A*S*S-0.13993E-02*A*S*S*S-0.57353E-00000299
                     205*A*A+0.11329E-03*A*A*S-0.19416E-03*A*A*S*S+0.74911E-04*A*A*S*S*S00000300
                     3-0.16187E-06*A*A*A-0.79239E-06*A*A*A*S+0.22558E-05*A*A*A*S*S-0.99200000301
                     418E-06*A*A*A*S*S*S                                                00000302
                  C                                                                     00000323
                  C SLOPE FACTOR (DI/DD)* VS SOLIDITY AND ALPHA 1   FIG 177             00000324
                  C                                                                     00000325
                  C   CAUTION  THIS POLYNOMIAL GENERATED FOR SOLIDITIES FROM 0.6 TO 1.4 10000325
                  C                                                                     20000325
 0006                0FIGHF(A,S)=.81324E+00-.17818E+01*S+.13558E+01*S*S-.35174E+00*S*S*S00000326
                     1-.40846E-02*A+.18322E-01*A*S-.21692E-01*A*S*S+.76075E-02*A*S*S*S+.00000327
                     218174E-03*A*A-.83518E-03*A*A*S+.10421E-02*A*A*S*S-.38235E-03*A*A*S00000328
                     3*S*S-.94842E-06*A*A*A+.86041E-05*A*A*A*S-.12163E-04*A*A*A*S*S+.46710000328
                     421E-05*A*A*A*S*S*S                                                20000328
 0007                 READ(5,700)(BETA(I),I=1,15)                                              5
 0008                 READ(5,700)(ADENCE(I),I=1,15)                                            6
```

Table D-17. Program CHECK, Listing and Output

```
FORTRAN IV G LEVEL 0, MOD 0            MAIN              DATE = 67160          16/30/48                PAGE 0002

  0009                READ(5,700)(ASLOPN(I),I=1,15)                                        7
  0010                READ(5,700)(ADEVAT(I),I=1,15)                                        8
  0011                READ(5,700)(ASLOPM(I),I=1,15)                                        9
  0012                READ(5,700)(ASLOPD(I),I=1,15)                                       10
  0013                S=0.8                                                               11
  0014                A=0.0                                                               12
  0015                I=1                                                                 13
  0016              1 DENCE=FIGAF(A,S)                                                   101
  0017                CDENCE(I)=DENCE                                                    102
  0018                AE=ADENCE(I)                                                       103
  0019                DE=AE-DENCE                                                        104
  0020                DDENCE(I)=DE                                                       105
  0021                PE=100.*DE/AE                                                  1   105
  0022                PDENCE(I)=PE                                                   2   105
  0023                SLOPN=FIGCF(A,S)                                                   106
  0024                CSLOPN(I)=SLOPN                                                    107
  0025                AN=ASLOPN(I)                                                       108
  0026                DN=AN-SLOPN                                                        109
  0027                DSLOPN(I)=DN                                                       110
  0028                PN=100.*DN/AN                                                  1000110
  0029                PSLOPN(I)=PN                                                   2000110
  0030                DEVAT=FIGDF(A,S)                                                   111
  0031                CDEVAT(I)=DEVAT                                                    112
  0032                AT=ADEVAT(I)                                                       113
  0033                DT=AT-DEVAT                                                        114
  0034                DDEVAT(I)=DT                                                       115
  0035                PT=100.*DT/AT                                                  1   115
  0036                PDEVAT(I)=PT                                                   2   115
  0037                SLOPM=FIGGF(A,S)                                                   116
  0038                CSLOPM(I)=SLOPM                                                    117
  0039                AM=ASLOPM(I)                                                       118
  0040                DM=AM-SLOPM                                                        119
  0041                DSLOPM(I)=DM                                                       120
  0042                PM=100.*DM/AM                                                  1   120
  0043                PSLOPM(I)=PM                                                   2   120
  0044                SLOPD=FIGHF(A,S)                                                   121
  0045                CSLOPD(I)=SLOPD                                                    122
  0046                AD=ASLOPD(I)                                                       123
  0047                DD=AD-SLOPD                                                        124
  0048                DSLOPD(I)=DD                                                       125
  0049                PD=100.*DD/AD                                                  1   125
  0050                PSLOPD(I)=PD                                                   2   125
  0051                IF(I-15)2,3,3                                                      126
  0052              2 I=I+1                                                              127
  0053                A=A+5.                                                             128
  0054                GO TO 1                                                            129
  0055              3 WRITE(6,750)S                                                      130
  0056                WRITE(6,751)                                                       131
```

Table D-17. Program CHECK, Listing and Output (cont.)

```
0057                 DO 4 I=1,15                                                      132
0058               4 WRITE(6,757)BETA(I),ADENCE(I),CDENCE(I),DDENCE(I),PDENCE(I)       133
0059                 WRITE(6,752)                                                      134
0060                 WRITE(6,753)                                                      135
0061                 DO 5 I=1,15                                                      136
0062               5 WRITE(6,757)BETA(I),ASLOPN(I),CSLOPN(I),DSLOPN(I),PSLOPN(I)       137
0063                 WRITE(6,754)                                                      138
0064                 DO 6 I=1,15                                                      139
0065               6 WRITE(6,757)BETA(I),ADEVAT(I),CDEVAT(I),DDEVAT(I),PDEVAT(I)       140
0066                 WRITE(6,755)                                                      141
0067                 WRITE(6,753)                                                      142
0068                 DO 7 I=1,15                                                      143
0069               7 WRITE(6,757)BETA(I),ASLOPM(I),CSLOPM(I),DSLOPM(I),PSLOPM(I)       144
0070                 WRITE(6,756)                                                      145
0071                 WRITE(6,753)                                                      146
0072                 DO 8 I=1,15                                                      147
0073               8 WRITE(6,757)BETA(I),ASLOPD(I),CSLOPD(I),DSLOPD(I),PSLOPD(I)       148
0074             700 FORMAT(8F8.3)                                                    149
0075             7500FORMAT(1H1,9X,74HCOMPARISON OF ACTUAL VALUES IN NASA SP-36 WITH VA   150
                    1LUES CALCULATED BY AXCOM2//43X,11HSOLIDITY = ,F3.1//)            151
0076             7510FORMAT(//33X,34HZERO CAMBER INCIDENCE VERSUS ANGLE/3X,14HANGLE, DE   152
                    1GREES,5X,16HACTUAL INCIDENCE,2X,20HCALCULATED INCIDENCE,2X,19HACTU   153
                    2AL - CALCULATED,5X,13HPERCENT ERROR/)                             154
0077             752 FORMAT(//36X,27HSLOPE FACTOR N VERSUS ANGLE/)                     155
0078             7530FORMAT(3X,14HANGLE, DEGREES,6X,13HACTUAL FACTOR,5X,17HCALCULATED F   156
                    1ACTOR,3X,19HACTUAL - CALCULATED,6X,13HPERCENT ERROR/)             157
0079             7540FORMAT(//39X,22HDEVIATION VERSUS ANGLE//3X,14HANGLE, DEGREES,5X,16   158
                    1HACTUAL DEVIATION,2X,20HCALCULATED DEVIATION,2X,19HACTUAL - DEVIAT   159
                    2ION,5X,13HPERCENT ERROR/)                                         160
0080             755 FORMAT(1H1,36X,27HSLOPE FACTOR M VERSUS ANGLE/)                   161
0081             756 FORMAT(//39X,32HSLOPE FACTOR DI/DD VERSUS ANGLE/)                 162
0082             757 FORMAT(5F20.10)   .                                               163
0083                 END
```

Table D-17. Program CHECK, Listing and Output (cont.)

```
        COMPARISON OF ACTUAL VALUES IN NASA SP-36 WITH VALUES CALCULATED BY AXCOM2

                                 SOLIDITY = 0.8



                                ZERO CAMBER INCIDENCE VERSUS ANGLE
ANGLE, DEGREES      ACTUAL INCIDENCE  CALCULATED INCIDENCE  ACTUAL - CALCULATED      PERCENT ERROR

    0.0                 0.0                 -0.0009329878        0.0009329878        0.0932987332
    5.0000000000        0.3299999833         0.3080989718        0.0219010115        6.6366682053
   10.0000000000        0.6799999475         0.6169836521        0.0630162954        9.2671022415
   15.0000000000        0.9899999499         0.9257200956        0.0642798543        6.4929141998
   20.0000000000        1.3099994659         1.2343072891        0.0756921768        5.7780303955
   25.0000000000        1.6199998856         1.5427494049        0.0772504807        4.7685480118
   30.0000000000        1.9299993515         1.8510446548        0.0789546967        4.0909175873
   35.0000000000        2.2299995422         2.1591939926        0.0708055496        3.1751365662
   40.0000000000        2.5499992371         2.4671907425        0.0828084946        3.2473926544
   45.0000000000        2.8299999237         2.7750444412        0.0549554825        1.9418897629
   50.0000000000        3.1199998856         3.0827503204        0.0372495651        1.1938962936
   55.0000000000        3.3899993896         3.3903064728       -0.0003070831       -0.0090584978
   60.0000000000        3.6199996856         3.6977157593       -0.0777158737       -2.1468467712
   65.0000000000        3.8299999237         4.0049800873       -0.1749801636       -4.5686721802
   70.0000000000        4.0099992752         4.3120946884       -0.3020954132       -7.5335502625

                              SLOPE FACTOR N VERSUS ANGLE

ANGLE, DEGREES        ACTUAL FACTOR     CALCULATED FACTOR   ACTUAL - CALCULATED      PERCENT ERROR

    0.0                -0.0389999971        -0.0343636572       -0.0046363398       11.8880500793
    5.0000000000       -0.0499999970        -0.0483931080       -0.0016068891        3.2137775421
   10.0000000000       -0.0609999970        -0.0621372499        0.0011372529       -1.8643474579
   15.0000000000       -0.0739999413        -0.0760737062        0.0020737648       -2.8023862839
   20.0000000000       -0.0879999995        -0.0906807184        0.0026807189       -3.0462713242
   25.0000000000       -0.1039999723        -0.1064355373        0.0024355650       -2.3418893814
   30.0000000000       -0.1209999919        -0.1238162518        0.0028162599       -2.3274869919
   35.0000000000       -0.1409999728        -0.1433003545        0.0023003817       -1.6314764023
   40.0000000000       -0.1619999409        -0.1653655767        0.0033656359       -2.0775537491
   45.0000000000       -0.1859999895        -0.1904897094        0.0044897199       -2.4138278961
   50.0000000000       -0.2119999528        -0.2191501260        0.0071501732       -3.3727235794
   55.0000000000       -0.2409999967        -0.2518250346        0.0108250380       -4.4917144775
   60.0000000000       -0.2769999504        -0.2889920473        0.0119920969       -4.3292751312
   65.0000000000       -0.3209999800        -0.3311289549        0.0101289749       -3.1554431915
   70.0000000000       -0.3759999871        -0.3787130713        0.0027130842       -0.7215649486

                                DEVIATION VERSUS ANGLE

ANGLE, DEGREES      ACTUAL DEVIATION  CALCULATED DEVIATION  ACTUAL - DEVIATION,      PERCENT ERROR

    0.0                 0.0                 -0.0014475845        0.0014475845        0.1447584033
    5.0000000000        0.0599999987         0.0814747810       -0.0214747824      -35.7912902832
   10.0000000000        0.1299999952         0.1593298316       -0.0293298364      -22.5614013672
   15.0000000000        0.2099999785         0.2358062267       -0.0258062482      -12.2886896133
   20.0000000000        0.2999999523         0.3145923018       -0.0145923495       -4.8641147614
   25.0000000000        0.3999999762         0.3993784785        0.0006214976        0.1553744078
   30.0000000000        0.5099999905         0.4938524365        0.0161475539        3.1661853790
   35.0000000000        0.6299999952         0.6017042994        0.0282956958        4.4913787842
   40.0000000000        0.7599999905         0.7266232967        0.0333766937        4.3916702271
   45.0000000000        0.8999999762         0.8722926378        0.0277073383        3.0785923004
   50.0000000000        1.0599994659         1.0424118042        0.0175876617        1.6592140198
   55.0000000000        1.2500000000         1.2406597137        0.0093402863        0.7472229004
   60.0000000000        1.4799995422         1.4707336426        0.0092658997        0.6260744929
   65.0000000000        1.7500000000         1.7363204956        0.0136795044        0.7816859484
   70.0000000000        2.0699996948         2.0411033630        0.0288963318        1.3959579468
```

Table D- 17. Program CHECK,Listing and Output (cont.)

```
                                   SLOPE FACTOR M VERSUS ANGLE

ANGLE, DEGREES        ACTUAL FACTOR      CALCULATED FACTOR   ACTUAL - CALCULATED        PERCENT ERROR

     0.0                  0.3099999428        0.3104162812       -0.0004163384        -0.1343027353
     5.0000000000         0.3119999766        0.3125761747       -0.0005761981        -0.1846788526
    10.0000000000         0.3149999976        0.3147908449        0.0002091527         0.0663976669
    15.0000000000         0.3169999719        0.3171648979       -0.0001649261        -0.0520271473
    20.0000000000         0.3209999800        0.3198031187        0.0011968613         0.3728539944
    25.0000000000         0.3239999413        0.3228106499        0.0011892915         0.3670653105
    30.0000000000         0.3279999495        0.3262923956        0.0017075539         0.5205957294
    35.0000000000         0.3329999447        0.3303530812        0.0026468635         0.7948539853
    40.0000000000         0.3379999995        0.3350979686        0.0029020309         0.8585889935
    45.0000000000         0.3439999819        0.3406320214        0.0033679605         0.9790582657
    50.0000000000         0.3499999642        0.3470600843        0.0029398799         0.8399657607
    55.0000000000         0.3569999933        0.3544869423        0.0025130510         0.7039358616
    60.0000000000         0.3649999499        0.3630179167        0.0019820333         0.5430228710
    65.0000000000         0.3750000000        0.3727575541        0.0022424459         0.5979855657
    70.0000000000         0.3879999518        0.3838108182        0.0041891336         1.0796728134

                                  SLOPE FACTOR DI/DO VERSUS ANGLE/
ANGLE, DEGREES        ACTUAL FACTOR      CALCULATED FACTOR   ACTUAL - CALCULATED        PERCENT ERROR

     0.0                  0.0769999623        0.0754218698        0.0015780926         2.0494718557
     5.0000000000         0.0789999962        0.0780347586        0.0009652376         1.2218189240
    10.0000000000         0.0809999704        0.0802936554        0.0007063150         0.8719941378
    15.0000000000         0.0829999447        0.0826053023        0.0003946424         0.4754729667
    20.0000000000         0.0859999657        0.0853770375        0.0006229281         0.7243353128
    25.0000000000         0.0899999738        0.0890154839        0.0009844899         1.0938777924
    30.0000000000         0.0939999819        0.0939274430        0.0000725389         0.0771690011
    35.0000000000         0.1019999981        0.1005203128        0.0014796853         1.4506711960
    40.0000000000         0.1109999418        0.1092003584        0.0017995834         1.6212463379
    45.0000000000         0.1209999919        0.1203768849        0.0006231070         0.5149644613
    50.0000000000         0.1319999695        0.1344547272       -0.0024547577        -1.8596649170
    55.0000000000         0.1499999762        0.1518397331       -0.0018397570        -1.2265043259
    60.0000000000         0.1719999909        0.1729413271       -0.0009413362        -0.5472884774
    65.0000000000         0.1979999542        0.1981655955       -0.0001656413        -0.0836572051
    70.0000000000         0.2269999981        0.2279177904       -0.0009177923        -0.4043137431
```

Table D-17. Program CHECK,Listing and Output (cont.)

APPENDIX E

PROPOSED DESIGN OF AN IMPROVED INLET DUCT

The present inlet duct is deficient because of the shape of its bellmouth, because of the small velocities that occur in it during operation which make accurate determination of volume flow rates impossible, and because it has no provision to eliminate effects of atmospheric gusts or winds.

The entrance bellmouth should have more gradual changes in wall curvature to eliminate local separations at the entrance to the cylindrical duct. It was stated earlier that the velocity head in this duct with 36 in. diameter is about 0.6 in. of water, a value too small for accurate measurements. To avoid large fluctuations of the read-out of the Texas Instruments pressure gauge, for small variation in flow rate, the velocity head should be increased to about 6 in. of water or 33 lb/ft^2, at a volume flow rate of 360 $\text{ft}^3\text{/sec}$, giving a response at the instrument of about 8000 counts. For an assumed incompressible flow with a mass density ρ_i of 0.002378 $\text{lb sec}^2\text{/ft}^4$, and a velocity head q_{i1} of 33 lb/ft^2, the velocity V_i in the measuring plane of the inlet duct would have to be

$$V_i = \sqrt{\frac{2\, q_{i1}}{\rho_i}} \qquad \text{(ft/sec)} \qquad (6)$$

Hence the required flow area is 360/166 = 2.16 ft^2, corresponding to a circular area with 19.9 in. diameter. Because of the small pressure rise of the compressor it is necessary to convert the velocity head at the measuring plane into static pressure rise by arranging an optimum diffuser between this section and the inlet pipe to the compressor that has a diameter of 36 in. Test data of Reference 11 show that the included diffuser angle should be 8° for the present application. Larger diffuser angles produce separation with associated flow instabilities, and smaller angles require ducts with increased lengths where the boundary layer growth is excessive and reduces pressure recovery. For a diffuser angle of 8° the length L of the diffuser is

$$L = \frac{36 - 19.9}{2 \tan 4^\circ} = 116 \text{ in.}$$

Figure E-1 shows the design of the proposed inlet duct. A well designed bellmouth from a diameter of 48 in. to the throat of 19.9 in. requires an axial length of about 26 in., giving a total length of the duct of 116 + 26 = 142 in. Ahead of the bellmouth inlet a structure will be attached to support several layers of fine mesh screen to eliminate flow disturbances by gusts in the surrounding atmosphere. The whole duct is mounted on a trolley which can be rolled onto the apron outside the test cell to permit simple attachment to and removal from the presently installed cylindrical inlet duct. It is recommended also that an additional honeycomb flow straightener be installed at the entrance of this duct.

The bellmouth and the diffuser could be molded out of plastics, reinforced by fiberglass, by using a wooden template which is split at the smallest diameter.

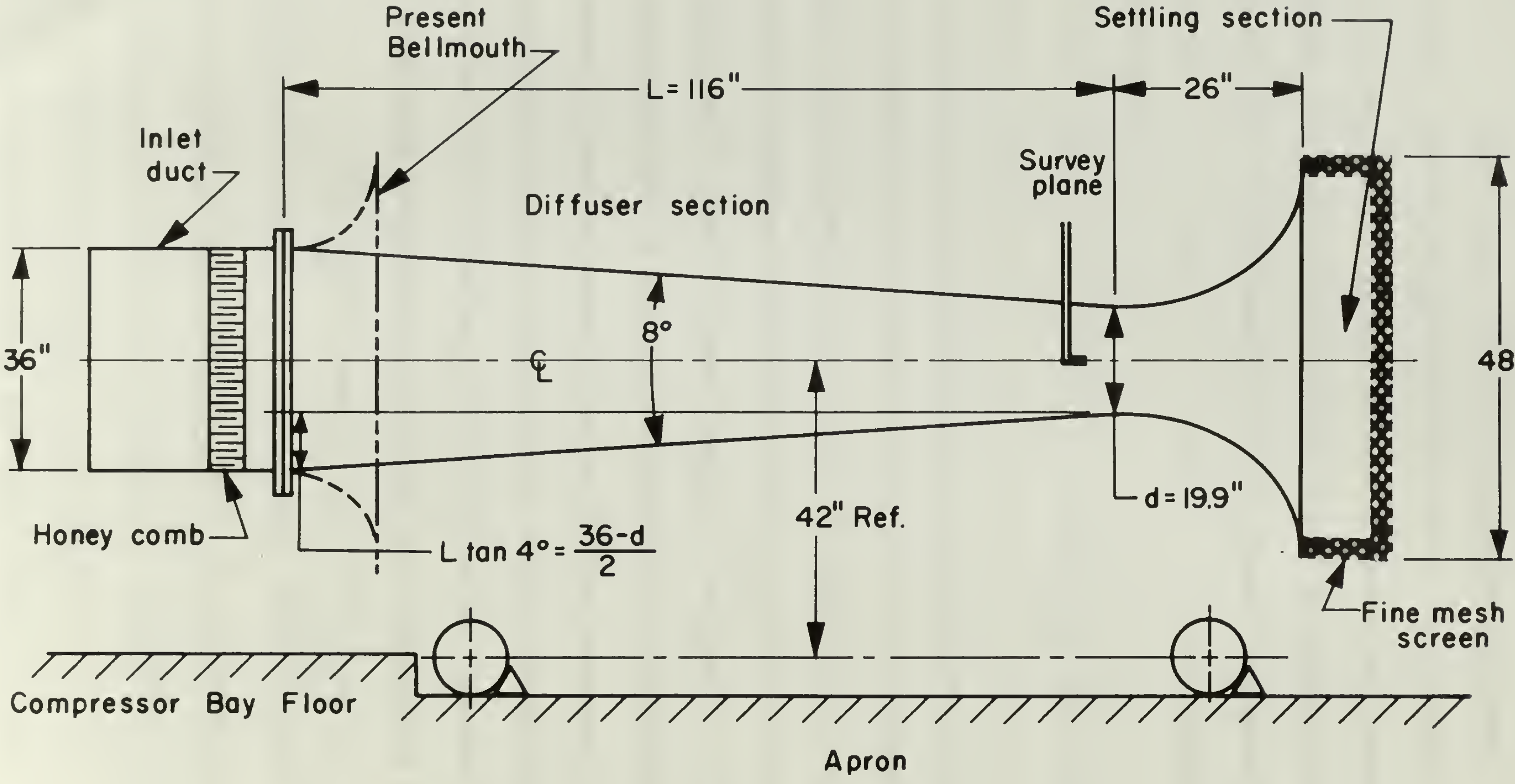

FIG. E-1 PROPOSED IMPROVED INLET DUCT

INITIAL DISTRIBUTION LIST

		Copies
1.	Defense Documentation Center Cameron Station Alexandria, Virginia 22314	20
2.	Library Naval Postgraduate School Monterey, California 93940	2
3.	Commander, Naval Air Systems Command Navy Department Washington, D. C. 20360	1
4.	Commander, Naval Ship Systems Command Navy Department Washington, D. C. 20360	1
5.	Dr. O. H. Johnson Naval Air Systems Command (Code 330 B) Navy Department Washington, D. C. 20360	1
6.	Capt. A. Bodnaruk, USN Naval Ship Systems Command (Code 6140) Navy Department Washington, D. C. 20360	1
7.	Office of Naval Research (Power Branch) Attn: Mr. J. K. Patton, Jr. Navy Department Washington, D. C. 20360	1
8.	Chairman, Department of Aeronautics Naval Postgraduate School Monterey, California 93940	3
9.	Professor M. H. Vavra Department of Aeronautics Naval Postgraduate School Monterey, California 93940	3
10.	Lt. B. C. Marshall Air Antisubmarine Squadron 35 Fleet Post Office San Francisco, California 96601	4

DOCUMENT CONTROL DATA - R&D

(Security classification of title, body of abstract and indexing annotation must be entered when the overall report is classified)

1. ORIGINATING ACTIVITY *(Corporate author)* Naval Postgraduate School Monterey, California 93940	**2a. REPORT SECURITY CLASSIFICATION** UNCLASSIFIED **2b. GROUP** -

3. REPORT TITLE

EFFECT OF STATOR BLADE ORIENTATION ON THE PERFORMANCE OF AN AXIAL FLOW COMPRESSOR

4. DESCRIPTIVE NOTES *(Type of report and inclusive dates)*

Thesis

5. AUTHOR(S) *(Last name, first name, initial)*

Marshall, Bruce C., Lieutenant, U. S. Navy

6. REPORT DATE September 1967	**7a. TOTAL NO. OF PAGES** 199	**7b. NO. OF REFS** 11
8a. CONTRACT OR GRANT NO.	**9a. ORIGINATOR'S REPORT NUMBER(S)**	
b. **PROJECT NO.**		
c.	**9b. OTHER REPORT NO(S)** *(Any other numbers that may be assigned this report)*	
d. Unlimited dist		

10. AVAILABILITY/LIMITATION NOTICES

~~This document is subject to special export controls and each transmittal to foreign nationals may be made only with prior approval of the Naval Postgraduate School~~.

11. SUPPLEMENTARY NOTES -	**12. SPONSORING MILITARY ACTIVITY** Commander, Naval Air Systems Command Department of the Navy Washington, D. C. 20360

13. ABSTRACT

A mean streamline analysis of the effect of stator blade orientation on the performance of an axial flow compressor was performed by means of a computer program. Measurements were made on a 3-stage axial flow compressor at the Naval Postgraduate School at six stator stagger angles between 23.8^{o} and 44.3^{o} for a fixed orientation of the rotor blades. Maximum efficiency and pressure ratio were measured at a stator stagger angle of 31.8^{o}. Results at other blade settings showed that by varying stator stagger angle with flow rate optimum efficiencies and pressure ratios can be achieved over a wide range of operating conditions.

The results of the analysis were compared with the measured results. Suggestions are made for improving the manner of adapting cascade test data to performance predictions.

By applying a non-dimensional deflection coefficient it could be shown that minimum work input corresponded to maximum efficiency.

The test compressor has a tip diameter of 36 in. and a hub/tip ratio of 0.6. The blading tested is of the free-vortex type with a design degree of reaction of 0.5. Tip speed was about 185 ft/sec.

14. KEY WORDS	LINK A		LINK B		LINK C	
	ROLE	WT	ROLE	WT	ROLE	WT
compressor						
compressor performance						
axial flow						
variable stator						
stator blade orientation						

DD FORM 1 NOV 65 1473 (BACK)
S/N 0101-807-6821

A-31409

thesM3555
Effect of stator blade orientation on th
3 2768 002 12799 5
DUDLEY KNOX LIBRARY